



**Universiteit
Leiden**
The Netherlands

Cardiovascular computed tomography for diagnosis and risk stratification of coronary artery disease

Werkhoven, J.M. van

Citation

Werkhoven, J. M. van. (2011, June 23). *Cardiovascular computed tomography for diagnosis and risk stratification of coronary artery disease*. Retrieved from <https://hdl.handle.net/1887/17733>

Version: Corrected Publisher's Version

License: [Licence agreement concerning inclusion of doctoral thesis in the Institutional Repository of the University of Leiden](#)

Downloaded from: <https://hdl.handle.net/1887/17733>

Note: To cite this publication please use the final published version (if applicable).

Cardiovascular
Computed Tomography
for Diagnosis and Risk Stratification
of Coronary Artery Disease

J.M. van Werkhoven

**Cardiovascular Computed Tomography
for Diagnosis and Risk Stratification
of Coronary Artery Disease**

J.M. van Werkhoven



The research described in this thesis was performed at the departments of Cardiology and Radiology of the Leiden University Medical Center, Leiden, the Netherlands.

Design: Judith A. van Werkhoven

Lay-out:: Optima Grafische Communicatie, Rotterdam, The Netherlands

Printed by: Optima Grafische Communicatie, Rotterdam, The Netherlands

ISBN: 978-94-6169-078-4

Copyright © 2011 J.M. van Werkhoven, The Hague, The Netherlands. All rights reserved. No parts of this book may be reproduced or transmitted, in any form or by any means, without prior permission by the author.

Financial support for the costs associated with the publication of this thesis was gratefully received from: Astellas Pharma BV, AstraZeneca BV, B.Braun Medical BV, Boehringer Ingelheim BV, Boston Scientific Benelux BV, Bracco Imaging Europe BV, Meda Pharma BV, Merck Sharp & Dohm BV, Philips Healthcare, Sanofi-Aventis BV, Servier Nederland Pharma BV, St Jude Medical BV, Stichting Imago, and Toshiba Medical Systems BV.

Cardiovascular Computed Tomography for Diagnosis and Risk Stratification of Coronary Artery Disease

Proefschrift

ter verkrijging van

de graad van Doctor aan de Universiteit Leiden,
op gezag van Rector Magnificus prof.mr. P.F. van der Heijden,
volgens besluit van het College voor Promoties
te verdedigen op donderdag 23 juni 2011

klokke 16:15 uur

door

Jacob Marinus van Werkhoven

geboren te 's Gravenhage
in 1983

Promotiecommissie

Promotores: Prof. dr. J.J. Bax
Prof. dr. J.W. Jukema
Prof. dr. A. de Roos

Overige leden: Prof. dr. P.J. de Feyter (Erasmus Universiteit, Rotterdam)
Prof. dr. J.H.C. Reiber
Prof. dr. M.J. Schalij
dr. J.H.M. Schreur (MC Haaglanden, Den Haag)
Prof. dr. E.E. Van der Wall

The research described in this thesis was supported by a grant from the Netherlands Society of Cardiology and the Interuniversity Cardiology Institute of the Netherlands.

“l’existence précède l’essence”
(Jean-Paul Sartre)

Table of Contents

Chapter 1:	General introduction and outline	10
Part 1	Cardiovascular Computed Tomography for diagnosis of coronary artery disease	
Chapter 2:	Multi-slice computed tomography coronary angiography: anatomic vs functional assessment in clinical practice Minerva Cardioangiol 2008	20
Chapter 3:	Diagnostic accuracy of computed tomography coronary angiography in patients with an intermediate pre-test likelihood for coronary artery disease Am J Cardiol 2010	38
Chapter 4:	Invasive versus noninvasive evaluation of coronary artery disease J Am Coll Cardiol Img 2008	50
Chapter 5:	Anatomic correlates of a normal perfusion scan using 64-slice computed tomographic coronary angiography Am J Cardiol 2008	68
Chapter 6:	Comparison of Non-Invasive Multi-Slice Computed Tomography Coronary Angiography versus Invasive Coronary Angiography and Fractional Flow Reserve for the Evaluation of Men with Known Coronary Artery Disease Am J Cardiol 2009	82
Chapter 7:	Combined non-Invasive anatomic and functional assessment with MSCT and MRI for the detection of significant coronary artery disease in patients with an intermediate pre-test likelihood Heart 2010	94

Chapter 8: Predictive value of multislice computed tomography variables of atherosclerosis for ischemia on stress-rest single-photon emission computed tomography
Circ Cardiovasc Imaging 2010 112

Chapter 9: Impact of clinical presentation and pre-test likelihood on the relation between coronary calcium score and computed tomography coronary angiography
Am J Cardiol 2010 132

Part 2 Cardiovascular computed tomography for risk stratification of coronary artery disease

Chapter 10: The value of multi-slice computed tomography coronary angiography for risk stratification
J Nucl Cardiol 2009 146

Chapter 11: Prognostic value of multislice computed tomography and gated single-photon emission computed tomography in patients with suspected coronary artery disease
J Am Coll Cardiol 2009 168

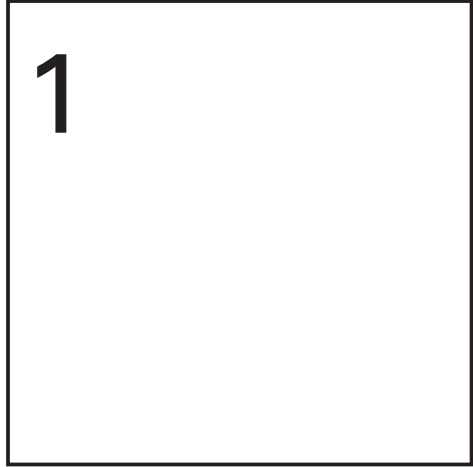
Chapter 12: Incremental prognostic value of multi-slice computed tomography coronary angiography over coronary artery calcium scoring in patients with suspected coronary artery disease
Eur Heart J 2009 186

Chapter 13: Incremental prognostic value of left ventricular function analysis over non-invasive coronary angiography with multi-detector computed tomography
J Nucl Cardiol 2010 204

Chapter 14: Multi-slice computed tomography coronary angiography for risk stratification in patients with an intermediate pre-test likelihood.
Heart 2009 218

Chapter 15:	Diabetes: prognostic value of computed tomography coronary angiography--comparison with a nondiabetic population Radiology 2010	232
Chapter 16:	Influence of smoking on the prognostic value of cardiovascular computed tomography coronary angiography Eur Heart J 2011	252
Part 3	Future perspectives	
Chapter 17:	Myocardial perfusion imaging to assess ischemia using multislice computed tomography Expert Rev Cardiovasc Ther 2009	268
Chapter 18:	Diastolic heart function assessed with MDCT: feasibility study in comparison with tissue doppler J Am Coll Cardiol Img 2011	282
	Summary and Conclusions	303
	Samenvattingen en Conclusies	311
	List of Publications	321
	Dankwoord	331
	Curriculum Vitae	335

Chapter 1



General Introduction and Outline of the Thesis

General Introduction

Coronary artery disease (CAD) is one of the leading causes of mortality and morbidity. Worldwide 3.8 million men and 3.4 million women die of CAD each year.¹ In 2007 11,876 people died of CAD in the Netherlands.² Currently approximately 1 in 25 patients in the Netherlands have CAD, and the prevalence is expected to increase by 40% until 2025, due to demographic changes in the Dutch population.

CAD is caused by the development of atherosclerotic lesions in the coronary arteries. The process of atherosclerosis is induced by endothelial dysfunction, inflammation and the influx of cholesterol in the artery wall.³ This process is mediated by multiple risk factors including age, gender, smoking, hypertension, hypercholesterolemia, diabetes mellitus, obesity, and family history. Formation and early progression of atherosclerosis occurs asymptotically. Acute symptoms may develop when an atherosclerotic plaque ruptures causing coronary thrombosis and acute coronary occlusion. Stable or chronic symptoms develop due to atherosclerosis progression not resulting in coronary occlusions. As the lesion progresses it may start to block the coronary artery, thereby affecting myocardial blood flow. At first this stenosis is counterbalanced by vasodilatation of the coronary artery. However, as the stenosis progresses further, myocardial perfusion and function decrease and patients start to experience chest pain. Complaints generally become apparent at first during exercise or stress. During rest, adequate myocardial blood flow can usually be maintained, however during exercise or stress the myocardial blood flow can no longer be increased to cope with increased oxygen demand.

Currently many diagnostic tools are used to detect the presence of CAD, varying from clinical assessment, blood markers, and the electrocardiogram (ECG), to invasive and non-invasive cardiac imaging. The latter plays an important role in both diagnosis and risk stratification of patients with suspected or known CAD.

Imaging of CAD

The presence of CAD can be identified by direct anatomic assessment of coronary atherosclerosis and stenosis. In contrast, CAD may also be diagnosed indirectly by assessment of myocardial perfusion and function in rest and during exercise or stress. Several anatomic and functional imaging techniques are currently used, of which the invasive modalities are considered the golden standard.

Invasive imaging

Invasive selective coronary angiography is used extensively as a diagnostic tool in both acute and outpatient settings. Using a transfemoral catheter a contrast agent is selectively injected into the ostium of a coronary artery. Simultaneous fluoroscopy allows for high resolution images of the coronary arteries and of luminal narrowing caused by stenotic lesions.⁴ In addition to standard fluoroscopic assessment of coronary arteries, coronary angiography has evolved to a platform for intracoronary imaging and measurement using intravascular ultrasound (IVUS), virtual histology (VH), Doppler flow measurement, and the fractional flow reserve (FFR). IVUS and VH provide a set of transversal ultrasound images of the vessel wall, thereby enabling direct assessment of coronary atherosclerosis. In contrast, Doppler flow and FFR measure coronary blood flow and coronary blood flow reserve and are used to evaluate the hemodynamic effect of lesions detected during preceding coronary angiography.

Non-invasive imaging

Although invasive cardiac imaging techniques are considered the golden standard, these techniques are associated with complications. Although severe complications occur in only a very small proportion of patients, invasive imaging is nevertheless generally restricted to individuals with a high pre-test likelihood of CAD. Non-invasive imaging was developed to identify or rule out the presence of CAD in patients with a lower pre-test likelihood of CAD, and has gained widespread popularity in the last decades. The development of stress echocardiography, single photon emission computed tomography (SPECT), positron emission tomography (PET), and magnetic resonance imaging (MRI) has enabled non-invasive evaluation of myocardial perfusion and function. Stress echocardiography uses ultrasound to image the myocardium and can identify patients with CAD by detecting impaired wall motion due to decreased blood flow resulting from a coronary stenosis.⁵ SPECT and PET assess myocardial perfusion by use of radioisotope tracers which are injected into the bloodstream. The blood-borne SPECT and PET tracers distribute throughout the myocardium and respectively emit gamma radiation and positrons, which can be detected externally by a gamma camera.⁶ A perfusion defect caused by coronary stenosis is indicated by decreased emissions from the corresponding myocardial segments. Sets of images obtained during distinct intervals of the cardiac cycle can be looped to assess wall motion. MRI is also used to assess myocardial perfusion and wall motion, however without the use of ionizing radiation. MRI uses a magnetic field to align the nuclear magnetism of hydrogen atoms in the body. The alignment of these hydrogen atoms are subsequently altered by a radio frequency field which results in the hydrogen atoms producing an electromagnetic signal which can be detected by an MRI scanner.⁷ Different tissue types can be distinguished from each other by the different electromagnetic signals. To assess myocardial perfusion, MRI contrast agents,

which alter the electromagnetic signal emitted from the myocardium, are injected into the bloodstream.⁸

In addition to these non-invasive functional imaging techniques, non-invasive assessment of coronary anatomy has become feasible with the more recent introduction and rapid technical advances of non-invasive imaging using computed tomography (CT). The CT scanner generates a set of cross sectional images of the body, obtained with an X-ray tube and detector row rotating around the longitudinal z-axis of the body.⁹ Non-contrast enhanced CT allows for visualization of coronary calcifications as a marker for CAD, and can quantify the extent and severity of coronary calcification by use of the coronary calcium score (CS). Contrast enhanced CT coronary angiography (CTA) provides direct visualization of the coronary arteries and allows for direct detailed assessment of coronary atherosclerosis and stenosis severity.⁹

Objective and outline of the thesis

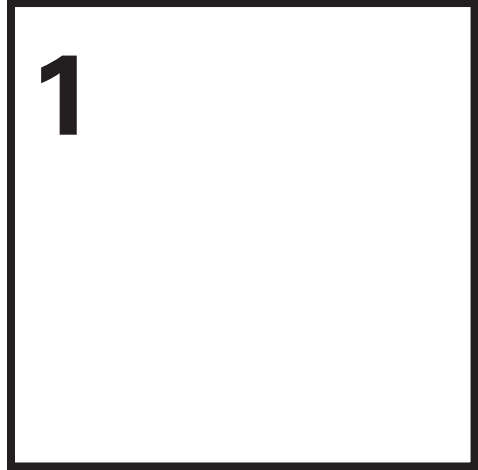
CTA is a relatively new imaging technique; the objective of the thesis is therefore to explore the value of CTA for diagnosis and risk stratification of CAD in patients presenting with suspected and known CAD, in order to further define its role in clinical practice. In Part 1 of the thesis the value of CTA for diagnosis of CAD, and its relationship to existing diagnostic imaging modalities is described. Chapter 2 reviews the technique and potential implementation of CTA in clinical practice relative to existing non-invasive imaging modalities. In Chapter 3 the diagnostic accuracy of CTA is studied specifically in patients with an intermediate pre-test likelihood, as this is the population of choice for non-invasive diagnostic imaging strategies. In Chapter 4 multiple non-invasive and invasive cardiac imaging techniques are compared to evaluate their ability to detect CAD. Chapter 5 describes the prevalence of atherosclerotic lesion on CTA in patients with normal myocardial perfusion as assessed on SPECT. In Chapter 6 the relationship between CTA, invasive coronary angiography and FFR is described. Chapter 7 assesses the complementary value of CTA and myocardial perfusion imaging using MRI. In Chapter 8 the predictive value of CTA for perfusion defects on SPECT is evaluated in detail. Chapter 9 describes the effects of patient clinical presentation and pre-test likelihood on the relationship between CS and CTA. In Part 2 of the thesis the value of CTA for risk stratification is evaluated; in addition the prognostic value of CTA is compared to other non-invasive imaging techniques used for risk stratification. A review of this topic is provided in Chapter 10. In Chapter 11 the prognostic value of CTA is compared to the prognostic value of myocardial perfusion imaging using SPECT. Chapter 12 describes the incremental prognostic value of CTA over CS testing. The incremental prognostic value of left ventricular function over CTA is discussed in Chapter 13. In Chapter 14 the prognostic

value of CTA is evaluated specifically in patients with an intermediate pre-test likelihood for CAD. Chapter 15 evaluates the prognostic value of CTA in diabetic patients and compares it to a non-diabetic population. The prognostic value of CTA in smokers compared to non-smokers is discussed in Chapter 16. Future perspectives of CTA are discussed in Part 3 of the thesis. The potential value of CTA for perfusion imaging is reviewed in Chapter 17, and the feasibility of diastolic function assessment using CTA is discussed in Chapter 18.

References

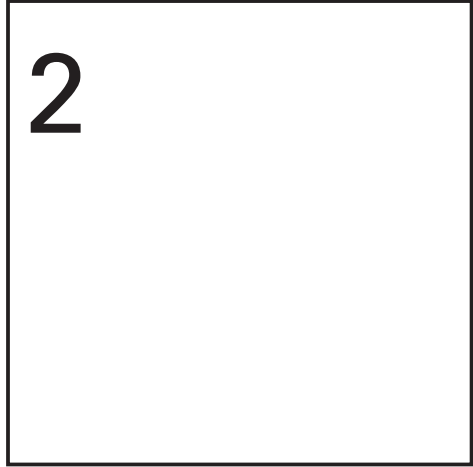
1. Mackay J, Mensah GA. The Atlas of Heart Disease and Stroke. World Health Organization; 2004.
2. Hoeymans N, Melse JM, Schoemaker CG. Gezondheid en determinanten. Deelrapport van de Volksgezondheid Toekomst Verkenning 2010 Van gezond naar beter. RIVM-rapport nr. 270061006. 2010.
3. Libby P, Theroux P. Pathophysiology of coronary artery disease. *Circulation* 2005;111:3481-8.
4. Brusckhe AV, Sheldon WC, Shirey EK, et al. A half century of selective coronary arteriography. *J Am Coll Cardiol* 2009;54:2139-44.
5. Stress Echocardiography. In: Feigenbaum H, Armstrong WF, Ryan T, editors. *Feigenbaum's Echocardiography*. 6th ed. Philadelphia: Lippincott Williams & Wilkins; 2005. p. 488-522.
6. Zaret BL, Beller GA. *Clinical Nuclear Cardiology*. 3rd ed. Philadelphia: Mosby; 2005.
7. Doyle M. Overview of Cardiovascular Magnetic Resonance Imaging. In: Biederman RW, Doyle M, Yamrozik J, editors. *Cardiovascular MRI Tutorial*. 1st ed. Philadelphia: Lippincott Williams & Wilkins; 2008. p. 3-8.
8. Doyle M. Myocardial Perfusion and Viability. In: Biederman RW, Doyle M, Yamrozik J, editors. *Cardiovascular MRI Tutorial*. 1st ed. Philadelphia: Lippincott Williams & Wilkins; 2008. p. 133-44.
9. de Feyter PJ, Krestin GP. *Computed Tomography of the Coronary Arteries*. 2nd ed. London: Informa; 2008.

Part 1



Cardiovascular computed tomography for diagnosis of coronary artery disease

Chapter 2



Multi-slice computed tomography coronary
angiography: anatomic vs functional assessment
in clinical practice

Abstract

Non-invasive imaging plays an increasingly important role in the diagnosis and risk stratification of coronary artery disease. Several techniques such as stress echocardiography and myocardial perfusion imaging have become available to assess cardiac function and myocardial perfusion. With the arrival of multi-slice computed tomography coronary angiography (CTA), non-invasive imaging of coronary anatomy has also become possible. Studies concerning the diagnostic accuracy have demonstrated a good agreement with conventional coronary angiography resulting in a sensitivity and specificity of approximately 86% and 96% respectively. The high negative predictive value of 97% renders it particularly useful to rule out the presence of coronary artery disease in patients with an intermediate pre-test likelihood. Moreover comparative studies have demonstrated that anatomic imaging with CTA may provide information complementary to the traditionally used techniques for functional assessment. From these studies can be derived that only approximately 50% of significant stenoses on CTA are functionally relevant; a large proportion of significant (>50%) lesions on CTA does not result in perfusion abnormalities. Alternatively, many patients with a normal perfusion CTA show considerable atherosclerosis on CTA. Therefore the combined use of these techniques may enhance the assessment of the presence and extent of coronary artery disease. In the future diagnostic algorithms combining non-invasive anatomic and functional imaging need to be evaluated in large patient populations to establish their efficacy, safety, and cost effectiveness. Importantly, these investigations should result in the development of comprehensive guidelines on the use of CTA in clinical practice as well.

Introduction

Coronary artery disease (CAD) is one of the leading causes of death in the western world. In the diagnosis and risk stratification of this condition, imaging plays an increasingly important role. The golden standard for detecting CAD is conventional coronary angiography which enables visualization of the coronary lumen. This is a highly accurate and robust diagnostic technique, but because of its invasive nature it is less suitable as a first line diagnostic test. In the past decades non-invasive imaging has been developed for this purpose and functions as a gatekeeper for conventional coronary angiography. Several techniques such as stress echocardiography and myocardial perfusion imaging have become available to assess cardiac function and myocardial perfusion. Myocardial perfusion imaging with single photon emission computed tomography (SPECT) in particular is widely available and frequently used. With the arrival of multi-slice computed tomography coronary angiography (CTA), non-invasive coronary angiography has become possible. The technique has matured rapidly and its introduction has resulted in a shift from pure functional imaging to non-invasive assessment of coronary anatomy as well. In the present review we will provide an overview of the current status of CTA, and its clinical implications.

CTA technique

Background

Accurate imaging of coronary anatomy with CTA is governed by several basic principles. To ensure detailed evaluation of the coronary arteries as well as coronary stenosis, a high spatial resolution is necessary. This is determined by the minimal slice thickness. Other factors are a high temporal resolution, ECG gating, and sufficient coverage, which are all needed to minimize artefacts due to cardiac and respiratory motion. Temporal resolution (shutter speed) is determined by the rotation time, number of X-ray beams, and the reconstruction protocol used. It needs to be high because of the constant motion of the heart and coronary arteries. ECG gating is used to essentially 'freeze' the heart during an optimal phase of the cardiac cycle with the least cardiac motion. Sufficient images of each cardiac phase are obtained by using an overlapping scan protocol. Finally, respiratory motion is counteracted by performing data acquisition during an inspiratory breath hold. Sufficient coverage (i.e. number of slices) ensures a short scan time during a single breath hold.

Technological advances

CTA technology evolved rapidly starting with the first 4-slice spiral CT scanner in 2000.^{1, 2} At first, the development of new scanners focused on the number of slices. This increased the coverage and thereby reduced scan time. These advancements enabled a shorter breath

hold which reduced the prevalence of uninterpretable scans caused by breathing artefacts, and arrhythmias. Currently 64-slice scanners are the industry standard.

Recent development of new scan technology has moved into different directions. To increase temporal resolution a dual source computed tomography (DSCT) system has been developed, which integrates two X-ray tubes into one scan system, thereby increasing the temporal resolution to 83 ms.^{3, 4} This improvement results in superior image quality as well as less dependency on heart rate control.^{5, 6} Another improvement has been a reduction of the radiation dose by the development of prospective ECG gating. With this “step-and-shoot” protocol images are made during a fixed part of the RR interval, typically end diastolic. Since data are acquired only during this interval the radiation dose can be substantially lowered to approximately 1.1-3.0 mSv.⁷ Finally, entire cardiac coverage in one heart beat can be obtained by the recently introduced 320-slice CT system.^{8, 9} Because of the wide detector array a complete volume of the heart can be scanned without the need for overlapping scans. This significantly lowers the scan time, which counters problems with arrhythmias, decreases the radiation dose, and reduces the amount of contrast needed.

Scan protocol

Patient preparation is an important component of non-invasive coronary angiography. Before each scan, patients should be informed about the procedure, and heart rate is monitored. Most centers administer beta-blockers to patients with heart rates above 65 beats per minute, typically with oral beta-blockers (metoprolol 50 -100 mg), but intravenous beta blockers are also used. Importantly, only patients with sinus rhythm should be studied while imaging should not be performed in patients with arrhythmias. Finally, some centers also administer sublingual nitrates which dilate the coronary arteries thereby enhancing image quality. Importantly, only patients with sinus rhythm should be studied while imaging should not be performed in patients with arrhythmias.

After patient preparation, several exploratory scans are performed to determine accurate start and end positions. Finally, the ECG gated contrast enhanced scan is performed during administration of approximately 80-140 ml of iodinated contrast agent, followed by 40-50 ml saline for optimal arterial enhancement.

After the data have been acquired, the cardiac phase with the least motion is identified and used to reconstruct a dataset of the entire heart. Reconstructions are transferred to an offline workstation for further analysis. The presence of coronary artery stenosis is typically evaluated by assessing the axial images in combination with processed images included 3D volume rendered and curved multiplanar reconstructions or maximum intensity projections. (Figure 1)

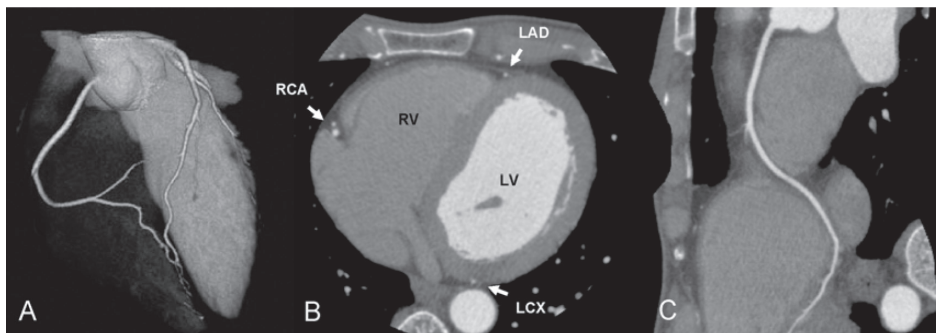


Figure 1. Examples of different reconstruction techniques used for the offline evaluation of CTA exams. Panel A shows a three dimensional volume rendered reconstruction of the right and left coronary arteries. In panel B an axial cross section is depicted in which the left anterior descending coronary artery (LAD), right coronary artery (RCA), and left circumflex artery (LCX) are clearly visible. A multi-planar reconstruction of the right coronary artery is shown in panel C.

Diagnostic accuracy of CTA

Interpretability

The diagnostic accuracy of CTA for the detection of significant CAD (>50% lumen diameter), has been assessed in many comparative studies.^{2, 6, 10-26} With each generation of scanners better image quality, a lower number of uninterpretable scans, and an increased diagnostic accuracy has been obtained. Indeed, although 4-slice CTA showed promising diagnostic accuracy, up to 30% of segments were uninterpretable and had to be excluded from analysis.^{2, 10, 17} The number of uninterpretable scans decreased substantially with 16-slice CTA,^{15, 16, 19} and with the current 64-slice scanners the rate of uninterpretable segments is approximately 4%.²⁷

64-slice CTA

A recent meta-analysis by Abulla et al. has evaluated the diagnostic accuracy of 64-slice CTA compared to conventional coronary angiography.²⁷ The authors included 19 studies that evaluated the native coronary arteries in a total of 1,740 patients. On a patient level the following diagnostic accuracy was observed: sensitivity 86%; specificity 96%, positive predictive value 83%, and negative predictive value 97%. Recently, results from a multi-center trial have been reported by Miller et al.²⁶ The authors included 316 patients with a calcium score ≤ 600 , of which 291 patients underwent conventional coronary angiography. On a patient level a sensitivity and specificity of respectively 83%, and 91% were observed. Accordingly, these multi-center data confirm the observations from previous single center studies.^{11-13, 18, 20-22, 24, 25} An example of the excellent concordance between 64-slice CTA and conventional coronary angiography is illustrated in Figure 2.

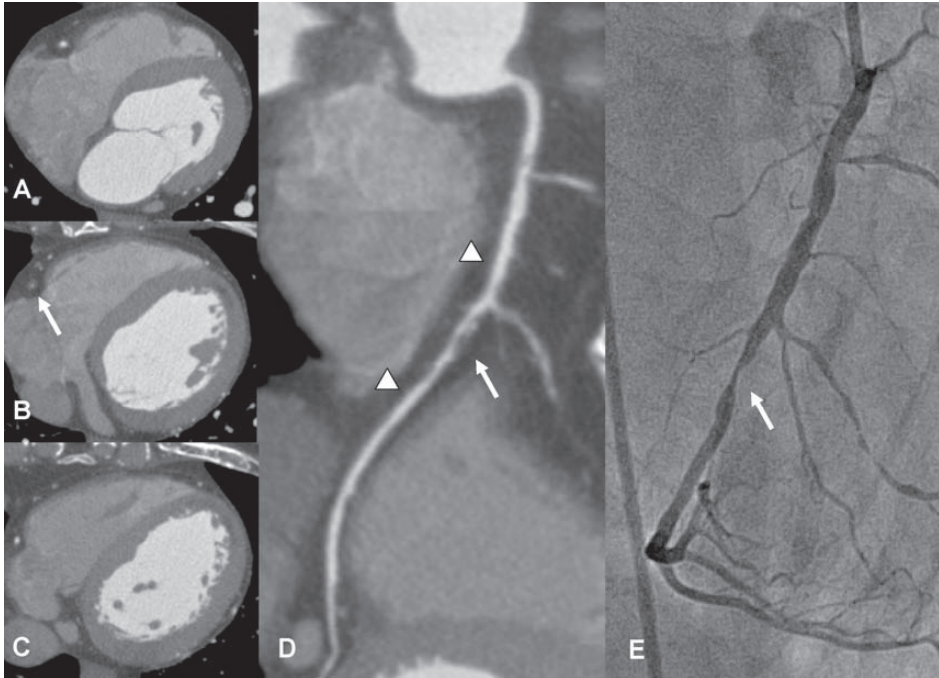


Figure 2. Patient with a significant coronary artery stenosis in the right coronary artery (panels A-D) on CTA. In panels A-C axial slices of the heart are shown at three levels of the right coronary artery corresponding with the markers in panel D: top arrowhead (panel A), middle arrow (panel B), and bottom arrowhead (panel C). While in panels A and C the coronary lumen is clearly visible, substantial reduction of the coronary lumen is visible in panel B. Findings were confirmed by conventional coronary angiography (panel E).

DSCT

The diagnostic accuracy of DSCT has been evaluated in several studies.^{6, 14, 23} In a study by Weustink et al. including 100 patients, the DSCT scanner yielded a high diagnostic accuracy with a sensitivity of 99%, specificity 87%, positive predictive value 96%, and negative predictive value 95% on a patient level.⁶ Because of the increased temporal resolution (83 ms), a high diagnostic accuracy could be obtained even in patients with a high heart rate. This is further emphasized in the study by Ropers et al. who evaluated the influence of heart rate on the diagnostic accuracy of DSCT.⁵ In total, 100 patients were scanned without premedication with beta blockers, allowing comparison of the diagnostic accuracy between 56 patients with a heart rate <65 and 44 patients with a heart rate \geq 65. Although the per-segment evaluability was slightly lower in patients with a high heart rate, no decrease in diagnostic accuracy was observed.

Potential use of CTA in clinical practice

Possible indications

Stable chest pain

The majority of studies on the diagnostic accuracy of CTA have been performed in patients with stable chest pain complaints and referred for coronary angiography due to a high pre-test likelihood for CAD. As a result, most data have been obtained in populations with a high prevalence of CAD. However, non-invasive imaging may be more valuable in patients with a lower likelihood of disease.²⁸ The relationship between pre-test probability and the usefulness of CTA was recently studied by Meijboom et al. who evaluated the diagnostic accuracy of CTA among patients with a high, intermediate, or low pre-test likelihood. In patients with a high pre-test likelihood for CAD, the additional value of CTA was limited. In contrast, in patients with an intermediate pre-test likelihood, a negative CTA scan allowed reduction of the post test probability of CAD to 0%.²⁹ Accordingly these data indicate that the main strength of CTA may be to rule out CAD in patients with a low to intermediate pre-test likelihood.

Acute chest pain

CTA may also be proven useful in patients presenting with acute chest pain. In this clinical setting, it is important to obtain a rapid diagnosis to avoid unnecessary hospitalization as well as incorrect discharge of patients.^{30, 31} Several studies have evaluated the feasibility of CTA in this population.³²⁻³⁶ In a large randomized controlled trial by Goldstein et al., 197 low risk chest pain patients were randomized into a CTA group (n=99) and a standard of care group (n=98).³⁷ In the CTA group, CAD was ruled out in 67 (68%) of 99 patients. In 24 patients with an intermediate or non-diagnostic CT exam a nuclear stress study was performed for further evaluation. In the remaining 8 patients CTA detected severe disease. These patients were directly referred for conventional coronary angiography. An important finding of this study was that the implemented algorithm significantly reduced the diagnostic time compared to the standard of care (3.4 h vs. 15.0 h, $p < 0.001$), while also lowering the costs (\$1,586 vs. \$1,872, $p < 0.001$). Accordingly, initial data suggests that in patients with an intermediate likelihood without ECG changes and elevated enzymes, in whom diagnosis may be particularly challenging, CTA may be useful.³⁸ Nevertheless, further evaluation of the accuracy, safety, and cost-effectiveness of CTA in this setting is warranted.

Asymptomatic patients

In general use of CTA is considered to be inappropriate in asymptomatic patients because of the associated radiation burden. However several subpopulations have been identified that may benefit from evaluation with CTA, such as patients referred for preoperative cardiac evaluation,³⁹ or patients with left bundle branch block.⁴⁰ Also, in patients with

dilated cardiomyopathy CTA may be useful for identification of idiopathic versus ischemic etiology.⁴¹

Previous revascularization

In patients with previous revascularization (percutaneous coronary intervention or bypass grafting) imaging with CTA is possible but is frequently challenging.^{42, 43} The assessability of in-stent restenosis is hampered by the occurrence of metal artefacts caused by the stent struts. As a result, high rates of uninterpretable stents have been reported. The routine use of CTA in patients with previous coronary stenting is therefore not recommended.²⁸ However in selected patients with larger stent diameter, results with 64-slice CTA have been promising. Cademartiri et al evaluated 182 patients with a total of 192 stents (diameter ≥ 2.5 mm) and demonstrated a sensitivity and specificity of 95% and 93%. Moreover, a negative predictive value of 99% was obtained indicating that in selected patients, CTA may be used to rule out in-stent restenosis.^{28, 44, 45}

CTA imaging of bypass grafts is less affected by motion than the coronary arteries, thereby allowing good visualization of graft patency or stenosis. In general, high accuracies in the range of 90% to 100% have been reported.^{46, 47} However, the assessment of grafts can be affected by surgical metal clips which may render the graft uninterpretable. Furthermore, assessment of the native coronary arteries or segments distal to the anastomosis may be difficult due to the frequent presence of extensive coronary calcifications in combination with small vessel size. As a result, higher rates of unevaluable segments as compared to patients without previous coronary artery bypass grafting have been reported.⁴³ Thus, while coronary artery bypass grafts can be assessed accurately, assessment on a patient level remains challenging. The routine use of CTA is therefore not recommended in patients with previous bypass graft surgery.²⁸

Integration into current clinical practice

Anatomy versus function

Traditional non-invasive diagnostic imaging strategies have focused on the assessment of myocardial perfusion and function. Accordingly, the presence of CAD was determined based on the presence of inducible perfusion or wall motion abnormalities, indicating the presence of ischemia. With the arrival of CTA it has become possible to assess cardiac anatomy non-invasively as well. To understand the relative values of these techniques several studies comparing CTA to myocardial perfusion imaging have been performed.^{32, 48-50} An overview of the studies comparing 64-slice CTA to myocardial perfusion imaging using SPECT is shown in Table 1. From these studies can be derived that only approximately 50% of significant stenoses on CTA are functionally relevant; a large proportion of significant (>50%) lesions on CTA does not result in perfusion abnormalities. Alternatively, many patients with a normal perfusion scan show considerable atherosclerosis on CTA. Accordingly, these

Table 1. Overview of studies comparing 64-slice CTA to myocardial perfusion imaging (MPI).

	n	CTA \leq 50%		CTA >50%	
		MPI -	MPI +	MPI -	MPI +
Schuijf(50)	114	37 (90%)	4 (10%)	40 (55%)	33 (45%)
Hacker(49)	26	12 (86%)	2 (14%)	4 (33%)	8 (67%)
Gaemperli(48)	91	53 (96%)	2 (4%)	18 (50%)	18 (50%)
Galagher(32)	85	66 (90%)	7 (10%)	6 (50%)	6 (50%)

studies illustrate the discrepancy between anatomic and functional testing; CTA detects atherosclerosis, functional testing evaluates the presence of hemodynamically significant lesions. As a result, the techniques may be considered to provide complementary information on the presence and severity of CAD. The combined use of these techniques may therefore potentially enhance the diagnostic workup of patients presenting with chest pain complaints.

Combined anatomic and functional imaging

Two approaches can be used to combine the information from CTA and myocardial perfusion imaging. The first is fusion of the anatomic and functional information, either by hybrid imaging or by retrospective fusion of datasets.^{51, 52} The advantage of this approach is that it allows accurate allocation of perfusion defects to the corresponding coronary arteries.⁵³ A disadvantage however is the associated radiation dose while information on both anatomy and function may not be required in all patients.

An alternative approach to combining anatomic and functional imaging therefore might be sequential imaging. A flow chart advocating such a strategy has been recently published and is provided in Figure 3.⁵⁴ Patients presenting with an intermediate pre-test likelihood may benefit the most from CTA. In these patients, CTA can be used as an initial imaging technique to rule out the presence of CAD. Patients with a normal CTA can be safely discharged and do not require further testing. In patients with non-obstructive atherosclerosis (<50%) medical therapy and aggressive risk factor modification may be indicated. Invasive imaging and revascularization may not be needed as the likelihood of ischemia is still low. On the other hand, the likelihood of hemodynamically relevant CAD is high in patients with a severely abnormal CTA, including left main or three vessel disease. These patients may be referred for conventional coronary angiography immediately. Finally, in patients with a borderline stenosis or an equivocal CTA, functional imaging remains required to determine the further management and in general, only patients with ischemia should be referred for conventional coronary angiography in combination with possible revascularization. An example of a patient with a significant stenosis on CTA with a corresponding perfusion defect on SPECT is shown in Figure 4.

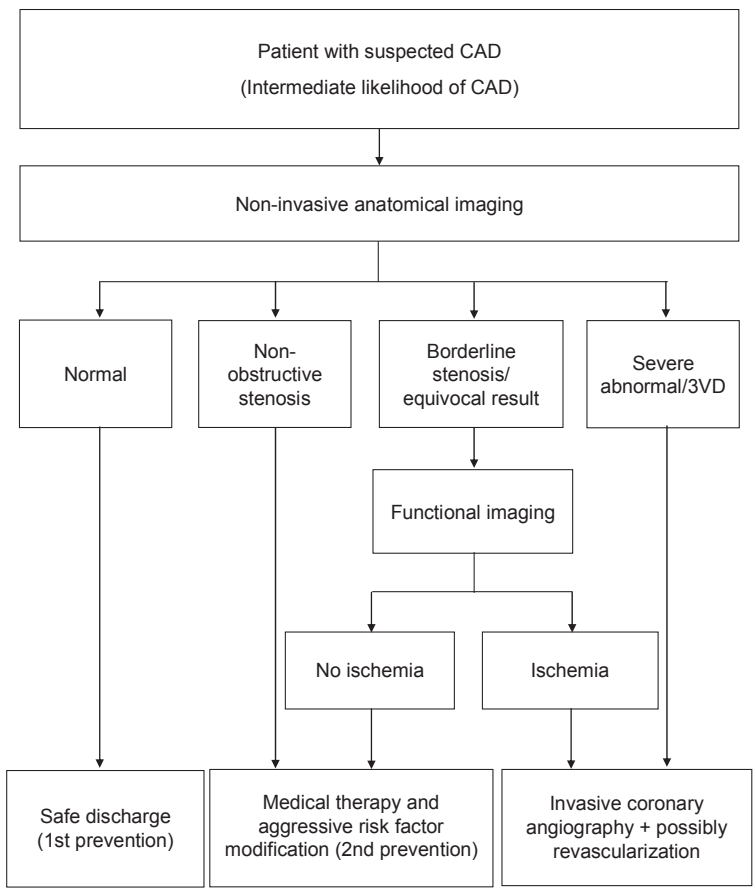


Figure 3. A flow chart describing the combined use of non-invasive anatomical and functional imaging in patients with an intermediate pre-test likelihood of coronary artery disease (CAD). Reprinted with permission from reference 54.

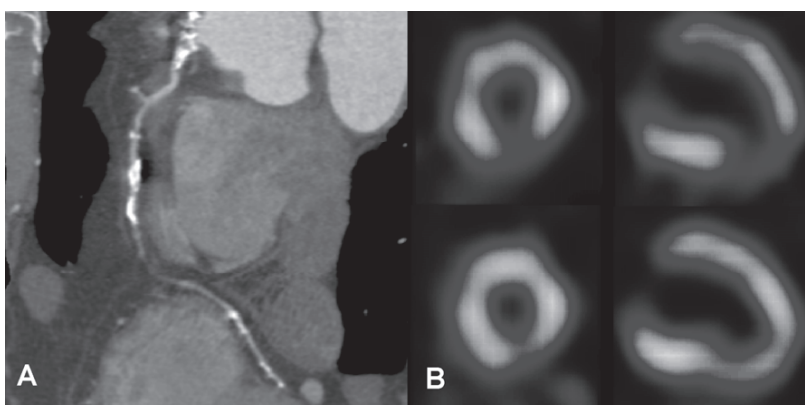


Figure 4. Example of a patient with a significant stenosis in the right coronary artery on CTA (panel A), which resulted in a partially reversible perfusion defect on SPECT (panel B).

Future perspectives

Plaque imaging

Acute coronary syndromes (ACS) are a major cause of morbidity and mortality worldwide.⁵⁵ Since CTA allows direct evaluation of the presence and (to some extent) composition of atherosclerosis, the technique may potentially be useful to identify patients with plaque characteristics suggesting a high risk for plaque rupture. Several studies have identified differences in plaque composition between patients presenting with ACS and patients with stable CAD.⁵⁶⁻⁵⁸ Motoyama et al. studied the characteristics of culprit lesions in 38 patients with ACS and compared them to the lesions observed in 33 patients presenting with stable angina pectoris.^{55, 57} The authors observed significantly more positive remodeling, non-calcified plaque, and spotty calcifications in the culprit lesions of ACS patients. Similar findings have been reported in other studies.^{56, 58} Although these data suggest that the assessment of plaque characteristics may be of clinical relevance, accurate and reproducible quantification remains challenging. Leber et al. recently reported on the accuracy of 64-slice CTA to classify and quantify plaque volumes in the proximal coronary arteries.^{55, 59} CTA was compared with intravascular ultrasound in 19 patients with 36 vessels. CTA detected calcified and mixed plaque with high accuracy (95% and 94%, respectively) but accuracy was lower for non-calcified lesion (83%). When regarding plaque volume, non-calcified plaque and mixed plaque volumes were systematically underestimated whereas calcified plaque volume was overestimated by CTA. Importantly the presence of features associated with plaque vulnerability, including the presence of large lipid cores and spotty calcifications, was also assessed. A lipid pool was correctly identified in 70% of sections and spotty calcification patterns in 90% of sections. The authors concluded that imaging of plaque characteristics related to ACS may be possible with CTA, but that evaluation of plaque burden is only moderately concordant with intravascular ultrasound.

These preliminary studies demonstrate the ability of CTA to provide information on atherosclerotic plaque patterns. Potentially, this information may be used for risk stratification, although only limited outcome data of CTA are currently available.^{60, 61}

CTA perfusion imaging

Another potential feature of CTA is the evaluation of myocardial perfusion, which has generated substantial interest. Based on differences in the attenuation values during contrast administration, differentiation between territories with normal and abnormal perfusion is possible. Indeed, using the same protocol as used for coronary angiography, areas of previous myocardial infarction are identified as hypoenhanced regions.⁶²⁻⁶⁴ Similar to MRI, identification of scar tissue is possible with delayed enhancement imaging. Using this technique myocardial segments with scar tissue appear as hyperenhanced regions.^{65, 66} An excellent

agreement has been shown between infarct imaging with CTA and other techniques including magnetic resonance imaging and SPECT.^{63, 67}

Importantly, preliminary data suggest that CTA can also be used to assess the presence of inducible perfusion abnormalities indicating the presence of ischemia.⁶⁸ However, the administration of adenosine may frequently induce tachycardia, which in turn may hamper simultaneous assessment of the coronary arteries. The introduction of new generation scanners such as 256- and 320-slice CT however may substantially facilitate combined evaluation of coronary anatomy and stress perfusion in a single procedure.⁶⁹ Further studies should demonstrate whether CTA may indeed have the potential to provide combined assessment of anatomy and function in a single session.

Conclusions

With the current generation scanners CTA has become a robust non-invasive imaging technique. Studies concerning the diagnostic accuracy have demonstrated a good agreement with conventional coronary angiography. The high negative predictive value of CTA renders it particularly useful to rule out the presence of CAD in patients with an intermediate pre-test likelihood. Comparative studies have demonstrated that anatomic imaging with CTA may provide information complementary to the traditionally used techniques for functional assessment. Moreover, the combined use of these techniques may enhance the assessment of the presence and extent of CAD. In the future diagnostic algorithms combining non-invasive anatomic and functional imaging need to be evaluated in large patient populations to establish their efficacy, safety, and cost effectiveness. Importantly, these investigations should result in the development of comprehensive guidelines on the use of CTA in clinical practice as well.

References

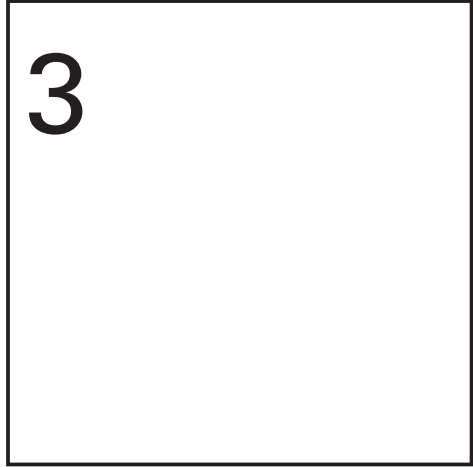
1. Hu H, He HD, Foley WD, et al. Four multidetector-row helical CT: image quality and volume coverage speed. *Radiology* 2000;215:55-62.
2. Nieman K, Oudkerk M, Rensing BJ, et al. Coronary angiography with multi-slice computed tomography. *Lancet* 2001;357:599-603.
3. Achenbach S, Ropers D, Kuettner A, et al. Contrast-enhanced coronary artery visualization by dual-source computed tomography--initial experience. *Eur J Radiol* 2006;57:331-5.
4. Flohr TG, McCollough CH, Bruder H, et al. First performance evaluation of a dual-source CT (DSCT) system. *Eur Radiol* 2006;16:256-68.
5. Ropers U, Ropers D, Pflederer T, et al. Influence of heart rate on the diagnostic accuracy of dual-source computed tomography coronary angiography. *J Am Coll Cardiol* 2007;50:2393-8.
6. Weustink AC, Meijboom WB, Mollet NR, et al. Reliable high-speed coronary computed tomography in symptomatic patients. *J Am Coll Cardiol* 2007;50:786-94.
7. Husmann L, Valenta I, Gaemperli O, et al. Feasibility of low-dose coronary CT angiography: first experience with prospective ECG-gating. *Eur Heart J* 2008;29:191-7.
8. Kitagawa K, Arbab-Zadeh A, Hannon KM, et al. Comparison of 256X0.5mm and 64X0.5mm Multidetector Computed Tomography Image Quality and Accuracy in a Custom-Designed, Motion-Simulating Phantom of Coronary Artery Stenosis (abstract 1902). American Heart Association Scientific Sessions 2007.
9. Motoyama S, Sarai M, Anno H, et al. Image Quality of Coronary CT Angiography in 256-slice CT (abstract 2758). American Heart Association Scientific Sessions 2007.
10. Achenbach S, Giesler T, Ropers D, et al. Detection of coronary artery stenoses by contrast-enhanced, retrospectively electrocardiographically-gated, multislice spiral computed tomography. *Circulation* 2001;103:2535-8.
11. Ehara M, Surmely JF, Kawai M, et al. Diagnostic accuracy of 64-slice computed tomography for detecting angiographically significant coronary artery stenosis in an unselected consecutive patient population: comparison with conventional invasive angiography. *Circ J* 2006;70:564-71.
12. Hausleiter J, Meyer T, Hadamitzky M, et al. Non-invasive coronary computed tomographic angiography for patients with suspected coronary artery disease: the Coronary Angiography by Computed Tomography with the Use of a Submillimeter resolution (CACTUS) trial. *Eur Heart J* 2007;28:3034-41.
13. Herzog C, Zwerner PL, Doll JR, et al. Significant coronary artery stenosis: comparison on per-patient and per-vessel or per-segment basis at 64-section CT angiography. *Radiology* 2007;244:112-20.
14. Heuschmid M, Burgstahler C, Reimann A, et al. Usefulness of noninvasive cardiac imaging using dual-source computed tomography in an unselected population with high prevalence of coronary artery disease. *Am J Cardiol* 2007;100:587-92.
15. Hoffmann U, Moselewski F, Cury RC, et al. Predictive value of 16-slice multidetector spiral computed tomography to detect significant obstructive coronary artery disease in patients at high risk for coronary artery disease: patient-versus segment-based analysis. *Circulation* 2004;110:2638-43.
16. Kaiser C, Bremerich J, Haller S, et al. Limited diagnostic yield of non-invasive coronary angiography by 16-slice multi-detector spiral computed tomography in routine patients referred for evaluation of coronary artery disease. *Eur Heart J* 2005;26:1987-92.
17. Kopp AF, Schroeder S, Kuettner A, et al. Non-invasive coronary angiography with high resolution multidetector-row computed tomography. Results in 102 patients. *Eur Heart J* 2002;23:1714-25.
18. Leschka S, Alkadhi H, Plass A, et al. Accuracy of MSCT coronary angiography with 64-slice technology: first experience. *Eur Heart J* 2005;26:1482-7.
19. Mollet NR, Cademartiri F, Nieman K, et al. Multislice spiral computed tomography coronary angiography in patients with stable angina pectoris. *J Am Coll Cardiol* 2004;43:2265-70.

20. Mollet NR, Cademartiri F, Van Mieghem CA, et al. High-resolution spiral computed tomography coronary angiography in patients referred for diagnostic conventional coronary angiography. *Circulation* 2005;112:2318-23.
21. Raff GL, Gallagher MJ, O'Neill WW, et al. Diagnostic accuracy of noninvasive coronary angiography using 64-slice spiral computed tomography. *J Am Coll Cardiol* 2005;46:552-7.
22. Ropers D, Rixe J, Anders K, et al. Usefulness of multidetector row spiral computed tomography with 64- x 0.6-mm collimation and 330-ms rotation for the noninvasive detection of significant coronary artery stenoses. *Am J Cardiol* 2006;97:343-8.
23. Scheffel H, Alkadhi H, Plass A, et al. Accuracy of dual-source CT coronary angiography: First experience in a high pre-test probability population without heart rate control. *Eur Radiol* 2006;16:2739-47.
24. Schuijff JD, Pundziute G, Jukema JW, et al. Diagnostic accuracy of 64-slice multislice computed tomography in the noninvasive evaluation of significant coronary artery disease. *Am J Cardiol* 2006;98:145-8.
25. Shabestari AA, Abdi S, Akhlaghpour S, et al. Diagnostic performance of 64-channel multislice computed tomography in assessment of significant coronary artery disease in symptomatic subjects. *Am J Cardiol* 2007;99:1656-61.
26. Late-Breaking Clinical Trial Abstracts From the American Heart Association's Scientific Sessions 2007. *Circulation* 2008;116:2627-33.
27. Abdulla J, Abildstrom SZ, Gotzsche O, et al. 64-multislice detector computed tomography coronary angiography as potential alternative to conventional coronary angiography: a systematic review and meta-analysis. *Eur Heart J* 2007;28:3042-50.
28. Schroeder S, Achenbach S, Bengel F, et al. Cardiac computed tomography: indications, applications, limitations, and training requirements: Report of a Writing Group deployed by the Working Group Nuclear Cardiology and Cardiac CT of the European Society of Cardiology and the European Council of Nuclear Cardiology. *Eur Heart J* 2007.
29. Meijboom WB, Van Mieghem CA, Mollet NR, et al. 64-slice computed tomography coronary angiography in patients with high, intermediate, or low pretest probability of significant coronary artery disease. *J Am Coll Cardiol* 2007;50:1469-75.
30. Lee TH, Ting HH, Shammash JB, et al. Long-term survival of emergency department patients with acute chest pain. *Am J Cardiol* 1992;69:145-51.
31. Pope JH, Aufderheide TP, Ruthazer R, et al. Missed diagnoses of acute cardiac ischemia in the emergency department. *N Engl J Med* 2000;342:1163-70.
32. Gallagher MJ, Ross MA, Raff GL, et al. The diagnostic accuracy of 64-slice computed tomography coronary angiography compared with stress nuclear imaging in emergency department low-risk chest pain patients. *Ann Emerg Med* 2007;49:125-36.
33. Goldstein JA, Gallagher MJ, O'Neill WW, et al. A randomized controlled trial of multi-slice coronary computed tomography for evaluation of acute chest pain. *J Am Coll Cardiol* 2007;49:863-71.
34. Hoffmann U, Nagurney JT, Moselewski F, et al. Coronary multidetector computed tomography in the assessment of patients with acute chest pain. *Circulation* 2006;114:2251-60.
35. Meijboom WB, Mollet NR, Van Mieghem CA, et al. 64-Slice CT coronary angiography in patients with non-ST elevation acute coronary syndrome. *Heart* 2007;93:1386-92.
36. Rubinshtein R, Halon DA, Gaspar T, et al. Usefulness of 64-slice cardiac computed tomographic angiography for diagnosing acute coronary syndromes and predicting clinical outcome in emergency department patients with chest pain of uncertain origin. *Circulation* 2007;115:1762-68.
37. Goldstein JA, Gallagher MJ, O'Neill WW, et al. A randomized controlled trial of multi-slice coronary computed tomography for evaluation of acute chest pain. *J Am Coll Cardiol* 2007;49:863-71.
38. Kramer CM, Budoff MJ, Fayad ZA, et al. ACCF/AHA 2007 clinical competence statement on vascular imaging with computed tomography and magnetic resonance: a report of the American College of Cardiology Foundation/American Heart Association/American College of Physicians

- Task Force on Clinical Competence and Training: developed in collaboration with the Society of Atherosclerosis Imaging and Prevention, the Society for Cardiovascular Angiography and Interventions, the Society of Cardiovascular Computed Tomography, the Society for Cardiovascular Magnetic Resonance, and the Society for Vascular Medicine and Biology. *Circulation* 2007;116:1318-35.
39. Meijboom WB, Mollet NR, Van Mieghem CA, et al. Pre-operative computed tomography coronary angiography to detect significant coronary artery disease in patients referred for cardiac valve surgery. *J Am Coll Cardiol* 2006;48:1658-65.
 40. Ghostine S, Caussin C, Daoud B, et al. Non-invasive detection of coronary artery disease in patients with left bundle branch block using 64-slice computed tomography. *J Am Coll Cardiol* 2006;48:1929-34.
 41. Andreini D, Pontone G, Pepi M, al. Diagnostic accuracy of multidetector computed tomography coronary angiography in patients with dilated cardiomyopathy. *J Am Coll Cardiol* 2007;49:2044-50.
 42. Rixe J, Achenbach S, Ropers D, et al. Assessment of coronary artery stent restenosis by 64-slice multi-detector computed tomography. *Eur Heart J* 2006;27:2567-72.
 43. Ropers D, Pohle FK, Kuettner A, et al. Diagnostic accuracy of noninvasive coronary angiography in patients after bypass surgery using 64-slice spiral computed tomography with 330-ms gantry rotation. *Circulation* 2006;114:2334-41.
 44. Cademartiri F, Schuijff JD, Pugliese F, et al. Usefulness of 64-slice multislice computed tomography coronary angiography to assess in-stent restenosis. *J Am Coll Cardiol* 2007;49:2204-10.
 45. Schuijff JD, Pundziute G, Jukema JW, et al. Evaluation of patients with previous coronary stent implantation with 64-section CT. *Radiology* 2007;245:416-23.
 46. Meyer TS, Martinoff S, Hadamitzky M, et al. Improved noninvasive assessment of coronary artery bypass grafts with 64-slice computed tomographic angiography in an unselected patient population. *J Am Coll Cardiol* 2007;49:946-50.
 47. Malagutti P, Nieman K, Meijboom WB, et al. Use of 64-slice CT in symptomatic patients after coronary bypass surgery: evaluation of grafts and coronary arteries. *Eur Heart J* 2007;28:1879-85.
 48. Gaemperli O, Schepis T, Koepfli P, et al. Accuracy of 64-slice CT angiography for the detection of functionally relevant coronary stenoses as assessed with myocardial perfusion SPECT. *Eur J Nucl Med Mol Imaging* 2007;34:1162-71.
 49. Hacker M, Jakobs T, Hack N, et al. Sixty-four slice spiral CT angiography does not predict the functional relevance of coronary artery stenoses in patients with stable angina. *Eur J Nucl Med Mol Imaging* 2007;34:4-10.
 50. Schuijff JD, Wijns W, Jukema JW, et al. Relationship between noninvasive coronary angiography with multi-slice computed tomography and myocardial perfusion imaging. *J Am Coll Cardiol* 2006;48:2508-14.
 51. Gaemperli O, Schepis T, Valenta I, et al. Cardiac image fusion from stand-alone SPECT and CT: clinical experience. *J Nucl Med* 2007;48:696-703.
 52. Rispler S, Keidar Z, Ghersin E, et al. Integrated single-photon emission computed tomography and computed tomography coronary angiography for the assessment of hemodynamically significant coronary artery lesions. *J Am Coll Cardiol* 2007;49:1059-67.
 53. Gaemperli O, Kaufmann PA. Hybrid cardiac imaging: more than the sum of its parts? *J Nucl Cardiol* 2008;15:123-6.
 54. Schuijff JD, Jukema JW, van der Wall EE, et al. The current status of multislice computed tomography in the diagnosis and prognosis of coronary artery disease. *J Nucl Cardiol* 2007;14:604-12.
 55. Virmani R, Burke AP, Farb A, et al. Pathology of the vulnerable plaque. *J Am Coll Cardiol* 2006;47:C13-C18.

56. Hoffmann U, Moselewski F, Nieman K, et al. Noninvasive assessment of plaque morphology and composition in culprit and stable lesions in acute coronary syndrome and stable lesions in stable angina by multidetector computed tomography. *J Am Coll Cardiol* 2006;47:1655-62.
57. Motoyama S, Kondo T, Sarai M, et al. Multislice computed tomographic characteristics of coronary lesions in acute coronary syndromes. *J Am Coll Cardiol* 2007;50:319-26.
58. Schuijff JD, Beck T, Burgstahler C, et al. Differences in plaque composition and distribution in stable coronary artery disease versus acute coronary syndromes; non-invasive evaluation with multi-slice computed tomography. *Acute Card Care* 2007;9:48-53.
59. Leber AW, Becker A, Knez A, et al. Accuracy of 64-slice computed tomography to classify and quantify plaque volumes in the proximal coronary system: a comparative study using intravascular ultrasound. *J Am Coll Cardiol* 2006;47:672-7.
60. Min JK, Shaw LJ, Devereux RB, et al. Prognostic value of multidetector coronary computed tomographic angiography for prediction of all-cause mortality. *J Am Coll Cardiol* 2007;50:1161-70.
61. Pundziute G, Schuijff JD, Jukema JW, et al. Prognostic value of multislice computed tomography coronary angiography in patients with known or suspected coronary artery disease. *J Am Coll Cardiol* 2007;49:62-70.
62. Henneman MM, Schuijff JD, Jukema JW, et al. Comprehensive cardiac assessment with multislice computed tomography: evaluation of left ventricular function and perfusion in addition to coronary anatomy in patients with previous myocardial infarction. *Heart* 2006;92:1779-83.
63. Henneman MM, Schuijff JD, Dibbets-Schneider P, et al. Comparison of multislice computed tomography to gated single-photon emission computed tomography for imaging of healed myocardial infarcts. *Am J Cardiol* 2008;101:144-8.
64. Ko SM, Seo JB, Hong MK, et al. Myocardial enhancement pattern in patients with acute myocardial infarction on two-phase contrast-enhanced ECG-gated multidetector-row computed tomography. *Clin Radiol* 2006;61:417-22.
65. Habis M, Capderou A, Ghostine S, et al. Acute myocardial infarction early viability assessment by 64-slice computed tomography immediately after coronary angiography: comparison with low-dose dobutamine echocardiography. *J Am Coll Cardiol* 2007;49:1178-85.
66. Lardo AC, Cordeiro MA, Silva C, et al. Contrast-enhanced multidetector computed tomography viability imaging after myocardial infarction: characterization of myocyte death, microvascular obstruction, and chronic scar. *Circulation* 2006;113:394-404.
67. Sanz J, Weeks D, Nikolaou K, et al. Detection of healed myocardial infarction with multidetector-row computed tomography and comparison with cardiac magnetic resonance delayed hyperenhancement. *Am J Cardiol* 2006;98:149-55.
68. George RT, Silva C, Cordeiro MA, et al. Multidetector computed tomography myocardial perfusion imaging during adenosine stress. *J Am Coll Cardiol* 2006;48:153-60.
69. George RT, Lardo AC, Kitagawa K, et al. Combined Perfusion and Non-Invasive Coronary Angiography in Patients with Suspected Coronary Disease using 256 Row, 0.5mm Slice Thickness non-Helical Multi-Detector Computed Tomography (abstract 2589). American Heart Association Scientific Sessions 2007.

Chapter 3



Diagnostic accuracy of computed tomography
coronary angiography in patients with an
intermediate pre-test likelihood for coronary
artery disease

JM van Werkhoven, MW Heijenbrok, JD Schuijf, JW Jukema, MM Boogers, EE van
der Wall, JHM Schreur, JJ Bax

Abstract

Data on the diagnostic accuracy of multi-slice computed tomography coronary angiography (CTA) have been mostly derived in patients with a high pre-test likelihood for coronary artery disease (CAD). Systematic comparison with invasive angiography in patients with intermediate pre-test likelihood is scarce. The purpose of the present study was to determine the diagnostic accuracy of CTA in patients without known CAD with an intermediate pre-test likelihood. 61 patients (61% male, and average age 57 ± 9 years) referred for invasive coronary angiography underwent additional 64-slice CTA. 920 segments were identified on invasive coronary angiography of which 885 (96%) were interpretable on CTA. Invasive coronary angiography identified a significant stenosis ($\geq 50\%$ luminal narrowing) in 29 segments, of which 23 were detected on CTA. As a result, sensitivity, specificity, positive predictive value and negative predictive value were 79%, 98%, 61%, and 99% respectively. On a patient level, sensitivity, specificity, positive predictive value, and negative predictive value were respectively 100%, 89%, 76%, and 100%. Importantly, CTA correctly ruled out the presence of significant stenosis in 66% (40 of 61) of the total population. In conclusion, the current study confirms that CTA has an excellent diagnostic accuracy in the target population of patients with an intermediate pre-test likelihood. Notably, the high negative predictive value allowed rule out of significant stenosis in a large proportion of patients. CTA may therefore be used as a highly effective gatekeeper for invasive coronary angiography.

Introduction

Recently, non-invasive anatomic imaging has become possible with the introduction of multi-slice computed tomography coronary angiography (CTA). Numerous studies have shown that CTA has a high diagnostic accuracy for the evaluation of significant CAD ($\geq 50\%$ luminal narrowing) as compared to invasive coronary angiography.¹⁻⁷ Accordingly, the technique has been proposed as a tool to rule out significant CAD and thus serve as a non-invasive gatekeeper for invasive coronary angiography. However thus far, almost all studies investigating the diagnostic accuracy of CTA have been performed in populations with a high pre-test likelihood for CAD. Nevertheless, this population is unlikely to benefit from CTA as the majority of patients will require invasive coronary angiography anyway. In contrast, patients with an intermediate pre-test likelihood of CAD may derive far more benefit from a non-invasive alternative for coronary angiography and may in fact represent the target population for this technique. Unfortunately, only very limited data are currently available in patients with an intermediate pre-test likelihood, and systematic comparison with invasive coronary angiography is scarce. For this reason the purpose of the present study was to specifically address the diagnostic accuracy of CTA in patients with an intermediate pre-test likelihood for CAD.

Methods

In this prospective cohort study, 61 patients with an intermediate pre-test likelihood for CAD and referred for invasive diagnostic coronary angiography underwent additional evaluation with CTA within a period of 14 days. An intermediate pre-test likelihood was defined according to the Diamond and Forrester criteria as a pre-test likelihood of CAD between 13.4% and 87.2%, as previously described.⁸ Patients were excluded from the study if they met one of the following exclusion criteria for CTA: cardiac arrhythmias, renal insufficiency (serum creatinine >120 mmol/L), known hypersensitivity to iodine contrast media, and pregnancy. Finally patients were excluded in the occurrence of a cardiac event (worsening angina, revascularization, or myocardial infarction) in the period between the 2 examinations. The study was approved by the local medical ethics committee (Medical Center Haaglanden, The Hague, The Netherlands) and all patients gave written informed consent.

All examinations were performed using a 64-slice MSCT scanner (Lightspeed VR 64, GE Healthcare, Milwaukee, MI, USA). Patient's heart rate and blood pressure were monitored before each scan. In the absence of contraindications, patients with a heart rate exceeding the threshold of 65 beats per minute were administered beta-blocking medication (50-100 mg metoprolol, oral or 5-10 mg metoprolol, intravenous).

Before the helical scan, a non-enhanced electrocardiographically gated scan, prospectively triggered at 75% of the R-R interval, was performed to measure the coronary calcium score (CS), and to determine the start and end positions of the helical scan. Following the calcium scan a retrospectively electrocardiographically gated helical scan was performed using the following scan parameters: collimation 64 x 0.625 mm; rotation time 0.35 s; tube voltage 120 kV, and tube current 600 mA (with tube modulation to reduce the radiation dose). A bolus of 80 ml iomeprol (Iomeron 400, Bracco, Milan, Italy) was injected at 5 ml/s followed by 40 ml saline flush. The helical scan was automatically triggered using a bolus tracking technique (SmartPrep), when the attenuation level in the region of interest reached the predefined threshold (baseline attenuation + 100 Hounsfield units). Datasets were reconstructed from the retrospectively gated raw data with an effective slice thickness of 0.625 mm. Coronary arteries were evaluated using the reconstructed dataset with the least motion artifacts, typically an end-diastolic phase.

Post-processing of the MSCT calcium scans and coronary angiograms was performed on a dedicated workstation (Advantage, GE Healthcare, Waukesha, Wisconsin, USA). The total CS was calculated from the non-enhanced calcium scan using the Agatston method. Subsequently, coronary anatomy was evaluated using the contrast-enhanced helical examinations. Coronary arteries were divided into 17 segments according to a modified American Heart Association classification.⁹ All studies were interpreted by two experienced observers blinded to the results of coronary angiography. First image quality was assessed and scored as good, average (reduced image quality but diagnostic quality), and poor (low diagnostic image quality). Next, the presence of significant stenosis ($\geq 50\%$ luminal narrowing) was evaluated using axial slices, curved multiplanar reconstructions, and maximum intensity projections.

Invasive diagnostic coronary angiography was performed according to standard techniques. Coronary angiograms were evaluated by an observer blinded to the CTA results using offline quantitative software (QCA-CMS, version 6.0, Medis, Leiden, The Netherlands) for quantitative coronary angiography (QCA). Coronary arteries were divided into 17 segments according to a modified American Heart Association classification and QCA was performed in lesions exceeding 30% luminal narrowing on visual assessment.⁹ Each segment was evaluated for the presence of $\geq 50\%$ luminal narrowing on QCA. Obstructive CAD was defined as luminal narrowing of $\geq 50\%$. Accordingly, sensitivity, specificity, positive and negative predictive values (including 95% confidence intervals), and positive and negative likelihood ratios for the detection of stenoses $\geq 50\%$ luminal narrowing on QCA were calculated on segmental, vessel and patient levels.

Results

All 61 patients were clinically referred for invasive diagnostic coronary angiography because of chest pain suspect for CAD and an intermediate pre-test likelihood according to the Diamond and Forrester criteria. Characteristics of the study population are listed in Table 1. Briefly, the average age was 57 ± 9 years, and the population consisted of 61% male patients. The majority of patients presented with atypical angina (82%), non-anginal chest pain was observed in 13%, and typical angina in 5%.

Table 1. Patient characteristics

Men/Women	37/24
Age (years) (range)	57 ± 9 (35-75)
Heart rate (beats per minute) (range)	58 ± 8 (41-78)
Average calcium score (Agatston) (range)	198 ± 323 (0-1505)
B-blocking medication	37 (61%)
Diabetes mellitus	15 (25%)
Hypertension	38 (62%)
Hypercholesterolemia†	38 (62%)
Current smoker	20 (33%)
Body mass index ≥ 30 kg/m ²	14 (23%)
Non-anginal chest pain	8 (13%)
Atypical angina pectoris	50 (82%)
Typical angina pectoris	3 (5%)
Nr. of coronary arteries narrowed on invasive coronary angiography	
None	45 (74%)
1	8 (13%)
>1	8 (13%)

On invasive coronary angiography 920 coronary segments were identified of which 35 segments (3.8%) were uninterpretable on CTA, leaving 885 segments for further analysis. The image quality was good in 753 segments (85%), average image quality was observed in 100 segments (11%) and image quality was poor in the remaining 32 segments (4%). On invasive coronary angiography a significant stenosis was identified in 29 segments (3.3%). CTA correctly ruled out the presence of significant stenosis in 841 of 856 segments while a significant stenosis was correctly identified in 23 of 29 segments. CTA overestimated disease severity in 15 segments without significant disease on invasive coronary angiography, while 6 segments were incorrectly scored as non-significant on CTA. Accordingly the sensitivity and specificity were respectively 79% and 98% on a segment level. The positive predictive value was 61% and the negative predictive value 98%. The positive likelihood ratio was 39.5 compared to a negative likelihood ratio of 0.21.

In total 183 vessels were identified. Significant stenosis was observed in 26 vessels on invasive coronary angiography. CTA correctly identified a significant stenosis in 22 of 26 vessels. Significant stenosis was ruled out in 148 of 157 vessels. CTA overestimated disease severity in 9 vessels without significant stenosis on invasive coronary angiography, while disease severity was underestimated in 4 vessels. The sensitivity, specificity, positive predictive value, and negative predictive value on a vessel level were respectively 85%, 94%, 71% and 93%. Positive and negative likelihood ratios were 14.2 and 0.16 respectively.

In the 61 included patients significant CAD was observed in 16 patients (26%) on invasive coronary angiography. CTA correctly identified significant CAD in all 16 patients with significant disease on invasive coronary angiography. On the other hand, CTA correctly ruled out significant disease in 40 of 45 patients without significant stenosis on invasive coronary angiography, representing 66% of the total population. Disease severity was overestimated in 5 patients without a significant stenosis on invasive coronary angiography. Importantly CTA did not underestimate disease severity. This resulted in a sensitivity and specificity of respectively 100% and 89%. The positive predictive value was 76% and the negative predictive value of 100%. The positive likelihood ratio was 9.1 compared to a negative likelihood ratio of 0.00. The results of all analyses, including positive and negative predictive values with 95% confidence intervals, are listed in Table 2.

Discussion

The main finding of this study is that CTA has an excellent diagnostic accuracy in patients without known CAD and with an intermediate pre-test likelihood for CAD. Importantly, the observed negative predictive value was consistently high on a patient, vessel and segment level. As a result, CTA allowed accurate rule out of significant CAD in 66% of the total population. These findings indicate that CTA may be used as a highly accurate and effective gatekeeper for invasive coronary angiography in this target population for non-invasive imaging.

The diagnostic accuracy of CTA has been studied extensively. In early single center studies an average weighted sensitivity of 97.5 (95%-confidence interval 96-99) and specificity of 91 (95%-confidence interval 87.5-95) have been observed.⁵ More recently several prospective multi-center studies have been published showing similar sensitivities and specificities.^{1, 3, 4} Importantly however, almost all data on the diagnostic accuracy of CTA have been obtained in patients with a high pre-test probability for CAD. Nonetheless, the role of CTA may be limited in this population as the majority of patients will require invasive coronary angiography anyway. In contrast, only very limited data are available in patients with an intermediate

Table 2. Diagnostic accuracy of multi-slice computed tomography coronary angiography

Variable	Segmental Analysis	Vessel Analysis	Patient Analysis
Excluded	35/920 (3.8%)	0%	0%
Sensitivity	23/29 (79%, 64-94%)	22/26 (85%, 71-99%)	16/16 (100%, 100-100%)
Specificity	841/856 (98%, 97-99%)	148/157 (94%, 90-98%)	40/45 (89%, 80-98%)
Positive predictive value	23/38 (61%, 46-77%)	22/31 (71%, 55-87%)	16/21 (76%, 58-94%)
Negative predictive value	841/847 (99%, 99-100%)	148/152 (97%, 94-100%)	40/40 (100%, 100-100%)
Diagnostic accuracy	864/885 (98%, 97%-99%)	170/183 (93%, 89-97%)	56/61 (92%, 85-99%)
Positive likelihood ratio	39.5	14.2	9.1
Negative likelihood ratio	0.21	0.16	0.00

pre-test likelihood although it is precisely this population that may benefit the most from CTA. However, since according to Bayes theorem pre-test probability directly affects the diagnostic performance of a test, it is important to realize that diagnostic modalities should be validated across the full range of pre-test probabilities. The relationship between pre-test probability and the diagnostic benefit of CTA was recently studied by Meijboom et al. among patients with a high, intermediate, or low pre-test likelihood. In patients with a high pre-test likelihood for CAD, observations on CTA failed to substantially change the post-test probability for significant CAD. Thus, a normal CTA examination did not result in sufficient reduction of post-test probability to reliably rule out the presence of significant CAD. These data further underline the limited clinical value of CTA in this patient group. In contrast, in patients with a low and intermediate pre-test likelihood, a negative CTA scan was able to reduce the post test probability of CAD to 0%.¹⁰ Particularly in patients with an intermediate pre-test probability CTA was most beneficial as the largest changes from pre-test probability to post-test probability were observed.

The findings of the current study confirm the usefulness of CTA in patients with intermediate pre-test likelihood. In all patients with a negative CTA study, invasive coronary angiography confirmed the absence of significant CAD resulting in a negative predictive value of 100%. These observations are in line with Meijboom et al. who also observed a negative predictive value of 100% in their subanalysis of patients with an intermediate pre-test likelihood.¹¹ Similarly, Leber et al. reported a high negative predictive value of 99% in their study using dual-source computed tomography in patients with an intermediate pre-test likelihood.¹² Thus, when CTA is applied in a patient population with intermediate pre-test likelihood, the need for further imaging will be restricted to only those patients with an abnormal CTA examination. In the current study, the presence of significant CAD could be ruled out in a large proportion of patients; a negative CTA study was obtained in 66% of the patient population. Similar percentages were reported by Meijboom et al. (52%) and Leber et al. (68%). Thus, when appropriately applied, use of CTA may avoid invasive coronary angiography in the majority of patients. Indeed, the high negative predictive value and the small proportion of patients needing further testing support CTA as a highly effective gatekeeper for invasive coronary angiography in patients with an intermediate pre-test likelihood of CAD. Interestingly, this concept has been further strengthened by preliminary cost-effectiveness data. Min et al. recently explored the value of CTA (n=1647) as a first line test as compared to myocardial perfusion imaging (n=6588) using single photon emission computed tomography (SPECT) in patients with mainly low to intermediate pre-test likelihood. Importantly, in this low risk population, lower referral rates to invasive coronary angiography and overall lower healthcare costs were observed in patients undergoing CTA as a first line test compared to SPECT, with similar event rates in both groups during follow-up.¹³

This prospective study was performed in a relatively small patient population. Larger studies are necessary to more accurately approximate the sensitivity and specificity of CTA in a broad population of patients with an intermediate pre-test likelihood. Importantly, these investigations should take into account variations in patient characteristics which in addition to pre-test probability may also have an effect on diagnostic accuracy. These data are mandatory to further determine the predictive value of CTA in various populations. Currently 64-slice CTA is still associated with a high radiation exposure, although the radiation dose of CTA has substantially decreased with the use of dedicated dose reduction techniques that have recently become available.¹⁴⁻¹⁷ Importantly, low-dose computed tomography with prospective ECG-triggering has recently been shown to reduce radiation burden while maintaining diagnostic image quality and a high diagnostic accuracy.^{18, 19}

Conclusion

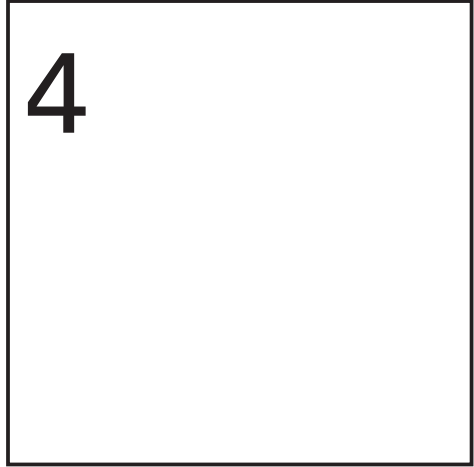
The current study confirms that CTA has an excellent diagnostic accuracy in the target population of patients with an intermediate pre-test likelihood. Notably, the high negative predictive value allowed rule out of significant stenosis in a large proportion of patients. CTA may therefore be used as a highly effective gatekeeper for invasive coronary angiography.

References

1. Miller JM, Rochitte CE, Dewey M, et al. Diagnostic Performance of Coronary Angiography by 64-Row CT. *N Engl J Med* 2008;359:2324-36.
2. Schuijff JD, Pundziute G, Jukema JW, et al. Diagnostic accuracy of 64-slice multislice computed tomography in the noninvasive evaluation of significant coronary artery disease. *Am J Cardiol* 2006;98:145-8.
3. Budoff MJ, Dowe D, Jollis JG, et al. Diagnostic performance of 64-multidetector row coronary computed tomographic angiography for evaluation of coronary artery stenosis in individuals without known coronary artery disease: results from the prospective multicenter ACCURACY (Assessment by Coronary Computed Tomographic Angiography of Individuals Undergoing Invasive Coronary Angiography) trial. *J Am Coll Cardiol* 2008;52:1724-32.
4. Meijboom WB, Meijs MFL, Schuijff JD, et al. Diagnostic Accuracy of 64-slice Computed Tomography Coronary Angiography: A Prospective Multicenter, Multivendor Study. *J Am Coll Cardiol* 2008;52:2135-44.
5. Abdulla J, Abildstrom SZ, Gotzsche O, et al. 64-multislice detector computed tomography coronary angiography as potential alternative to conventional coronary angiography: a systematic review and meta-analysis. *Eur Heart J* 2007;28:3042-50.
6. Mowatt G, Cook JA, Hillis GS, et al. 64-Slice computed tomography angiography in the diagnosis and assessment of coronary artery disease: systematic review and meta-analysis. *Heart* 2008;94:1386-93.
7. Pundziute G, Schuijff JD, Jukema JW, et al. Prognostic value of multislice computed tomography coronary angiography in patients with known or suspected coronary artery disease. *J Am Coll Cardiol* 2007;49:62-70.
8. Diamond GA, Forrester JS. Analysis of probability as an aid in the clinical diagnosis of coronary-artery disease. *N Engl J Med* 1979;300:1350-8.
9. Austen WG, Edwards JE, Frye RL, et al. A reporting system on patients evaluated for coronary artery disease. Report of the Ad Hoc Committee for Grading of Coronary Artery Disease, Council on Cardiovascular Surgery, American Heart Association. *Circulation* 1975;51:5-40.
10. Meijboom WB, Van Mieghem CA, Mollet NR, et al. 64-slice computed tomography coronary angiography in patients with high, intermediate, or low pretest probability of significant coronary artery disease. *J Am Coll Cardiol* 2007;50:1469-75.
11. Meijboom WB, Van Mieghem CA, Mollet NR, et al. 64-slice computed tomography coronary angiography in patients with high, intermediate, or low pretest probability of significant coronary artery disease. *J Am Coll Cardiol* 2007;50:1469-75.
12. Leber AW, Johnson T, Becker A, et al. Diagnostic accuracy of dual-source multi-slice CT-coronary angiography in patients with an intermediate pretest likelihood for coronary artery disease. *Eur Heart J* 2007;28:2354-60.
13. Min JK, Kang N, Shaw LJ, et al. Costs and clinical outcomes after coronary multidetector CT angiography in patients without known coronary artery disease: comparison to myocardial perfusion SPECT. *Radiology* 2008;249:62-70.
14. Hausleiter J, Meyer T, Hadamitzky M, et al. Radiation dose estimates from cardiac multislice computed tomography in daily practice: impact of different scanning protocols on effective dose estimates. *Circulation* 2006;113:1305-10.
15. Hsieh J, Londt J, Vass M, et al. Step-and-shoot data acquisition and reconstruction for cardiac x-ray computed tomography. *Med Phys* 2006;33:4236-48.
16. Husmann L, Valenta I, Gaemperli O, et al. Feasibility of low-dose coronary CT angiography: first experience with prospective ECG-gating. *Eur Heart J* 2008;29:191-7.
17. Rybicki FJ, Otero HJ, Steigner ML, et al. Initial evaluation of coronary images from 320-detector row computed tomography. *Int J Cardiovasc Imaging* 2008;24:535-46.

18. Herzog BA, Husmann L, Burkhard N, et al. Accuracy of low-dose computed tomography coronary angiography using prospective electrocardiogram-triggering: first clinical experience. *Eur Heart J* 2008;29:3037-42.
19. Scheffel H, Alkadhi H, Leschka S, et al. Low-dose CT coronary angiography in the step-and-shoot mode: diagnostic performance. *Heart* 2008;94:1132-1137.

Chapter 4



Invasive versus noninvasive evaluation of coronary artery disease

JD Schuijf, JM van Werkhoven, G Pundziute, JW Jukema, I Decramer,
MP Stokkel, P Dibbets-Schneider, MJ. Schalij, JHC Reiber,
EE van der Wall, W Wijns, JJ Bax

Abstract

Preliminary comparisons have suggested that abnormal myocardial perfusion studies correlate well with significant luminal stenosis on MDCT coronary angiography. However atherosclerotic coronary lesions may be detectable by MDCT even in the presence of normal myocardial perfusion. The objective of this study was to compare the diagnostic information obtained from noninvasive characterization of coronary artery disease by multi-detector computed tomography (MDCT) and myocardial perfusion imaging (MPI), and to compare findings with invasive coronary angiography and intravascular ultrasound (IVUS). MDCT, MPI and conventional coronary angiography were performed in 70 patients. In addition, IVUS was performed in 53 patients. Quantitative information was obtained by quantitative coronary angiography (QCA) and IVUS assessment of plaque burden and minimal luminal area. Of 26 patients with an abnormal MPI study, 23 (88%) showed significant stenosis on MDCT. As compared to QCA, MDCT showed a sensitivity of 96% and specificity of 67% for the detection of stenoses $\geq 50\%$ diameter narrowing in these patients. The mean diameter stenosis on QCA was 76% and the mean minimal lumen area in IVUS was 3.3 mm². On the other hand, 27 (84%) of 44 patients with normal MPI had evidence of coronary atherosclerosis on MDCT (luminal stenosis $\geq 50\%$: n = 15, luminal stenosis $< 50\%$: n = 12, sensitivity of 100% and specificity of 83% as compared to QCA). IVUS showed substantial plaque burden (mean: 58.9% \pm 18.1% of cross-sectional area), but presence of a stenosis (minimal lumen area < 4.0 mm²) in only 14 patients (mean minimal lumen area, 5.8 \pm 3.3 mm²). Only 7 patients with normal myocardial perfusion scans demonstrated absence of coronary atherosclerosis by MDCT. In conclusion, a considerable plaque burden can be observed on MDCT even in the absence of myocardial perfusion abnormalities. This does not constitute a false-positive MDCT result, but rather reflects the fact that MDCT can detect atherosclerotic lesions that are not flow-limiting. Clinically, it is important to make a clear distinction between the presence of plaque and the presence of stenosis in MDCT.

Introduction

Traditionally, the evaluation and management of patients with suspected coronary artery disease (CAD) has been based on the noninvasive detection of ischemia followed by invasive coronary angiography to confirm the presence of luminal stenosis. There is generally a very good correlation between the stress myocardial perfusion or echo studies and quantitative angiography. However, it is well established that acute coronary events, usually result from voluminous atherosclerotic lesions but may not be associated with significant luminal obstruction. Intravascular ultrasound (IVUS) studies have demonstrated that even significant atherosclerosis burden may not always result in luminal obstruction, and may be frequently associated with normal myocardial perfusion.^{1, 2} The recent introduction of 64-slice multi-detector computed tomography (MDCT) has allowed the opportunity to noninvasively characterize the atherosclerotic lesions and define luminal and vessel wall alterations alike. The technique has been demonstrated to have a high diagnostic accuracy as compared to invasive coronary angiography.³ It is conceivable that the majority of patients with abnormal MPI will also show high-grade stenoses on MDCT. In addition, MDCT should allow recognition of plaque burden in patients with normal perfusion.^{4, 5} These patients with normal perfusion may only show minimal changes on invasive coronary angiography despite definitive atherosclerotic disease. Accordingly, the purpose of the present study was to compare the diagnostic information obtained from noninvasive characterization of CAD by MDCT and MPI, and to compare findings with invasive coronary angiography and IVUS.

Methods

Patients and study protocol

The study group consisted of symptomatic patients who presented to the outpatient clinic (Leiden, the Netherlands and Aalst, Belgium) for the evaluation of chest pain. Noninvasive imaging with gated SPECT and MDCT was performed, and based on clinical presentation and/or imaging results, 70 of these patients were referred for invasive coronary angiography in combination with IVUS and enrolled in the present study. Exclusion criteria were contraindications to MDCT,⁶ and the presence of unstable angina, heart failure, myocardial infarction or revascularization between the imaging procedures. Data of 15 patients have been previously reported in a study comparing MDCT and MPI.⁵ The study protocol was approved by the institutional ethics committee and informed consent was obtained in all patients.

Clinical characteristics of the study population are presented in Table 1. Of the 70 patients (mean age, 62 ± 11 years) included in the study, 46 (66%) were male. Diagnosis of CAD was established in 5 (7%) and suspected in the remaining 65 (93%) patients. Of the patients

Table 1. Clinical characteristics of the study population (n=70).

Gender (M/F)	46/24
Age (years)	62 ± 11
Risk factors for CAD	
Diabetes Mellitus	21 (30%)
Hypertension	46 (66%)
Hypercholesterolemia	35 (50%)
Positive family history	27 (39%)
Current smoking	25 (36%)
Obese (BMI ≥ 30 kg/m ²)	14 (20%)
Average BMI (30 kg/m ²)	27.0 ± 4.0
Previous CAD	
Previous myocardial infarction	5 (7%)
Anterior/inferior	4/1
Previous PCI	4 (6%)
Agatston calcium score	435 ± 789
Heart rate (bpm) during MDCT	63 ± 9
LVEF on gated SPECT	58 ± 14%
Nr of significantly stenosed vessels on QCA	
0	32 (46%)
1	17 (24%)
2	13 (19%)
3	8 (11%)

with known CAD, 4 had previous percutaneous coronary intervention (with stent placement in 2 patients) whereas 1 patient had previous coronary artery bypass grafting (CABG). In the latter patients, 2 bypassed (grafted) coronary vascular territories were excluded from analysis. In all patients MPI, MDCT and conventional coronary angiography (with QCA) were performed. In 53 patients, additional vascular imaging with IVUS was performed in a total of 109 coronary arteries. In the remaining 17 patients, IVUS imaging was not possible due to the presence of left main stenoses, severe coronary stenosis or total occlusion (n=10), and technical problems or time constraints during conventional coronary angiography (n=7).

Multi-detector computed tomography coronary angiography

MDCT coronary angiography was performed using either an Aquilion 64 (Toshiba Medical Systems, Japan) or a Sensation 64 (Siemens, Germany).

First, a prospective coronary calcium scan was performed prior to MDCT angiography with a collimation 4 × 3.0 mm, gantry rotation time 500 ms, the tube voltage 120 kV and tube current 200 mA. The temporal window was set at 75% after the R-wave for electrocardiographically triggered prospective reconstruction. For the contrast enhanced scan, collimation was either 64 × 0.5 mm or 64 × 0.6 mm, respectively. The tube current was 300 mA, at 120 kV. Non-ionic contrast material was administered in the antecubital vein with an amount of 80 to 110 ml for 64-slice

MDCT, depending on the total scan time, and a flow rate of 5 ml/sec (Iomeron 400®), followed by a saline flush. Subsequently, data sets were reconstructed and transferred to a remote workstation as previously described.⁶ Coronary calcium score was derived using dedicated software. Coronary calcium was identified as a dense area in the coronary artery exceeding the threshold of 130 HU. The global Agatston score as well as per coronary artery was recorded for each patient.

MDCT angiographic examinations were evaluated in consensus by 2 experienced readers including an interventional cardiologist blinded to the SPECT data for the presence of atherosclerosis. Coronary arteries were divided into 17 segments according to the modified American Heart Association classification.⁷ Each segment was evaluated for the presence of any atherosclerotic plaque using axial images and curved multiplanar reconstructions. Coronary plaques were defined as structures >1 mm² within and/or adjacent to the coronary artery lumen, which could be clearly distinguished from the vessel lumen and the surrounding pericardial tissue, as previously described.⁸ To describe the degree of stenosis, abnormal segments were further classified as showing 1. non-obstructive disease (<50% luminal narrowing), 2. borderline stenosis (50% to 70% luminal narrowing) or severe stenosis, showing ≥70% luminal narrowing. To describe the extent of disease on MDCT, for each patient and vessel, the number of segments showing disease as well as significant (≥50% luminal narrowing) was determined. Data were recorded on a patient and vessel basis and in the vessel-based analysis, the left main coronary artery was considered part of the left anterior descending coronary artery.

Myocardial perfusion imaging

In all patients, stress MPI (using either technetium-99m tetrofosmin or technetium-99m sestamibi) was performed with symptom-limited bicycle exercise or pharmacological (dipyridamole, adenosine or dobutamine) stress.⁹ Data were acquired with either a dual-head SPECT camera (Vertex Epic ADAC Pegasus) or a triple-head SPECT camera (GCA 9300/HG, Toshiba Corp., Tokyo, Japan) followed by reconstruction into long- and short-axis projections perpendicular to the heart-axis; data were presented in polar map format (normalized to 100%), and a 17-segment model was used in which myocardial segments were allocated to the territories of the different coronary arteries as previously described.^{10, 11} Perfusion defects were identified on the stress images (segmental tracer activity less than 75% of maximum) and divided into ischemia (reversible defects, with ≥10% increase in tracer uptake on the resting images) or scar tissue (irreversible defects).⁵ Accordingly, examinations were classified as being either normal or abnormal, the latter being further divided in those demonstrating reversible defects and those demonstrating irreversible defects. The gated images were used to assess regional wall motion to improve differentiation between perfusion abnormalities and attenuation artifacts.¹² The left ventricular ejection fraction was derived from the gated SPECT data using previously validated and automated software (quantitative gated SPECT [QGS]; Cedars-Sinai Medical Center, Los Angeles, CA); gating was only performed at rest.

Conventional coronary angiography

Conventional coronary angiography was performed according to standard clinical protocols. Quantitative coronary angiography (QCA) was performed using QCA-CMS 6.0 (Medis, Leiden, the Netherlands). For each coronary artery, the most severe stenosis was identified. The tip of the catheter was used for calibration and after automated vessel contour detection with manual correction if needed, percentage diameter stenosis was calculated.

Intravascular ultrasound

IVUS imaging was performed with 2.9Fr 20-MHz catheters (Eagle Eye, Volcano, Brussels, Belgium). After intracoronary administration of nitrates, the IVUS catheter was advanced to the distal portion of coronary artery under fluoroscopic guidance. Using automated pullback device, the transducer was withdrawn at a continuous speed of 0.5 mm/s up to the coronary ostium. Cine runs before and during contrast injection were performed to confirm the position of the IVUS transducer before IVUS evaluation was started. All data were stored digitally and were analysed off-line with the use of QCU-CMS 4.0 (Medis, Leiden, The Netherlands). After motion correction had been applied, coronary arteries were divided into segments according to the modified American Heart Association classification (7 using coronary ostia and side branches as landmarks. In each coronary segment, the frame with the most severe cross-sectional area of narrowing was selected for analysis. In addition, proximal and distal reference sites that had the largest lumen area by IVUS in the proximal and distal portion of the vessel segment in the 10 mm adjacent (but before any side-branch) to the lesion site were selected. Subsequently, lumen and external elastic membrane (EEM) contours were manually traced to determine lumen area and EEM area at the lesion site and proximal and distal reference site. EEM area was defined as the area that was circumscribed by the border between the hypochoic media zone and the surrounding echocardiographically bright adventitia. Plaque plus media area was calculated as the difference between the EEM and the lumen area. Based on these parameters, minimal lumen area (MLA), lesion plaque area, lesion plaque burden, lumen area stenosis, lumen diameter stenosis and corrected lumen area stenosis were calculated per coronary segment as previously described.^{1, 2} Briefly, lesion plaque burden was defined as plaque plus media area divided by the EEM area, resulting in the lesion percentage area stenosis due to plaque. Lumen area stenosis was calculated by subtracting the lumen area at the lesion site from the lumen area at the reference site and subsequently dividing by the lumen area at the reference site. In addition, vascular remodelling was determined. The number of lesions with positive remodelling was determined by calculating the remodelling index (RI) by dividing the lesion EEM area by the average of the proximal and distal reference EEM area. Subsequently, positive remodelling was defined as a $RI \geq 1.0$, whereas $RI < 1.0$ was classified as negative remodeling.¹³

Statistical analysis

Data were analysed on a per-patient and per-vessel basis and for the corresponding calculations, the coronary artery and coronary segment showing the most severe stenosis on either QCA or IVUS were used respectively. Continuous variables were described by mean \pm SD. Comparisons between patient groups were performed using the independent samples T test for continuous variables and the χ^2 test with Yates' correction was used for comparison of categorical variables. A P-value <0.05 was considered statistically significant. All statistical analyses were performed using SPSS (SPSS Institute, Chicago, Illinois, USA).

Results

Comparison of MDCT with MPI and invasive angiography

The results of the analysis on a patient basis ($n=70$) are presented in Table 2 and Figure 1. Abnormal perfusion on SPECT was noted in 26 (37%) patients. The abnormal perfusion was associated with an average coronary calcium score of 751 ± 1143 . Calcium scores ≥ 400 were observed in 11 (42%) patients. MDCT coronary angiography demonstrated atherosclerosis in all 26 patients; severe stenosis was observed in 14 patients, 9 patients revealed borderline stenosis, and the remaining 3 patients presented with non-obstructive disease. The average number of diseased segments was 6.4 ± 3.1 , whereas the average number of significantly stenosed segments was 2.5 ± 2.5 per patient. Considering the most severe stenosis per patient on conventional angiography, QCA showed an average percentage stenosis of $75.9\% \pm 19.2\%$ with 23 patients showing significant stenosis ($\geq 50\%$ luminal narrowing). When validating MDCT results against QCA, the sensitivity of MDCT to detect coronary artery stenoses $\geq 50\%$ luminal narrowing was 96% (22/23) and specificity was 67% (2/3). The remaining 44 (63%) of 70 patients demonstrated a normal myocardial perfusion on SPECT imaging. In these patients,

Table 2. Angiographic characteristics (MDCT and QCA) for patients with respectively abnormal and normal perfusion (patient based analysis).

	MPI abnormal (n=26 patients)	MPI normal (n=44 patients)	P -value
Calcium Score	751 ± 1143	255 ± 415	0.051
MDCT			
Normal	0	7 (16%)	
Abnormal	26 (100%)	37 (84%)	0.083
Non-obstructive stenosis	3 (12%)	22 (59%)	
Borderline stenosis	9 (35%)	12 (32%)	
Severe stenosis	14 (54%)	3 (8%)	<0.001
Diseased segments	6.4 ± 3.1	5.0 ± 3.0	0.080
Segments with $>50\%$ stenosis	2.5 ± 2.5	0.61 ± 1.2	0.001
QCA	$75.9 \pm 19.2\%$	$26.7 \pm 17.7\%$	<0.001

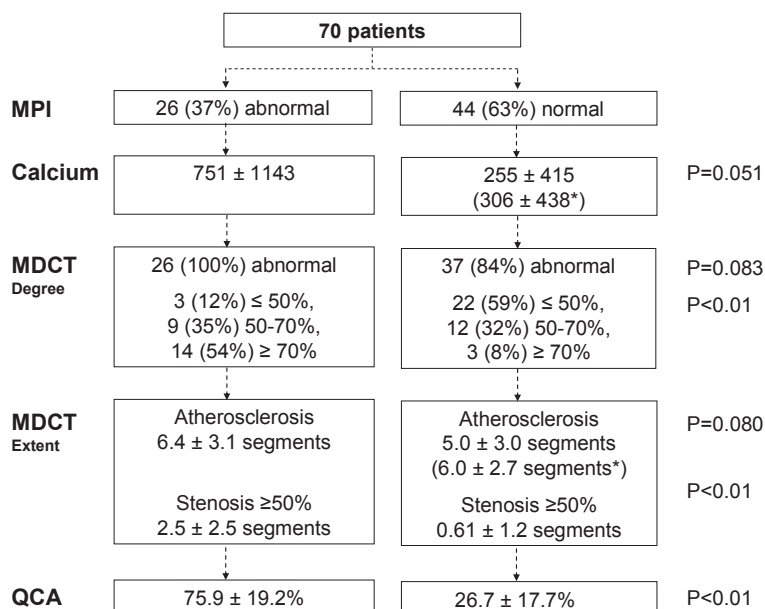


Figure 1. Flow chart describing the MDCT and QCA findings in 70 patients with respectively abnormal and normal MPI results. Note the discrepancy between the imaging modalities in patients with normal MPI. In the majority of these patients MDCT was abnormal, with no significant difference in the number of segments with atherosclerosis either (as compared to patients with abnormal perfusion). However, number of significantly stenosed segments was significantly lower in patients with normal MPI, as also reflected by minimal luminal narrowing on QCA.

* Average in patients with atherosclerosis on MDCT.

average coronary calcium score was 255 ± 415 ($P=0.051$ as compared to patients with abnormal perfusion). In total, a calcium score ≥ 400 was observed in 8 (18%). MDCT was abnormal in 37 (84%) patients with 22 patients showing non-obstructive disease, 12 borderline stenosis and 3 patients showing severe stenosis. The average number of diseased segments (5.0 ± 3.0) was statistically insignificantly lower than the patients with abnormal perfusion scans (6.4 ± 3.1 , $P=0.08$). After excluding patients with completely normal coronary arteries, average number of diseased segments was 6.0 ± 2.7 ($P=0.10$). However, average number of segments with significant stenosis was significantly lower (0.61 ± 1.2 , $P<0.01$) as compared to patients with abnormal perfusion. Average percentage lumen stenosis of the most severe lesion on QCA was also considerably lower ($26.7\% \pm 17.7\%$, $P<0.01$) compared to patients with abnormal SPECT. All 9 patients with significant stenosis on QCA were detected by MDCT (sensitivity 100%), while MDCT correctly demonstrated absence of stenosis in 29/35 patients (specificity 83%).

Upon analysis by vascular territories instead of patient basis, abnormal myocardial perfusion was noted in 36 (17%) of 208 vascular territories with ischemia in 33 and fixed perfusion defects in 3 vascular territories (Table 3). In the remaining 172 (83%) vascular territories myocardial perfusion was normal.

Table 3. Angiographic characteristics (MDCT and QCA) of coronary arteries with respectively abnormal and normal perfusion in the corresponding vascular territory (vessel based analysis).

	MPI abnormal (n=36 vessels)	MPI normal (n=172 vessels)	P -value
Calcium score	281 ± 590	116 ± 232	0.13
MDCT			
Normal	0	45 (26%)	
Abnormal	36 (100%)	127 (74%)	<0.01
Non-obstructive stenosis	10 (28%)	93 (54%)	
Borderline stenosis	10 (28%)	27 (16%)	
Severe stenosis	16 (44%)	7 (4%)	<0.01
Diseased segments	2.6 ± 1.3	1.7 ± 1.3	<0.01
Segments with >50% stenosis	1.1 ± 1.2	0.29 ± 0.67	<0.01
QCA	71.0% ± 22.1%	22.7% ± 19.1%	<0.01

Comparison of MDCT with MPI, invasive angiography and IVUS

MPI was abnormal in 17 of 53 (32%) of patients in whom IVUS imaging was available. IVUS imaging of the coronary artery corresponding to the territory with abnormal perfusion could not be performed in 4 patients. These patients were therefore excluded from the patient based analysis, but the available data were included in the vessel based analysis. Accordingly, on a patient basis, MPI was abnormal in 13 of 49 (27%) patients. Average coronary calcium score in these patients was 355 ± 355 with 3 (18%) patients showing calcium scores ≥ 400 . In all patients, MDCT was abnormal with severe stenosis in 4 (31%), borderline stenosis in 7 (54%) and non-obstructive lesions in 2 (31%) patients. The average number of MDCT-verified diseased segments was 5.5 ± 3.0 , whereas the average number of significantly stenosed segments was 1.5 ± 1.2 . Average percent luminal narrowing as determined by QCA was relatively low in these patients ($68.5\% \pm 18.5\%$), possibly due to the exclusion of patients with severe stenosis in whom IVUS imaging could not be performed. Nonetheless, mean MLA was 3.3 ± 1.2 mm² with an average lesion plaque area and plaque burden of respectively 10.7 ± 4.9 mm² and $74.3\% \pm 8.8\%$, confirming the presence of potentially flow-limiting stenoses. Moreover, 9 (69%) lesions were associated with constrictive remodelling.

Normal perfusion was observed in the remaining 36 (73%) patients. Average coronary calcium score was 247 ± 395 ($P=0.41$ as compared to patients with abnormal perfusion). In these patients, calcium scores exceeded 400 in 7 (19%) patients. MDCT revealed atherosclerosis in 32 (89%), of which 18 patients showed non-obstructive disease, 11 patients had borderline stenosis and 3 severe stenosis. Mean number of diseased segments was similar to that of patients with abnormal perfusion, 5.4 ± 3.1 ($P=0.92$) compared to patients with abnormal perfusion, but the mean number of significantly stenosed segments was

significantly lower, 0.58 ± 0.91 ($P=0.028$). Considering only the most severe percent luminal stenosis per patient, mean luminal narrowing of only $26.2\% \pm 15.6\%$ was observed on QCA, indicating minimal angiographic stenosis. In line with these observations, preservation of the lumen was confirmed by IVUS with an average MLA of 5.8 ± 3.3 mm², significantly higher as compared to patients with abnormal MPI ($P<0.01$). Nonetheless, considerable atherosclerosis was identified on IVUS with an average lesion plaque area of 8.7 ± 4.3 mm², not significantly different compared to patients with perfusion abnormalities ($P=0.17$). Also substantial plaque burden was observed, with an average of $58.9\% \pm 18.1\%$ ($P<0.01$) of the lesion cross-sectional area as compared to abnormal MPI. A positive remodeling was identified in 16 (44%) of patients with normal MPI, as compared to 31% in patients with abnormal MPI ($P=0.39$) (Table 4). The results are summarized in Figure 2, whereas in Figure 3, an example of a patient with MDCT and IVUS-verified significant atherosclerotic burden is presented who had normal myocardial perfusion.

Table 4. IVUS characteristics of the most severe lesion in patients with respectively abnormal and normal perfusion on MPI (patient based analysis).

	MPI abnormal (n=13 patients)	MPI normal (n=36 patients)	P-value
Reference section			
EEM area (mm ²)	14.2 ± 5.8	14.6 ± 4.5	0.68
Lumen area (mm ²)	8.5 ± 3.4	9.6 ± 3.7	0.28
Lesion section			
EEM area (mm ²)	14.0 ± 5.6	14.5 ± 4.8	0.76
MLA (mm ²)	3.3 ± 1.2	5.8 ± 3.3	<0.01
Lesion plaque area (mm ²)	10.7 ± 4.9	8.7 ± 4.3	0.17
Lesion plaque burden (%)	74.3 ± 8.8	58.9 ± 18.1	<0.01
Lumen area stenosis (%)	66.9 ± 13.8	41.7 ± 23.1	<0.01
Lumen diameter stenosis (%)	44.1 ± 14.1	25.3 ± 15.8	<0.01
Corrected lumen area stenosis (%)	77.2 ± 9.1	61.5 ± 20.1	<0.01
Reference section			
Positive remodeling (n, %)	4 (31%)	16 (44%)	0.39

Upon analysis by vessel basis, 15 (14%) of 109 coronary arteries were associated with abnormal perfusion in the corresponding vascular territory during MPI. The average coronary calcium score was 120 ± 115 per vessel. In all coronary arteries with abnormal perfusion, atherosclerosis was identified on MDCT, with non-obstructive stenosis in 5 (33%), borderline stenosis in 6 (40%) and severe stenosis in 4 (27%). With regard to the extent of disease on MDCT, a mean of 2.5 ± 1.2 diseased segments per vessel was observed, while mean of significantly diseased segments was 1.0 ± 1.0 . Mean extent of stenosis on QCA was $63.4 \pm 23.5\%$. In the remaining 94 (86%) coronary arteries without perfusion abnormalities, average coronary calcium score was 94 ± 178 ($P=0.62$) as compared to coronary arteries

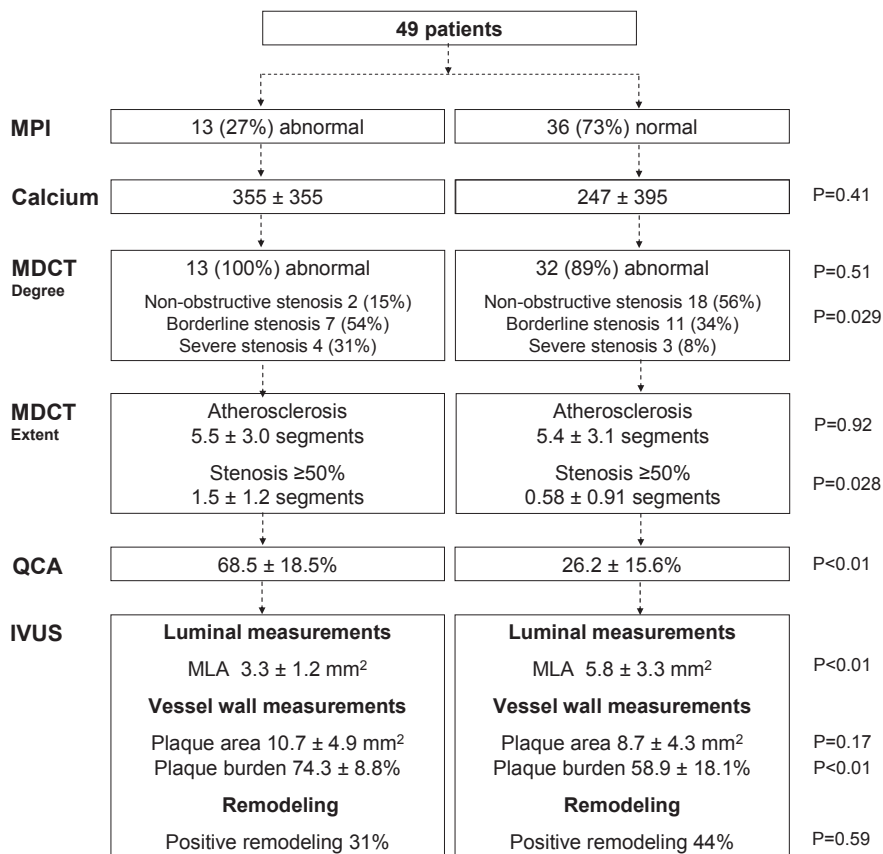


Figure 2. Flowchart describing the observations in 49 patients in whom additional IVUS imaging was performed. In almost all patients with normal MPI, the presence of atherosclerosis was observed on MDCT with negligible luminal narrowing identified on QCA. IVUS imaging confirmed the presence of substantial atherosclerosis (mean lesion plaque burden 58.9%), yet without luminal compromise (mean MLA 5.8 mm²).

with abnormal perfusion. On MDCT, atherosclerosis was absent in 19 (20%), while the average degree of luminal stenosis on QCA was 21.4% ± 13.8%. Further details of the IVUS measurements on a vessel basis are provided in Table 5. Finally, as shown in Figure 4, significant differences in IVUS measurements were observed when comparing patients with and without atherosclerosis on MDCT.

Discussion

The present study, upon comparison of MDCT to MPI showed that abnormal perfusion was always associated with an abnormal MDCT, with a majority of patients showing significant luminal stenosis. In these patients, significant CAD was also observed on invasive imaging verified by an mean

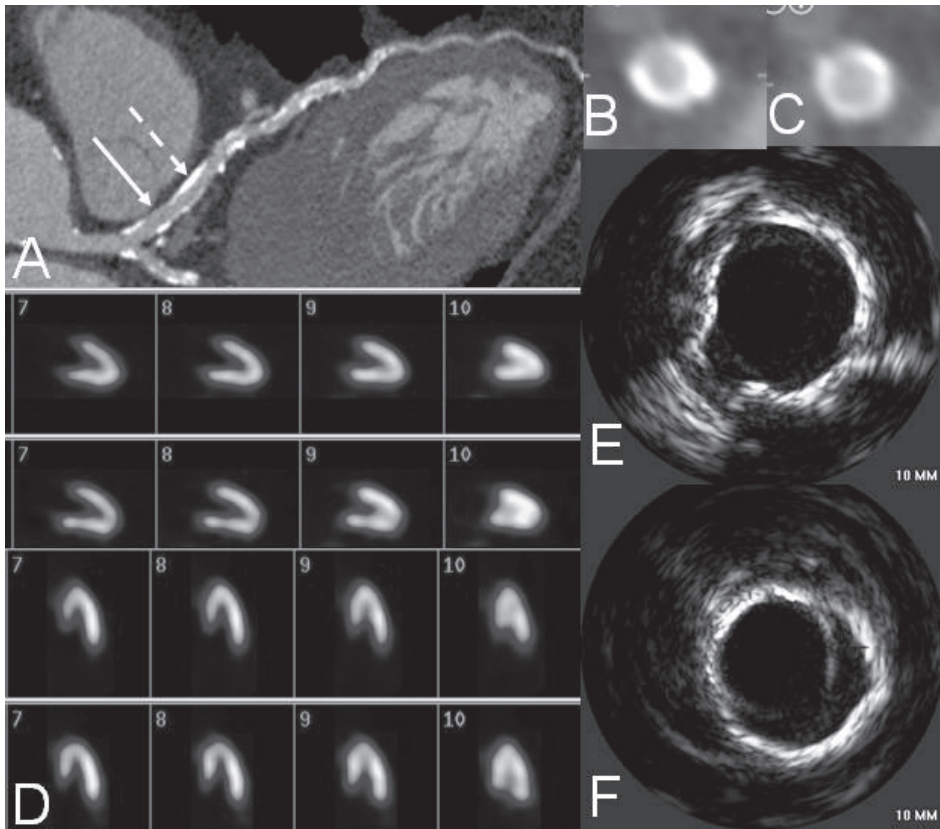
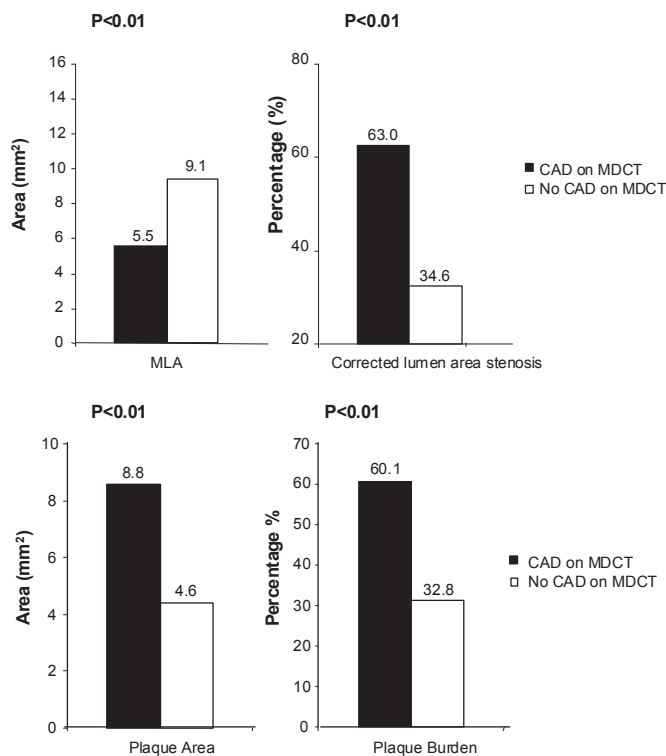


Figure 3. A 60-year old male presented to the outpatient clinic with dyspnea and an elevated risk profile for coronary artery disease, including hypertension, hypercholesterolemia and smoking. Contrast enhanced MDCT coronary angiography revealed considerable atherosclerosis in the left anterior descending coronary artery (Panel A). Panels B and C are cross-sectional images of the areas indicated by the arrows in Panel A. In contrast, myocardial perfusion imaging (Panel D), which was performed during exercise stress (first and third panel) and rest (second and fourth panel), showed normal perfusion. However, also during intravascular ultrasound imaging (Panels E and F), considerable plaque burden was demonstrated, yet with preservation the coronary lumen.

percent diameter stenosis of $75.9 \pm 19.2\%$ on conventional invasive angiography as well as a mean MLA $<4.0 \text{ mm}^2$ by IVUS. Thus, in case of advanced CAD, the different imaging modalities appear to be in agreement with abnormal results obtained with all invasive and noninvasive techniques. However, in symptomatic patients who showed normal myocardial perfusion, MDCT revealed significant atherosclerotic burden; in these patients the invasive coronary angiography and QCA demonstrated only minor lesions with a mean diameter stenosis $26.7 \pm 17.7\%$. IVUS clarified the discrepancy by revealing considerable lesion plaque burden ($58.9 \pm 18.1\%$ of cross-sectional area) which often spared the lumen (mean MLA, $5.8 \pm 3.3 \text{ mm}^2$) due to positive remodelling. These findings are intuitively expected, and pathologically well established, and are reconfirmed in the present study by employing multi-modality invasive and noninvasive imaging strategies.

Table 5. IVUS characteristics in coronary arteries with respectively abnormal and normal perfusion in the corresponding vascular territory (vessel based analysis).

	MPI abnormal (n=15 vessels)	MPI normal (n=94 vessels)	P-value
Reference section			
EEM area (mm ²)	15.6 ± 6.1	15.1 ± 5.4	0.57
Lumen area (mm ²)	9.3 ± 4.1	9.8 ± 3.5	0.45
Lesion section			
EEM area (mm ²)	14.4 ± 5.3	14.0 ± 5.2	0.85
MLA (mm ²)	3.6 ± 1.5	6.5 ± 3.6	<0.01
Lesion plaque area (mm ²)	10.8 ± 4.6	7.6 ± 4.0	<0.01
Lesion plaque burden (%)	73.5 ± 9.0	52.4 ± 17.5	<0.01
Lumen area stenosis (%)	63.9 ± 18.0	33.2 ± 20.8	<0.01
Lumen diameter stenosis (%)	41.9 ± 15.8	19.4 ± 13.6	<0.01
Corrected lumen area stenosis (%)	76.2 ± 10.0	55.1 ± 18.7	<0.01
Remodeling			
Positive remodeling	5 (33%)	49 (52%)	0.17

**Figure 4.** Differences in IVUS measurements between coronary arteries with CAD and without CAD as determined on MDCT. Panel A: MLA (mm²) and corrected lumen area stenosis (%). Panel B: plaque area (mm²) and plaque burden (%). All measurements were significantly different between coronary arteries with and without CAD identified on MDCT.

Hemodynamically relevant stenoses

The flow-limiting lesions as determined by MPI were also associated with significant focal luminal narrowing on MDCT as well as invasive imaging. In total, 14 patients showed severe stenosis on MDCT, confirmed by a stenosis $\geq 70\%$ luminal narrowing on QCA in all patients. In all patients with abnormal MPI, a mean percent diameter stenosis of $75.9 \pm 19.2\%$ was observed whereas IVUS showed mean MLA of 3.3 ± 1.3 mm². This observation is in consonance with an earlier report that compared IVUS measurements in 70 coronary lesions to gated SPECT and observed a 3.3 mm²-MLA of coronary lesions corresponding to a positive SPECT study.¹ Similar findings have been obtained in other studies employing fractional flow reserve (^{13, 14} indicating an agreement among various imaging modalities in the presence of hemodynamically relevant CAD.

Atherosclerosis in the presence of normal perfusion

In 63% of our patients, a normal MPI study was obtained. In these patients, only mild luminal narrowing (mean diameter stenosis $26.7\% \pm 17.7\%$) was observed during conventional invasive coronary angiography; 23% of patients had normal coronary angiograms (QCA < 20% luminal narrowing). However, MDCT revealed normal coronary arteries only in 7 (16%) patients. In addition, the extent of disease, as reflected by a mean number of abnormal segments per patient, was not significantly different from patients with abnormal MPI. The presence of extensive atherosclerotic disease in such cases with normal MPI was confirmed by IVUS, which showed considerable plaque burden (average 58.9 ± 18.1 of cross-sectional area). These lesions were positively remodelled and did not inflict significant luminal stenosis (mean MLA of 5.8 ± 3.3 mm²). The presence of extensive atherosclerotic disease in the setting of normal myocardial perfusion has been described previously. In a large cohort of 1195 patients without historical CAD extensive atherosclerosis, as reflected by a calcium score > 400, was observed in 31% of patients with normal MPI studies.¹⁵ The presence of substantial disease has also been previously described in angiographically normal segments; Mintz et al showed in a large series of consecutive patients that atherosclerosis was commonly present in angiographic reference segments and less than 7% of segments were classified as entirely normal by IVUS imaging.¹⁶

Accordingly, various imaging modalities provide distinct morphological and functional information about coronary atherosclerotic disease. Conventional coronary angiography and MPI detect anatomically significant and hemodynamically relevant stenoses, respectively. In contrast, the techniques remain limited in depicting the disease in its earlier stages, or even when the disease is mature but does not compromise luminal integrity due to expansive vascular remodelling.

Clinical implications

The current study reconfirms the expectation that the patients with perfusion defects on MPI indicating hemodynamically obstructive stenoses and representing advanced CAD, revealed

significant stenoses on MDCT as well as invasive angiography with QCA and IVUS. On the other hand, patients with (pre-clinical) atherosclerosis may present with normal perfusion on MPI, with (nearly) normal invasive angiography/QCA, but many of these patients may demonstrate extensive atherosclerosis in absence of obstructive stenoses on MDCT, verified subsequently by the IVUS observations. Thus, the presence of atherosclerotic plaque in MDCT in the setting of a normal MPI does not constitute a false-positive result. Much rather, it reflects the fact that MDCT can detect atherosclerotic lesions that are not flow limiting - as confirmed by IVUS in our study. Clinically, it is important to make a clear distinction between the presence of plaque and the presence of stenosis in MDCT. Since the large positively remodelled lesions are harbingers of plaque rupture it remains to be determined whether such advanced characterization of atherosclerotic lesions will result in superior prognostification of patients.

Study limitations

In the present study, MDCT examinations were visually assessed, as no validated quantification algorithms are currently available. Moreover, it is important to realize that interpretation of MDCT results is seriously limited in presence of calcific lesions. Also, IVUS imaging was not performed in all vessels in every patient. Furthermore, the current observations should be confirmed in less selected populations that would decrease the influence of selection bias. Finally, as the patients underwent multiple examinations, the radiation burden in the current study was high. The radiation dose of MDCT in particular is high, although the recent development of dose reduction strategies such as tube modulation or snapshot pulse scanning mode will result in considerably lower radiation exposures.

Conclusion

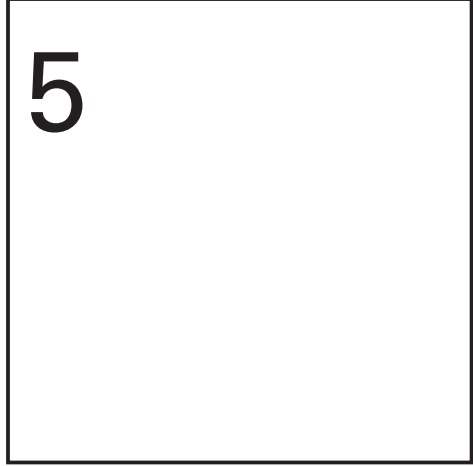
The current findings demonstrate a good agreement between noninvasive imaging techniques (MPI, MDCT) and invasive techniques (angiography, QCA and IVUS) in patients with flow-limiting CAD. These patients exhibited abnormal perfusion on MPI, predominantly obstructive atherosclerosis on MDCT, and obstructive stenoses on invasive quantitative angiography and IVUS. In another subset of symptomatic patient population with normal myocardial perfusion, MDCT uncovered considerable atherosclerosis in a large proportion of patients. Although invasive angiography did not confirm severe coronary lesions, the presence of MDCT-based atherosclerosis was validated by IVUS examination.

Accordingly, considerable plaque burden can be observed on MDCT without inducing perfusion abnormalities on MPI. Rather than MDCT being false positive, atherosclerosis without flow-limiting luminal narrowing is detected.

References

1. Nishioka T, Amanullah AM, Luo H, et al. Clinical validation of intravascular ultrasound imaging for assessment of coronary stenosis severity: comparison with stress myocardial perfusion imaging. *J Am Coll Cardiol* 1999;33:1870-8.
2. Rodes-Cabau J, Candell-Riera J, Angel J, et al. Relation of myocardial perfusion defects and nonsignificant coronary lesions by angiography with insights from intravascular ultrasound and coronary pressure measurements. *Am J Cardiol* 2005;96:1621-6.
3. Vanhoenacker PK, Heijenbrok-Kal MH, Van Heste R, et al. Diagnostic performance of multi-detector CT angiography for assessment of coronary artery disease: meta-analysis. *Radiology* 2007;244:419-28.
4. Hacker M, Jakobs T, Hack N, et al. Sixty-four slice spiral CT angiography does not predict the functional relevance of coronary artery stenoses in patients with stable angina. *Eur J Nucl Med Mol Imaging* 2007;34:4-105. Schuijff JD, Wijns W, Jukema JW, et al. Relationship between noninvasive coronary angiography with multi-slice computed tomography and myocardial perfusion imaging. *J Am Coll Cardiol* 2006;48:2508-14.
6. Schuijff JD, Pundziute G, Jukema JW, et al. Diagnostic accuracy of 64-slice multislice computed tomography in the noninvasive evaluation of significant coronary artery disease. *Am J Cardiol* 2006;98:145-8.
7. Austen WG, Edwards JE, Frye RL, et al. A reporting system on patients evaluated for coronary artery disease. Report of the Ad Hoc Committee for Grading of Coronary Artery Disease, Council on Cardiovascular Surgery, American Heart Association. *Circulation* 1975;5:5-40.
8. Leber AW, Knez A, Becker A, et al. Accuracy of multidetector spiral computed tomography in identifying and differentiating the composition of coronary atherosclerotic plaques: a comparative study with intracoronary ultrasound. *J.Am.Coll.Cardiol.* 2004;43:1241-7.
9. Bavelaar-Croon CD, America YG, Atsma DE, et al. Comparison of left ventricular function at rest and post-stress in patients with myocardial infarction: Evaluation with gated SPECT. *J Nucl.Cardiol* 2001;8:10-8.
10. Cerqueira MD, Weissman NJ, Dilsizian V, et al. Standardized myocardial segmentation and nomenclature for tomographic imaging of the heart: a statement for healthcare professionals from the Cardiac Imaging Committee of the Council on Clinical Cardiology of the American Heart Association. *Circulation* 2002;105:539-42.
11. Hachamovitch R, Hayes SW, Friedman JD, et al. Stress myocardial perfusion single-photon emission computed tomography is clinically effective and cost effective in risk stratification of patients with a high likelihood of coronary artery disease (CAD) but no known CAD. *J Am Coll.Cardiol* 2004;43:200-8.
12. Smanio PE, Watson DD, Segalla DL, et al. Value of gating of technetium-99m sestamibi single-photon emission computed tomographic imaging. *J.Am.Coll.Cardiol.* 1997;30:1687-92.
13. Briguori C, Anzuini A, Airolidi F, et al. Intravascular ultrasound criteria for the assessment of the functional significance of intermediate coronary artery stenoses and comparison with fractional flow reserve. *Am J Cardiol* 2001;87:136-41.
14. Abizaid AS, Mintz GS, Mehran R, et al. Long-term follow-up after percutaneous transluminal coronary angioplasty was not performed based on intravascular ultrasound findings: importance of lumen dimensions. *Circulation* 1999;100:256-61.
15. Berman DS, Wong ND, Gransar H, et al. Relationship between stress-induced myocardial ischemia and atherosclerosis measured by coronary calcium tomography. *J.Am.Coll.Cardiol.* 2004;44:923-30.
16. Mintz GS, Painter JA, Pichard AD, et al. Atherosclerosis in angiographically "normal" coronary artery reference segments: an intravascular ultrasound study with clinical correlations. *J Am Coll Cardiol* 1995;25:1479-85.

Chapter 5



Anatomic correlates of a normal perfusion scan using 64-slice computed tomographic coronary angiography

JM van Werkhoven, JD Schuijf, JW Jukema, LJ Kroft, MPM Stokkel,
P Dibbets-Schneider, G Pundziute, A Scholte, EE van der Wall, JJ Bax

Abstract

Both myocardial perfusion imaging (MPI) and multi-slice computed tomography (MSCT) are currently used to detect coronary artery disease (CAD). However, MSCT permits early detection of atherosclerosis, while myocardial perfusion is still normal. In addition, MPI can be normal despite the presence of high risk CAD (left main and balanced 3-vessel CAD). In this study, the range of anatomical findings on MSCT in patients with a normal MPI was evaluated. In 180 patients presenting with chest pain, MPI (with gated single photon emission computed tomography (SPECT)) and 64-slice MSCT were performed. In patients with a normal MPI, the prevalence of completely normal coronary arteries, non-obstructive CAD, and obstructive CAD were determined on MSCT. The occurrence of high risk CAD, including left main and 3-vessel disease, was also evaluated. A normal MPI and adequate MSCT were obtained in 97 (54%) patients (50% female patients, average age 58 ± 12 years, 5% known CAD). A total of 38 patients (39%) showed normal coronary anatomy, whereas non-significant and significant CAD was observed in respectively 37 (38%), and 18 (19%) patients. Importantly, only 4 (4%) patients presented with high risk CAD on 64-slice MSCT, 2 with left main and 2 with 3-vessel disease. In conclusion, a normal MPI can be associated with a wide range of anatomical observations and cannot exclude the presence of both non-obstructive and obstructive CAD, importantly however, the prevalence of high-risk CAD was rare.

Introduction

Recently, non-invasive coronary angiography using multi-slice computed tomography (MSCT) has attracted a lot of attention. Studies using 64-slice MSCT have reported a high sensitivity (ranging from 85% to 100%), and even higher specificity (ranging from 92% to 97%) to detect significant ($\geq 50\%$ luminal narrowing) coronary lesions.¹⁻⁶ In addition, MSCT can also detect subclinical atherosclerosis, in the absence of stenotic coronary lesions, resulting in normal perfusion on myocardial perfusion imaging (MPI).^{7, 8} MSCT thus provides anatomical information rather than information on functional consequences of coronary artery disease (CAD). To explore the range of anatomical abnormalities underlying a normal MPI, a head-to-head comparison was performed between MSCT and MPI in patients with a normal MPI.

Methods

The study population consisted of 180 patients, who underwent MPI and 64-slice MSCT sequentially, in random order. Patients presented with suspected or known CAD. Suspected CAD was defined as having no history of CAD, and known CAD was defined as having evidence of CAD on previous diagnostic tests prior to the MPI and MSCT examinations in this study. Exclusion criteria were: atrial fibrillation, renal insufficiency (serum creatinine > 120 mmol/L), known allergy to iodine contrast media, and pregnancy. The pre-test likelihood of CAD was determined for patients without known CAD using the Diamond and Forrester method, with a risk threshold of $< 13.4\%$, for low risk, $> 87.2\%$ for high risk, and between 13.4 and 87.2% for intermediate risk. The study was part of an ongoing study protocol comparing MSCT with MPI,⁸ and was approved by the hospitals medical ethics committee. Informed consent was obtained in all patients.

The included patients were scanned using a 64-slice MSCT scanner (Aquillion 64, Toshiba Medical Systems, Tokyo, Japan). Prior to each scan, heart rate and blood pressure were monitored. In the absence of contraindications, patients with a heart rate exceeding the threshold of 70 beats per minute were given beta-blocking medication (50-100 mg metoprolol, oral).

Before the helical scan, a non-enhanced prospective electrocardiographically-gated scan, prospectively triggered at 75% of the R-R interval with 4×3.0 mm collimation, was performed to measure the coronary calcium score, and to determine the start and end positions of the helical scan. Optimal rotation time and pitch for the helical scan were automatically calculated by the scanner during a breath hold exercise. Subsequently, scan time was based on rotation time, pitch, and scan length.

The following helical scan parameters were used: collimation 64 x 0.5 mm; rotation time 0.4 s; pitch factor between 0.2 and 0.3; tube voltage 120 kV or 135 kV; tube current 300 (range 250-400 mA). A bolus of 90-105 ml contrast agent (Iomeron 400 i.v.) was injected at 5 ml/s followed by 50 ml saline flush.

A region of interest, used for triggering the scan, was placed in the aorta descendens in a single slice defined at the upper limit of the scanning field. The helical scan was automatically triggered when the attenuation level in the region of interest reached baseline + 100 Hounsfield units. All patients were scanned during a single breath hold of 8-11 seconds.

Using electrocardiographically-gated post processing and scanner software, the best phase was reconstructed with an interval of 0.3 mm. With a test slice in the various phases of the heart cycle other suitable R-R intervals were examined for additional reconstructions. Coronary arteries were evaluated using the reconstruction dataset with the least motion artifacts.

MSCT and calcium score (Agatston) scans were evaluated with a dedicated workstation (Vitrea 2, Vital Images, USA). All MSCT scans were interpreted by two experienced observers blinded to the results of MPI. Discrepancies in interpretation were resolved by consensus. For each patient, total coronary calcium score was determined and graded into four groups: 0, 1-100, 101-400, and > 400. Coronary anatomy on MSCT was assessed on a patient level and on a vessel level using axial slices, and curved multiplanar reconstructions. In each patient the presence of CAD was determined. Further differentiation was made between non-significant and significant CAD, using a diameter stenosis of $\geq 50\%$ as a threshold for significant lesions. Finally, the presence of high risk scans, defined as obstructive left main and 3-vessel disease, was also ascertained.

Each patient underwent a 2-day gated stress-rest MPI using technetium-99 tetrofosmin or technetium-99 sestamibi (500 MBq) with a symptom limited bicycle test or pharmacological stress using adenosine (0.14 mg/kg/min for 6 minutes), or dobutamine (up to a maximum dose of 40 $\mu\text{g}/\text{kg}/\text{min}$ in 15 min). Patients were instructed to withhold beta-blocking medication 48 hours prior to exercise or dobutamine stress, and patients were instructed to withhold calcium antagonists 24 hours before pharmacological stress using adenosine. Patients were also told to withhold caffeine starting the day before adenosine stress testing.

The images were acquired on a triple-head (GCA 9300/HG, Toshiba Corp., Tokyo, Japan) single photon emission computed tomography (SPECT) camera equipped with low energy high resolution collimators. A 20% window was used around the 140-keV energy peak of $^{99\text{m}}\text{Tc}$. Ninety projections (step-and-shoot mode; 35 s per projection; total imaging time, 23 min) were obtained over a 360 degree circular orbit. Data were stored in a 64 x 64

matrix. The raw scintigraphic data were reconstructed with filtered back projection using a Butterworth filter (cutoff frequency, 0.26 cycle per pixel, order 9). Using the gated images, attenuation correction was performed by evaluating wall motion in segments with perfusion defects thought to be caused by attenuation artifacts.

Gated SPECT examinations were judged by two experienced observers who were blinded to the results of MSCT. Quantitative assessment of left ventricular function, and wall thickening was performed using previously validated, and automated software (quantitative gated SPECT (QGS); Cedars-Sinai Medical Center, Los Angeles, CA).⁹ By estimating and displaying the endo- and epicardial surfaces, the left ventricular ejection fraction was derived.

The myocardium was divided into segments using a 17-segment model described elsewhere.¹⁰ Segmental myocardial perfusion was analyzed quantitatively (QGS software) and segmental tracer activity was categorized on a 4-point scale: 1 = normal tracer activity > 75%; 2 = tracer activity 50%-75%; 3 = tracer activity 25%-50%; 4 = tracer activity < 25%. Perfusion defects on stress images were considered present when tracer activity was < 75% of maximum. When significant fill-in (> 10%) of perfusion defects was observed on the resting images, segments were classified as ischemic, whereas defects without fill-in (\leq 10%) were considered scar tissue.¹¹

Continuous variables were expressed as mean and standard deviation. Proportions were expressed in percentages. Continuous variables were compared using one-way Anova, and student's t-test. Proportions were compared using Chi-square with Yates' correction. A P-value of <0.05 was considered to indicate statistical significance. Statistical analysis was performed using SPSS 12.0 software.

Results

The study population consisted of 180 patients who had undergone both an MPI study and a MSCT examination. A normal MPI was observed in 105 (58%) of these patients. Due to an uninterpretable MSCT caused by an irregular heart, 4 patients had to be excluded. Also 4 patients with an abnormal left ventricular ejection fraction (< 50%) on MPI were excluded, leaving 97 patients for analysis. These patients presented with non-anginal chest pain (34%), atypical chest pain (62%), and typical chest pain (4%). A low, intermediate, and high likelihood for disease was noted in respectively 6 (7%), 82 (89%), and 4 (4%) of the 92 patients without known CAD. Patient characteristics of both the patients with a normal and abnormal MPI are provided in Table 1.

Table 1. Patient characteristics of patients with a normal and abnormal myocardial perfusion scan

Variable	Normal (n=97)	Abnormal (n=75)	P-value
Male/Female	49/48	51/24	<0.05
Age (years)	58±12	55±12	NS
Suspected coronary artery disease	92 (95%)	61 (81%)	<0.05
Known coronary artery disease	5 (5%)	14 (19%)	<0.05
Previous coronary angioplasty	2 (2%)	5 (7%)	NS
Previous coronary bypass	0 (0%)	4 (5%)	<0.05
Previous myocardial infarction	0 (0%)	9 (12%)	<0.05
Average ejection fraction	67±10	58±12	<0.05
Diabetes mellitus	45 (46%)	42 (56%)	NS
Hypertension	51 (53%)	35 (47%)	NS
Hypercholesterolemia	38 (39%)	32 (43%)	NS
Current Smoker	30 (30%)	27 (36%)	NS
Obesity (BMI ≥ 30)	22 (23%)	15 (20%)	NS

During MPI, a bicycle stress test was performed in 53 (55%) patients, whereas pharmacological stress with adenosine or dobutamine was used in respectively 42 (43%) and 2 (2%) patients. In patients undergoing bicycle stress, at least 85% of maximum heart rate was achieved if no stress-induced symptoms or changes in electrocardiogram or blood pressure occurred. The two patients undergoing dobutamine stress also reached at least 85% of maximum heart rate. In the 97 patients with a diagnostic MSCT scan, 291 vessels could be analyzed, of which 2 (1%) were uninterpretable due to motion artifacts caused by a high heart rate. The average heart rate during data acquisition was 67±15 bpm. Average calcium score was 165±319.

As shown in Figure 1, coronary calcium was absent in 38 (39%) patients. A calcium score of 1-100 was observed in 25 (26%) patients, a score of 101-400 in 21 (22%) patients, and only 12 (12%) had a calcium score > 400. Of note, one patient (1%) was excluded from the calcium score analysis due to a missing calcium scan. Comparison of calcium scores and MSCT showed that the average calcium score in patients with a completely normal MSCT scan was significantly lower than the average calcium score in patients with non-obstructive or obstructive CAD (3.3±11.1 versus 223±363.6, and 306.8±323.3 respectively). The average calcium score in the high risk CAD group was 559.8±615.5, but due to the low number of patients not significantly different from the other groups (Figure 2).

MSCT identified 38 (39%) patients without CAD, 37 (38%) patients with non-obstructive CAD, and 22 (23%) patients with obstructive CAD (at least 1 significant (≥50%) stenosis) as illustrated in Figure 3. The characteristics of patients without CAD, with non-obstructive CAD, and with obstructive CAD are compared in Table 2. Analysis on a vessel basis resulted

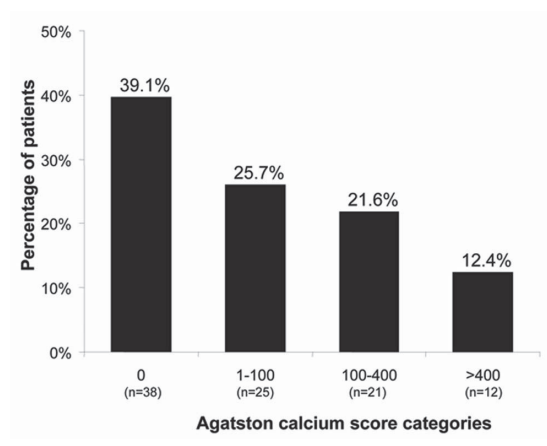


Figure 1. Distribution of coronary calcium score categories in the study population.

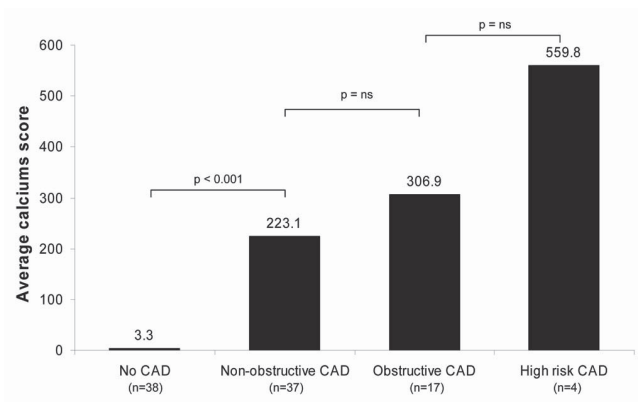


Figure 2. Average coronary calcium scores for patients without CAD, non-obstructive CAD, obstructive CAD and high-risk CAD. The extent of coronary calcium increased in parallel to the severity of CAD on MSCT.

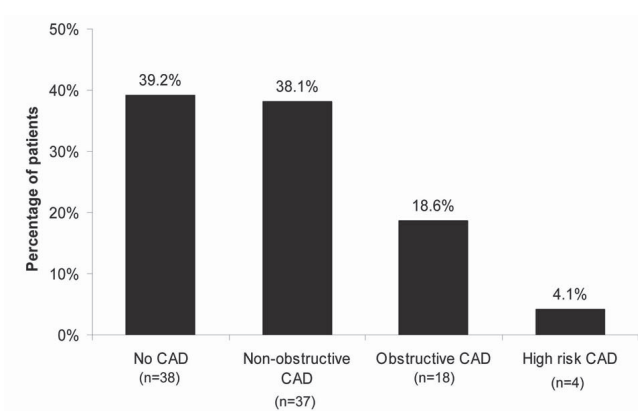


Figure 3. Distribution of anatomical findings observed on MSCT. In the majority of patients, either no CAD or non-obstructive CAD was observed, whereas high-risk CAD was demonstrated in only 4% of patients.

Table 2. Patient characteristics for patients with normal, non-obstructive, and obstructive coronary artery disease (CAD)

Variable	Normal (n=38)	Non-obstructive CAD (n=37)	Obstructive CAD (n=22)	P-value
Male/Female	15/23	19/18	15/7	NS
Age (years)	53±10	61±12	62±11	0.001
Diabetes mellitus	12 (32%)	19 (51%)	14 (64%)	NS
Hypertension	16 (42%)	22 (60%)	13 (59%)	NS
Hypercholesterolemia†	14 (37%)	24 (65%)	13 (59%)	NS
Current smoker	10 (26%)	12 (32%)	8 (36%)	NS
Obesity	4 (11%)	11 (30%)	7 (32%)	NS
Average of risk factors	1.9±1.0	2.6±1.6	2.7±1.2	NS
Average ejection fraction	67±10	67±11	65±8	NS
Known coronary artery disease	0 (0%)	3 (8%)	2 (9%)	NS
Pre-test likelihood (n=92)				
Low	3 (8%)	1 (3%)	2 (10%)	NS
Intermediate	34 (90%)	30 (88%)	18 (90%)	NS
High	1 (3%)	3 (9%)	0 (0%)	NS

in the following: 139 (46%) vessels without atherosclerosis, 124 (41%) vessels with non-obstructive CAD, and 39 (13%) vessels with obstructive CAD.

In the 59 patients with both non-obstructive and obstructive CAD, 9 (15%), 13 (22%), and 37 (63%) had 1-, 2-, and 3-vessel disease respectively. Regarding only patients with non-obstructive CAD, 1, 2, and 3 vessels were diseased in 8 (22%), 9 (24%), and 20 (54%) patients respectively, resulting in an average number of diseased vessels of 2.5±0.8. The opposite was observed when the number of coronary arteries with obstructive lesions was considered. In patients with obstructive CAD, the majority had either 1 (46%) or 2 (37%) significantly diseased vessels (Figure 4). The average number of significantly diseased vessels in all patients with obstructive CAD including high risk patients was 1.6±0.7.

Of the 97 patients studied with a normal perfusions scan, only 4 (4%) patients presented with high-risk CAD of which 2 patients had obstructive 3-vessel disease, and 2 patients had obstructive left main disease (see Figure 4). The various anatomical correlates in patients with a normal MPI are shown in Figure 5.

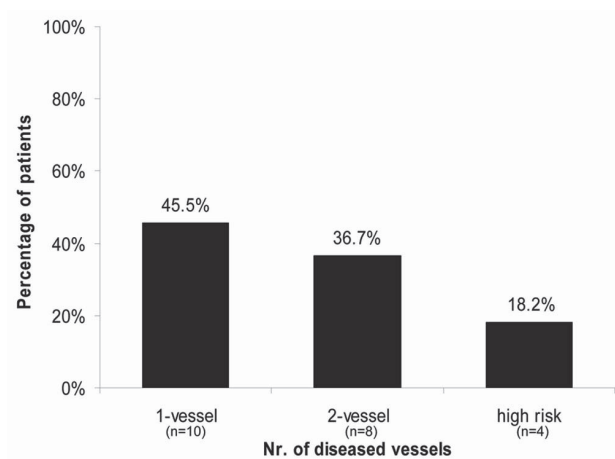


Figure 4. Bar graph showing the number of obstructively diseased vessels in patients with obstructive CAD (at least 1 significant stenosis).

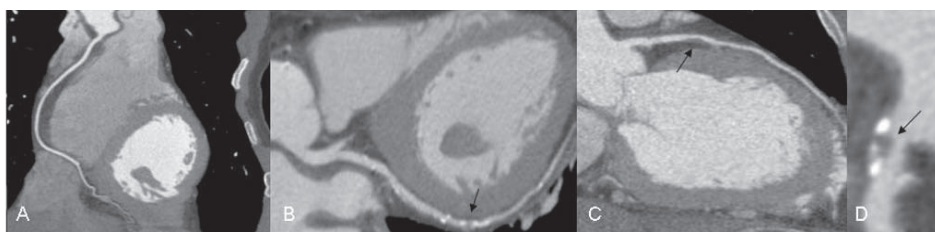


Figure 5. The anatomical correlates of a normal MPI included normal coronary anatomy (right coronary artery, panel A), non-obstructive CAD (circumflex artery, panel B), obstructive CAD (left anterior descending artery, panel C), and high risk CAD (left main artery, panel D).

Discussion

Patients with a normal MPI can have a wide range of atherosclerotic burden as reflected by the presence of calcium as well as significant stenoses on 64-slice MSCT. Although calcium was absent in a large part of the study population (39%), a considerable amount of patients (34%) presented with intermediate to high calcium score, indicating the presence of substantial atherosclerosis. When examined with MSCT, atherosclerosis was absent in 39% of the patients, while the majority of the population showed either non-obstructive (38%) or obstructive atherosclerosis (19%). Importantly, high risk CAD (defined as obstructive left main or 3-vessel disease) was observed only in a small proportion (4%) of the studied patients.

The relation between MPI and calcium has been previously investigated in several studies. Berman et al. explored the relation between atherosclerosis determined by electron beam

computed tomography calcium scoring and MPI in a large group of predominantly low risk, asymptomatic patients (n = 1,195). Coronary calcifications were absent in only 22% of individuals with a normal MPI.¹² Moreover, extensive calcifications (calcium score >400) were observed in a considerable higher proportion of patients with normal MPI (31%) as compared to 13% in the current study. This discrepancy may partially be explained by differences in patient populations; for example, more women (who had lower calcium scores) were included in the present study. A study by Blumenthal et al. had a comparable outcome.¹³ Like our results, these studies revealed only a modest relation between the extent of coronary calcium and ischemia with a widespread distribution of calcium scores in patients with normal MPI.

Høilund-Carslen et al. recently published observations on the anatomical correlates of MPI using conventional coronary angiography.¹⁴ Obstructive CAD was reported in 18% of the 235 patients with a normal MPI. Thus far, only a few studies have non-invasively evaluated the coronary anatomy with MSCT in patients undergoing MPI. Hacker et al. studied a cohort of 38 patients in which 55% had no perfusion defects on MPI.¹⁵ MSCT detected one or more significant lesions in 8 (38%) of those 21 patients. A recent study by Schuijff et al. reported similar findings.⁸

The available evidence indicates that a normal MPI is associated with a wide range of atherosclerotic findings on MSCT and cannot be used to rule out the presence of atherosclerosis. Still, a normal MPI is associated with an excellent long-term prognosis and a hard annual event rate < 1%.¹⁶ Future studies are thus needed to understand the prognostic value of a normal MPI in the presence of coronary atherosclerosis.

Homogeneously reduced perfusion in patients with high-risk CAD (3-vessel and left main disease) is thought to be a potential cause of a “false” normal MPI study.¹⁷⁻¹⁹ In the current study, the prevalence of high risk CAD in patients with a normal MPI was evaluated, and the results revealed that left main or 3-vessel disease was only present in a small amount of patients (4%). Only limited comparative data using coronary angiography are thus far available. Fujimoto et al. determined the lesion characteristics in 58 ischemic heart disease patients with false negative MPI examinations.²⁰ No patients with 3-vessel disease were observed, and only 1 (2%) patient presented with obstructive left main CAD. Høilund-Carslen et al., encountered only 5 (2%) cases of 3-vessel disease, in line with the current findings.¹⁴ Accordingly, these observations suggest that balanced 3-vessel disease may not be a frequent cause of “false” normal MPI findings.

Several limitations need to be acknowledged. No direct comparison with invasive coronary angiography was available. However, previous studies have reported on the diagnostic

accuracy of 64-slice MSCT in direct comparison with invasive angiography.¹⁻⁶ Despite the excellent diagnostic accuracy of MSCT, uninterpretable segments due to calcium or motion remain problematic. For this reason, 4 (4%) patients with uninterpretable MSCT examinations were excluded in the current analysis. Thus, the uninterpretability of a small proportion of MSCT examinations must be taken into account when comparing MSCT and MPI for their efficacy in detecting CAD. Moreover, the proportion of diabetic patients was relatively high in the current study, resulting in an increased likelihood of CAD. Whether the current findings apply to a non-diabetic population remains to be determined. Finally, the radiation burden of MSCT remains a limitation of this imaging modality. However, a reduction in radiation burden is anticipated with the new generation 128- and 256-slice MSCT scanners and dose-modulation strategies that are currently being developed.

Conclusion

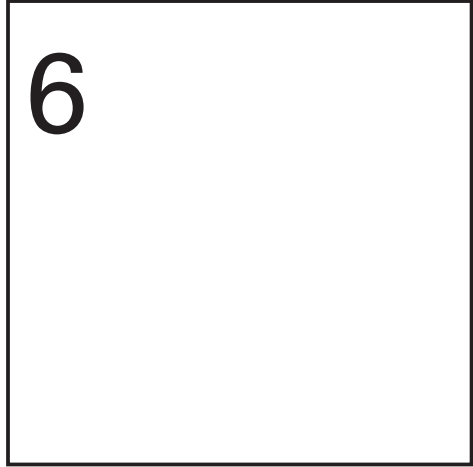
A normal MPI can be associated with a wide range of anatomical observations and cannot exclude the presence of both non-obstructive and obstructive CAD, importantly however, the prevalence of high-risk CAD was rare.

References

1. Ehara M, Surmely JF, Kawai M, et al. Diagnostic accuracy of 64-slice computed tomography for detecting angiographically significant coronary artery stenosis in an unselected consecutive patient population - Comparison with conventional invasive angiography. *Circ J* 2006;70:564-71.
2. Leber AW, Knez A, von Ziegler F, et al. Quantification of obstructive and nonobstructive coronary lesions by 64-slice computed tomography - A comparative study with quantitative coronary angiography and intravascular ultrasound. *J Am Coll Cardiol* 2005;46:147-54.
3. Leschka S, Alkadhi H, Plass A, et al. Accuracy of MSCT coronary angiography with 64-slice technology: first experience. *Eur Heart J* 2005;26:1482-7.
4. Mollet NR, Cademartiri F, van Mieghem CA, et al. High-resolution spiral computed tomography coronary angiography in patients referred for diagnostic conventional coronary angiography. *Circulation* 2005;112:2318-23.
5. Raff GL, Gallagher MJ, O'Neill W, et al. Diagnostic accuracy of noninvasive coronary angiography using 64-slice spiral computed tomography. *J Am Coll Cardiol* 2005;46:552-7.
6. Schuijff JD, Pundziute G, Jukema JW, et al. Diagnostic accuracy of 64-slice multislice computed tomography in the Noninvasive evaluation of significant coronary artery disease. *Am J Cardiol* 2006;98:145-8.
7. Hacker M, Jakobs T, Matthiesen F, et al. Comparison of spiral multidetector CT angiography and myocardial perfusion imaging in the noninvasive detection of functionally relevant coronary artery lesions: First clinical experiences. *J Nucl Med* 2005;46:1294-1300.
8. Schuijff JD, Wijns W, Jukema JW, et al. The relationship between non-invasive coronary angiography with multi-slice computed tomography and myocardial perfusion imaging. *J Am Coll Cardiol* 2006;48:2508-14.
9. Sharir T, Berman DS, Waechter PB, et al. Quantitative analysis of regional motion and thickening by gated myocardial perfusion SPECT: Normal heterogeneity and criteria for abnormality. *J Nucl Med* 2001;42:1630-8.
10. Cerqueira MD, Weissman NJ, Dilsizian V, et al. Standardized myocardial segmentation and nomenclature for tomographic imaging of the heart - A statement for healthcare professionals from the Cardiac Imaging Committee of the Council on Clinical Cardiology of the American Heart Association. *Circulation* 2002;105:539-42.
11. Beeres SL, Bax JJ, Dibbets P, et al. Effect of intramyocardial injection of autologous bone marrow-derived mononuclear cells on perfusion, function, and viability in patients with drug-refractory chronic ischemia. *J Nucl Med* 2006;47:574-80.
12. Berman DS, Wong ND, Gransar H, et al. Relationship between stress-induced myocardial ischemia and atherosclerosis measured by coronary calcium tomography. *J Am Coll Cardiol* 2004;44:923-30.
13. Blumenthal RS, Becker DM, Yanek LR, et al. Comparison of coronary calcium and stress myocardial perfusion imaging in apparently healthy siblings of individuals with premature coronary artery disease. *Am J Cardiol* 2006;97:328-33.
14. Hoiland-Carlsen PF, Johansen A, Christensen HW, et al. Potential impact of myocardial perfusion scintigraphy as gatekeeper for invasive examination and treatment in patients with stable angina pectoris: observational study without post-test referral bias. *Eur Heart J* 2006;27:29-34.
15. Hacker M, Jakobs T, Hack N, et al. Sixty-four slice spiral CT angiography does not predict the functional relevance of coronary artery stenoses in patients with stable angina. *Eur J Nucl Med Mol Imaging* 2007;34:4-10.
16. Underwood SR, Anagnostopoulos C, Cerqueira M, et al. Myocardial perfusion scintigraphy: the evidence - A consensus conference organised by the British Cardiac Society, the British Nuclear Cardiology Society and the British Nuclear Medicine Society, endorsed by the Royal College

- of Physicians of London and the Royal College of Radiologists. *Eur J Nucl Med Mol Imaging* 2004;31:261-91.
17. Duvernoy CS, Ficaro EP, Karabajakian MZ, et al. Improved detection of left main coronary artery disease with attenuation-corrected SPECT. *J Nucl Cardiol* 2000;7:639-48.
 18. Hung GU, Chen CP, Yang KT. Incremental value of ischemic stunning on the detection of severe and extensive coronary artery disease in dipyridamole Tl-201 gated myocardial perfusion imaging. *Int J Cardiol* 2005;105:108-10.
 19. Williams KA, Schuster RA, Williams KA, et al. Correct spatial normalization of myocardial perfusion SPECT improves detection of multivessel coronary artery disease. *J Nucl Cardiol* 2003;10:353-60.
 20. Fujimoto S, Wagatsuma K, Uchida Y, et al. Study of the predictors and lesion characteristics of ischemic heart disease patients with false negative results in stress myocardial perfusion single-photon emission tomography. *Circ J* 2006;70:297-303.

Chapter 6



Comparison of Non-Invasive Multi-Slice
Computed Tomography Coronary Angiography
versus Invasive Coronary Angiography and
Fractional Flow Reserve for the Evaluation of Men
with Known Coronary Artery Disease

JM van Werkhoven, JD Schuijf, JW Jukema, G Pundziute, A de Roos,
MJ Schalij, EE van der Wall, JJ Bax

Abstract

Computed tomography coronary angiography (MSCT) can accurately detect the presence of atherosclerosis non-invasively. However, a discrepancy has been observed between MSCT and non-invasive functional imaging. The purpose of the present study was to evaluate the correlation between MSCT and invasive fractional flow reserve (FFR) in men with known coronary artery disease (CAD). 33 patients (average age 57 ± 11 years) clinically referred for coronary angiography underwent MSCT and FFR. Coronary angiography and MSCT were evaluated for non-significant (30-50% luminal narrowing) and significant stenosis (>50% luminal narrowing). Abnormal FFR was defined as ≤ 0.75 . A total of 36 vessels were evaluated with FFR, with 8 (22%) showing reduced FFR. MSCT was normal (completely normal or <30% luminal narrowing in 11 (31%), non-significant lesions were observed in 13 vessels (36%), and significant stenosis in 12 vessels (33%). Abnormal FFR was observed in only 58% of vessels with lesions >50% on MSCT. Nevertheless, the agreement between normal MSCT and FFR was excellent; FFR was normal in all 11 vessels with normal MSCT. In conclusion, significant stenoses on MSCT frequently do not result in reduced FFR. A normal MSCT study however can accurately rule out the presence of hemodynamically significant lesions in men with known CAD.

Introduction

Multi-slice computed tomography coronary angiography (MSCT) is increasingly used as a non-invasive imaging technique capable of accurately detecting the presence of atherosclerosis.¹⁻⁶ However, a considerable discrepancy has been observed when comparing anatomic imaging with MSCT to myocardial perfusion imaging (MPI).⁷⁻¹⁰ In these comparative studies, a large proportion of significant lesions on MSCT were not associated with a perfusion defect on MPI. Possibly, invasive functional testing using fractional flow reserve (FFR) may provide a more accurate comparison, since measurements are performed directly in the coronary arteries.¹¹ Only one previous study has addressed the diagnostic accuracy of MSCT to predict the presence of reduced FFR.¹² The purpose of the present study was to further assess the relationship between the anatomic information observed on MSCT and invasive functional testing using FFR in men with known coronary artery disease (CAD).

Methods

In total 33 patients were included in the study. Patients were clinically referred for coronary angiography and underwent additional testing including 1) FFR measurements during the cardiac catheterization procedure and 2) MSCT within 2 months before or after conventional coronary angiography. Conventional coronary angiography, FFR and MSCT results were obtained in 36 vessels. Patients were excluded from the study if they met one of the following exclusion criteria for MSCT: cardiac arrhythmia, renal insufficiency (serum creatinine > 120 mmol/L), known allergy to iodine contrast media, and pregnancy. Patients were also excluded if a cardiac event (worsening angina, revascularization, or myocardial infarction) occurred between the procedures. The study was part of an ongoing research protocol approved by the hospitals medical ethics committee, and all patients gave informed consent.

Patients were scanned using a 64-slice scanner (Aquillion 64, Toshiba Medical Systems, Tokyo, Japan) using a previously published scan protocol.¹³ Before each examination, heart rate and blood pressure were monitored. In the absence of contraindications, patients with a heart rate exceeding the threshold of 65 beats per minute were given beta-blocking medication (50-100 mg metoprolol, oral).

The presence of calcium and the status of the coronary arteries were both evaluated using a dedicated workstation (Vitrea 2, Vital Images, USA, and Advantage, GE healthcare, USA). All studies were interpreted by two experienced observers blinded to the results of coronary angiography and FFR. Discrepancies in interpretation were resolved by consensus.

The coronary calcium score was calculated using the Agatston method. MSCT coronary angiography studies were evaluated using an intention to diagnose strategy regardless of image quality. In each vessel the presence of atherosclerosis was evaluated, and lesions were graded as having a diameter stenosis of either >30% or >50% luminal narrowing. Lesions with a stenosis >50% were deemed significant. A normal MSCT was defined as completely normal or <30% luminal narrowing.

Conventional coronary angiography was performed according to standard techniques. Quantitative analysis by an observer blinded to the MSCT and FFR results using an offline software program (QCA-CMS, version 6.0, Medis, Leiden, The Netherlands). After catheter based calibration, quantitative coronary angiography of the most severe lesions was performed with automated vessel contour detection in end-diastolic frames. Vessels were classified as having a diameter stenosis of either >30% or >50% luminal narrowing, and lesions with a stenosis >50% were deemed significant. A normal coronary angiography was defined as completely normal or <30% luminal narrowing. FFR measurements were performed in the distal and very proximal coronary artery during maximal hyperaemia obtained by intravenous injection of a bolus of adenosine (6 ug/ml in 7 ml). A 0.014 inch pressure guidewire (Brightwire 2, Volcano Corps., San Diego, USA) was advanced 1-2 mm into the proximal artery to measure proximal pressure, and advanced further, into the distal coronary artery to measure distal pressure. The FFR of the vessel was calculated as the ratio of distal pressure to proximal pressure, and a value of ≤ 0.75 was used as a cutoff point for significantly impaired coronary function.

Continuous variables were expressed as mean with standard deviation, and where compared using the student's t-test. Proportions were expressed in percentages. First MSCT observations were compared to coronary angiography. Secondly, MSCT and conventional coronary angiography were compared to FFR to determine the relation between stenotic lesions and FFR measurements. All comparisons were performed on a vessel basis. Statistical analyses were performed using SPSS software (version 12.0, SPSS Inc, Chicago, IL, USA). A p-value <0.05 was deemed significant.

Results

In total 33 patients were included in the study. An overview of the characteristics of these patients is provided in Table 1. During conventional coronary angiography, an FFR measurement was obtained in the left anterior descending artery (n= 25), the right coronary artery (n = 9), and the left circumflex artery (n = 2), resulting in 38 vessels for analysis.

Table 1. Patient characteristics

Age (years)	57±11
Known coronary artery disease	30 (91%)
Diabetes mellitus	3 (9%)
Hypertension	14 (42%)
Hypercholesterolemia†	12 (36%)
Current Smoker	7 (21%)
Positive family history of cardiovascular disease	12 (36%)
Body mass index ≥ 30 Kg/m ²	8 (24%)
Heart rate during scan (beats per minute)	59±12
Average calcium score (Agatston units)	554±1588
Significant stenosis on coronary angiography	19 (58%)

Using the contrast enhanced MSCT images, 11 (31%) of 36 vessels were classified as normal (completely normal or <30% luminal narrowing). Atherosclerotic lesions exceeding 30% luminal narrowing were detected in 25 (69%) vessels. Of these 25 vessels, 13 (36%) vessels had atherosclerotic disease between 30% and 50% diameter stenosis, and in 12 (33%) vessels the diameter stenosis exceeded 50% luminal narrowing.

A total of 18 (50%) coronary arteries were normal (completely normal or <30% luminal narrowing) on conventional coronary angiography. Lesions with a diameter stenosis >30% were detected in the remaining 18 vessels (50%), of which 9 (25%) showed a non-significant stenosis (30-50% luminal narrowing) and 9 (25%) a significant stenosis (>50% luminal narrowing). Using the pressure guidewire, an average FFR of 0.83 ± 0.13 was measured. Normal FFR (>0.75) was observed in 28 (78%) vessels while FFR was abnormal in the remaining 8 (22%) vessels.

On MSCT 11 vessels were graded as normal (completely normal or <30% luminal narrowing). All 11 vessels were also graded normal on conventional coronary angiography. MSCT showed non-significant lesions (30-50% diameter stenosis) in 13 vessels, of which 5 were normal and 8 showed non-significant disease on conventional coronary angiography. Thus MSCT correctly identified 30-50% luminal narrowing in 8 of 13 vessels (62%). A significant lesion was observed in 12 vessels on MSCT. All 9 vessels with luminal narrowing >50% on conventional coronary angiography were detected; however MSCT overestimated the severity of disease in 3 vessels. Significant lesions were therefore correctly identified in 9 of 12 vessels (75%). Although an overestimation of disease was observed in some cases, MSCT correctly ruled out significant disease in all 25 vessels classified as <50% on MSCT.

Hemodynamically significant disease on FFR was observed in 7 of 12 vessels (58%) with >50% luminal narrowing on MSCT. Of note, abnormal FFR was also observed in 1 of 13 vessels (8%) with atherosclerosis between 30% and 50% luminal narrowing. Importantly, FFR was normal

in all 11 coronary arteries classified as normal on MSCT. Finally, on average FFR decreased significantly with increasing stenosis severity; further details are provided in Figure 1.

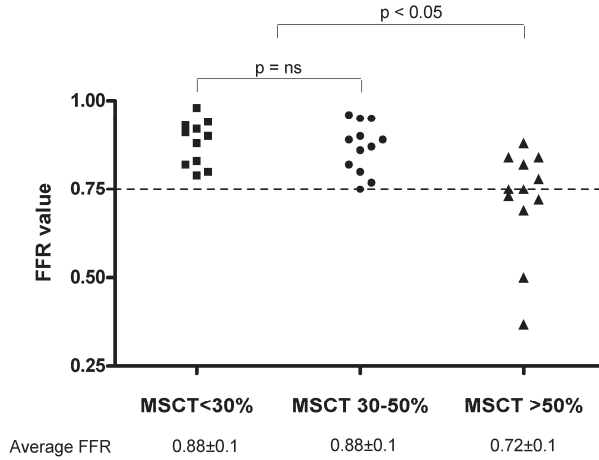


Figure 1. Scatter plot of FFR values in vessels with <30%, 30-50% and >50% luminal narrowing on MSCT. Average FFR was significantly reduced in patients with >50% luminal narrowing on MSCT.

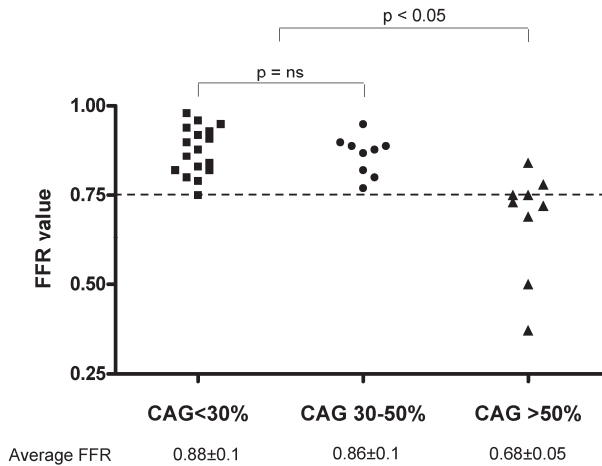


Figure 2. Scatter plot of FFR values in vessels with <30%, 30-50% and >50% luminal narrowing on conventional coronary angiography. Average FFR was significantly reduced in patients with >50% luminal narrowing on conventional coronary angiography.

When evaluating the relation between conventional coronary angiography and FFR, 7 of 9 vessels with >50% luminal narrowing on conventional coronary angiography were associated with hemodynamically significant disease on FFR.(Figure 2) Abnormal FFR was observed in 1 of 18 vessels (6%) with normal or <30% luminal narrowing on conventional

coronary angiography. On average the FFR was significantly decreased in vessels with >50% stenosis on conventional coronary angiography compared to vessels with normal or non-significant CAD.

Discussion

The main findings of this comparative study between MSCT and coronary angiography with FFR in men with known CAD are as follows: Although non-invasive anatomical imaging with MSCT correlates well with conventional coronary angiography, the agreement between an abnormal MSCT (>50% luminal narrowing) and FFR is relatively low. A large proportion (42%) of significant (>50%) lesions on MSCT did not result in a functional abnormality on FFR. Importantly however, the absence of any lesion exceeding 30% luminal narrowing on MSCT, was associated with consistent normal FFR values, suggesting that normal coronary anatomy on MSCT can accurately rule out the presence of hemodynamically significant CAD.

One previous study has been published comparing non-invasive anatomical imaging with 64-slice MSCT to FFR.¹² In this retrospective study the diagnostic accuracy of MSCT and coronary angiography using FFR as the reference standard was assessed. In total 89 stenoses were evaluated and a poor correlation was observed between MSCT and FFR. These results are in line with the current study in which a large proportion of significant stenoses on MSCT did not result in reduced FFR as well.

The inaccuracy of MSCT to precisely estimate degree of stenosis has been suggested as a potential cause of this discrepancy. Indeed, several studies have shown that MSCT has a tendency to overestimate the degree of stenosis.¹ Also in the present study, MSCT more frequently classified patients as having stenosis either 30-50% or >50% luminal narrowing as compared to conventional coronary angiography. However, similar to MSCT, conventional coronary angiography also fails to accurately predict reduced coronary flow reserve. In the current study 78% of vessels with a significant stenosis (>50% luminal narrowing) on conventional coronary angiography were associated with reduced FFR. In a meta-analysis by Christou et al. combining 18 studies with 1316 patients, a concordance of 61% between the presence of intermediate lesions of 30-70% luminal narrowing on coronary angiography and an abnormal FFR (using a cutoff value of 0.75) was observed.¹⁴ When considering only lesions exceeding 70% luminal narrowing, the concordance increased slightly to 67%, indicating still a poor relation between degree of stenosis and reduced flow reserve. In the current study the concordance between significant stenosis on conventional coronary angiography and abnormal FFR seemed higher compared to the concordance between

significant stenosis on MSCT and FFR. To some extent this may be explained again by the tendency of MSCT to overestimate the degree of stenosis. Nevertheless, also conventional coronary angiography still frequently failed to accurately predict reduced FFR.

Comparable values have been reported in previous studies comparing MSCT to non-invasive MPI. In general, abnormal MSCT studies were associated with ischemia in approximately only 40% to 60% of studies.⁷⁻¹⁰ In line with these observations, only 58% of significant (>50% stenosis) lesions on MSCT resulted in abnormal FFR in our current study as well. These findings highlight the fact that even on a vessel basis using invasive measurements, the relation between significant epicardial coronary stenosis and functional consequences is poor. Accordingly, in the presence of an abnormal MSCT study, functional testing remains essential to determine appropriate management.

An important finding of this study is that a normal MSCT (completely normal or <30% luminal narrowing) was consistently associated with a normal FFR. Also in previous comparisons of MSCT to MPI, MSCT has been shown to have a high negative predictive value for ischemia.¹⁵ However, in contrast to our study, still small but not negligible proportions of normal MSCT studies were associated with abnormal MPI studies in these investigations.^{8, 10} A recent study reported that abnormal MPI was observed in 10% of patients having coronary arteries without any evidence of luminal narrowing or coronary plaque on MSCT.¹⁰ In some of these patients, the occurrence of attenuation artefacts may have hampered accurate evaluation of myocardial perfusion. More likely however, findings may have been influenced by intrinsic differences between FFR and MPI. While FFR detects epicardial coronary lesions that are severe enough to result in ischemia, MPI is also affected by abnormalities occurring at smaller levels of the coronary circulation. As a consequence, dysfunction of microvascular arterioles - which can occur in the presence of longstanding arterial hypertension and diabetes mellitus - can also result in abnormal MPI despite the absence of epicardial stenosis.¹⁶ Accordingly, one may intuitively expect a higher agreement between MSCT and FFR as both technique evaluate and exclude CAD at macrovascular level. Indeed, comparisons of conventional coronary angiography and FFR have also indicated excellent concordance over 95% between normal coronary arteries and FFR values,¹⁴ in line with the current study. These are important observations, as a normal FFR has been demonstrated to confer excellent prognosis and can safely defer patients from percutaneous intervention.^{17, 18} Consequently, one may presume that also patients with a normal MSCT study have a low likelihood of coronary events and do not require invasive coronary angiography with possible intervention. Thus far only limited prognostic data on MSCT are available although preliminary data suggest that a normal MSCT study is indeed associated with excellent prognosis.¹⁹⁻²¹

Conclusion

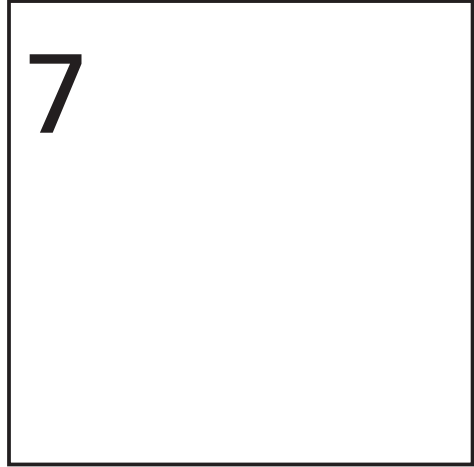
Significant stenoses on MSCT frequently do not result in reduced FFR. A normal MSCT study however can accurately rule out the presence of hemodynamically significant lesions in men with known CAD.

References

1. Hamon M, Biondi-Zoccai GG, Malagutti P, et al. Diagnostic performance of multislice spiral computed tomography of coronary arteries as compared with conventional invasive coronary angiography: a meta-analysis. *J Am Coll Cardiol* 2006;48:1896-910.
2. Hausleiter J, Meyer T, Hadamitzky M, et al. Non-invasive coronary computed tomographic angiography for patients with suspected coronary artery disease: the Coronary Angiography by Computed Tomography with the Use of a Submillimeter resolution (CACTUS) trial. *Eur Heart J* 2007;28:3034-41.
3. Leber AW, Knez A, von Ziegler F, et al. Quantification of obstructive and nonobstructive coronary lesions by 64-slice computed tomography: a comparative study with quantitative coronary angiography and intravascular ultrasound. *J Am Coll Cardiol* 2005;46:147-54.
4. Mollet NR, Cademartini F, Van Mieghem CAG, et al. High-resolution spiral computed tomography coronary angiography in patients referred for diagnostic conventional coronary angiography. *Circulation* 2005;112:2318-23.
5. Raff GL, Gallagher MJ, O'Neill WW, et al. Diagnostic accuracy of noninvasive coronary angiography using 64-slice spiral computed tomography. *J Am Coll Cardiol* 2005;46:552-7.
6. Schuijf JD, Pundziute G, Jukema JW, et al. Diagnostic accuracy of 64-slice multislice computed tomography in the noninvasive evaluation of significant coronary artery disease. *Am J Cardiol* 2006;98:145-8.
7. Gaemperli O, Schepis T, Koepfli P, et al. Accuracy of 64-slice CT angiography for the detection of functionally relevant coronary stenoses as assessed with myocardial perfusion SPECT. *Eur J Nucl Med Mol Imaging* 2007;34:1162-71.
8. Hacker M, Jakobs T, Hack N, et al. Sixty-four slice spiral CT angiography does not predict the functional relevance of coronary artery stenoses in patients with stable angina. *Eur J Nucl Med Mol Imaging* 2007;34:4-10.
9. Rispler S, Keidar Z, Ghersin E, et al. Integrated single-photon emission computed tomography and computed tomography coronary angiography for the assessment of hemodynamically significant coronary artery lesions. *J Am Coll Cardiol* 2007;49:1059-67.
10. Schuijf JD, Wijns W, Jukema JW, et al. The relationship between non-invasive coronary angiography with multi-slice computed tomography and myocardial perfusion imaging. *J Am Coll Cardiol* 2006;48:2508-14.
11. Pijls NH, De Bruyne B, Peels K, et al. Measurement of fractional flow reserve to assess the functional severity of coronary-artery stenoses. *N Engl J Med* 1996;334:1703-8.
12. Meijboom WB, Van Mieghem CA, Van Pelt N, et al. Comprehensive assessment of coronary artery stenoses: computed tomography coronary angiography versus conventional coronary angiography and correlation with fractional flow reserve in patients with stable angina. *J Am Coll Cardiol* 2008;52:636-43.
13. Schuijf JD, Pundziute G, Jukema JW, et al. Diagnostic accuracy of 64-slice multislice computed tomography in the noninvasive evaluation of significant coronary artery disease. *Am J Cardiol* 2006;98:145-8.
14. Christou MA, Siontis GC, Katritsis DG, et al. Meta-analysis of fractional flow reserve versus quantitative coronary angiography and noninvasive imaging for evaluation of myocardial ischemia. *Am J Cardiol* 2007;99:450-6.
15. Di Carli MF, Hachamovitch R. New technology for noninvasive evaluation of coronary artery disease. *Circulation* 2007;115:1464-80.
16. Camici PG, Crea F. Coronary microvascular dysfunction. *N Engl J Med* 2007;356:830-40.
17. Pijls NH, van Schaardenburgh P, Manoharan G, et al. Percutaneous coronary intervention of functionally nonsignificant stenosis: 5-year follow-up of the DEFER Study. *J Am Coll Cardiol* 2007;49:2105-11.

18. Silber S, Albertsson P, Aviles FF, et al. Guidelines for percutaneous coronary interventions. The Task Force for Percutaneous Coronary Interventions of the European Society of Cardiology. *Eur Heart J* 2005;26:804-47.
19. Gilard M, Le Gal G, Cornily J, et al. Midterm Prognosis of Patients With Suspected Coronary Artery Disease and Normal Multislice Computed Tomographic Findings. *Arch Intern Med* 2007;165:1686-9.
20. Min JK, Shaw LJ, Devereux RB, et al. Prognostic value of multidetector coronary computed tomographic angiography for prediction of all-cause mortality. *J Am Coll Cardiol* 2007;50:1161-70.
21. Pundziute G, Schuijff JD, Jukema JW, et al. Prognostic value of multislice computed tomography coronary angiography in patients with known or suspected coronary artery disease. *J Am Coll Cardiol* 2007;49:62-70.

Chapter 7



Combined non-Invasive anatomic and functional assessment with MSCT and MRI for the detection of significant coronary artery disease in patients with an intermediate pre-test likelihood

JM van Werkhoven, MW Heijenbrok, JD Schuijf, JW Jukema,
EE van der Wall, JHM Schreur, JJ Bax.

Abstract

The objective of this study was to compare magnetic resonance myocardial perfusion imaging (MRI) to anatomical assessment with multi-slice computed tomography coronary angiography (MSCT) and conventional coronary angiography. 53 patients (60% male, average age 57 ± 9 years, 83% intermediate pre-test likelihood) underwent 1.5 Tesla MRI, 64-slice MSCT, and conventional coronary angiography. The presence of significant stenosis ($\geq 50\%$ luminal narrowing) was determined on MSCT and conventional coronary angiography. Ischemia on MRI was defined as a stress perfusion abnormality in the absence of delayed contrast enhancement. A significant stenosis was observed on MSCT in 15 (28%) patients, while ischemia on MRI was observed in 19 (36%). In the 38 patients without significant stenosis on MSCT, normal perfusion was observed in 29 (76%). In patients with a significant stenosis on MSCT, ischemia was observed in 10 (67%). In all patients without significant stenosis on MSCT and normal perfusion on MRI ($n=29$), significant stenosis was absent on conventional coronary angiography. All patients with both MSCT and MRI abnormal ($n=10$) had significant stenoses on conventional coronary angiography. In conclusion, the anatomic and functional data obtained with MSCT and MRI is complementary for the assessment of CAD. These findings support the sequential or combined assessment of anatomy and function.

Introduction

Coronary artery disease (CAD) remains one of the leading causes of morbidity and mortality in the Western world. In this regard, non-invasive imaging modalities play an increasingly important role. Following the recent development of non-invasive anatomic imaging using multi-slice computed tomography coronary angiography (MSCT), non-invasive imaging of atherosclerosis has received particular interest. Using this technique, fast evaluation of coronary anatomy has become possible, enabling stenosis detection with a high diagnostic accuracy compared to conventional coronary angiography.^{1, 2} Notably, also subclinical atherosclerosis, possibly warranting more targeted anti-atherosclerotic therapy, can easily be identified with this technique.

However, non-invasive anatomic imaging (MSCT angiography) is unable to predict ischemia, which is needed to guide decisions concerning potential revascularization. Several studies comparing the relationship between MSCT and functional imaging of myocardial perfusion using single photon emission computed tomography (SPECT) and positron emission tomography (PET) have indeed shown a discrepancy between non-invasive anatomic and functional imaging, suggesting that these techniques may provide complementary information regarding the presence, extent and severity of CAD.^{3, 4}

In addition to the currently available nuclear imaging techniques, myocardial perfusion abnormalities reflecting ischemia may also be appreciated using magnetic resonance imaging (MRI).^{5, 6} Myocardial perfusion imaging using stress MRI has a good diagnostic accuracy compared to non-invasive functional imaging using SPECT and PET, and invasive imaging using fractional flow reserve.⁷⁻⁹ Because of its high spatial resolution and the lack of ionizing radiation, MRI may possibly be used as an alternative to SPECT and PET for combined anatomic and functional imaging in combination with MSCT. Currently, the potential complementary relation between MSCT and MRI perfusion imaging has not been investigated. Therefore the purpose of this study was to compare myocardial perfusion imaging with MRI to anatomical assessment with MSCT and conventional coronary angiography.

Methods

Patient population and study protocol

In this prospective cohort study, 53 consecutive patients referred for conventional diagnostic coronary angiography because of suspected CAD underwent additional evaluation with MSCT and cardiovascular MRI within a period of 14 days. Patients were excluded from the study if they met one of the following exclusion criteria for MSCT: cardiac arrhythmias,

renal insufficiency (serum creatinine >120 mmol/L), known hypersensitivity to iodine contrast media, and pregnancy. Further exclusion criteria for MRI were: cardiac pacemakers or intracranial aneurysm clips, and claustrophobia. Finally patients were excluded in the occurrence of a cardiac event (worsening angina, revascularization, or myocardial infarction) in the period between the 3 examinations.

Baseline characteristics of the patients were recorded, and their pre-test likelihood of CAD was determined using the Diamond and Forrester method, with a risk threshold of <13.4% for low risk, >87.2% for high risk, and between 13.4% and 87.2% for intermediate risk, as previously described.¹⁰ The study was approved by the local medical ethics committee (Medical Centre Haaglanden, The Hague, The Netherlands) and all patients gave written informed consent.

Quantitative coronary angiography

Conventional coronary angiography was performed according to standard techniques. Quantitative coronary angiography (QCA) analysis of the most severe lesion was performed for each coronary artery by an observer blinded to the MSCT and MRI results using an offline software program (QCA-CMS, version 6.0, Medis, Leiden, The Netherlands). Coronary arteries were divided into 17 segments according to the modified American Heart Association classification and QCA was performed in lesions exceeding 30% luminal narrowing on visual assessment.¹¹ A significant stenosis was defined on a patient and vessel level as $\geq 50\%$ luminal narrowing on QCA.

Multi-slice computed tomography

All examinations were performed using a 64-slice MSCT scanner (Lightspeed VR 64, General Electrics, Milwaukee, MI, USA). Patient's heart rate and blood pressure were monitored before each scan. In the absence of contraindications, patients with a heart rate exceeding the threshold of 65 beats per minute were administered beta-blocking medication (50-100 mg metoprolol, oral or 5-10 mg metoprolol, intravenous).

Before the helical scan, a non-enhanced electrocardiographically (ECG)-gated scan, prospectively triggered at 75% of the R-R interval, was performed to measure the coronary calcium score (CS). The retrospectively ECG gated helical scan was performed using the following scan parameters: collimation 64 x 0.625 mm; rotation time 0.35 s; tube voltage 120 kV, and tube current 600 mA (with tube modulation to reduce the radiation dose). A bolus of 80 ml iomeprol (Iomeron 400, Bracco, Milan, Italy) was injected at 5 ml/s followed by 40 ml saline flush. Datasets were reconstructed from the retrospectively gated raw data with an effective slice thickness of 0.625 mm.

Post-processing of the MSCT calcium scans and coronary angiograms was performed on a dedicated workstation (Advantage, GE Healthcare, Waukesha, Wisconsin, USA). The total CS was calculated using the Agatston method. Coronary anatomy was evaluated using the contrast-enhanced helical examinations. Coronary arteries were divided into 17 segments according to the modified American Heart Association classification.¹¹ All studies were interpreted by two experienced observers blinded to the results of coronary angiography and MRI with an intention to diagnose strategy. Discrepancies in interpretation were resolved by consensus. MSCT results were classified on a patient and vessel level as normal (no identifiable plaque or wall irregularities), non-significant, non-obstructive CAD (<50% luminal narrowing) or significant, obstructive CAD ($\geq 50\%$ luminal narrowing).

Magnetic resonance imaging

MRI was performed with a 1.5 Tesla scanner (Symphony, Siemens, Erlangen, Germany), using a multi-channel surface coil array. A first pass MRI perfusion scan was performed during adenosine stress to determine the presence of hypo-enhancement indicative of a perfusion defect during stress. After first pass perfusion imaging delayed contrast-enhanced MRI was performed to determine the presence of areas with hyper-enhancement indicating scar tissue. The integration of the 2 datasets provides differentiation between ischemia and scar tissue.^{12, 13} Studies were analyzed per patient and per vascular territory. To assess MRI results per vascular territory, the myocardium was divided into segments using a modified 17-segment model described elsewhere, without the apex.¹⁴ Segments 1, 2, 7, 8, 13, and 14 were allocated to the left anterior descending artery, segments 3, 4, 9, 10, and 15 to the right coronary artery, and finally segments 5, 6, 11, 12, and 16 were allocated to the left circumflex artery.

First pass stress perfusion MRI

During the examination, pharmacological stress was applied using adenosine infusion. In order to obtain maximum vasodilatory effect, patients were instructed to abstain from smoking, tea, and coffee, and were asked to stop anti-anginal medication and beta-blockers for 24 hours before the examination.

The first pass of 0.1 mmol/kg gadolinium-DOTA (Dotarem, Guerbet, Gorinchem, the Netherlands) injected at a rate of 3 ml/s was assessed after 6 minutes of adenosine infusion (140 $\mu\text{g}/\text{kg}/\text{min}$) in 3 short-axis slices at the basal, mid and apical level of the LV. Using the following parameters: TrueFISP with a notched saturation pulse, inversion time 230 ms, repetition time/echo time 427 ms/ 1.53 ms, flip angle 8°, matrix 256 by 122, field of view 341 by 420 mm, slice thickness of 8 mm with a slice gap of 8 mm.

The images were evaluated by 2 experienced observers blinded to the MSCT and QCA results using dedicated software (MASS, version 5.1, Medis, Leiden, The Netherlands). Using the short-axis acquisitions, first pass stress perfusion MRI scans were visually scored using the proposed modified 17-segment model, without the apex.¹⁴ Each segment was graded on a 5-point scale (0=no hypo-enhancement, 1=hypo-enhancement 1 to 25% of left ventricular (LV) wall thickness, 2=hypo-enhancement 26 to 50% of LV wall thickness, 3=hypo-enhancement 51-75% of LV wall thickness, and 4=hypo-enhancement 76-100% of LV wall thickness.¹⁵

Delayed contrast-enhanced MRI

Delayed contrast-enhanced MRI was obtained 15 minutes after infusion of gadolinium in 3 short-axis slices at the basal, mid and apical level of the LV, using inversion recovery Turbo-Flash technique (repetition time/echo time 705 ms/ 4.30 ms, flip angle 25°, matrix 256 by 166, field of view 341 by 420 mm, and a slice thickness of 6 mm). The inversion time was adjusted to null normal myocardium.

The images were evaluated by 2 experienced observers blinded to the MSCT and QCA results using dedicated software (MASS, version 5.1, Medis, Leiden, The Netherlands). Hyper-enhancement on the delayed contrast-enhanced MR images was scored according to the same segment model used for the analysis of first pass stress perfusion MRI.¹⁴ Each segment was graded on a 5-point scale (0 = no hyper-enhancement, 1=hyper-enhancement 1 to 25% of LV wall thickness, 2=hyper-enhancement 26 to 50% of LV wall thickness, 3=hyper-enhancement 51-75% of LV wall thickness, and 4=hyper-enhancement 76-100% of LV wall thickness.¹⁵

Differentiation between ischemia and scar

Ischemia was defined as the presence of hypo-enhancement during first pass stress perfusion in the absence of hyper-enhancement on the delayed contrast-enhanced MRI. In segments with scar the degree of hyper-enhancement (1% through 100% of LV wall thickness) was subtracted from the degree of hypo-enhancement during the first pass perfusion to differentiate between partially reversible defects and total irreversibility. Segments with partial reversibility were subsequently graded as ischemic.

Data analysis

Continuous variables were expressed as mean with standard deviation, and proportions were expressed in percentages. MSCT observations were compared to QCA to evaluate the ability of MSCT to detect significant stenosis ($\geq 50\%$ luminal narrowing). Secondly, MSCT was compared to MRI to determine the relation between anatomic assessment with MSCT

and ischemia on MRI. Finally flow charts were created to determine the relationship between MSCT, MRI and QCA. Comparisons were performed on a patient and vascular territory level.

Results

Patients were clinically referred for invasive coronary angiography because of chest pain suspect for CAD. All characteristics of the study population are listed in Table 1. Briefly, the average age was 57 ± 9 years, and the population consisted of 60% male patients. The majority of patients (83%) presented with an intermediate pre-test likelihood of CAD.

Table 1. Patient characteristics

Gender (male)	32 (60%)
Age (yrs)	57 ± 9
Risk Factors	
Diabetes	8 (15%)
Hypertension	30 (57%)
Hypercholesterolemia	29 (55%)
Family history CAD	23 (43%)
Current Smoking	16 (30%)
Obesity (BMI ≥ 30)	9 (17%)
Pre-test likelihood of CAD	
Low	3 (6%)
Intermediate	44 (83%)
High	6 (11%)
Significant CAD on QCA	15 (28%)
1-vessel disease	7 (13%)
2-vessel disease	6 (11%)
3-vessel disease	2 (4%)

Multi-slice computed tomography

The heart rate exceeded 65 beats per minute in 35 patients (66%), and in these patients additional beta-blocking medication was administered. As a result, the average heart rate during MSCT was 59 ± 8 beats per minute. The average CS of the population was 251 ± 487 . Calcifications were present in 37 patients (70%), and a CS > 400 was observed in 10 patients (19%).

On a patient level, the MSCT angiogram was classified as normal in 14 (26%) patients, non-significant, non-obstructive CAD ($< 50\%$ luminal narrowing) in 24 (45%), and significant, obstructive CAD ($\geq 50\%$ luminal narrowing) was observed in the remaining 15 (28%) patients. On a vessel level, normal coronary anatomy was present in 83 (52%) vessels,

non-significant disease (<50% luminal narrowing) in 51 (32%), and significant disease (\geq 50% luminal narrowing) in 25 (16%) vessels.

Magnetic resonance imaging

First pass perfusion MRI during adenosine stress revealed normal myocardial perfusion in 34 patients (64%). A perfusion defect was observed in the remaining 19 patients (36%). During the delayed contrast-enhanced scan hyper-enhancement was observed in 3 patients (6%). In these patients the first pass perfusion defects were only partially attributable to scar. Thus on a patient level ischemia was absent in 34 (64%) patients while a perfusion abnormality indicative of ischemia was observed in the remaining 19 (36%) patients. On a vascular level, 126 (79%) territories showed no hypo-enhancement during first pass perfusion MRI. Thus, hypo-enhancement was seen in the remaining 33 (21%) vascular territories. During delayed contrast-enhanced MRI hyper-enhancement was observed in 4 of the territories showing first pass perfusion abnormalities. In one territory partial reversibility was observed while in the remaining 3 territory the abnormalities observed during first pass perfusion were entirely attributable to scar tissue. Accordingly, on a vascular territory level, perfusion abnormalities indicative of ischemia were present in 30 (19%) vascular territories.

Relation between anatomic and functional imaging

Relation between MSCT and QCA

The agreement between MSCT and QCA for the detection of significant CAD is shown in Table 2A. MSCT correctly identified 13 of 15 (87%) significant, obstructive lesions on QCA (\geq 50%) and accurately ruled out the presence of significant disease in 36 of 38 (95%) patients without significant lesions on QCA. In Table 2B the relationship between MSCT and QCA is illustrated on a vessel level. MSCT correctly identified 20 of 25 (80%) significant, obstructive stenoses and was able to correctly rule out a significant lesion in 129 of 134 (96%) vessels without significant lesions on QCA.

Relation between MSCT and MRI

Figure 1 (Panel A) illustrates the complementary value of MSCT and MRI. Only 67% of patients with a significant, obstructive lesion (\geq 50% luminal narrowing) on MSCT showed ischemia on MRI. Vice versa, a significant, obstructive stenosis was observed in 15% of patients with normal perfusion on MRI. A similar complementary value between MSCT and MRI was observed when assessing the relation between MSCT and MRI on a vascular territory level (Figure 1, Panel B).

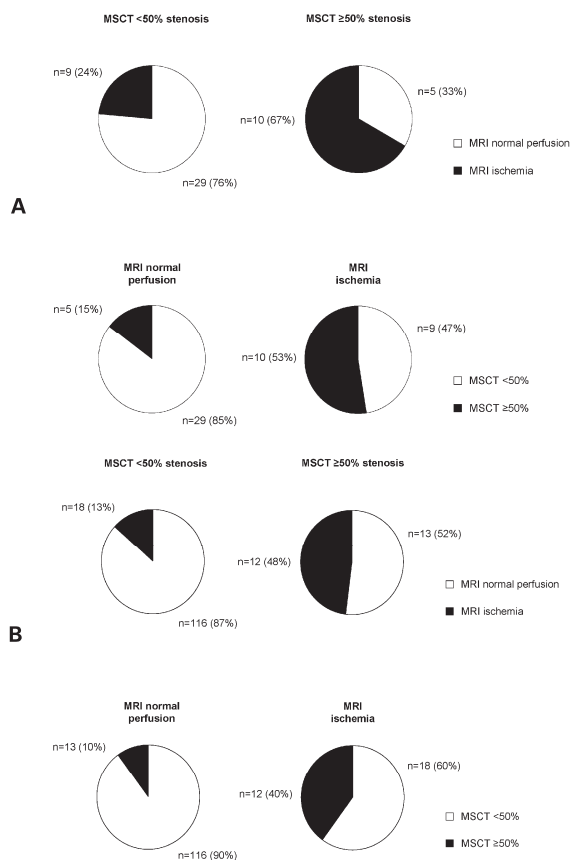
Figure 2 further illustrates the complimentary value of MRI to MSCT. In this Figure, the results of MRI and QCA are presented in patients with a normal MSCT, non-significant,

Table 2a. Agreement between MSCT and QCA on a patient level.

		QCA <50%	QCA ≥50%
MSCT			
<50%	(n = 38)	36 (95%)	2 (13%)
≥50%	(n = 15)	2 (5%)	13 (87%)
Total		38	15

Table 2b. Agreement between MSCT and QCA on a vessel level.

		QCA <50%	QCA ≥50%
MSCT			
<50%	(n = 134)	129 (96%)	5 (20%)
≥50%	(n = 25)	5 (4%)	20 (80%)
Total		134	25

**Figure 1.** Pie charts depicting the relationship between the anatomic information obtained by MSCT and the functional information from MRI on a patient level (Panel A) and on a vascular territory level (Panel B).

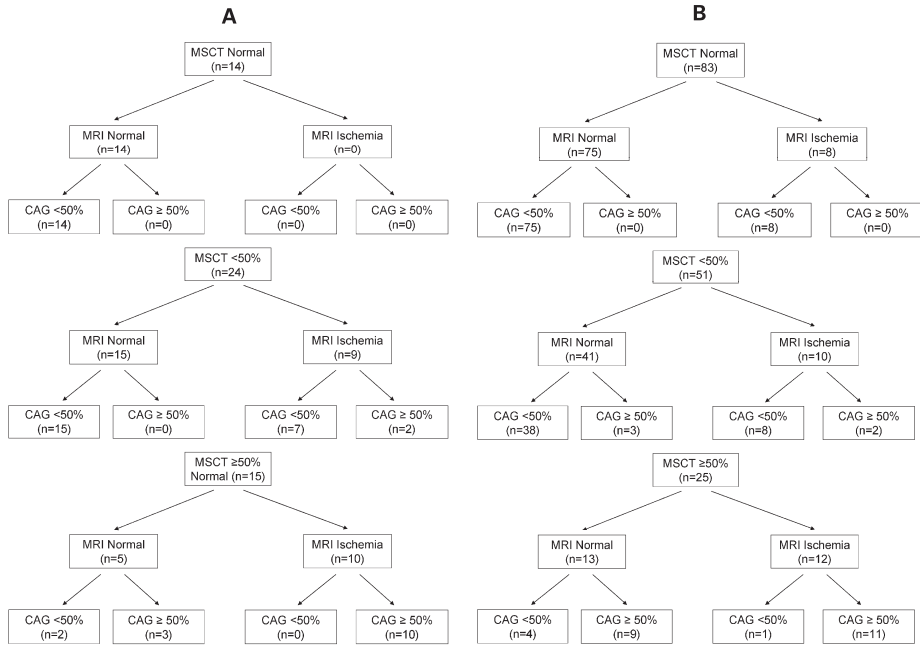


Figure 2. Flow charts describing the relationship between MSCT, MRI and QCA on a patient level (Panel A) and on a vascular territory level (Panel B). These flow charts illustrate the complimentary value of MRI in patients with non-significant and significant stenosis on MSCT.

non-obstructive CAD (MSCT <50% luminal narrowing) and in patients with significant, obstructive CAD (MSCT ≥50% luminal narrowing). Importantly, MRI was normal in all patients with a normal MSCT (n=14, 100%). Furthermore, no significant stenoses were observed on QCA in these patients as well. In the 24 patients with non-significant, non-obstructive CAD (<50% luminal narrowing) on MSCT, MRI was normal in 15 (63%) while ischemia was observed in 9 (37%). Thus, approximately 1 out of 3 people with non-significant, non-obstructive CAD (<50% narrowing) had ischemia on perfusion MRI. In two patients classified as having non-significant CAD on MSCT a significant stenosis was observed on QCA. Importantly, ischemia was observed on MRI in both of these patients. Nevertheless, in all patients without significant stenosis on MSCT and normal perfusion on MRI, absence of a significant stenosis was confirmed on QCA.

Finally, in the 15 patients with a significant stenosis on MSCT (≥50% luminal narrowing), MRI was normal in 5 (33%) and ischemia was observed in 10 (67%). In other words, 1 out of 3 patients with a significant stenosis on MSCT had normal perfusion on MRI. Two patients were classified as having a significant stenosis on MSCT while QCA was non-significant. Ischemia on MRI was absent in both of these patients. Importantly however, in all patients with both a significant stenosis on MSCT and ischemia on MRI the presence of a significant

stenosis was confirmed on QCA. Similar findings were observed on a vascular territory level. An example of a patient with a perfusion defect on MRI, a significant stenosis on MSCT and a significant stenosis on QCA is presented in Figure 3.

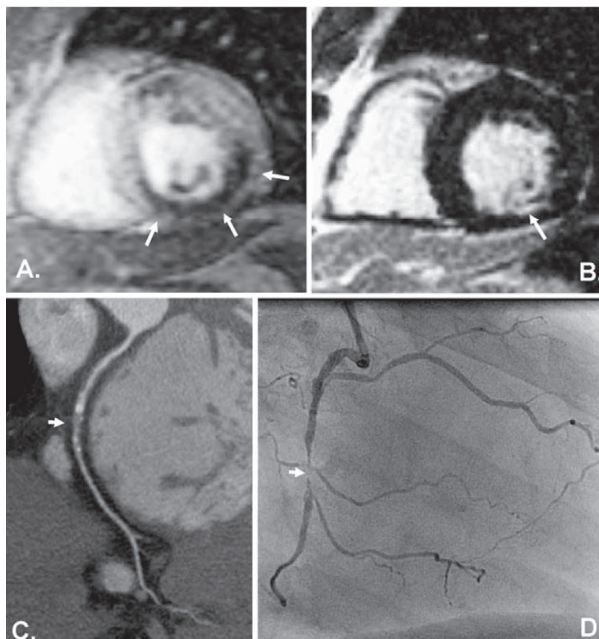


Figure 3. Case example of a patient with a large perfusion defect in the inferior wall on MRI during first pass perfusion (Panel A) and a small area showing delayed enhancement (Panel B) suggesting the presence of predominantly ischemia in addition to a small region of scar tissue. On MSCT a corresponding high-grade stenosis was identified in the right coronary artery (Panel C). On coronary angiography the right coronary angiography was occluded with collaterals originating from the right ventricular branch (Panel D).

Discussion

The main finding of the current study is that MSCT coronary angiography and MRI perfusion imaging may provide complementary information regarding the presence, extent and severity of CAD.

Complementary value of MSCT and MRI

In patients with a significant stenosis on MSCT, normal perfusion on MRI was observed in 33%, suggesting that still a large proportion of significant stenoses on MSCT have no effect on myocardial perfusion (not associated with stress-inducible ischemia). Simultaneously, these findings indicate that normal perfusion on MRI cannot rule out the presence of significant atherosclerosis. Indeed a significant stenosis was still observed in approximately 1 out

of 6 of patients without evidence of ischemia on MRI. Although currently no comparison has been available between MSCT and MRI perfusion imaging, several previous studies have assessed the relationship between conventional coronary angiography and MRI.^{13, 16-18} In a meta-analysis by Nandalur et al. significant stenosis on conventional coronary angiography was associated with abnormal perfusion on MRI in 58% to 97% of patients.¹⁸ Initially, this correlation seems higher than that observed in the current study when comparing MSCT to MRI. However, differences in methodology such as the use of different cut-offs (50%, 70% and 75% luminal narrowing) for significant stenosis as well as a differences in disease prevalence (on average \approx 60% in the meta-analysis by Nandalur et al. compared to \approx 30% in the current study) may have exerted major influence on individual observations.¹⁹

In patient populations more comparable to our current study in patients with an intermediate pre-test likelihood, the relationship between coronary anatomy and myocardial perfusion has been studied by comparing MSCT to SPECT or PET imaging.^{3, 4} In the study by Schuijff et al., only 50% of patients with a significant (\geq 50%) lesion on MSCT had an abnormal perfusion on SPECT.⁴ Conversely, normal perfusion on SPECT was unable to rule out the presence of significant CAD or atherosclerosis in general. In a more recent study by Gaemperli et al. the MSCT observations were corroborated by invasive coronary angiography.²⁰ The predictive value of obstructive CAD on MSCT was 58% for the prediction of a reversible perfusion defect on SPECT. Importantly, the accuracy of MSCT to identify abnormal perfusion on SPECT was similar to that of quantitative coronary angiography. These observations support the notion that the low predictive value of MSCT for reversible perfusion defects is not caused by inaccuracies in stenosis detection with MSCT but merely reflects inherent differences of the techniques. The results of the current study comparing MSCT to MRI perfusion imaging are in line with those observed when comparing MSCT to nuclear perfusion imaging, and further support that MSCT and MRI may provide complementary information with regard to the identification of the presence, extent and severity of CAD.

Combined anatomic and functional imaging

The combined assessment of coronary anatomy and myocardial perfusion may not only provide complementary information regarding different aspects of CAD, but may also result in a higher diagnostic accuracy for the detection of hemodynamically significant coronary artery lesions as has been suggested in preliminary work by Rispler et al.²¹ In a study population of 56 patients, hybrid imaging using a SPECT MSCT scanner resulted in improved specificity and positive predictive value for the identification of hemodynamically significant coronary lesions. In line with these results the addition of MRI to MSCT improved identification of significant stenosis on QCA in the current study; all patients with both a significant stenosis on MSCT and ischemia on MRI were associated with a significant stenosis on QCA. Conversely,

in all patients without significant stenosis on MSCT and normal perfusion on MRI, absence of a significant stenosis was confirmed on QCA.

Possibly, diagnostic accuracy may improve even further on a vessel basis by fusing both MSCT and MRI perfusion datasets into a single, three-dimensional anatomic representation of the heart with overlying coronary anatomy. This approach may enable accurate allocation of perfusion defects to the corresponding stenosis. Gaemperli et al. assessed the accuracy of cardiac image fusion by combining MSCT and SPECT.²² The authors concluded that in almost one third of patients, fusion of MSCT and SPECT resulted in increased diagnostic performance, especially in functionally relevant lesions in distal segments and diagonal branches and in vessels with extensive disease or calcifications. Fusion of MSCT and MRI perfusion datasets may potentially provide similar information in the future.

Clinical implications

The combination of anatomic imaging for identification of atherosclerosis and functional imaging for assessment of myocardial perfusion may improve risk stratification and have important implications for patient management.²³ Recently, a flow chart incorporating anatomic and functional imaging has been suggested which separates patients into three groups for management: the first group with normal coronary anatomy who can be safely discharged, a second group with non-flow limiting stenosis requiring medical treatment and aggressive risk factor modification and a final group of patients with a flow-limiting stenosis requiring further evaluation with conventional coronary angiography with potentially revascularization.²⁴

Such diagnostic strategies initially proposed the use of SPECT imaging for assessment of ischemia in combination with anatomical assessment using MSCT. Indeed, SPECT imaging remains the most robust and extensively used modality for assessment of ischemia. However, the combination of SPECT and MSCT, although having the potential to improve patient management, is associated with an increased radiation burden.²⁵ Because of the lack of ionizing radiation, MRI may be considered a promising alternative to SPECT for combined anatomic and functional assessment with MSCT, although the limited availability of MRI perfusion imaging and the associated costs currently inhibit the widespread use of this technique. Therefore the utilization of MRI in this setting will remain largely dependent on local availability.

Study limitations

Both MSCT and MRI have some general limitations. Even though the diagnostic accuracy of MSCT is high, images are of poor quality in still a small percentage of patients. This percentage is expected to continue to decrease with newer generation scanners. Another

limitation of MSCT is the considerable radiation dose associated with the currently used 64-slice system. Radiation burden can however be decreased using newer generation scanners and protocols.^{26, 27}

A general limitation of MRI includes the relatively longer examination times which can be uncomfortable for some patients. Furthermore a limitation of the clinical applicability of MRI perfusion imaging is the wide variation in scan protocols, scanners and data analysis methodologies that currently exist. In the present study a qualitative approach was used similar to previously published studies.^{9, 13, 28, 29} Other studies have used quantitative methodologies which have the advantage of decreased inter-observer variability. However their disadvantages include that quantification may be time consuming while optimal and standardized approaches have not yet been defined.

Conclusion

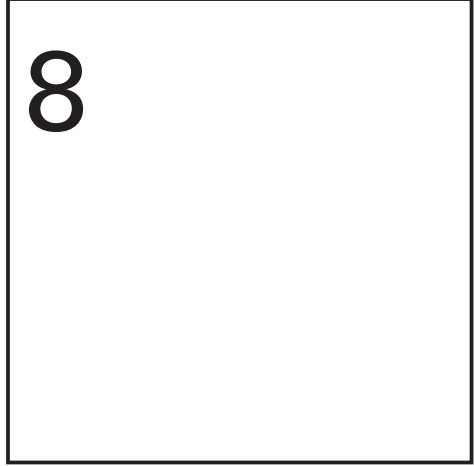
The anatomic and functional data obtained with MSCT and MRI provide complementary information regarding the assessment of CAD. These findings support the sequential or combined assessment of anatomy and function in patients presenting with suspected CAD.

References

1. Miller JM, Rochitte CE, Dewey M, et al. Diagnostic Performance of Coronary Angiography by 64-Row CT. *N Engl J Med* 2008;359:2324-36.
2. Meijboom WB, Meijns MFL, Schuijff JD, et al. Diagnostic Accuracy of 64-slice Computed Tomography Coronary Angiography: A Prospective Multicenter, Multivendor Study. *J Am Coll Cardiol* 2008;52:2135-44.
3. Di Carli MF, Dorbala S, Curillova Z, et al. Relationship between CT coronary angiography and stress perfusion imaging in patients with suspected ischemic heart disease assessed by integrated PET-CT imaging. *J Nucl Cardiol* 2007;14:799-809.
4. Schuijff JD, Wijns W, Jukema JW, et al. Relationship between noninvasive coronary angiography with multi-slice computed tomography and myocardial perfusion imaging. *J Am Coll Cardiol* 2006;48:2508-14.
5. Klocke FJ, Simonetti OP, Judd RM, et al. Limits of detection of regional differences in vasodilated flow in viable myocardium by first-pass magnetic resonance perfusion imaging. *Circulation* 2001;104:2412-6.
6. Lee DC, Simonetti OP, Harris KR, et al. Magnetic resonance versus radionuclide pharmacological stress perfusion imaging for flow-limiting stenoses of varying severity. *Circulation* 2004;110:58-65.
7. Costa MA, Shoemaker S, Futamatsu H, et al. Quantitative magnetic resonance perfusion imaging detects anatomic and physiologic coronary artery disease as measured by coronary angiography and fractional flow reserve. *J Am Coll Cardiol* 2007;50:514-22.
8. Schwitter J, Nanz D, Kneifel S, et al. Assessment of myocardial perfusion in coronary artery disease by magnetic resonance: a comparison with positron emission tomography and coronary angiography. *Circulation* 2001;103:2230-5.
9. Schwitter J, Wacker CM, van Rossum AC, et al. MR-IMPACT: comparison of perfusion-cardiac magnetic resonance with single-photon emission computed tomography for the detection of coronary artery disease in a multicentre, multivendor, randomized trial. *Eur Heart J* 2008;29:480-9.
10. Diamond GA, Forrester JS. Analysis of probability as an aid in the clinical diagnosis of coronary-artery disease. *N Engl J Med* 1979;300:1350-8.
11. Austen WG, Edwards JE, Frye RL, et al. A reporting system on patients evaluated for coronary artery disease. Report of the Ad Hoc Committee for Grading of Coronary Artery Disease, Council on Cardiovascular Surgery, American Heart Association. *Circulation* 1975;51:5-40.
12. Fuster V, Kim RJ. Frontiers in cardiovascular magnetic resonance. *Circulation* 2005;112:135-44.
13. Klem I, Heitner JF, Shah DJ, et al. Improved detection of coronary artery disease by stress perfusion cardiovascular magnetic resonance with the use of delayed enhancement infarction imaging. *J Am Coll Cardiol* 2006;47:1630-8.
14. Cerqueira MD, Weissman NJ, Dilsizian V, et al. Standardized myocardial segmentation and nomenclature for tomographic imaging of the heart - A statement for healthcare professionals from the Cardiac Imaging Committee of the Council on Clinical Cardiology of the American Heart Association. *Circulation* 2002;105:539-42.
15. Wu E, Judd RM, Vargas JD, et al. Visualisation of presence, location, and transmural extent of healed Q-wave and non-Q-wave myocardial infarction. *Lancet* 2001;357:21-8.
16. Giang TH, Nanz D, Coulden R, et al. Detection of coronary artery disease by magnetic resonance myocardial perfusion imaging with various contrast medium doses: first European multi-centre experience. *Eur Heart J* 2004;25:1657-65.
17. Nagel E, Klein C, Paetsch I, et al. Magnetic resonance perfusion measurements for the noninvasive detection of coronary artery disease. *Circulation* 2003;108:432-7.

18. Nandalur KR, Dwamena BA, Choudhri AF, et al. Diagnostic performance of stress cardiac magnetic resonance imaging in the detection of coronary artery disease: a meta-analysis. *J Am Coll Cardiol* 2007;50:1343-53.
19. Min JK, Shaw L. Noninvasive Diagnostic and Prognostic Assessment of Individuals With Suspected Coronary Artery Disease. *Circ Cardiovasc Imaging* 2008;1:270-81.
20. Gaemperli O, Schepis T, Valenta I, et al. Functionally relevant coronary artery disease: comparison of 64-section CT angiography with myocardial perfusion SPECT. *Radiology* 2008;248:414-23.
21. Rispler S, Keidar Z, Ghersin E, et al. Integrated single-photon emission computed tomography and computed tomography coronary angiography for the assessment of hemodynamically significant coronary artery lesions. *J Am Coll Cardiol* 2007;49:1059-67.
22. Gaemperli O, Schepis T, Valenta I, et al. Cardiac image fusion from stand-alone SPECT and CT: clinical experience. *J Nucl Med* 2007;48:696-703.
23. van Werkhoven JM, Schuijf JD, Gaemperli O, et al. Prognostic value of multislice computed tomography and gated single-photon emission computed tomography in patients with suspected coronary artery disease. *J Am Coll Cardiol* 2009;53:623-32.
24. Schuijf JD, Jukema JW, van der Wall EE, et al. The current status of multislice computed tomography in the diagnosis and prognosis of coronary artery disease. *J Nucl Cardiol* 2007;14:604-12.
25. Einstein AJ. Radiation risk from coronary artery disease imaging: how do different diagnostic tests compare? *Heart* 2008;94:1519-21.
26. Husmann L, Valenta I, Gaemperli O, et al. Feasibility of low-dose coronary CT angiography: first experience with prospective ECG-gating. *Eur Heart J* 2008;29:191-7.
27. Rybicki FJ, Otero HJ, Steigner ML, et al. Initial evaluation of coronary images from 320-detector row computed tomography. *Int J Cardiovasc Imaging* 2008;24:535-46.
28. Cury RC, Cattani CA, Gabure LA, et al. Diagnostic performance of stress perfusion and delayed-enhancement MR imaging in patients with coronary artery disease. *Radiology* 2006;240:39-45.
29. Schuijf JD, Kaandorp TA, Lamb HJ, et al. Quantification of myocardial infarct size and transmural-ity by contrast-enhanced magnetic resonance imaging in men. *Am J Cardiol* 2004;94:284-8.

Chapter 8



Predictive value of multislice computed tomography variables of atherosclerosis for ischemia on stress-rest single-photon emission computed tomography

JE van Velzen, JD Schuijf, JM van Werkhoven, BA Herzog,
AP Pazhenkottil, E Boersma, FR de Graaf, AJ Scholte, LJ Kroft,
A de Roos, MP Stokkel, JW Jukema, PA Kaufmann, EE van der Wall,
JJ Bax

Abstract

Previous studies have shown that the presence of stenosis alone on multislice computed tomography (MSCT) has a limited positive predictive value for the presence of ischemia on myocardial perfusion imaging (MPI). The purpose of this study was to assess which variables of atherosclerosis on MSCT angiography are related to ischemia on MPI. Both MSCT and MPI were performed in 514 patients. On MSCT, the calcium score, degree of stenosis ($\geq 50\%$ and $\geq 70\%$ stenosis), plaque extent and location were determined. Plaque composition was classified as non-calcified, mixed or calcified. Ischemia was defined as a summed difference score ≥ 2 on a per patient basis. Ischemia was observed in 137 patients (27%). On a patient basis, multivariate analysis showed that the degree of stenosis (presence of $\geq 70\%$ stenosis, OR 3.5), plaque extent and composition (mixed plaques ≥ 3 , OR 1.7 and calcified plaques ≥ 3 , OR 2.0) and location (atherosclerotic disease in left main coronary artery and/or proximal left anterior descending coronary artery, OR 1.6) were independent predictors for ischemia on MPI. In addition, MSCT variables of atherosclerosis such as plaque extent, composition and location had significant incremental value for the prediction of ischemia over the presence of $\geq 70\%$ stenosis. In conclusion, in addition to the degree of stenosis, MSCT variables of atherosclerosis describing plaque extent, composition and location are predictive of the presence of ischemia on MPI.

Introduction

Over the past decade, multislice computed tomography (MSCT) angiography has emerged as a non-invasive modality for visualization of the coronary arteries. Recently, several studies have addressed the diagnostic accuracy of MSCT as compared to invasive coronary angiography reporting high accuracies for the detection of 50% stenosis.¹ Importantly, the high negative predictive value of 99% indicates that the technique may be particularly useful for ruling out the presence of coronary artery disease (CAD) in patients with lower likelihood of CAD. On the other hand, while MSCT angiography provides insight into the severity and extent of anatomical disease, it is currently unable to evaluate the hemodynamical relevance of CAD. In fact, previous studies have revealed a large discrepancy between the presence of atherosclerosis on MSCT angiography and the presence of ischemia during functional testing.²⁻⁵ These investigations demonstrated that approximately only half of obstructive stenoses ($\geq 50\%$ luminal narrowing) on MSCT were associated with abnormal perfusion, whereas a large proportion of obstructive lesions on MSCT did not result in perfusion abnormalities. Therefore, identification of anatomical MSCT variables of atherosclerosis that are associated with ischemia on MPI, in addition to the presence of obstructive CAD, may improve selection of further diagnostic and/or therapeutic management. Thus, the purpose of this study was to identify variables of atherosclerosis on MSCT angiography that are related to ischemia on MPI, in addition to the presence of obstructive CAD.

Methods

Patients and study protocol

The study population consisted of 524 patients who were clinically referred for functional and anatomical imaging because of chest pain or an elevated risk profile as part of an ongoing registry addressing the relative merits of MSCT in relation to other imaging techniques. Patients underwent both myocardial perfusion imaging (MPI) with stress-rest gated single photon emission computed tomography (SPECT) and MSCT within 3 months in two different institutions. Patients were included at the University Hospital in Zurich, Switzerland ($n=263$) and at the Leiden University Medical Center, Leiden, the Netherlands ($n=261$). Exclusion criteria were: known CAD (previous myocardial infarction, percutaneous coronary intervention and coronary artery bypass surgery), atrial fibrillation, renal insufficiency (glomerular filtration rate <30 ml/min), known allergy to iodine contrast and pregnancy. The clinical symptoms of included patients were recorded and patients were further classified as having a low, intermediate or high pre-test likelihood of obstructive CAD using the method described by Diamond and Forrester.⁶

Stress-rest gated MPI

Patients were instructed to withhold beta-blocking medication and calcium antagonists 48 hours before examination and caffeine 12 hours before examination. For each center a different gated MPI protocol was used. In Leiden (n=261) a two-day gated stress-rest SPECT protocol was performed using either technetium-99 tetrofosmin (500 MBq) or technetium-99m sestamibi (500 MBq). In patients that were able to exercise, symptom-limited bicycle test was performed and in patients unable to exercise pharmacological stress was performed using adenosine or dobutamine. In Zurich (n=263) a one day gated stress-rest SPECT was performed using adenosine stress and technetium-99m tetrofosmin (300 MBq at peak stress and 900 MBq at rest). The images were acquired on a triple-head SPECT camera (GCA 9300/HG, Toshiba Corp., Tokyo, Japan) or a dual-head detector camera (Millennium VG & Hawk-eye, General Electric Medical Systems, Milwaukee, WI, USA; or Vertex Epic ADAC Pegasus, Philips Medical Systems, Eindhoven, the Netherlands). All cameras were equipped with low energy high resolution collimators. A 20% window was used with a 140-keV energy peak of technetium-99m, and data were stored in a 64x64 matrix. Subsequently, stress-rest gated MPI datasets were quantitatively evaluated using previously validated automated software.⁷ The data were reconstructed into long- and short-axis perpendicular to the heart axis. A 20-segment model was used in which the myocardial segments were assigned to the different perfusion territories. Each segment was scored by an experienced observer according to the standard scoring scale of 0-4 (normal, mild, moderate, severe reduction or absence of uptake). The total segmental perfusion scores during stress and rest were added to calculate the summed stress score (SSS) and the summed rest score (SRS), respectively. The summed difference score (SDS) was calculated as the sum of difference between the SRS and SSS. Ischemia was defined as a $SDS \geq 2$ and severe ischemia was defined as a $SDS \geq 8$.⁸ On a per vessel basis, the presence of ischemia was assessed visually in the corresponding vascular territory. Consequently, ischemia in the anterior and septal wall was allocated to the left anterior descending coronary artery, ischemia in the lateral wall was allocated to the left circumflex coronary artery and ischemia in the inferior wall was allocated to the right coronary artery.⁹

MSCT coronary angiography

Heart rate and blood pressure were evaluated before each scan. If a patient's heart rate was above 65 beats per minute and no contra-indications existed, beta-blocking medication was administered one hour before the examination (50-100 mg metoprolol orally or 5-10 mg metoprolol intravenously).

In the first 41 patients data acquisition was performed using a 16-slice MSCT scanner (Aquilion 16, Toshiba Medical Systems, Tokyo, Japan) with a collimation of 16 x 0.5 mm, a gantry rotation time of 400 ms, tube voltage of 120 kV and tube current of 250 to 350 mA.

A 64-slice MSCT scanner (Aquilion 64, Toshiba Medical Systems, Tokyo, Japan or General Electrics Lightspeed VCT, Milwaukee, WI, USA) was used for the remaining 483 patients with a collimation of 64 x 0.5 mm, a gantry rotation time of 400 ms, tube voltage of 100 to 135 kV and tube current of 250 to 350 mA, depending on body shape. First, a non-contrast enhanced low dose scan prospectively triggered at 75% of the R-R interval was performed before helical scanning. This examination was used for calcium scoring and followed by a triggered helical scan. For the 16-slice MSCT non-ionic contrast (Iomeron 400, Bracco, Milan, Italy) was administered in the ante-cubital vein, with a dose of 130 to 140 ml and a flow-rate of 4 ml/s, followed by a saline flush. For 64-slice MSCT, 80 to 110 ml contrast was administered with a flow rate of 5 ml/s followed by a saline flush. Automatic detection of peak enhancement in the descending aorta was used for timing. Subsequently data sets were reconstructed at the best phase of the R-R interval and transferred to dedicated work stations (Vitrea2, Vital Images, USA, or Advantage, GE Healthcare, USA).

The non-contrast enhanced CT images were used to calculate the calcium score using the Agatston method.¹⁰ MSCT angiographic examinations were evaluated in consensus by 2 experienced readers including an interventional cardiologist blinded to stress-rest SPECT findings. A 17-segment model modified according to the American Heart Association was used and for each segment was determined if atherosclerosis was present using axial and/or orthogonal images and curved multiplanar reconstructions. If atherosclerosis was present, the degree of stenosis was graded as non-obstructive (<50% stenosis), obstructive (≥50% stenosis) and severely obstructive (≥70% stenosis). Additionally, the extent of atherosclerosis was determined by assessing the number of diseased segments. Consequently, plaques were scored according to plaque composition (non-calcified, mixed or calcified). Non-calcified plaques were regarded as plaques having a lower CT attenuation compared to the contrast lumen and no visible calcifications, calcified plaques were plaques with predominantly high CT attenuation and without non-calcified plaque elements, and mixed plaques were plaques consisting of both non-calcified and calcified elements. Lastly, the location of disease was classified as being present in left main coronary artery (LM) and/or proximal left anterior descending coronary artery (LAD) or not (example provided in Figure 1).

Statistical analysis

Continuous data were expressed as mean and standard deviation, and categorical data were expressed in numbers and percentages. Binary logistic regression analysis was performed to determine the predictive value of MSCT variables of atherosclerosis for presence of ischemia on MPI on both a patient and vessel basis. First univariate analysis of baseline clinical risk variables (age and gender), calcium score and MSCT variables was performed. To analyze the predictive value of variables of atherosclerosis on MSCT (degree of stenosis, plaque

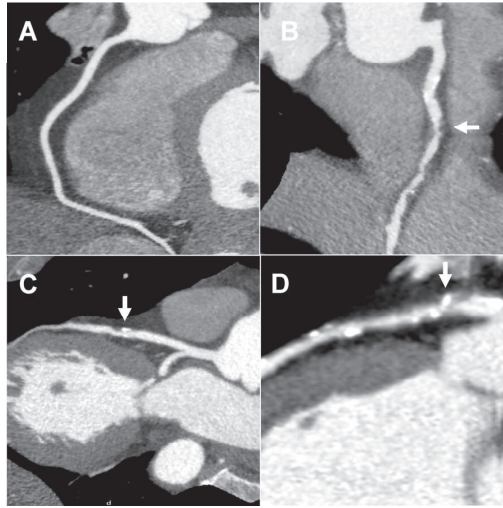


Figure 1. Examples of the classification of different variables of atherosclerosis on MSCT. Panel A: Assessment of the presence of atherosclerosis: curved multiplanar reconstruction (MPR) of right coronary artery (RCA) revealing the absence of atherosclerosis. Panel B: Assessment of the degree of stenosis: MPR showing a lesion resulting in $\geq 50\%$ stenosis in the mid RCA (arrow). Panel C: Assessment of the extent and composition of atherosclerotic disease: MPR of the left anterior descending coronary artery (LAD) revealing a single mixed plaque (arrow). Panel D: Assessment of location of atherosclerosis: MPR of the LAD demonstrating the presence of an atherosclerotic lesion in the left main coronary artery and proximal LAD (arrow).

extent, composition and location), optimal binary cutoffs were created for analysis. For each variable, an odds ratio with 95% confidence interval (OR (CI 95%)) was calculated.

The current study used 2 generations of MSCT scanners (16-slice and 64-slice), thus to correct for scanner type, scanner type was included in the univariate analysis. In addition, interaction was assessed between scanner type and MSCT variables of atherosclerosis (describing degree of stenosis, plaque extent, composition and location). In this analysis, no interaction was demonstrated between MSCT scanner type and MSCT variables of atherosclerosis (data not shown).

The intention was to build a multivariate model that combines clinical variables and MSCT variables of atherosclerosis for the prediction of ischemia on MPI, in a stepwise fashion. The first model consisted of clinical risk variables only. Consequently, the presence of (severely) obstructive CAD was added, followed by plaque extent and composition (≥ 3 mixed plaques and ≥ 3 calcified plaques). Finally, plaque location (atherosclerotic disease in the LM and/or proximal LAD) was added to the model. For each next iterative step, variables may not remain statistically significant. Thus, all variables with a p-value < 0.15 were kept in the model in order not to miss clinically relevant predictors of ischemia.

The performance of the final multivariate model for prediction of ischemia on both a patient and vessel basis was studied with respect to discrimination and calibration. Discrimination was quantified by a measure of concordance, the c-index. For binary outcomes the c-index is identical to the area under the receiver operating characteristic (ROC) curve. The c-index lies between 0.5 and 1, and is better if closer to one.¹¹ Calibration refers to whether the predicted risks agree with the observed risk frequencies. Calibration was measured with the Hosmer-Lemeshow goodness-of-fit test ($p > 0.10$ considered to indicate lack of deviation between the model and observed event rates). Statistical analysis was performed using SPSS software (version 16.0, SPSS inc., Chicago, IL, USA) and SAS software (The SAS system 6.12, Cary, NC, USA: SAS Institute Inc). A p-value < 0.05 was considered statistically significant.

Results

Patient characteristics

In total, 524 patients were enrolled in the present study. In 10 patients (2%) the MSCT data set was not interpretable because of an irregular or elevated heart rate and these patients were excluded from the analysis. Therefore, 514 patients were included in the analysis. Baseline patient characteristics are described in Table 1.

Table 1. Baseline patient characteristics

Male	302 (59%)
Age (years)	60 ± 11
Obesity (BMI ≥ 30 kg/m ²)	111 (22%)
Diabetes	155 (30%)
Hypercholesterolemia	209 (41%)
Hypertension	287 (56%)
Positive family history for CAD	191 (37%)
Smoking currently	153 (30%)
Pre-test likelihood	
Low pre-test likelihood	113 (22%)
Intermediate pre-test likelihood	334 (65%)
High pre-test likelihood	67 (13%)
Symptoms patient population	
Typical chest pain	78 (15%)
Atypical chest pain	146 (28%)
Non-anginal chest pain	41 (8%)
Asymptomatic	181 (35%)
Other (dyspnea, tiredness, dizziness ect.)	68 (13%)

Stress-rest gated MPI results

In 87 patients symptom-limited bicycle test was performed and in the remaining 427 patients pharmacological stress was applied using either adenosine (n=395) or dobutamine (n=32). MPI imaging results are presented in Table 2. The mean SSS was 2.8 ± 4.5 , the mean SRS was 1.5 ± 3.0 and the mean SDS was 1.3 ± 3.6 . Ischemia ($\text{SDS} \geq 2$) was observed in 137 patients (27%). Within this group, 16 patients (3%) were shown to have severe ischemia ($\text{SDS} \geq 8$).

Baseline MSCT results

Average heart rate during MSCT acquisition was 63 ± 10 beats per minute. The baseline calcium score and MSCT imaging results are shown in Table 2. The mean calcium score was 324 ± 751 .

MSCT predictors for ischemia on MPI: patient based analysis

Results of the univariate analysis regarding the predictive value of MSCT variables for ischemia on MPI (patient basis) are listed in Table 3. As demonstrated, scanner type (16-slice or 64-slice) was not related to the presence of ischemia on MPI. To determine the independent predictive value of MSCT variables of atherosclerosis for ischemia on MPI, multivariate models were created including MSCT variables of atherosclerosis corrected for baseline clinical variables and the presence of severely obstructive CAD (Table 4). Interestingly, several MSCT variables of atherosclerosis remained predictive of ischemia on MPI in

Table 2. Imaging results of MPI, calcium score and MSCT angiography

MPI	
Normal perfusion ($\text{SDS} < 2$)	374 (73%)
Ischemia ($\text{SDS} \geq 2$)	137 (27%)
Severe ischemia ($\text{SDS} \geq 8$)	16 (3%)
Calcium score	
0	174 (34%)
1-100	140 (27%)
101-400	88 (17%)
>400	112 (22%)
MSCT angiography	
Degree	
Presence of non-obstructive CAD	354 (69%)
Presence of obstructive CAD ($\geq 50\%$)	157 (31%)
Presence of severely obstructive CAD ($\geq 70\%$)	83 (16%)
Extent and Composition	
Non-calcified plaques ≥ 3	39 (8%)
Mixed plaques ≥ 3	93 (18%)
Calcified plaques ≥ 3	126 (25%)
Location	
LM and/or proximal LAD diseased	74 (15%)

Table 3. Univariate analysis for prediction of ischemia on MPI on patient basis

	OR (CI 95%)	P-value
Clinical	2.0 (1.4-3.8)	<0.001
Calcium score		
1-100	0.6 (0.4-0.9)	0.02
101-400	1.2 (0.7-2.0)	0.48
>400	4.8 (3.1-7.5)	<0.001
MSCT angiography		
MSCT scanner type (64-slice)	1.3 (0.7-2.6)	0.46
Degree		
Number of obstructive segments	1.4 (1.3-1.6)	<0.001
Presence obstructive CAD	5.4 (3.5-8.3)	<0.001
Presence severely obstructive CAD	6.8 (4.1-11.2)	<0.001
Extent and Composition		
Number of non-calcified plaques	1.1 (1.0-1.2)	0.15
Number of mixed plaques	1.3 (1.2-1.4)	<0.001
Number of calcified plaques	1.3 (1.2-1.4)	<0.001
Non-calcified plaques ≥ 3	0.9 (0.4-2.0)	0.86
Mixed plaques ≥ 3	3.9 (2.5-6.3)	<0.001
Calcified plaques ≥ 3	3.3 (2.2-5.1)	<0.001
Location		
LM and/or proximal LAD diseased	3.4 (2.2-5.3)	<0.001

the multivariate model. Regarding contrast enhanced MSCT coronary angiography, degree of stenosis (presence of $\geq 50\%$ and $\geq 70\%$ stenosis), extent and composition (presence of ≥ 3 mixed plaques and/or ≥ 3 calcified plaques) and location (atherosclerotic disease in LM and/or proximal LAD) remained independent predictors of ischemia. An example of a patient with all predictors on MSCT is provided in Figure 2.

MSCT predictors for ischemia on MPI: vessel based analysis

Results of the univariate analysis regarding the predictive value of MSCT variables for ischemia on MPI (vessel basis) are listed in Table 5. To determine the independent predictive value of MSCT variables of atherosclerosis for ischemia on MPI on a vessel basis, multivariate models were created including MSCT variables of atherosclerosis which were corrected for baseline clinical risk variables (Table 6). Interestingly, several MSCT variables of atherosclerosis remained predictive of ischemia on MPI in the multivariate model on a vessel basis. Indeed, degree of stenosis (presence of $\geq 50\%$ and $\geq 70\%$ stenosis) and extent and composition (presence of ≥ 2 mixed plaques and/or ≥ 2 calcified plaques) remained significant independent predictors of ischemia.

Table 4. Multivariate models for prediction of ischemia on MPI on patient basis

	OR (CI 95%)	P-value
Model I		
Clinical	2.0 (1.4-3.8)	<0.001
Model II		
Clinical	1.6 (1.1-2.3)	0.01
Presence obstructive CAD	5.0 (3.3-7.7)	<0.0001
Model III		
Clinical	1.7 (1.2-2.5)	0.006
Presence severely obstructive CAD	6.2 (3.7-10.4)	<0.0001
Model IV		
Clinical	1.6 (1.1-2.3)	0.02
Presence severely obstructive CAD	3.8 (2.2-6.7)	<0.0001
Mixed plaques ≥ 3	2.0 (1.2-3.5)	0.012
Calcified plaques ≥ 3	2.3 (1.5-3.7)	<0.0001
Model V		
Clinical	0.7 (1.1-2.4)	0.008
Presence severely obstructive CAD	4.2 (2.5-7.3)	<0.0001
Calcified plaques ≥ 3	1.9 (1.2-3.1)	0.01
LM and/or proximal LAD diseased	1.8 (1.1-3.0)	0.03
Model VI		
Clinical	1.6 (1.1-2.4)	0.01
Presence severely obstructive CAD	3.5 (2.0-6.3)	<0.0001
Mixed plaques ≥ 3	1.7 (0.9-3.1)	0.053
Calcified plaques ≥ 3	2.0 (2.2-3.3)	0.007
LM and/or proximal LAD diseased	1.6 (0.9-2.7)	0.107

Incremental value of angiographic MSCT variables of atherosclerosis to predict ischemia on MPI

In total, 157 patients (31%) had obstructive CAD and 83 patients (16%) had severely obstructive CAD on MSCT. Regarding these patients, 80 patients (51%) and 52 patients (63%) revealed ischemia on MPI, respectively. Moreover, of the 259 patients with at least one of the significant predictors on MSCT, only 119 patients (33%) showed ischemia on MPI. Example of a patient demonstrating only one significant predictor and a normal MPI is provided in Figure 3. In addition, of the 22 patients with all of the significant predictors on MSCT (describing degree of stenosis, plaque extent, composition, and location), 18 patients (82%) showed ischemia on MPI.

Finally, the performance of the multivariate models for prediction of ischemia on both a patient (model V in Table 4) and vessel basis (model IV in Table 6) were studied with respect to discrimination and calibration. Discrimination was quantified by a measure of concordance, the c-index. In this model, plaque extent, composition and location had significant incremental value over clinical risk stratification and the presence of severely obstructive

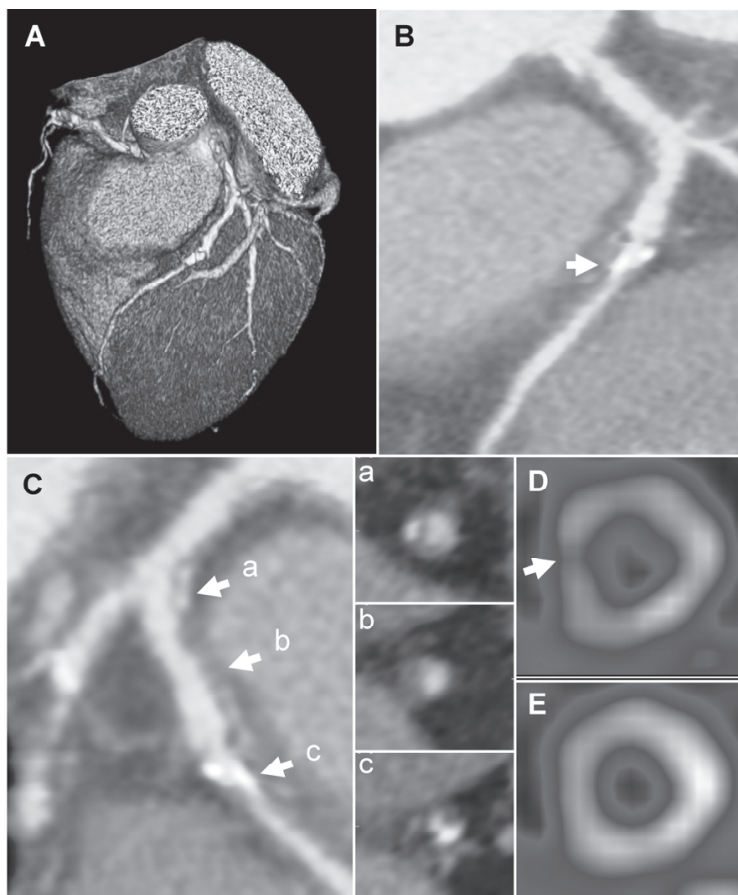


Figure 2. Example of a 72-year-old male patient exhibiting all the significant predictors on multislice computed tomography (MSCT) for prediction of ischemia on myocardial perfusion imaging (MPI). In panel A, a 3D volume rendered reconstruction is provided, showing the left anterior descending coronary artery (LAD). Panel B: A curved multiplanar reconstruction (MPR) of the LAD is shown demonstrating the presence of obstructive CAD ($\geq 50\%$) in the proximal segment (arrow). Panel C: Another curved MPR of the LAD is shown in a different view, revealing the presence of multiple diseased segments (cross sectional images a, b and c), the presence of obstructive lesion in the LAD (arrow c) and the presence of mixed plaque (cross sectional images a, b and c). Panel D: Stress single photon emission computed tomography (SPECT) short axis image showing the presence of a perfusion defect, particularly evident in the antero-septal region (arrow). Panel E: Rest SPECT short axis image demonstrating normal perfusion.

CAD ($p < 0.05$) for the prediction of ischemia on both a patient and vessel basis (Figure 4 and Figure 5, respectively). The performance of the model (calibration) was assessed by the Hosmer-Lemeshow goodness-of-fit test ($p > 0.10$ considered to indicate lack of deviation between the model and observed event rates). As demonstrated in Figure 6, on both a patient and vessel basis, the estimated risk of the models showed good agreement with the observed risk frequencies.

Table 5. Univariate analysis for prediction of ischemia on MPI on vessel basis

	OR (CI 95%)	P-value
Clinical	1.9 (2.5-1.4)	<0.001
MSCT angiography		
Degree		
Number of obstructive segments	2.0 (1.7-2.4)	<0.001
Presence obstructive CAD	4.0 (3.0-5.3)	<0.001
Presence severely obstructive CAD	5.3 (3.6-7.8)	<0.001
Extent and Composition		
Number of non-calcified plaques	1.2 (1.0-1.4)	0.08
Number of mixed plaques	1.6 (1.4-1.8)	<0.001
Number of calcified plaques	1.4 (1.2-1.6)	<0.001
Non-calcified plaques ≥ 2	1.0 (0.6-1.9)	0.91
Mixed plaques ≥ 2	3.0 (2.1-4.2)	<0.001
Calcified plaques ≥ 2	2.1 (1.5-2.9)	<0.001

Table 6. Multivariate models for prediction of ischemia on MPI on vessel basis

	OR (CI 95%)	P-value
Model I		
Clinical	1.9 (2.5-1.4)	<0.001
Model II		
Clinical	1.8 (1.4-2.2)	<0.001
Presence obstructive CAD	3.8 (2.8-5.0)	<0.001
Model III		
Clinical	1.8 (1.5-2.2)	<0.001
Presence severely obstructive CAD	5.0 (3.3-7.3)	<0.001
Model IV		
Clinical	1.8 (1.4-2.2)	<0.001
Presence severely obstructive CAD	3.5 (2.3-5.3)	<0.001
Mixed plaques ≥ 2	1.9 (1.3-2.8)	<0.001
Calcified plaques ≥ 2	1.8 (1.3-2.5)	<0.001

Discussion

The main findings of the present study can be summarized as follows. In a population with predominantly low-to-intermediate pre-test likelihood for CAD, MSCT variables of atherosclerosis such as plaque extent, composition and location were significant predictors of ischemia on MPI, over the presence of obstructive CAD. Moreover, the incremental value of angiographic MSCT variables of atherosclerosis over clinical risk stratification and the presence of severely obstructive CAD was investigated. In this model, plaque extent, composition (presence of ≥ 3 mixed plaques and/or ≥ 3 calcified plaques) and location (ath-

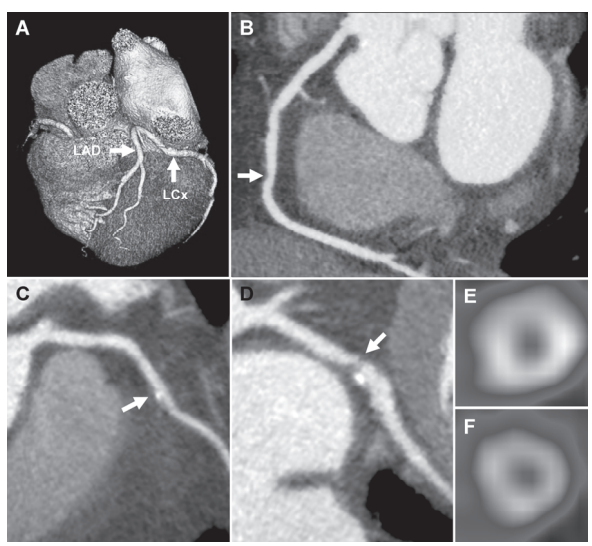


Figure 3. Example of a 69 year-old female patient exhibiting an obstructive lesion on multislice computed tomography (MSCT) while myocardial perfusion imaging (MPI) showed normal perfusion. A 3D volume rendered reconstruction is provided in panel A, showing the left anterior descending coronary artery (LAD) and left circumflex coronary artery (LCx). Panel B: A curved multiplanar reconstruction (MPR) of the right coronary artery (RCA) is shown demonstrating the presence of non-obstructive non-calcified plaque (arrow). Panel C: A curved MPR of the LAD is shown revealing the presence of a single non-obstructive mixed plaque (arrow). Panel D: A curved MPR of LCx is shown demonstrating the presence of obstructive lesion (however <70%) in the mid LAD (arrow). Panel E: Single photon emission computed tomography (SPECT) short axis image showing normal perfusion in stress and rest (panel F).

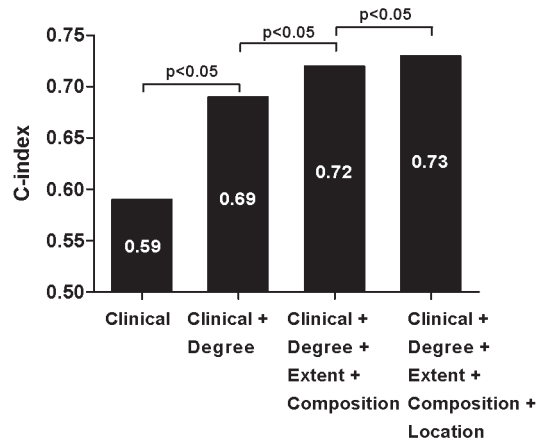


Figure 4. Bars representing the c-index (area under the curve) on the y-axis illustrating the incremental predictive value of angiographic multislice computed tomography (MSCT) variables of atherosclerosis for the prediction of ischemia on myocardial perfusion imaging (MPI) on a patient basis. The addition of the degree of stenosis (presence of $\geq 70\%$ stenosis) provided incremental predictive information to baseline clinical variables for the prediction of ischemia on MPI on a patient basis. Furthermore the addition of extent and composition of atherosclerosis (≥ 3 calcified plaques) and location (atherosclerotic disease in the left main coronary artery and/or proximal left anterior descending coronary artery) on MSCT resulted in further incremental predictive value over baseline clinical variables, and degree of stenosis on MSCT.

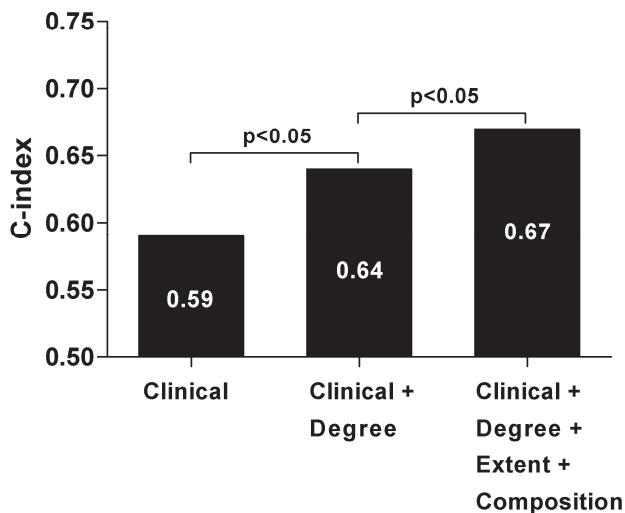


Figure 5. Bars representing the c-index (area under the curve) on the y-axis illustrating the incremental predictive value of angiographic multislice computed tomography (MSCT) variables of atherosclerosis for the prediction of ischemia on myocardial perfusion imaging (MPI) on a vessel basis. The addition of the degree of stenosis (presence of $\geq 70\%$ stenosis) provided incremental predictive information to baseline clinical variables for prediction of ischemia on MPI on a vessel basis. Furthermore the addition of extent and composition of atherosclerosis (≥ 2 mixed plaques and ≥ 2 calcified plaques) on MSCT resulted in further incremental predictive value over baseline clinical variables, and degree of stenosis on MSCT.

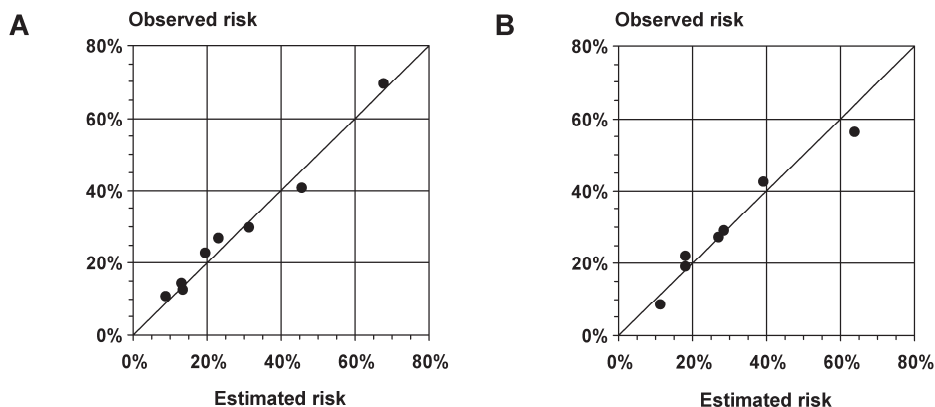


Figure 6. Hosmer-Lemeshow plot of estimated risk for ischemia on multislice computed tomography (MSCT) (x-axis) versus observed risk for ischemia on myocardial perfusion imaging (MPI) (y-axis) by decile of risk, on a patient (A) and vessel (B) basis. A calibration plot is shown for the prediction of ischemia on MPI (myocardial perfusion imaging) by the multivariate model of atherosclerosis variables on MSCT. Patient basis analysis is shown in panel A, describing model VI in Table 4. Vessel basis analysis is demonstrated in panel B, describing model IV in Table 5. The diagonal line in both plots demonstrates a good fit on both a patient and vessel basis. The Hosmer-Lemeshow goodness-of-fit test statistic was $p=0.93$ on a patient basis and $p=0.11$ on a vessel basis.

erosclerotic disease in LM and/or proximal LAD) further significantly enhanced prediction of ischemia over clinical risk stratification and the presence of severely obstructive CAD.

Previous investigations assessing the relation between MSCT and MPI demonstrated that normal coronary arteries on MSCT were highly associated with normal perfusion on MPI.¹² Accordingly, patients with normal coronary arteries on MSCT may be reassured and in general do not require further testing. Nevertheless, in a substantial number of patients MSCT will reveal the presence of atherosclerotic disease. However, previous comparisons demonstrated that only half of patients with stenosis of 50% or greater showed abnormal perfusion, resulting in a low positive predictive value of merely 50%.^{4, 5} Accordingly, with the expanding use of MSCT, clinicians will be increasingly confronted with patients having an obstructive lesion detected on MSCT but without information on the hemodynamic relevance. To determine further management, additional evaluation with functional imaging techniques remains necessary in these patients. However, if the likelihood of ischemia on MPI can be estimated more accurately based on MSCT results, a more appropriate selection of further testing and management can be achieved. Possibly, knowledge of the extent, composition, and location of atherosclerotic disease, as can be derived from MSCT, may enhance prediction of the presence of ischemia over the mere assessment of the degree of stenosis.

Extent and composition of atherosclerosis

In addition to the presence of a single stenotic lesion in the coronary arteries, previous studies have reported that diffuse atherosclerosis also contributes to ischemia.^{13, 14} By measuring coronary flow reserve, de Bruyne et al. demonstrated that diffuse atherosclerotic disease can cause a decline in coronary flow despite the absence of obstructive CAD.¹³ These findings suggest that the severity of perfusion abnormalities not only depends on the presence of obstructive disease but is also influenced by the atherosclerotic burden in the coronary artery. The current study is in line with these observations, suggesting that more extensive atherosclerotic plaque burden indicates a higher likelihood for ischemia. Moreover, the present results parallel previous studies comparing MPI with coronary calcium scoring.^{15, 16} He et al. studied the relationship between the presence of stress-induced ischemia on MPI and coronary artery calcium (CAC) and demonstrated in approximately 4000 asymptomatic patients that CAC was predictive of ischemia on MPI.¹⁶ However, only a minority of patients (22%) with an abnormal CAC had abnormal perfusion on MPI. Similarly, Berman et al. established that the frequency of abnormal perfusion was related to the magnitude of CAC abnormality.¹⁷ However, patients with normal MPI results frequently had extensive atherosclerosis on the basis of CAC criteria, indicating that a normal MPI did not exclude the presence of CAD. Conversely, the presence of CAC did not necessarily result in perfusion abnormalities on MPI. Therefore, although a relation exists between the extent of

atherosclerosis and ischemia, the extent alone may not be a strong predictor of ischemia. Importantly, to improve agreement of MSCT and MPI, integration of the extent of CAD with other variables of atherosclerosis identified on MSCT can refine identification of patients with ischemic MPI.

In the present study, extent of mixed and calcified plaque independently predicted the presence of ischemia on MPI. Indeed, mixed and calcified lesions are thought to typically represent the more advanced stages of atherosclerosis and thus linked with larger plaque volume and a higher extent of ischemia. Additionally, plaque composition on MSCT has previously been linked to abnormal perfusion on SPECT by Lin et al. in 163 patients.¹⁸ The authors demonstrated that the presence of mixed plaques was found to be the strongest independent predictor of abnormal perfusion (OR 1.6, $p=0.01$). The current and previous studies indicate that an association between extent and composition of atherosclerosis and a higher likelihood of ischemia may exist. Accordingly, plaque extent and composition should be taken into consideration when evaluating and reporting coronary MSCT angiograms. However, the exact underlying mechanisms remain largely unknown and should be further investigated.

Location of atherosclerosis

Location of atherosclerotic disease has been shown to influence myocardial perfusion. In general, the more proximal the location of stenosis, the more severe and extensive the corresponding perfusion abnormality will be. Conversely, the effect of distal lesions on myocardial perfusion will be limited as a smaller amount of myocardium is involved. In the current study, location of atherosclerotic disease in the LM and/or proximal LAD was demonstrated to be a predictor for the presence of ischemia on MPI. Similarly, previous studies have shown that patients with angiographically observed atherosclerotic disease in the LM and/or proximal LAD are at higher risk for events. Califf et al. developed the jeopardy score (an angiographic risk stratification score) which, in addition to severity of disease, incorporated location of atherosclerotic disease to estimate the amount of myocardium at risk.¹⁹ As more proximally located lesions were associated with a higher occurrence of events, the jeopardy score demonstrated to allow improved risk stratification as compared to other angiographic scoring techniques. Interestingly, Lin et al. adapted this scoring technique for MSCT angiography; the MSCT segment-at-risk score.¹⁸ Using this method, individuals with reversible defects could be more accurately identified.

Clinical implications

Recently, MSCT cardiac imaging has been increasingly applied for the evaluation of patients presenting with suspected CAD. The reported high negative predictive values of almost 100% precipitate MSCT as a particularly effective technique for ruling out the presence

of obstructive CAD. Accordingly, if patients show normal coronary arteries on MSCT angiography further testing is not required, whereas if atherosclerotic disease has been verified on MSCT, unfortunately no information is provided on the hemodynamical relevance. As a result, the decision which patient requires further functional testing or direct invasive evaluation with potential revascularization currently remains largely dependent on individual interpretation of the coronary arteries on MSCT angiography combined with pre-test likelihood and clinical judgment. Preferably, more information than merely presence of luminal narrowing is required from this technique. In our study several MSCT variables of atherosclerosis were identified which were associated with a higher likelihood of ischemia. Moreover, integration of all MSCT variables of atherosclerosis significantly improved prediction of the presence of ischemia on MPI. Possibly, these results may allow a more refined and individualized assessment of patients undergoing MSCT angiography and provide the basis for the development of an algorithm to improve identification of patients requiring more aggressive therapy or intervention.

However it is important to realize that in the current study, MSCT and MPI data were acquired in two different institutions with slightly different image acquisition protocols, which may have influenced our findings.

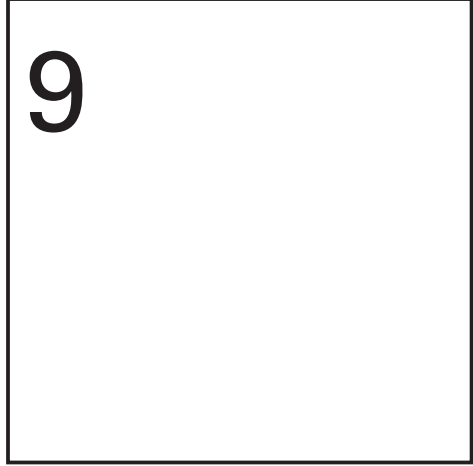
Conclusion

The results of the current study demonstrate that in addition to the presence of obstructive CAD, anatomical MSCT variables describing plaque extent, composition and location of atherosclerosis are independent predictors for the presence of ischemia on MPI.

References

1. Abdulla J, Abildstrom SZ, Gotzsche O, et al. 64-multislice detector computed tomography coronary angiography as potential alternative to conventional coronary angiography: a systematic review and meta-analysis. *Eur Heart J* 2007;28:3042-50.
2. Gaemperli O, Schepis T, Koepfli P, et al. Accuracy of 64-slice CT angiography for the detection of functionally relevant coronary stenoses as assessed with myocardial perfusion SPECT. *Eur J Nucl Med Mol Imaging* 2007;34:1162-71.
3. Gaemperli O, Schepis T, Valenta I, et al. Functionally relevant coronary artery disease: comparison of 64-section CT angiography with myocardial perfusion SPECT. *Radiology* 2008;248:414-23.
4. Hacker M, Jakobs T, Hack N, et al. Sixty-four slice spiral CT angiography does not predict the functional relevance of coronary artery stenoses in patients with stable angina. *Eur J Nucl Med Mol Imaging* 2007;34:4-10.
5. Schuijff JD, Wijns W, Jukema JW, et al. Relationship between noninvasive coronary angiography with multi-slice computed tomography and myocardial perfusion imaging. *J Am Coll Cardiol* 2006;48:2508-14.
6. Diamond GA, Forrester JS. Analysis of probability as an aid in the clinical diagnosis of coronary-artery disease. *N Engl J Med* 1979;300:1350-8.
7. Germano G, Kavanagh PB, Waechter P, et al. A new algorithm for the quantitation of myocardial perfusion SPECT. I: technical principles and reproducibility. *J Nucl Med* 2000;41:712-9.
8. Sharir T, Germano G, Kang X, et al. Prediction of myocardial infarction versus cardiac death by gated myocardial perfusion SPECT: risk stratification by the amount of stress-induced ischemia and the poststress ejection fraction. *J Nucl Med* 2001;42:831-7.
9. Cerqueira MD, Weissman NJ, Dilsizian V, et al. Standardized myocardial segmentation and nomenclature for tomographic imaging of the heart: a statement for healthcare professionals from the Cardiac Imaging Committee of the Council on Clinical Cardiology of the American Heart Association. *Circulation* 2002;105:539-42.
10. Agatston AS, Janowitz WR, Hildner FJ, et al. Quantification of coronary artery calcium using ultrafast computed tomography. *J Am Coll Cardiol* 1990;15:827-32.
11. Steyerberg EW, Harrell FE, Jr., Borsboom GJ, et al. Internal validation of predictive models: efficiency of some procedures for logistic regression analysis. *J Clin Epidemiol* 2001;54:774-81.
12. Schuijff JD, Wijns W, Jukema JW, et al. A comparative regional analysis of coronary atherosclerosis and calcium score on multislice CT versus myocardial perfusion on SPECT. *J Nucl Med* 2006;47:1749-55.
13. De Bruyne B, Hersbach F, Pijls NH, et al. Abnormal epicardial coronary resistance in patients with diffuse atherosclerosis but "Normal" coronary angiography. *Circulation* 2001;104:2401-6.
14. Marcus ML, Harrison DG, White CW, et al. Assessing the physiologic significance of coronary obstructions in patients: importance of diffuse undetected atherosclerosis. *Prog Cardiovasc Dis* 1988;31:39-56.
15. Anand DV, Lim E, Raval U, et al. Prevalence of silent myocardial ischemia in asymptomatic individuals with subclinical atherosclerosis detected by electron beam tomography. *J Nucl Cardiol* 2004;11:450-7.
16. He ZX, Hedrick TD, Pratt CM, et al. Severity of coronary artery calcification by electron beam computed tomography predicts silent myocardial ischemia. *Circulation* 2000;101:244-51.
17. Berman DS, Wong ND, Gransar H, et al. Relationship between stress-induced myocardial ischemia and atherosclerosis measured by coronary calcium tomography. *J Am Coll Cardiol* 2004;44:923-30.
18. Lin F, Shaw LJ, Berman DS, et al. Multidetector computed tomography coronary artery plaque predictors of stress-induced myocardial ischemia by SPECT. *Atherosclerosis* 2008;197:700-9.
19. Califf RM, Phillips HR, Hindman MC, et al. Prognostic value of a coronary artery jeopardy score. *J Am Coll Cardiol* 1985;5:1055-63.

Chapter 9



Impact of clinical presentation and pre-test likelihood on the relation between coronary calcium score and computed tomography coronary angiography

JM van Werkhoven, SM de Boer, JD Schuijf, F Cademartiri, E Maffei, JW Jukema, MJ. Boogers, LJ Kroft, A de Roos, JJ Bax

Abstract

The purpose of the current study was to assess the impact of clinical presentation and pre-test likelihood on the relationship between calcium score (CCS) and computed tomography coronary angiography (CTA), to determine the role of CCS as a gatekeeper to CTA in patients presenting with chest pain. In 576 patients with suspected coronary artery disease (CAD), CCS and CTA were performed. CCS was categorized as CCS 0, CCS 1-400 and CCS >400. On CTA the presence of significant CAD ($\geq 50\%$ luminal narrowing) was determined. Significant CAD was observed in 14 (5.8%) of 242 patients with CCS 0, in 94 (36.2%) of 260 patients with CCS 1-400, and in 60 (81.1%) of 74 patients with CCS >400. In patients with CCS 0, the prevalence of significant CAD increased from 3.9% to 4.1% and 14.3% in respectively non-anginal, atypical and typical chest pain, and from 3.4% to 3.9% and 27.3% with respectively a low, intermediate and high pre-test likelihood. In patients with CCS 1-400, the prevalence of significant CAD increased from 27.4% to 34.7% and 51.7% in respectively non-anginal, atypical and typical chest pain, and from 15.4% to 35.6% and 50% in respectively low, intermediate and high pre-test likelihood. In patients with CCS >400, the prevalence of significant CAD on CTA remained high (>72%) regardless of clinical presentation and pre-test likelihood. In conclusion, the relation between CCS and CTA is influenced by clinical presentation and pre-test likelihood. These factors should be taken into account when using CCS as a gatekeeper for CTA.

Introduction

Non-contrast enhanced computed tomography (CT) visualizes coronary calcium as a marker for coronary artery disease (CAD), and quantifies the presence and extent of coronary calcium by use of the coronary calcium score (CCS). More recently, contrast enhanced CT coronary angiography (CTA) has been introduced. This technique provides direct visualization of the coronary arteries and allows more detailed assessment of coronary atherosclerosis and stenosis severity. Several studies have suggested that CCS might be useful as a gatekeeper to CTA in diagnosis of significant CAD in patients presenting with chest pain. The absence of calcium could exclude the presence of significant CAD, indicating no need for further imaging, whereas patients with elevated CCS could be referred for CTA for additional information on stenosis severity. In order to evaluate the feasibility of such an approach, several comparative studies have been performed addressing the relationship between CCS and CTA in patients presenting with chest pain.¹⁻⁵ However, large discrepancies have been observed, which have been ascribed to differences in clinical characteristics of the studied populations. The purpose of the current study was therefore to systematically assess the impact of clinical presentation and pre-test likelihood on the relationship between CCS and CTA, to determine the role of CCS as a gatekeeper to CTA for diagnosis of significant CAD in patients presenting with chest pain.

Methods

The study population consisted of patients with suspected CAD who were clinically referred for further cardiac assessment because of chest pain. The included patients underwent both a CCS and CTA scan. Exclusion criteria were cardiac arrhythmias, renal insufficiency (defined as a glomerular filtration rate <30mL/min), known hypersensitivity to iodine contrast media, severe claustrophobia and pregnancy. In addition, patients with an uninterpretable CTA examination were excluded. Symptoms were classified as: typical angina, atypical angina, or non-anginal chest pain. Typical anginal chest pain was defined as combination of: 1) discomfort in the anterior chest, neck, shoulders, jaw, or arms; 2) precipitated by physical exertion or emotional stress; and 3) relieved by rest or nitroglycerin within minutes. Atypical chest pain was defined as chest pain with two of these 3 factors and non-anginal chest pain was defined as chest pain with less than 2 of these 3 factors.⁶ Pre-test likelihood was defined according to Diamond and Forrester criteria, which are based on previously observed prevalence's of significant CAD in age, gender and chest pain subgroups.⁷ Thresholds for low, intermediate and high pre-test likelihood were respectively; ≤ 13.4 , 13.5-87.2, and ≥ 87.3 .

The examination was performed using either a 64-detector row helical scanner (Aquilion 64; Toshiba Multi-slice system, Toshiba Medical Systems, Otawara, Japan) or a 320-detector row volumetric scanner (Aquilion ONE, Toshiba Medical Systems, Otawara, Japan). Before CCS and CTA examinations, the patients' heart rate and blood pressure were monitored. In the absence of contraindications, patients with a heart rate exceeding the threshold of 65 bpm were administered beta-blocking medication (50-100 mg metoprolol oral). Prior to the helical scan, a non-enhanced low-dose electrocardiographically gated scan was performed to measure CCS. The CCS scan was prospectively triggered at 70% or 75% of the R-R interval and performed using the following scan parameters: 4 x 3.0 mm or 2.5 mm collimation for 64-row CT, and single rotation wide volume acquisition (320 x 0.5 mm, reconstructed to 3 mm slices) for 320-row CT; gantry rotation time, 350-500 ms; tube voltage, 120 kV; and tube current, 200-250 mA.

For the 64-row contrast enhanced scan, collimation was 64 x 0.5 mm, tube voltage 100 to 135 kV and tube current 250 to 350 mA, depending on body mass index (BMI) and thoracic geometry. Non-ionic contrast material (Iomeron 400, Bracco, Milan) was administered with an amount of 80 to 110 ml followed by a saline flush with a flow rate of 5 ml/sec. For the 320-row contrast enhanced scan the heart was imaged in a single heartbeat, using prospective triggering with exposure interval depending on the heart rate. Scan parameters were: 320 X 0.5 mm collimation; 350 ms gantry rotation time, 100 to 135 kV tube voltage and a tube current of 400 to 580 mA, depending on body mass index. In total, 60 to 90 ml contrast material was administered with a rate of 5-6 ml/sec followed by a saline flush.

Post-processing of the CCS and CTA examinations was performed on dedicated workstations (Vitrea 2.0 or Vitrea FX 1.0, Vital Images, Minnetonka, MN, USA). The CCS was calculated using the Agatston method and patients were divided in three categories: CCS 0, CCS 1-400 and CCS >400. CTA angiograms were examined using the axial slices, curved multiplanar reconstructions, and maximum intensity projections. All CTA scans were interpreted by 2 experienced observers blinded to the results of CCS. CTA exams were classified according to the most severe lesion. In each patient, the presence of CAD was determined. Further differentiation was made between non-significant and significant CAD using a diameter stenosis $\geq 50\%$ as a threshold for significant lesions.

Continuous variables were expressed as mean values (\pm standard deviation) and categorical baseline data were expressed in numbers and percentages. Differences in baseline clinical variables between the CCS subgroups were compared using Anova, Student t and chi-square tests. The prevalence of significant CAD on CTA in each CCS category was determined according clinical presentation and pre-test likelihood. All statistical analyses were performed using SPSS software version 16.0 (SPSS, Chicago, Illinois, USA).

Results

The study population consisted of 602 patients presenting with chest pain who had undergone both CCS and CTA. In 26 (4.3%) of these patients, the CTA examination was uninterpretable because of the presence of motion artefacts, increased noise owing to a high body mass index, and breathing. After exclusion of these patients, a total of 576 remained for further analysis. The baseline characteristics of the patient population are presented in Table 1.

Table 1. Patient characteristics.

Variable	All (n=576)	CS 0 (n=242)	CS 1-400 (n=260)	CS >400 (n=74)	P-value
Men	273 (47%)	93 (38%)	137 (53%)	43 (58%)	0.001
Age (years)	56 ± 12	50 ± 11	59 ± 11	66 ± 9	<0.001
Diabetes Mellitus	105 (18%)	33 (14%)	49 (19%)	23 (31%)	0.003
Hypertension	254 (44%)	66 (27%)	136 (52%)	52 (70%)	<0.001
Hypercholesterolemia	199 (35%)	57 (24%)	106 (41%)	36 (49%)	<0.001
Current smokers	115 (20%)	49 (20%)	40 (15%)	26 (35%)	0.001
BMI ≥ 30 kg/m ²	109 (19%)	43 (18%)	48 (19%)	18 (24%)	0.48
Symptoms					0.017
Non-anginal chest pain	205 (36%)	103 (43%)	84 (32%)	18 (24%)	0.005
Atypical chest pain	249 (43%)	97 (40%)	118 (45%)	34 (46%)	0.42
Typical chest pain	122 (21%)	42 (17%)	58 (22%)	22 (30%)	0.06
Pre-test likelihood					<0.001
Low	117 (20%)	89 (37%)	26 (10%)	2 (3%)	<0.001
Intermediate	370 (64%)	131 (54%)	188 (72%)	51 (69%)	<0.001
High	89 (16%)	22 (9%)	46 (18%)	21 (28%)	<0.001

The median CCS of the study population was 7 (25th-75th percentile: 0-133). Calcium was absent in 242 patients (42%), a CCS of 1-400 was present in 260 patients (45.1%), and a CCS >400 in 74 patients (12.8%). Significant CAD was observed on CTA in 168 patients (29%). In the remaining 408 patients (71%) non-significant CAD was observed in 184 patients (32%) and 224 patients (39%) were classified as normal.

Figure 1 illustrates the CTA findings in the different CCS groups. In patients without any coronary calcium (CCS 0), significant CAD was observed in 14 patients (5.8%). In the group of patients with a CCS of 1-400, 94 patients (36.2%) had significant CAD on CTA. In patients with a high CCS >400, significant CAD was observed in 60 patients (81.1%).

Figures 2 and 3 illustrate the prevalence of significant CAD in the different CCS groups according to clinical presentation and pre-test likelihood.

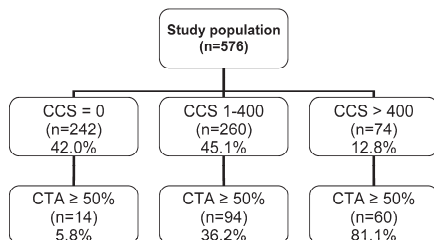


Figure 1. The prevalence of significant CAD on CTA per CCS category.

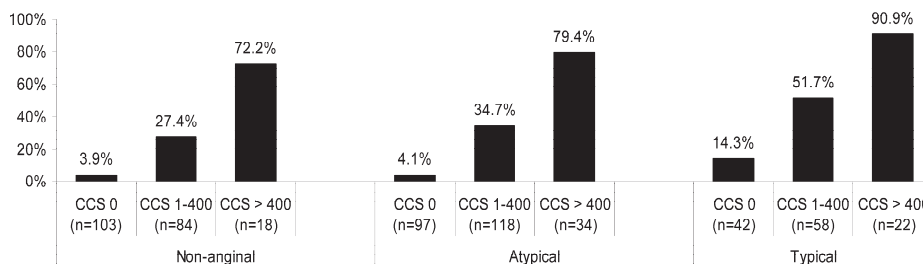


Figure 2. Prevalence of significant CAD on CTA in the various CCS categories according to patients' symptoms.

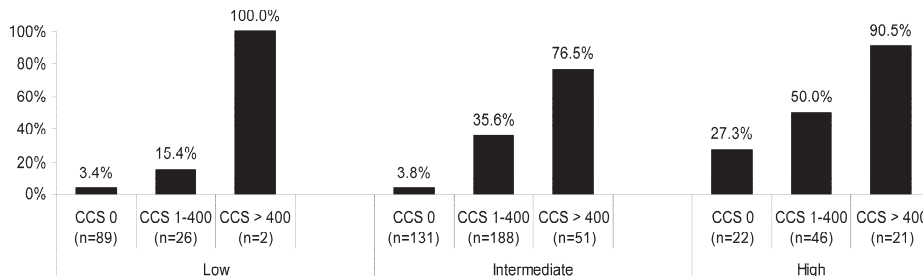


Figure 3. Prevalence of significant CAD on CTA in the various CCS categories, according to pre-test likelihood.

The impact of clinical presentation on the prevalence of significant CAD in each CCS category is illustrated in Figure 2. In patients with CCS 0, the prevalence of significant CAD was similar among patients with non-anginal and atypical complaints (respectively 3.9% and 4.1%, Figure 2). However, the prevalence increased to 14.3% in patients with typical chest pain. Accordingly, a CCS of 0 may not be useful to rule out significant CAD in patients presenting with typical chest pain complaints.

In patients with CCS 1-400, significant CAD was observed in 27.4% of patients with non-anginal chest pain. The prevalence increased to 34.7% and 51.7% in patients with atypical and typical chest pain, respectively. However, although there was an increase in

the prevalence of significant CAD according to the increase in severity of symptoms, the prevalence remained in an intermediate range.

In patients with a CCS >400, significant CAD was observed in 72.2% of patients with non-anginal complaints. The prevalence increased to 79.4% in atypical chest pain patients, and was highest (90.9%) in patients with typical chest pain. Although the prevalence of significant CAD increased with more severe chest pain symptoms, the prevalence was high in all patients with a CCS >400 regardless of clinical presentation.

The impact of pre-test likelihood on the prevalence of significant CAD in each CCS category is illustrated in Figure 3. In patients with a CCS 0, significant CAD was observed in 3.4% and 3.8% of patients with respectively a low and intermediate pre-test likelihood. The prevalence increased to 27.3% in patients with a high pre-test likelihood. Accordingly, a CCS of 0 may not be useful to rule out significant CAD in patients presenting with a high pre-test likelihood.

In patients with CCS 1-400, 15.4% of patients with a low pre-test likelihood had significant CAD. The prevalence of significant CAD increased to 35.6% in patients with intermediate pre-test likelihood and up to 50% in the high pre-test likelihood group. Although a large variance was observed in the prevalence of significant CAD on CTA according to increasingly higher pre-test likelihoods in patients with a CCS 1-400, the prevalence remained at an intermediate level.

In the group of patients with a CCS >400, a high prevalence of significant CAD was observed regardless of pre-test likelihood (Figure 3).

Discussion

The main finding of the current study is that the relation between CCS and CTA is highly influenced by clinical presentation and pre-test likelihood in patients presenting with chest pain. In each CCS category, the prevalence of significant CAD on CTA increased proportional to the severity of clinical presentation and pre-test likelihood. Clinical presentation and pre-test likelihood should therefore be taken into account when using CCS as a gatekeeper for CTA.

Several previous studies have assessed the relation between CCS and CTA in patients presenting with chest pain. A large proportion of these studies have specifically focused on the prevalence of significant CAD on CTA in patients with a CCS of 0. Within these

studies varying prevalences have been described, ranging between 1.7% in a recent study by Nieman et al. to 28% in a study by Haberl et al.¹⁻⁵ As a result of this large variation in reported prevalences, the value of a CCS of 0 to rule out significant CAD on CTA in chest pain patients has remained unclear.

Only a few comparative studies between CCS and CTA have been performed in chest pain patients with a CCS >0 .⁴ In patients with a CCS 1-400, Nieman et al. observed significant CAD on CTA in 35.4% of patients.⁴ The authors observed a high prevalence of 94% in patients with a CCS >400 . When using CCS as a gatekeeper for CTA, Nieman et al. propose that further downstream testing with CTA is necessary in patients with a CCS 1-400 and that the value of CTA may be limited in patients with a CCS >400 as the likelihood of subsequent significant CAD is high.

In patients with a CCS of 0, the prevalence of significant CAD on CTA increased from 3.9% and 4.1% in patients with non-anginal chest pain and atypical chest pain respectively to 14.3% in patients with typical chest pain. The prevalence of significant CAD on CTA in patients with a CCS of 0 increased from 3.4% and 3.8% in patients with a low and intermediate pre-test likelihood respectively to 27.3% in patients with a high pre-test likelihood. These observations may provide a valuable link between the discrepant findings described in previous comparative studies between CCS and CTA in patients with a CCS of 0. In the study by Haberl et al. all patients had an indication for invasive coronary angiography because of chest pain and signs of ischemia on conventional stress tests.³ As a result, the pre-test likelihood in this population was high, explaining the high prevalence (28%) of significant CAD in patients without calcium. In contrast, in a low to intermediate pre-test probability population, Nieman et al. observed a low prevalence of significant CAD similar to the prevalence observed in the subgroup of patients with a low or intermediate pre-test likelihood in the current study. Our observations suggest that when using CCS as a gatekeeper for CTA, the presence of significant CAD may be effectively ruled out in patients with non-anginal or atypical chest pain and in patients with a low or intermediate pre-test likelihood. However, a CCS of 0 may not reliably rule out the presence of significant CAD in patients with typical symptoms (17% of patients with a CCS 0 in the current) and patients with a high pre-test likelihood (9% of patients with a CCS 0 in the study population). In these patients additional evaluation with CTA may be necessary to confirm the presence or absence of significant CAD with more diagnostic certainty.

When assessing the relationship between CCS and CTA in patients with a CCS >0 , we observed that the prevalence of significant CAD on CTA in patients with a CCS 1-400 increased from 27.4% to 34.7% and 51.7% in patients with non-anginal, atypical and typical chest pain respectively. When regarding pre-test likelihood, the prevalence of significant

CAD on CTA in patients with a CCS 1-400 increased from 15.4% to 35.6% and 50% in patients with respectively a low, intermediate and high pre-test likelihood. Although the prevalence of significant CAD in patients with a CCS 1-400 was therefore influenced by clinical presentation and pre-test likelihood, the likelihood of significant CAD following a CCS 1-400 remained intermediate. When using CCS as a gatekeeper for CTA, further downstream testing with CTA therefore remains necessary in all patients with a CCS 1-400 (45% of current study population) to rule out the presence of significant CAD, regardless of clinical presentation and pre-test likelihood. In patients with a CCS >400, the prevalence of significant CAD on CTA remained high regardless of clinical presentation and pre-test likelihood. When using CCS as a gatekeeper, the value of CTA following a CCS >400 may be limited, as the presence of significant CAD can be ruled out in only a small proportion of patients. In patients with a CCS >400 (13% of total study population), it may therefore be more appropriate to proceed directly to functional imaging by means of myocardial perfusion imaging or to invasive coronary angiography to further determine the extent and severity of CAD, regardless of clinical presentation or pre-test likelihood.

The radiation dose remains a cause of concern for CTA. Currently traditional 64-row CTA protocols are still associated with high radiation exposure, although the radiation dose of CTA has recently decreased substantially.⁸⁻¹¹ Importantly, low-dose CTA with prospective ECG-triggering has recently been shown to reduce radiation burden while maintaining image quality and a high diagnostic accuracy.^{12, 13} The radiation burden with these novel acquisition techniques is approaching the level of diagnostic catheterization or even lower.¹⁴

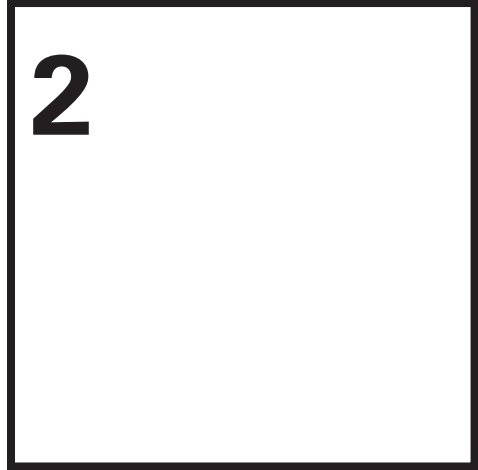
Conclusion

The relation between CCS and CTA is influenced by clinical presentation and pre-test likelihood. These factors should be taken into account when using CCS as a gatekeeper for CTA.

References

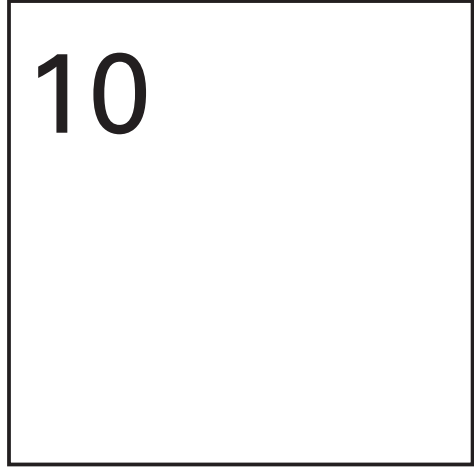
1. Akram K, O'Donnell RE, King S, et al. Influence of symptomatic status on the prevalence of obstructive coronary artery disease in patients with zero calcium score. *Atherosclerosis* 2008;203:533-7.
2. Gottlieb I, Miller JM, Arbab-Zadeh A, et al. The absence of coronary calcification does not exclude obstructive coronary artery disease or the need for revascularization in patients referred for conventional coronary angiography. *J Am Coll Cardiol* 2010;55:627-34.
3. Haberl R, Tittus J, Bohme E, et al. Multislice spiral computed tomographic angiography of coronary arteries in patients with suspected coronary artery disease: an effective filter before catheter angiography? *Am Heart J* 2005;149:1112-9.
4. Nieman K, Galema TW, Neefjes LA, et al. Comparison of the value of coronary calcium detection to computed tomographic angiography and exercise testing in patients with chest pain. *Am J Cardiol* 2009;104:1499-504.
5. Rubinshtein R, Gaspar T, Halon DA, et al. Prevalence and extent of obstructive coronary artery disease in patients with zero or low calcium score undergoing 64-slice cardiac multidetector computed tomography for evaluation of a chest pain syndrome. *Am J Cardiol* 2007;99:472-5.
6. Diamond GA. A clinically relevant classification of chest discomfort. *J Am Coll Cardiol* 1983;1:574-5.
7. Diamond GA, Forrester JS. Analysis of probability as an aid in the clinical diagnosis of coronary-artery disease. *N Engl J Med* 1979;300:1350-8.
8. Hausleiter J, Meyer T, Hadamitzky M, et al. Radiation dose estimates from cardiac multislice computed tomography in daily practice: impact of different scanning protocols on effective dose estimates. *Circulation* 2006;113:1305-10.
9. Hsieh J, Londt J, Vass M, et al. Step-and-shoot data acquisition and reconstruction for cardiac x-ray computed tomography. *Med Phys* 2006;33:4236-48.
10. Husmann L, Valenta I, Gaemperli O, et al. Feasibility of low-dose coronary CT angiography: first experience with prospective ECG-gating. *Eur Heart J* 2008;29:191-7.
11. Rybicki FJ, Otero HJ, Steigner ML, et al. Initial evaluation of coronary images from 320-detector row computed tomography. *Int J Cardiovasc Imaging* 2008;24:535-46.
12. Herzog BA, Husmann L, Burkhard N, et al. Accuracy of low-dose computed tomography coronary angiography using prospective electrocardiogram-triggering: first clinical experience. *Eur Heart J* 2008;29:3037-42.
13. Scheffel H, Alkadhi H, Leschka S, et al. Low-dose CT coronary angiography in the step-and-shoot mode: diagnostic performance. *Heart* 2008;94:1132-7.
14. Herzog BA, Wyss CA, Husmann L, et al. First Head-to-Head Comparison of Effective Radiation Dose from Low-Dose CT with Prospective ECG-Triggering versus Invasive Coronary Angiography. *Heart* 2009;95:1656-61.

Part 2



Cardiovascular computed tomography for risk stratification of coronary artery disease

Chapter 10



The Value of Multi-Slice Computed Tomography Coronary Angiography for Risk Stratification

JM van Werkhoven, JJ Bax, G Nucifora, JW Jukema, LJ Kroft,
A de Roos, JD Schuijf

Abstract

Multi-slice computed tomography coronary angiography (CTA) provides direct non-invasive anatomic assessment of the coronary arteries allowing for early identification of coronary artery disease (CAD). This information is useful for diagnosis of CAD, particularly the rule out of CAD. In addition, early identification of CAD with CTA may also be useful for risk stratification. The purpose of this review is to provide an overview of the current literature on the prognostic value of CTA and to discuss how the prognostic information obtained with CTA can be used to further integrate the technique into clinical practice. Non-invasive anatomic assessment of plaque burden, location, composition and remodeling using CTA may provide prognostically relevant information. This information has been shown to be incremental to the Framingham risk score, coronary artery calcium scoring and myocardial perfusion imaging. Characterization of atherosclerosis non-invasively has the potential to provide important prognostic information enabling a more patient tailored approach to disease management. Future studies assessing outcome after CTA based risk adjustments are needed to further understand the value of detailed non-invasive anatomic imaging.

Introduction

The introduction of multi-slice computed tomography coronary angiography (CTA) has changed the field of non-invasive imaging. In addition to existing functional imaging techniques assessing myocardial perfusion and wall motion, CTA currently provides direct non-invasive anatomic assessment of the coronary arteries. This allows for detection of coronary artery disease (CAD) at an earlier stage compared to functional imaging,¹ which may have important implications for the diagnosis as well as prognosis of CAD. For diagnosis, numerous studies support the use of CTA for rule out of the presence of CAD with a high accuracy.²⁻⁸ As a result the technique is increasingly used as a gatekeeper for further diagnostic testing. In addition, data are emerging that early identification of CAD with CTA may be useful for risk stratification. Since the first publications on the prognostic value of CTA in 2007 a number of studies have been published providing further insight into the potential value of non-invasive anatomic imaging for risk stratification.⁸⁻²¹ The purpose of this review is to provide an overview of the literature on the prognostic value of CTA and to discuss how the prognostic information obtained with CTA can be used to further integrate the technique into clinical practice.

Accuracy for risk stratification

Shift from stenosis to atherosclerosis

Diagnostic accuracy studies assessing the value of CTA have determined its ability to identify the presence or absence of significant stenosis ($\geq 50\%$ luminal narrowing).²²⁻²⁷ This threshold is important from a diagnostic point of view, as it can identify a cause for the patient's complaints as well as a treatment target for revascularization. Furthermore, patients with a significant stenosis on CTA may have worse outcome as compared to patients without significant CAD (^{14, 15, 18, 20}). Indeed, an annualized event rate for the occurrence of all cause mortality and myocardial infarction ranging between approximately 1% and 5% (^{14, 15, 18, 20}) has been observed in patients with significant CAD compared to approximately 0% to 2% in patients without significant CAD. However CTA can further differentiate patients as having non-significant CAD or completely normal coronary arteries. This is important as the presence of non-significant CAD may not necessarily be considered benign. (²⁸⁻³⁰ Indeed, myocardial infarction and unstable angina are frequently caused by lesions deemed to be non-significant prior to the event.³¹⁻³⁴ In line with this notion, the presence of non-significant CAD on CTA has been associated with an increased annualized event rates up to 1.5%, (^{14, 18, 20}) compared to a very low annualized event rates of $<0.7\%$ in patients with completely normal coronary anatomy.^{8-10, 12-14, 18, 20, 35} Accordingly, classification of patients as having normal anatomy, non-significant CAD or significant CAD may allow straightforward

and reliable risk stratification. However, it is conceivable that the prognostic information may be refined by further characterization of the observed atherosclerosis on segmental or plaque level. Potentially, such analysis may include identification of certain characteristics of lesions that may have a higher likelihood to cause thrombotic occlusion of the vessel and subsequent coronary events.

In the past, numerous histological studies have addressed the mechanism underlying coronary occlusion, thereby identifying three major causes, namely plaque erosion, the presence of calcified nodules and, in the majority of cases, plaque rupture.³⁶ In the setting of plaque rupture, the underlying plaque at the site of thrombus formation has been typically characterized as a lesion with a large lipid rich atheromatous necrotic core, with a ruptured thin fibrous cap and expansive remodeling. These findings have subsequently led to the hypothesis that plaque rupture is caused by rupture of the thin fibrous cap overlying a lesion with a large lipid-rich atheromatous necrotic core. (Figure 1) In addition to morphological characteristics of the plaque, the presence of inflammation, as reflected by macrophages and lymphocytes infiltration, also plays an important role. An overview of morphological

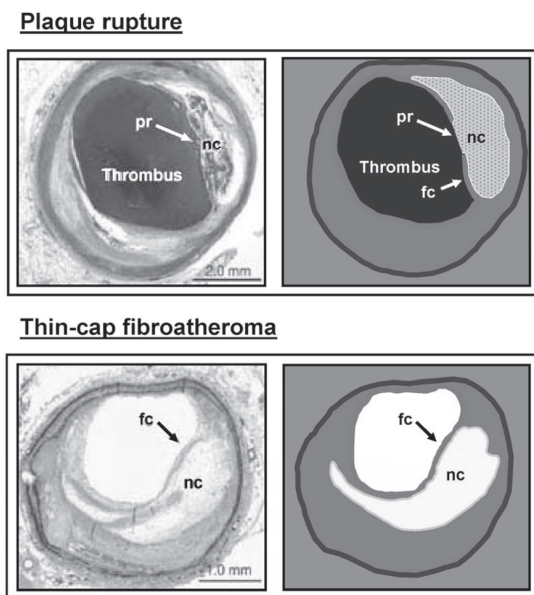


Figure 1. Thin capped fibroatheroma as a cause of plaque rupture. The top panel shows a histological specimen of a ruptured plaque. As can be observed in the specimen, the lumen is completely occluded by a large thrombus. The underlying plaque contains a large necrotic core (nc) and is covered by a thin fibrous cap (fc) which has ruptured (pr). These findings have subsequently led to the hypothesis that plaque rupture is caused by rupture of the thin fibrous cap of thin capped fibroatheroma plaques. A histological specimen of a thin capped fibroatheroma can be observed in the bottom panel. The plaque is characterized by a large necrotic atheromatous core (similar to the necrotic core observed in sites of plaque rupture), covered by a thin non-ruptured fibrous cap. Adapted and reprinted with permission from Jain et al. (80)

plaque characteristics associated with vulnerability is provided in Table 1.³⁷ Due to its ability to visualize the vessel wall, CTA may allow non-invasive identification of several characteristics associated with vulnerability including plaque burden, location, composition and remodeling.³⁸⁻⁴⁹

Table 1. Morphological markers of plaque vulnerability. Based on the table from Naghavi et al. (37)

Plaque
Plaque cap thickness
Plaque lipid core size
Plaque stenosis
Color
Collagen content versus lipid content, mechanical stability
Calcification burden and pattern
Pan arterial
Total coronary calcium burden
Total arterial burden of plaque including peripheral

Non-invasive characterization of atherosclerosis with CTA

Plaque burden and location

By combining plaque extent and severity throughout the coronary system, plaque burden can be either assessed quantitatively or semi-quantitatively with CTA by summation of the number of diseased and significantly diseased vessels or segments. Although plaque burden in itself does not directly imply plaque vulnerability, an increase in plaque burden is associated with an increased risk for vulnerable plaques. Several studies have attempted to create models of plaque burden using a modified AHA segment model of the coronary artery tree. In the study by Pundziute et al., increased number of segments with plaque as well as increased number of segments with significant stenosis were independent predictors of events when corrected for baseline clinical variables.⁸ Using similar scoring methods, other studies have also observed a higher risk for events in patients with increased number of segments with atherosclerosis.^{10, 16} Min et al. observed that a segmental involvement score allowed good differentiation between patients with a low and high risk for future events. In patients with more than 5 segments involved, an absolute event rate of 8.4% was observed compared to 2.5% in patients with a score ≤ 5 .¹⁶ In a next step, the extent and severity of atherosclerosis throughout the coronary artery tree was incorporated into the segmental severity score. Each coronary segment was graded according to stenosis severity (absent to severe plaque (0-3)) and the scores for all segments were combined. When using this segmental severity score an absolute event rate of 6.6% was observed in patients with a score >5 compared to 1.6% in patients with a score ≤ 5 .

In addition to plaque burden, plaque location should be considered as well, as vulnerable plaques are most often observed in proximal segments of the coronary artery tree.⁵⁰ The presence of proximal lesions is therefore associated with an increased risk of vulnerable plaques. Furthermore, plaque rupture in a proximal segment also increases the risk of a major cardiac event, due to the larger volume of myocardium that is at risk. Indeed, Pundziute et al. observed that the presence of left main plaque or proximal LAD plaque was an important independent predictor of events associated with a high event rate.⁸ Likewise, in the study by Min et al. the presence of any left main stenosis was also an independent predictor of events.¹⁶ Subsequently, the authors created a modified version of the Duke coronary artery score by combining both plaque burden and location into a single predictive model. As illustrated in Figure 2, events rates paralleled increasing disease severity as determined with this hierarchic model.

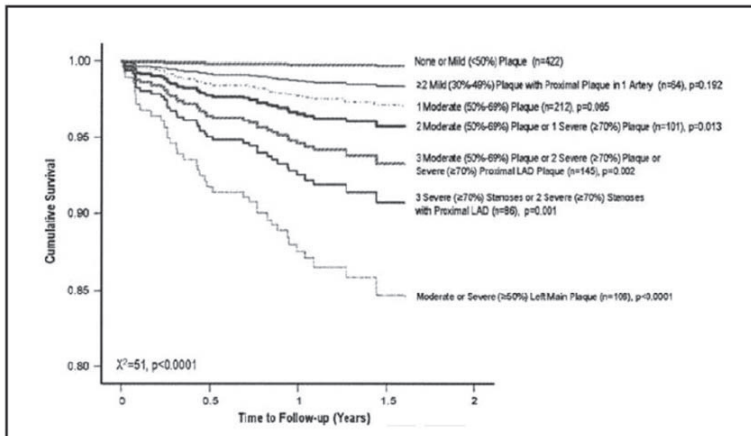


Figure 2. Prognostic value of CTA. Cumulative survival curves illustrating the risk of events in each category of the Duke Prognostic Coronary Artery Disease Index. The risk of events increases with increasingly higher disease severity categories. Reprinted with permission from Min et al. (16)

Plaque remodeling and plaque composition

To some extent, CTA allows assessment of plaque composition. A differentiation can be made between non-calcified plaques having low attenuation, calcified plaques with high attenuation and mixed plaques with both non-calcified and calcified elements.(Figure 3)⁴⁸ Furthermore, plaque remodeling, a marker of vulnerability, can also be appreciated.(Figure 4) In retrospective studies comparing observations on CTA between patients presenting with stable CAD and patients with suspected acute coronary syndrome (ACS), more outward plaque remodeling, non-calcified plaque and mixed plaque were observed in the latter.^{42, 51, 52} In subsequent prognostic investigations these characteristics have been further studied. Pundziute et al. assessed the prognostic value of different plaque characteristics and observed

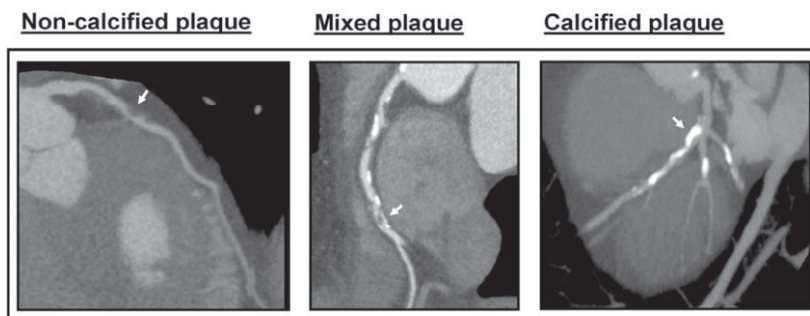


Figure 3. Plaque composition assessed with CTA. Curved multi-planar reconstructions showing three distinct plaque characteristics observed on CTA with non-calcified plaque (arrow, left panel), mixed plaque (arrow, mid panel) and calcified plaque (arrow, right panel).

Positive remodeling

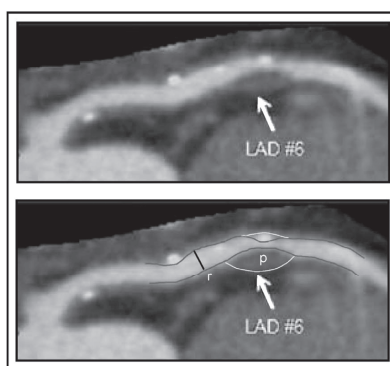


Figure 4. Example of a positively remodeled plaque. A multi-planar reconstruction of the left anterior descending coronary artery. In the proximal section of the vessel a large plaque can be observed between the lumen (purple line) and the vessel wall (yellow line). The diameter of the vessel at the plaque site is clearly larger compared to the diameter at the reference section (r), indicating positive remodeling (p). Adapted and reprinted with permission from Motoyama et al. (17)

that increased number of segments with mixed plaques was an independent predictor of events.⁸ Non-calcified plaque however has also been associated with an increased risk for events. Both the number of segments with mixed plaques as well as the number of segments with non-calcified plaque were independent predictors of events in a recent study by Van Werkhoven et al.²⁰ Furthermore, the presence of substantial non-calcified plaque burden was demonstrated to provide incremental prognostic value over the presence of significant stenosis on CTA. In a recent study by Motoyama et al. the concept of plaque morphology was investigated more extensively in 1059 patients during an average follow up of 27 months.¹⁷ The authors assessed the presence of two plaque characteristics, low attenuation plaque and positive remodeling, and recorded the occurrence of ACS during follow-up. In patients with a normal CTA study no events occurred. In patients with atherosclerosis

but without either high risk plaque feature (e.g. absence of both low attenuation plaque tissue and positive remodeling) the event rate was 0.49% whereas in patients with plaques positive for 1 high risk feature (either low attenuation or positive remodeling) the event rate increased to 3.7%. Finally, the majority of events occurred in patients with both high risk plaque features. In these patients an event rate as high as 22.2% was observed.(Figure 5) Accordingly, these findings may provide a proof of concept for the assessment of plaque composition on CTA for risk stratification.

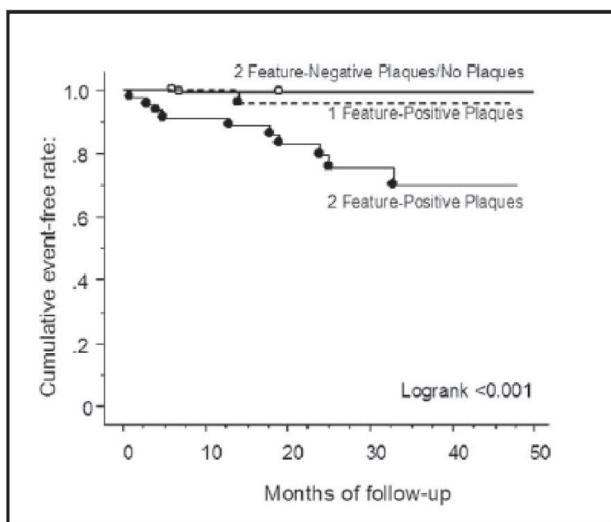


Figure 5. Prognostic value of low attenuation plaque and plaque remodeling features. Survival curves illustrating the prognostic value of 2 plaque features (low attenuation plaque and remodeling) associated with acute coronary syndrome. The event rate increased in patients with 1 feature positive plaques and was highest in patients with both high risk features. Reprinted with permission from Motoyama et al. (17)

Integration into clinical practice

Relation to existing tools for risk stratification

As outlined above, several investigations have demonstrated the feasibility of CTA for risk stratification. An important question however remains whether the technique provides incremental prognostic information to existing risk stratification methods. To a large extent, prognosis is determined using baseline clinical characteristics. To this end the Framingham score is widely used and provides an estimate of the risk of developing adverse coronary events.⁵³ The disadvantage of this method is that it is a population based screening tool, whereas CTA may provide a more patient specific approach. In a recent investigation by Hadamitzky et al., the value of risk stratification with CTA was compared to the Framingham risk score in a population of 1256 patients during an average follow-up of 18 months.¹⁵

Figure 6 illustrates the difference between the predicted risk based on the Framingham risk score and the observed risk according to findings on CTA. In patients without obstructive CAD on CTA, the observed risk was significantly lower than predicted by the Framingham risk score. In contrast significantly more events were observed in patients with obstructive CAD compared to the predicted event rate. CTA may therefore further refine risk stratification over conventional risk assessment alone.

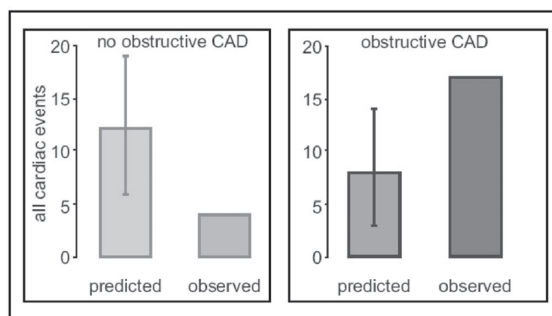


Figure 6. Prognostic value of CTA in addition to the Framingham risk score.

In patients without obstructive CAD, the observed risk was significantly lower than predicted by the Framingham risk score. In contrast significantly more events were observed in patients with obstructive CAD compared to the predicted event rate. Reprinted with permission from Hadamitzky et al. (15)

Of note, the incremental value of atherosclerosis over traditional risk assessment has been shown in the past for coronary artery calcium scoring (Figure 7).⁵⁴⁻⁵⁷ Based on numerous trials, coronary artery calcium scoring - performed either by electron beam computed tomography or CT - has been accepted as a robust tool for prognostification, especially in asymptomatic individuals.⁵⁸ In addition, the technique may be used in symptomatic patients to identify the presence and the extent of atherosclerosis.⁵⁹ However, the technique can only provide an estimate of total calcified plaque burden, and does not provide any information on the stenosis severity nor the presence and extent of non-calcified plaque burden. An important advantage of CTA therefore is the additional information on stenosis severity and plaque composition. In a study by Ostrom and colleagues, the incremental value of non-invasive coronary angiography with electron beam computed tomography over coronary calcium was assessed.¹⁸ The authors demonstrated that CTA-derived plaque burden, defined as the number of non-significantly or significantly diseased vessels, had independent and incremental value in predicting all-cause mortality independent of age, gender, conventional risk factors, and coronary artery calcium score. Similar findings were recently reported by Rubinshtein et al.¹⁹ In a more recent study the incremental prognostic value of both stenosis severity and plaque composition on CTA over the coronary artery calcium score was determined.²¹ In addition to stenosis severity the number of segments with non-calcified plaque as well as the number of segments with mixed plaque was shown

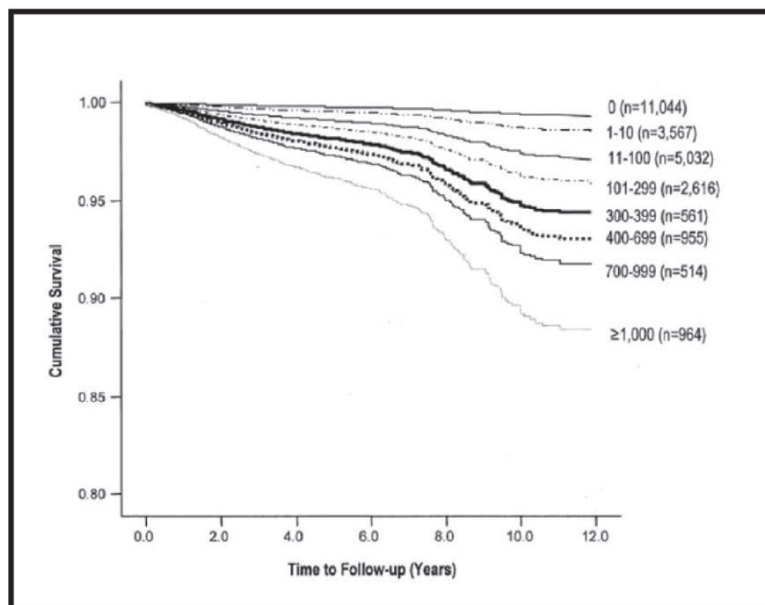


Figure 7. Prognostic value of coronary calcium scoring. Cumulative survival curves illustrating the event rate in increasingly higher calcium score categories. Reprinted with permission from Budoff et al. (55)

to be independently associated with increased risk for events. Accordingly, it appears that non-invasive measures of plaque extent, severity and composition not only provide improved diagnostic information but also incremental prognostic information over coronary artery calcium scoring.

Although risk stratification using non-invasive anatomic imaging is gaining momentum, traditionally functional imaging has been used extensively for this purpose. Particularly myocardial perfusion imaging is an established and important technique for prognosis. Patients with a normal perfusion have a very low event rate compared to increased event rates in patients with abnormal perfusion.⁶⁰⁻⁶⁶ Comparative studies between CTA and myocardial perfusion imaging have shown that CTA provides complementary information to myocardial perfusion imaging when regarding the diagnosis of CAD.⁽⁶⁷⁻⁷⁰⁾ The added value of this complementary information for risk stratification was recently determined.²⁰ Several CTA variables were able to provide prognostic information independent of myocardial perfusion imaging. On a patient level the presence of significant CAD ($\geq 50\%$ stenosis) was identified as a robust independent predictor. In addition to stenosis severity, plaque composition was shown to further enhance risk stratification, as illustrated in Figure 8.

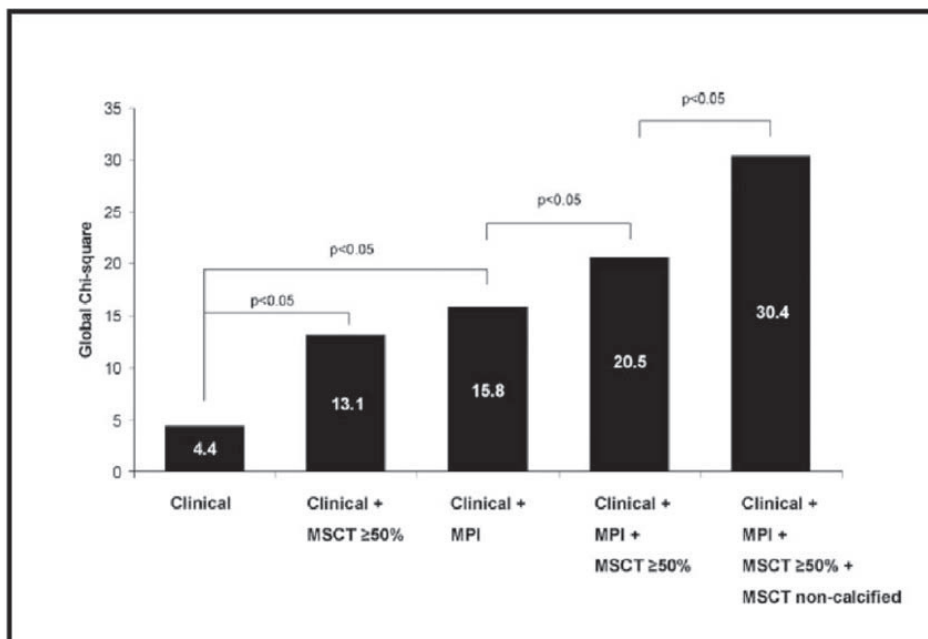


Figure 8. Incremental prognostic value of CTA over MPI. Bar graph illustrating the incremental prognostic value (depicted by chi-square value on the y axis) of CTA. The addition of CTA provides incremental prognostic information to baseline clinical variables and MPI. Furthermore, the addition of non-calcified plaque on CTA results in further incremental prognostic information over baseline clinical variables, MPI, and significant CAD ($\geq 50\%$ stenosis) on CTA. Reprinted with permission from Van Werkhoven et al. (20)

Patient populations

Symptomatic populations

CTA has been proposed for diagnosis of significant CAD in symptomatic patients presenting with an intermediate pre-test likelihood for significant stenosis. Based on the diagnostic accuracy of CTA for the detection of significant CAD on conventional coronary angiography, the comparative studies between CTA and myocardial perfusion imaging, and the limited prognostic data at the time, an algorithm has been proposed which integrates the use of these techniques for the diagnosis and management of this patient population.⁷¹ (Figure 9) The algorithm separates patients into three strategies for management: first, patients with normal coronary anatomy can be safely discharged, secondly patients with non-flow limiting atherosclerosis requiring medical treatment and aggressive risk factor modification and finally patients with a flow-limiting stenosis requiring further evaluation with conventional coronary angiography with potentially revascularization. The currently available outcome data support that the discharge of patients with a normal CTA study is safe as low events rates have been confirmed in these patients. (^{8-10, 12-14, 18, 20, 35} However in patients with atherosclerosis regardless of stenosis severity, assessment of plaque extent, composition,

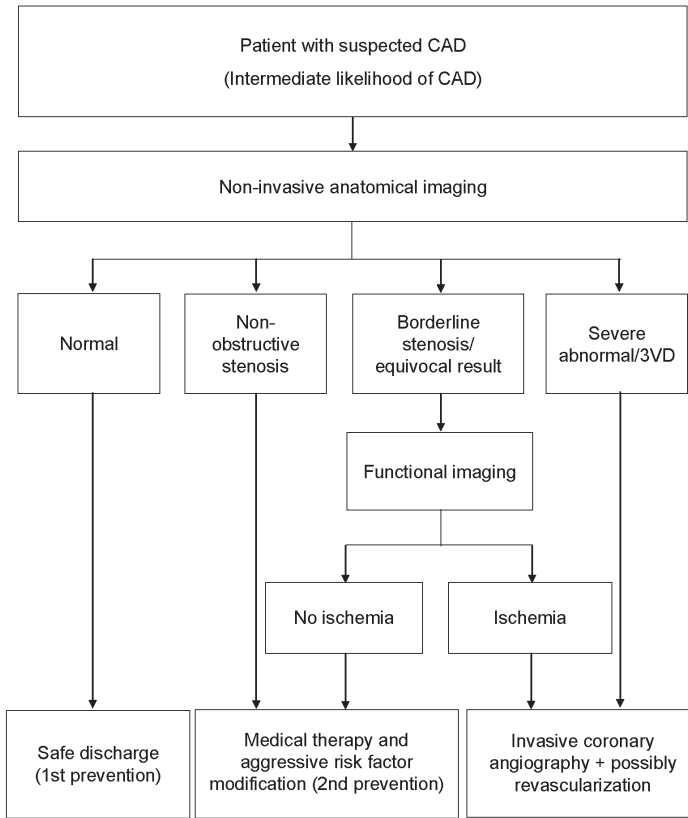


Figure 9. Algorithm illustrating the sequential use of CTA and functional imaging in patients with an intermediate pre-test likelihood. Reprinted with permission from Schuijff et al. (71)

location and remodeling may further improve risk stratification. As indicated by initial data, this information can be valuable both in patients with or without ischemia.²⁰

CTA is currently not recommended for diagnosis in other populations than those with an intermediate pre-test likelihood for significant CAD. It is however conceivable that in the future CTA may be used in other populations with the purpose of risk stratification. In symptomatic patients with a low pre-test likelihood for significant stenosis non-invasive imaging is generally not indicated for diagnosis. However assessment of atherosclerosis can be useful in identifying patients at increased risk of future events. As shown by Henneman et al., the prevalence of atherosclerosis in patients with a low pre-test likelihood is approximately 40% which illustrates that, although the pre-test likelihood for significant stenosis is low, atherosclerosis is nevertheless present in a large proportion of these patients. In patients with a high pre-test likelihood for significant stenosis functional data may be more relevant than CTA to determine need for revascularization. However, CTA can potentially be used as a

second line test for risk stratification as the anatomic information has been shown to provide incremental prognostic information to myocardial perfusion imaging alone.²⁰

Asymptomatic populations

Although only limited data are available in asymptomatic patient populations it is possible that CTA is valuable for risk stratification in these patients. On the one hand, CTA can be used to identify patients with severe CAD, such as triple vessel disease or left main disease, and who may benefit from aggressive intervention. On the other hand, CTA can be performed to document atherosclerosis for long-term risk assessment. In a recent study in 1000 asymptomatic individuals undergoing CTA the prevalence of atherosclerosis was reported to be 22%.¹¹ During a follow-up of 17 months, coronary events (unstable angina and revascularization) occurred in 15 (1.5%) individuals, all of which had atherosclerosis on CTA. However, the majority of events were revascularizations, triggered by the CTA results. In combination with the low overall event rate, these observations indicate the limited value of screening for atherosclerosis with CTA in this population. Accordingly, CTA is currently not acceptable as a general screening tool and CS testing or truly non-invasive approaches may be preferable. However, as proposed by Naghavi et al., non-invasive coronary angiography may potentially be used as a downstream test in the workup of asymptomatic individuals with high risk characteristics, following home- or office-based screening.³⁷ (Figure 10) Through selection of high risk patients with truly non-invasive techniques only a small subgroup of high risk patients remains in which further non-invasive and subsequent invasive imaging may be beneficial. Future studies will need to determine the value and feasibility of such a screening strategy.

Limitations

Although the available data support the potential clinical relevance of assessment of plaque characteristics on CTA, accurate quantification of plaque remains challenging, while requiring optimal image quality. Leber et al. have reported on the accuracy of 64-slice CTA to classify and quantify plaque volumes in the proximal coronary arteries as compared to intravascular ultrasound.⁷² CTA detected calcified and mixed plaque with high accuracy (95% and 94%, respectively) but accuracy was lower for non-calcified lesions (83%). When regarding plaque volume, non-calcified plaque and mixed plaque volumes were systematically underestimated whereas calcified plaque volume was overestimated by CTA. Novel software packages aimed at assessing plaque volume and plaque composition are currently being developed and may improve not only accuracy but also reproducibility of measurements.

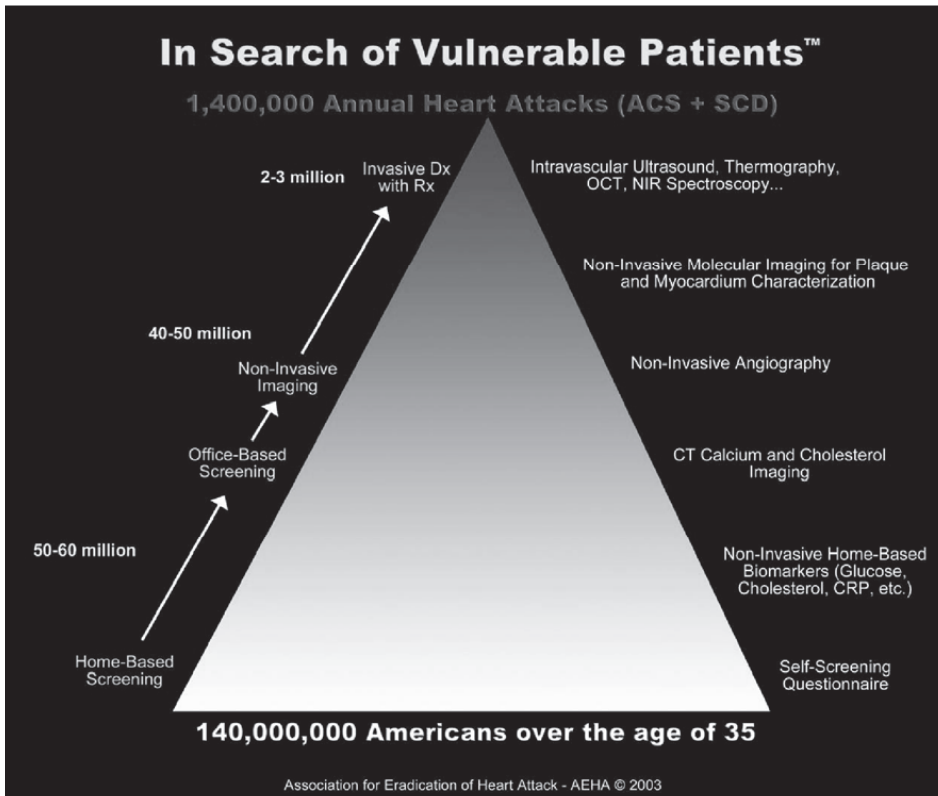


Figure 10. Potential screening algorithm for the identification of vulnerable plaque in asymptomatic individuals. An example of an algorithm with potential usefulness in the workup of high risk patients, to identify the presence of plaques with vulnerable characteristics. At the bottom of the pyramid individuals are selected for further non-invasive evaluation with CS testing and CTA based on home-based screening questionnaires and biomarker assessment. At the top of the pyramid a small subgroup remains warranting further invasive assessment. Ideally such an algorithm can be used to identify a subgroup of the general asymptomatic populations in need of aggressive primary prevention strategies. Reprinted with permission from Naghavi et al.(37)

In addition, the radiation dose remains a cause of concern for CTA. Currently traditional 64-slice CTA protocols are still associated with high radiation exposure, although the radiation dose of CTA has recently decreased substantially.⁷³⁻⁷⁶ Importantly, low-dose CTA with prospective ECG-triggering has recently been shown to reduce radiation burden while maintaining image quality and a high diagnostic accuracy.^{77, 78} Currently, the radiation burden with these novel acquisition techniques is approaching the level of diagnostic catheterization or even lower.⁷⁹

Conclusion

Non-invasive anatomic assessment of plaque burden, location, composition and remodeling using CTA may provide prognostically relevant information, incremental to not only the Framingham risk score, but also to other imaging approaches as coronary artery calcium scoring and myocardial perfusion imaging. Thus, non-invasive characterization of atherosclerosis has the potential to provide a more patient tailored approach to disease management. Future studies assessing outcome after CTA based risk adjustments are needed to further understand the value of detailed non-invasive anatomic imaging.

References

1. van Werkhoven JM, Schuijff JD, Jukema JW, et al. Anatomic correlates of a normal perfusion scan using 64-slice computed tomographic coronary angiography. *Am J Cardiol* 2008;101:40-5.
2. Miller JM, Rochitte CE, Dewey M, et al. Diagnostic Performance of Coronary Angiography by 64-Row CT. *N Engl J Med* 2008;359:2324-36.
3. Schuijff JD, Pundziute G, Jukema JW, et al. Diagnostic accuracy of 64-slice multislice computed tomography in the noninvasive evaluation of significant coronary artery disease. *Am J Cardiol* 2006;98:145-8.
4. Budoff MJ, Dowe D, Jollis JG, et al. Diagnostic performance of 64-multidetector row coronary computed tomographic angiography for evaluation of coronary artery stenosis in individuals without known coronary artery disease: results from the prospective multicenter ACCURACY (Assessment by Coronary Computed Tomographic Angiography of Individuals Undergoing Invasive Coronary Angiography) trial. *J Am Coll Cardiol* 2008;52:1724-32.
5. Meijboom WB, Meijis MFL, Schuijff JD, et al. Diagnostic Accuracy of 64-slice Computed Tomography Coronary Angiography: A Prospective Multicenter, Multivendor Study. *J Am Coll Cardiol* 2008;52:2135-44.
6. Abdulla J, Abildstrom SZ, Gotzsche O, et al. 64-multislice detector computed tomography coronary angiography as potential alternative to conventional coronary angiography: a systematic review and meta-analysis. *Eur Heart J* 2007;28:3042-50.
7. Mowatt G, Cook JA, Hillis GS, et al. 64-Slice computed tomography angiography in the diagnosis and assessment of coronary artery disease: systematic review and meta-analysis. *Heart* 2008;94:1386-93.
8. Pundziute G, Schuijff JD, Jukema JW, et al. Prognostic value of multislice computed tomography coronary angiography in patients with known or suspected coronary artery disease. *J Am Coll Cardiol* 2007;49:62-70.
9. Aldrovandi A, Maffei E, Palumbo A, et al. Prognostic value of computed tomography coronary angiography in patients with suspected coronary artery disease: a 24-month follow-up study. *Eur Radiol* 2009.
10. Carrigan TP, Nair D, Schoenhagen P, et al. Prognostic utility of 64-slice computed tomography in patients with suspected but no documented coronary artery disease. *Eur Heart J* 2009;30:362-71.
11. Choi EK, Choi SI, Rivera JJ, et al. Coronary computed tomography angiography as a screening tool for the detection of occult coronary artery disease in asymptomatic individuals. *J Am Coll Cardiol* 2008;52:357-65.
12. Gaemperli O, Valenta I, Schepis T, et al. Coronary 64-slice CT angiography predicts outcome in patients with known or suspected coronary artery disease. *Eur Radiol* 2008;18:1162-73.
13. Gilard M, Le Gal G, Cornily J, et al. Midterm Prognosis of Patients With Suspected Coronary Artery Disease and Normal Multislice Computed Tomographic Findings. *Arch Intern Med* 2007;165:1686-9.
14. Gopal A, Nasir K, Ahmadi N, et al. Cardiac computed tomographic angiography in an outpatient setting: an analysis of clinical outcomes over a 40-month period. *J Cardiovasc Comput Tomogr* 2009;3:90-5.
15. Hadamitzky M, Freissmuth B, Meyer T, et al. Prognostic Value of Coronary Computed Tomographic Angiography for Prediction of Cardiac Events in Patients With Suspected Coronary Artery Disease. *J Am Coll Cardiol Img* 2009;2:404-11.
16. Min JK, Shaw LJ, Devereux RB, et al. Prognostic value of multidetector coronary computed tomographic angiography for prediction of all-cause mortality. *J Am Coll Cardiol* 2007;50:1161-70.
17. Motoyama S, Sarai M, Harigaya H, et al. Computed tomographic angiography characteristics of atherosclerotic plaques subsequently resulting in acute coronary syndrome. *J Am Coll Cardiol* 2009;54:49-57.

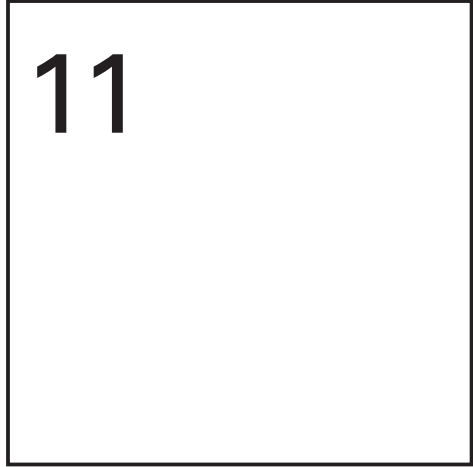
18. Ostrom MP, Gopal A, Ahmadi N, et al. Mortality incidence and the severity of coronary atherosclerosis assessed by computed tomography angiography. *J Am Coll Cardiol* 2008;52:1335-43.
19. Rubinshtein R, Halon DA, Gaspar T, et al. Cardiac computed tomographic angiography for risk stratification and prediction of late cardiovascular outcome events in patients with a chest pain syndrome. *Int J Cardiol* 2008;137:108-15.
20. van Werkhoven JM, Schuijf JD, Gaemperli O, et al. Prognostic value of multislice computed tomography and gated single-photon emission computed tomography in patients with suspected coronary artery disease. *J Am Coll Cardiol* 2009;53:623-32.
21. van Werkhoven JM, Schuijf JD, Gaemperli O, et al. Incremental prognostic value of multi-slice computed tomography coronary angiography over coronary artery calcium scoring in patients with suspected coronary artery disease. *Eur Heart J* 2009;30:2622-9.
22. Hamon M, Biondi-Zoccai GG, Malagutti P, et al. Diagnostic performance of multislice spiral computed tomography of coronary arteries as compared with conventional invasive coronary angiography: a meta-analysis. *J Am Coll Cardiol* 2006;48:1896-910.
23. Hausleiter J, Meyer T, Hadamitzky M, et al. Non-invasive coronary computed tomographic angiography for patients with suspected coronary artery disease: the Coronary Angiography by Computed Tomography with the Use of a Submillimeter resolution (CACTUS) trial. *Eur Heart J* 2007;28:3034-41.
24. Leber AW, Knez A, von Ziegler F, et al. Quantification of obstructive and nonobstructive coronary lesions by 64-slice computed tomography: a comparative study with quantitative coronary angiography and intravascular ultrasound. *J Am Coll Cardiol* 2005;46:147-54.
25. Mollet NR, Cademartiri F, Van Mieghem CAG, et al. High-resolution spiral computed tomography coronary angiography in patients referred for diagnostic conventional coronary angiography. *Circulation* 2005;112:2318-23.
26. Raff GL, Gallagher MJ, O'Neill WW, et al. Diagnostic accuracy of noninvasive coronary angiography using 64-slice spiral computed tomography. *J Am Coll Cardiol* 2005;46:552-7.
27. Schuijf JD, Pundziute G, Jukema JW, et al. Diagnostic accuracy of 64-slice multislice computed tomography in the noninvasive evaluation of significant coronary artery disease. *Am J Cardiol* 2006;98:145-8.
28. DeWood MA, Spores J, Notske R, et al. Prevalence of total coronary occlusion during the early hours of transmural myocardial infarction. *N Engl J Med* 1980;303:897-902.
29. Solomon HA, Edwards AL, Killip T. Prodromatan acute myocardial infarction. *Circulation* 1969;40:463-71.
30. Stowers M, Short D. Warning symptoms before major myocardial infarction. *Br Heart J* 1970;32:833-8.
31. Ambrose JA, Tannenbaum MA, Alexopoulos D, et al. Angiographic progression of coronary artery disease and the development of myocardial infarction. *J Am Coll Cardiol* 1988;12:56-62.
32. Little WC, Constantinescu M, Applegate RJ, et al. Can coronary angiography predict the site of a subsequent myocardial infarction in patients with mild-to-moderate coronary artery disease? *Circulation* 1988;78:1157-66.
33. Nobuyoshi M, Tanaka M, Nosaka H, et al. Progression of coronary atherosclerosis: is coronary spasm related to progression? *J Am Coll Cardiol* 1991;18:904-10.
34. Giroud D, Li JM, Urban P, et al. Relation of the site of acute myocardial infarction to the most severe coronary arterial stenosis at prior angiography. *Am J Cardiol* 1992;69:729-32.
35. Van Lingem R, Kakani N, Veitch A, et al. Prognostic and accuracy data of multidetector CT coronary angiography in an established clinical service. *Clin Radiol* 2009;64:601-7.
36. Virmani R, Burke AP, Farb A, et al. Pathology of the vulnerable plaque. *J Am Coll Cardiol* 2006;47:C13-C18.
37. Naghavi M, Libby P, Falk E, et al. From vulnerable plaque to vulnerable patient: a call for new definitions and risk assessment strategies: Part II. *Circulation* 2003;108:1772-8.

38. Achenbach S, Ropers D, Hoffmann U, et al. Assessment of coronary remodeling in stenotic and nonstenotic coronary atherosclerotic lesions by multidetector spiral computed tomography. *J Am Coll Cardiol* 2004;43:842-7.
39. Achenbach S, Moselewski F, Ropers D, et al. Detection of calcified and noncalcified coronary atherosclerotic plaque by contrast-enhanced, submillimeter multidetector spiral computed tomography: a segment-based comparison with intravascular ultrasound. *Circulation* 2004;109:14-7.
40. Becker CR, Nikolaou K, Muders M, et al. Ex vivo coronary atherosclerotic plaque characterization with multi-detector-row CT. *Eur Radiol* 2003;13:2094-8.
41. Cordeiro MA, Lima JA. Atherosclerotic plaque characterization by multidetector row computed tomography angiography. *J Am Coll Cardiol* 2006;47:C40-C47.
42. Hoffmann U, Moselewski F, Nieman K, et al. Noninvasive assessment of plaque morphology and composition in culprit and stable lesions in acute coronary syndrome and stable lesions in stable angina by multidetector computed tomography. *J Am Coll Cardiol* 2006;47:1655-62.
43. Komatsu S, Hirayama A, Omori Y, et al. Detection of coronary plaque by computed tomography with a novel plaque analysis system, 'Plaque Map', and comparison with intravascular ultrasound and angiography. *Circ J* 2005;69:72-7.
44. Leber AW, Knez A, Becker A, et al. Accuracy of multidetector spiral computed tomography in identifying and differentiating the composition of coronary atherosclerotic plaques: a comparative study with intracoronary ultrasound. *J Am Coll Cardiol* 2004;43:1241-7.
45. Leber AW, Becker A, Knez A, et al. Accuracy of 64-slice computed tomography to classify and quantify plaque volumes in the proximal coronary system: a comparative study using intravascular ultrasound. *J Am Coll Cardiol* 2006;47:672-7.
46. Motoyama S, Kondo T, Anno H, et al. Atherosclerotic plaque characterization by 0.5-mm-slice multislice computed tomographic imaging. *Circ J* 2007;71:363-6.
47. Pohle K, Achenbach S, MacNeill B, et al. Characterization of non-calcified coronary atherosclerotic plaque by multi-detector row CT: comparison to IVUS. *Atherosclerosis* 2007;190:174-80.
48. Schroeder S, Kopp AF, Baumbach A, et al. Noninvasive detection and evaluation of atherosclerotic coronary plaques with multislice computed tomography. *J Am Coll Cardiol* 2001;37:1430-5.
49. Schroeder S, Kuettner A, Leitritz M, et al. Reliability of differentiating human coronary plaque morphology using contrast-enhanced multislice spiral computed tomography: a comparison with histology. *J Comput Assist Tomogr* 2004;28:449-54.
50. Kolodgie FD, Burke AP, Farb A, et al. The thin-cap fibroatheroma: a type of vulnerable plaque: the major precursor lesion to acute coronary syndromes. *Curr Opin Cardiol* 2001;16:285-92.
51. Schuijff JD, Beck T, Burgstahler C, et al. Differences in plaque composition and distribution in stable coronary artery disease versus acute coronary syndromes; non-invasive evaluation with multi-slice computed tomography. *Acute Card Care* 2007;9:48-53.
52. Motoyama S, Kondo T, Sarai M, et al. Multislice computed tomographic characteristics of coronary lesions in acute coronary syndromes. *J Am Coll Cardiol* 2007;50:319-26.
53. Wilson PW, D'Agostino RB, Levy D, et al. Prediction of coronary heart disease using risk factor categories. *Circulation* 1998;97:1837-47.
54. Arad Y, Goodman KJ, Roth M, et al. Coronary calcification, coronary disease risk factors, C-reactive protein, and atherosclerotic cardiovascular disease events: the St. Francis Heart Study. *J Am Coll Cardiol* 2005;46:158-65.
55. Budoff MJ, Shaw LJ, Liu ST, et al. Long-term prognosis associated with coronary calcification: observations from a registry of 25,253 patients. *J Am Coll Cardiol* 2007;49:1860-70.
56. Detrano R, Guerci AD, Carr JJ, et al. Coronary calcium as a predictor of coronary events in four racial or ethnic groups. *N Engl J Med* 2008;358:1336-45.
57. Greenland P, LaBree L, Azen SP, et al. Coronary artery calcium score combined with Framingham score for risk prediction in asymptomatic individuals. *JAMA* 2004;291:210-5.

58. Greenland P, Bonow RO, Brundage BH, et al. ACCF/AHA 2007 clinical expert consensus document on coronary artery calcium scoring by computed tomography in global cardiovascular risk assessment and in evaluation of patients with chest pain: a report of the American College of Cardiology Foundation Clinical Expert Consensus Task Force (ACCF/AHA Writing Committee to Update the 2000 Expert Consensus Document on Electron Beam Computed Tomography) developed in collaboration with the Society of Atherosclerosis Imaging and Prevention and the Society of Cardiovascular Computed Tomography. *J Am Coll Cardiol* 2007;49:378-402.
59. Sarwar A, Shaw LJ, Shapiro MD, et al. Diagnostic and prognostic value of absence of coronary artery calcification. *JACC Cardiovasc Imaging* 2009;2:675-88.
60. Elhendy A, Schinkel A, Bax JJ, et al. Long-term prognosis after a normal exercise stress Tc-99m sestamibi SPECT study. *J Nucl Cardiol* 2003;10:261-6.
61. Elhendy A, Schinkel AFL, van Domburg RT, et al. Prognostic value of stress Tc-99m-tetrofosmin myocardial perfusion imaging in predicting all-cause mortality: a 6-year follow-up study. *European Journal of Nuclear Medicine and Molecular Imaging* 2006;33:1157-61.
62. Hachamovitch R, Berman DS, Kiat H, et al. Exercise myocardial perfusion SPECT in patients without known coronary artery disease: incremental prognostic value and use in risk stratification. *Circulation* 1996;93:905-14.
63. Stratmann HG, Williams GA, Wittry MD, et al. Exercise technetium-99m sestamibi tomography for cardiac risk stratification of patients with stable chest pain. *Circulation* 1994;89:615-22.
64. Thomas GS, Miyamoto MI, Morello AP, et al. Technetium 99m sestamibi myocardial perfusion imaging predicts clinical outcome in the community outpatient setting. The Nuclear Utility in the Community (NUC) Study. *J Am Coll Cardiol* 2004;43:213-23.
65. Underwood SR, Anagnostopoulos C, Cerqueira M, et al. Myocardial perfusion scintigraphy: the evidence - A consensus conference organised by the British Cardiac Society, the British Nuclear Cardiology Society and the British Nuclear Medicine Society, endorsed by the Royal College of Physicians of London and the Royal College of Radiologists. *European Journal of Nuclear Medicine and Molecular Imaging* 2004;31:261-91.
66. Shaw LJ, Iskandrian AE. Prognostic value of gated myocardial perfusion SPECT. *J Nucl Cardiol* 2004;11:171-85.
67. Gaemperli O, Schepis T, Koepfli P, et al. Accuracy of 64-slice CT angiography for the detection of functionally relevant coronary stenoses as assessed with myocardial perfusion SPECT. *Eur J Nucl Med Mol Imaging* 2007;34:1162-71.
68. Hacker M, Jakobs T, Hack N, et al. Sixty-four slice spiral CT angiography does not predict the functional relevance of coronary artery stenoses in patients with stable angina. *Eur J Nucl Med Mol Imaging* 2007;34:4-10.
69. Rispler S, Keidar Z, Ghersin E, et al. Integrated single-photon emission computed tomography and computed tomography coronary angiography for the assessment of hemodynamically significant coronary artery lesions. *J Am Coll Cardiol* 2007;49:1059-67.
70. Schuijff JD, Wijns W, Jukema JW, et al. The relationship between non-invasive coronary angiography with multi-slice computed tomography and myocardial perfusion imaging. *J Am Coll Cardiol* 2006;48:2508-14.
71. Schuijff JD, Jukema JW, van der Wall EE, et al. The current status of multislice computed tomography in the diagnosis and prognosis of coronary artery disease. *J Nucl Cardiol* 2007;14:604-12.
72. Leber AW, Becker A, Knez A, et al. Accuracy of 64-slice computed tomography to classify and quantify plaque volumes in the proximal coronary system: a comparative study using intravascular ultrasound. *J Am Coll Cardiol* 2006;47:672-7.
73. Hausleiter J, Meyer T, Hadamitzky M, et al. Radiation dose estimates from cardiac multislice computed tomography in daily practice: impact of different scanning protocols on effective dose estimates. *Circulation* 2006;113:1305-10.

74. Hsieh J, Londt J, Vass M, et al. Step-and-shoot data acquisition and reconstruction for cardiac x-ray computed tomography. *Med Phys* 2006;33:4236-48.
75. Husmann L, Valenta I, Gaemperli O, et al. Feasibility of low-dose coronary CT angiography: first experience with prospective ECG-gating. *Eur Heart J* 2008;29:191-7.
76. Rybicki FJ, Otero HJ, Steigner ML, et al. Initial evaluation of coronary images from 320-detector row computed tomography. *Int J Cardiovasc Imaging* 2008;24:535-46.
77. Herzog BA, Husmann L, Burkhard N, et al. Accuracy of low-dose computed tomography coronary angiography using prospective electrocardiogram-triggering: first clinical experience. *Eur Heart J* 2008;29:3037-42.
78. Scheffel H, Alkadhi H, Leschka S, et al. Low-dose CT coronary angiography in the step-and-shoot mode: diagnostic performance. *Heart* 2008;94:1132-7.
79. Herzog BA, Wyss CA, Husmann L, et al. First Head-to-Head Comparison of Effective Radiation Dose from Low-Dose CT with Prospective ECG-Triggering versus Invasive Coronary Angiography. *Heart* 2009.
80. Jain RK, Finn AV, Kolodgie FD, et al. Antiangiogenic therapy for normalization of atherosclerotic plaque vasculature: a potential strategy for plaque stabilization. *Nat Clin Pract Cardiovasc Med* 2007;4:491-502.

Chapter 11



Prognostic value of multislice computed tomography and gated single-photon emission computed tomography in patients with suspected coronary artery disease

JM van Werkhoven, JD Schuijf, O Gaemperli, J W Jukema, E Boersma, W Wijns, P Stolzmann, H Alkadhi, I Valenta, MPM Stokkel, G Pundziute, A Scholte, EE van der Wall, PA Kaufmann, JJ Bax

Abstract

Although MSCT is used for the detection of (CAD) in addition to MPI, its incremental prognostic value is unclear. The purpose of this study was therefore to study whether multi-slice computed tomography coronary angiography (MSCT) has incremental prognostic value over single photon emission computed tomography (SPECT) myocardial perfusion imaging (MPI) in patients with suspected coronary artery disease (CAD). In 541 patients (59% male, age 59 ± 11 years) referred for further cardiac evaluation, both MSCT and MPI were performed. The following events were recorded: all cause death, non-fatal infarction, and unstable angina requiring revascularization. In the 517 (96%) patients with an interpretable MSCT, significant CAD (MSCT $\geq 50\%$ stenosis) was detected in 158 (31%) patients, while abnormal perfusion (SSS ≥ 4) was observed in 168 (33%) patients. During follow-up (median 672 days, 25-75th percentile: 420-896), an event occurred in 23 (5.2%) patients. After correction for baseline characteristics in a multivariate model, MSCT emerged as an independent predictor of events with an incremental prognostic value to MPI. The annualized hard event rate (all-cause mortality and non-fatal infarction) in patients with none or mild CAD (MSCT $< 50\%$ stenosis) was 1.8% versus 4.8% in patients with significant CAD (MSCT $\geq 50\%$ stenosis). A normal MPI (SSS < 4) and abnormal MPI (SSS ≥ 4) were associated with an annualized hard event rate of 1.1% and 3.8% respectively. MSCT and MPI were synergistic and combined use resulted in significantly improved prediction (Log-rank test p -value < 0.005). In conclusion: MSCT is an independent predictor of events and provides incremental prognostic value to MPI. Combined anatomical and functional assessment may allow improved risk stratification.

Introduction

With the arrival of multi-slice computed tomography coronary angiography (MSCT), the focus of non-invasive imaging has shifted from functional imaging to a combination of both anatomical and functional imaging. Several studies have addressed the association between the anatomical and functional information obtained with MSCT and myocardial perfusion imaging (MPI) using single photon emission computed tomography (SPECT) respectively.¹⁻³ These comparative studies have shown that MSCT may provide complementary rather than overlapping diagnostic information when used in combination with MPI. Whether MSCT provides complementary information to MPI with regard to risk stratification remains to be determined. Interestingly, studies in the past have shown that MPI provides substantial incremental value over anatomical information obtained with invasive coronary angiography. However no studies have addressed this issue more recently.^{4, 5} Moreover, MSCT may have an important advantage over invasive coronary angiography due to its ability to provide information on plaque composition in addition to stenosis severity.⁶ Accordingly, the information obtained by MSCT may potentially enhance risk stratification by MPI. The aim of this study was therefore to assess in patients presenting with suspected coronary artery disease (CAD) whether MSCT has incremental prognostic value over MPI.

Methods

Patient selection

The study population consisted of 541 patients who prospectively underwent both MPI and MSCT within 3 months of each other. Enrollment of patients started in June 2003 and continued until December 2007. Follow-up information was obtained from the start of the study until August 2008. Patients were included at the University Hospital in Zurich, Switzerland (n=269); the Cardiovascular Center in Aalst, Belgium (n=17); and at the Leiden University Medical Center, The Netherlands (n=255). Patients were referred because of chest pain complaints, a positive exercise ECG test, or a high risk profile for cardiovascular disease. Exclusion criteria were: cardiac arrhythmias, renal insufficiency (serum creatinine >120 mmol/L), known hypersensitivity to iodine contrast media, and pregnancy. In addition, patients with a cardiac event in the period between MSCT and MPI, or an uninterpretable MSCT scan were excluded. The pre-test probability of CAD was determined using the Diamond and Forrester method, as previously described.⁷ The study was approved by the local ethics committees in all 3 participating centers and informed consent was obtained in all patients.

Myocardial perfusion imaging

Myocardial perfusion imaging was performed using gated SPECT. Two ECG-gated MPI protocols were used. A total of 272 patients underwent a 2-day gated stress-rest MPI using technetium-99m tetrofosmin (500 MBq), or technetium-99m sestamibi (500 MBq) with either a symptom limited bicycle test or pharmacological stress using adenosine (140 mcg/kg/min for 6 minutes) or dobutamine (up to 40 mcg/kg/min in 15 min). The remaining 269 patients underwent a 1-day stress-rest protocol with adenosine stress (140 mcg/kg/min during 7 minutes) using technetium-99m tetrofosmin (300 MBq at peak stress and 900 MBq at rest).

The images were acquired on a triple-head SPECT camera (GCA 9300/HG, Toshiba Corp., Tokyo, Japan) or a dual-head detector camera (Millennium VG & Hawkeye, General Electric Medical Systems, Milwaukee, WI, USA; or Vertex Epic ADAC Pegasus, Philips Medical Systems, Eindhoven, the Netherlands). All cameras were equipped with low energy high resolution collimators. A 20% window was used around the 140-keV energy peak of technetium-99m, and data were stored in a 64x64 matrix.

Stress and rest SPECT perfusion datasets were quantitatively evaluated using previously validated automated software.⁸ The myocardium was divided into a 20 segment model and for each segment myocardial perfusion was evaluated using a standard 5-point scoring system. The segmental perfusion scores during stress and rest were added together to calculate the summed stress score (SSS) and the summed rest score (SRS). The summed difference score (SDS) was calculated by subtracting the SRS from the SSS. Abnormal MPI was defined as $SSS \geq 4$ and severely abnormal MPI was defined as $SSS \geq 8$.

MSCT coronary angiography

In 33 patients the MSCT examination was performed using a 16-slice scanner (Aquilion16, Toshiba Medical Systems, Tokyo, Japan). The remaining 508 (94%) patients were scanned using a 64-slice MSCT scanner (Aquilion64, Toshiba Medical Systems, Tokyo, Japan; General Electrics LightSpeed VCT, Milwaukee, WI, US; or Sensation64, Siemens, Forchheim, Germany). Patient's heart rate and blood pressure were monitored before each scan. In the absence of contraindications, patients with a heart rate exceeding the threshold of 65 beats per minute were administered beta-blocking medication (50-100 mg metoprolol, oral or 5-10 mg metoprolol, intravenous).

Before the helical scan, a non-enhanced low dose prospective ECG-gated scan, prospectively triggered at 75% of the R-R interval was performed to measure the coronary calcium score (CS). The helical scan parameters have been previously described.^{3, 9}

Post-processing of the MSCT and CS scans was performed on dedicated workstations (Vitrea2, Vital Images, USA; Advantage, GE healthcare, USA; Syngo InSpace4D application, Siemens, Germany; and Aquarius, TeraRecon, USA). The CS was calculated using the Agatston method. Coronary anatomy was assessed in a standardized manner by dividing the coronary artery tree into 17 segments according to the modified American Heart Association classification. For each segment both the presence of atherosclerotic plaque as well as its composition was determined. Atherosclerotic lesions were deemed significant if the diameter stenosis was $\geq 50\%$. Lesions below this threshold were considered to be non-significant or mild. Plaque composition was graded as non-calcified plaque (plaques having lower density compared with the contrast-enhanced lumen), calcified plaque (plaques with high density), and mixed plaque (containing elements from both non-calcified and calcified plaque).

Follow-up

Patient follow-up data were gathered by three observers blinded to the baseline MSCT and MPI results using clinical visits or standardized telephone interviews. The following events were regarded as clinical endpoints: all cause mortality, non-fatal myocardial infarction, and unstable angina requiring revascularization. Non-fatal infarction was defined based on criteria of typical chest pain, elevated cardiac enzyme levels, and typical changes on the ECG. Unstable angina was defined according to the European Society of Cardiology guidelines as acute chest pain with or without the presence of ECG abnormalities, and negative cardiac enzyme levels.¹⁰ Patients with stable complaints undergoing an early elective revascularization within 60 days after imaging with MSCT or MPI were excluded from the survival analysis. Annualized event rates were calculated based on events per patient year follow-up.

Statistical analysis

Continuous variables were expressed as mean and standard deviation, and categorical baseline data were expressed in numbers and percentages. Cox regression analysis was used to determine the prognostic value of CS, MSCT, and MPI variables. First univariate analysis of baseline characteristics, CS, MSCT and MPI variables was performed using a composite endpoint of all cause mortality, non-fatal infarction, and unstable angina requiring revascularization. For each variable a hazard ratio with a 95%-confidence interval (95%-CI) was calculated. Using univariate analysis, optimal cutoffs (based on the number of segments affected) were created for plaque composition on MSCT. Finally multivariate models were created correcting MSCT and MPI for baseline risk factors. The incremental value of MSCT over baseline clinical variables and MPI was assessed by calculating the global chi-square.

Cumulative event rates for MSCT, MPI, and for MSCT and MPI combined were obtained by the Kaplan-Meier method using a composite endpoint of all cause mortality, non-fatal

infarction, and unstable angina requiring revascularization, and a hard composite endpoint of all cause mortality and non-fatal infarction. Statistical analyses were performed using SPSS software (version 12.0, SPSS Inc, Chicago, IL, USA) and SAS software (The SAS system 6.12, Cary, NC, USA: SAS Institute Inc). A p-value <0.05 was considered statistically significant.

Results

Patient characteristics

In the study population of 541 patients an uninterpretable MSCT examination was present in 24 patients (4%). Reasons for uninterpretability were the presence of motion artifacts, increased noise due to high body mass index, and breathing. In patients with an uninterpretable MSCT, MPI was abnormal ($SSS \geq 4$) in 9 (38%) patients and normal ($SSS < 4$) in the remaining 15 (62%) patients. After exclusion of these patients, a total of 517 patients remained for analysis. A complete overview of the baseline characteristics of these patients is presented in Table 1. The average age of the study cohort was 59 ± 11 years and 59% of patients were men. The majority of patients (65%) presented with an intermediate pre-test probability for of CAD, and a low or a high probability was present in respectively 22% and 13% of patients.

Table 1. Patient characteristics.

Gender (male)	303 (59%)
Age (yrs)	59 ± 11
Risk Factors	
Diabetes	156 (30%)
Hypertension	290 (56%)
Hypercholesterolemia	209 (40%)
Family history CAD	191 (37%)
Current Smoking	154 (30%)
Obesity (BMI ≥ 30)	111 (22%)
Pre-test likelihood of CAD	
Low	113 (22%)
Intermediate	336 (65%)
High	68 (13%)

MSCT and SPECT results

An exercise test was performed in 88 patients (17%), while pharmacological stress with adenosine was used in 397 patients (77%), and with dobutamine in 30 patients (6%). All MPI results are listed in Table 2. The gated SPECT images during rest and stress were normal ($SSS < 4$) in 349 (67%) patients. An abnormal MPI ($SSS \geq 4$) was present in 192 (33%) patients and severely abnormal MPI ($SSS \geq 8$) was present in 64 (13%) patients. During MSCT image

Table 2. Imaging results.

Calcium Score	
CS > 400	113 (22%)
CS > 1000	47 (9%)
MSCT	
Atherosclerosis	362 (70%)
Significant CAD	158 (31%)
Patients with non-calcified plaques	130 (25%)
Patients with mixed plaques	204 (40%)
Patients with calcified plaques	270 (52%)
MPI	
SSS <4 (normal)	349 (67%)
SSS 4-7	104 (20%)
SSS 8-12	44 (9%)
SSS ≥ 13	20 (4%)
SDS 0-1	378 (73%)
SDS 2-3	72 (14%)
SDS ≥ 4	67 (13%)

acquisition, an average heart rate of 63 ± 11 beats per minute was recorded. CS and MSCT results are listed in Table 2. The average CS was 325 ± 751 Agatston units. A CS >400 was present in 113 (22%) patients and CS was normal or ≤ 400 in 404 patients (78%). A CS >1000 was observed in 47 (9%) patients, while a CS ≤ 1000 was observed in the remaining 470 patients (91%). During the contrast enhanced helical scan, a completely normal MSCT examination was observed in 155 (30%) of patients. Atherosclerosis, both mild (<50% stenosis) and significant ($\geq 50\%$ stenosis), was observed in 362 (70%). Significant CAD with lesions $\geq 50\%$ stenosis was observed in 158 (31%) patients. Non-calcified plaques were observed in 130 patients (25%), mixed plaques in 204 patients (40%), and calcified plaques in 270 patients (52%).

The results of MSCT in relation to MPI are illustrated in Figure 1. This figure illustrates the complementary value of MSCT and MPI. Only approximately 50% of patients with a significant lesion ($\geq 50\%$ stenosis) showed a perfusion defect on MPI (SSS ≥ 4). Importantly, a significant stenosis was observed in 22% of patients with normal perfusion on MPI (SSS <4).

Follow-up results

Of the cohort of 517 patients, 35 (6.8%) were lost to follow-up, while 43 (8.3%) patients underwent early revascularization (within 60 days of MSCT or MPI). In the remaining 439 patients the median follow-up time achieved was 672 days (25-75th percentile: 420-896). During this time period an event occurred in 23 patients (5.2%). Death by any cause occurred in 8 patients (1.8%); in 2 the cause of death could be ascertained as cardiac. Non-fatal myocardial infarction occurred in 8 patients (1.8%) and 7 patients (1.6%) were hospitalized due to unstable angina pectoris.

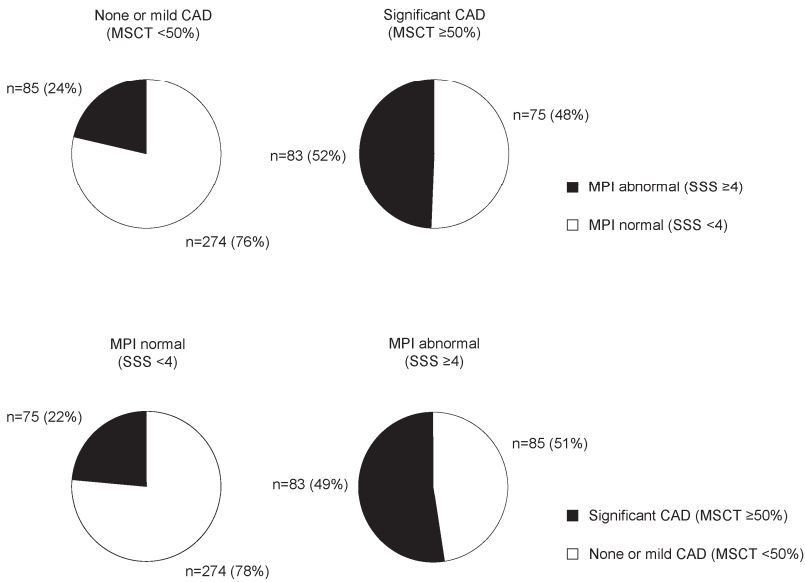


Figure 1. Pie charts depicting the relationship between the anatomic information obtained by MSCT and the functional information from MPI.

Univariate and multivariate analysis

Baseline univariate predictors of events are listed in Table 3. CS, MSCT and MPI were significant univariate predictors of events. Both CS >400 and CS >1000 were significant predictors. When regarding the MSCT results on a patient level, the presence of significant CAD ($\geq 50\%$ stenosis) was a strong significant predictor (hazard ratio 3.683 (95%-confidence interval (95%-CI): 1.611-8.420)), whereas the presence of any atherosclerosis was not (hazard ratio 3.087 (95%-CI: 0.917-10.388)). Importantly, plaque composition on MSCT was also identified as a predictor of events. On a patient level, the presence of ≥ 2 segments with non-calcified plaque (n=65) (hazard ratio 5.0 (95%-CI: 2.2-11.7)) or ≥ 3 segments with mixed plaque (n=68) (hazard ratio 3.5 (hazard ratio (95%-CI: 1.5-8.1)) were both significant predictors of events. Of the MPI variables, the SSS ≥ 4 was the strongest significant predictor of events (hazard ratio 4.0, 95% CI 1.7-9.3).

After univariate analysis multivariate models were created for both MSCT and MPI correcting for baseline risk factors. MSCT ($\geq 50\%$ stenosis) remained a significant predictor when corrected for CS > 400 or CS > 1000. However CS > 400 and CS > 1000 did not reach statistical significance. MPI also remained a significant predictor when corrected for CS > 400 or CS > 1000. In this model, CS > 1000 however also remained a significant independent predictor of events.

Table 3. Univariate predictors of events,

	HR (95%-CI)	p-value
Calcium Score		
CS > 400	3.007 (1.318-6.860)	0.009
CS > 1000	3.752 (1.392-10.114)	0.009
MSCT		
Atherosclerosis	3.087 (0.917-10.388)	0.069
Significant CAD	3.683 (1.611-8.420)	0.002
≥2 non-calcified plaques	5.0 (2.2-11.7)	<0.001
≥3 mixed plaques	3.5 (1.5-8.1)	<0.005
≥4 calcified plaques	1.5 (0.6-4.1)	0.409
MPI		
SSS ≥ 2	3.500 (1.513-8.094)	0.003
SSS ≥ 4	4.029 (1.742-9.319)	0.001
SSS ≥ 8	1.922 (0.653-5.656)	0.236
SDS ≥ 2	1.853 (0.783-4.381)	0.160
SDS ≥ 4	2.142 (0.724-6.336)	0.169

Subsequently, several multivariate models were created to assess the independent predictive value of different MSCT variables, corrected for MPI and baseline risk factors. On a patient level, no independent prognostic value over MPI and baseline risk factors was observed for the presence of any atherosclerosis on MSCT. In contrast, the observation of significant CAD on MSCT was however shown to provide independent prognostic value over MPI. When regarding plaque composition only the presence of 2 or more segments with non-calcified plaque was an independent significant predictor. Importantly, MPI remained an independent significant predictor of events in each multivariate model.

To assess the incremental prognostic value of these MSCT variables over baseline clinical variables and MPI, global chi-square scores were calculated. The results of this analysis are presented in Figure 4. This figure shows that information on the presence of significant stenosis obtained by MSCT has incremental prognostic value to both baseline clinical variables alone and baseline clinical variables and MPI combined. Finally the addition of non-calcified plaque on a patient basis resulted in further enhancement of risk stratification incremental to the combination of clinical variables, MPI, and significant stenosis on MSCT.

Event rates

The Kaplan-Meier survival curves in Figures 2 and 3 illustrate the different survival rates of the MPI and MSCT test outcomes both for the composite endpoint of all cause mortality, non-fatal myocardial infarction and unstable angina requiring revascularization (Log Rank p-value <0.001) as well as for the combined hard endpoint of all cause mortality and non-fatal myocardial infarction (Log Rank p-value <0.05). The annualized event rate (annualized

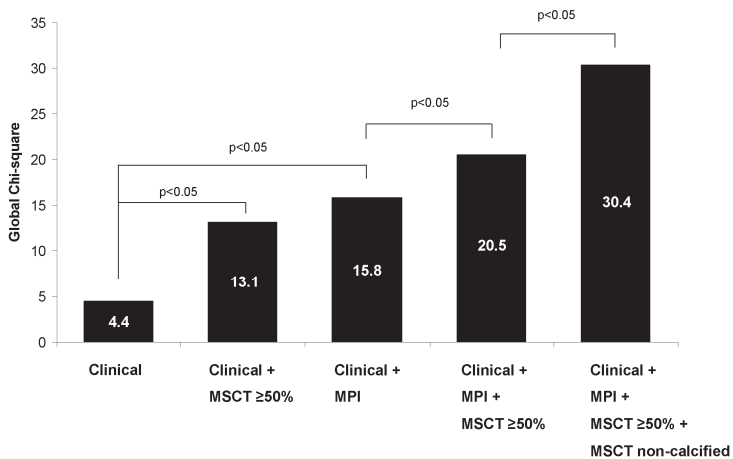


Figure 2. Bar graphs illustrating the incremental prognostic value (depicted by chi-square value on the y-axis) of MSCT. The addition of MSCT provides incremental prognostic information to baseline clinical variables and MPI. Furthermore the addition of non-calcified plaque on MSCT (≥ 2 segments with non-calcified plaque) results in further incremental prognostic information over baseline clinical variables, MPI, and significant CAD ($\geq 50\%$ stenosis) on MSCT.

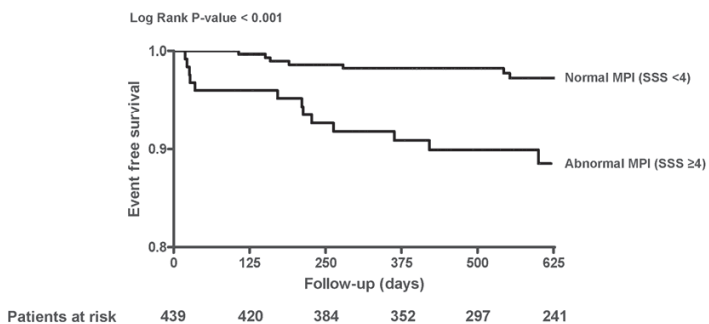


Figure 3a. Kaplan-Meier curves for all events (all cause mortality, non-fatal infarction, and unstable angina requiring revascularization) in patients with a normal MPI (SSS <4) or an abnormal MPI (SSS ≥ 4).

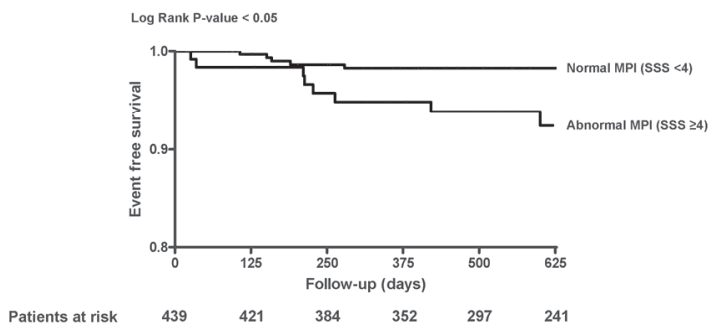


Figure 3b. Kaplan-Meier curves for hard events (all cause mortality and non-fatal infarction) in patients with a normal MPI (SSS <4) or an abnormal MPI (SSS ≥ 4).

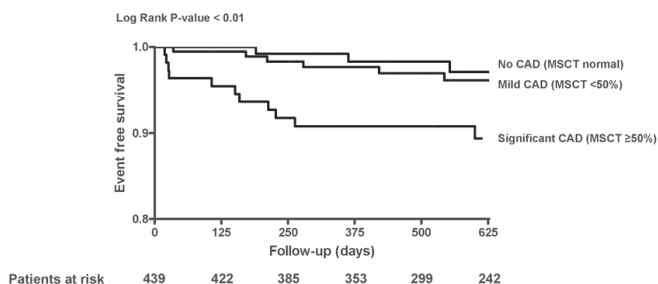


Figure 4a. Kaplan-Meier curves for all events (all cause mortality, non-fatal infarction, and unstable angina requiring revascularization) in patients with no CAD (MSCT normal), mild CAD (MSCT <50% stenosis) or significant CAD (MSCT ≥50% stenosis).

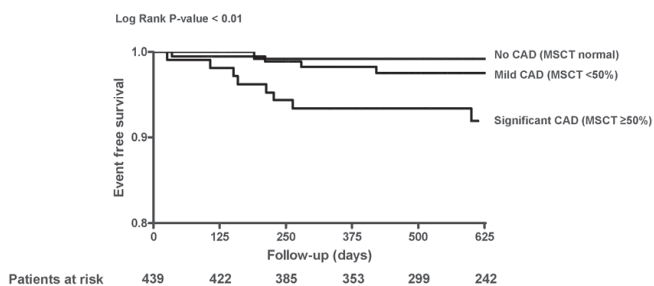


Figure 4b. Kaplan-Meier curves for hard events (all cause mortality and non-fatal infarction) in patients with no CAD (MSCT normal), mild CAD (MSCT <50% stenosis) or significant CAD (MSCT ≥50% stenosis).

event rate for hard events between parentheses) in patients with a normal MPI examination (SSS <4) was 1.5% (1.1%); the annualized event rate in patients with an abnormal MPI (SSS ≥4) was 6.0% (3.8%). The annualized event rate in patients with none or mild CAD (MSCT <50% stenosis) was 3.0% (1.8%). When these patients were further divided into patients with mild atherosclerosis and patients without any evidence of atherosclerosis, the annualized event rates were 2.0% (1.4%), and 1.1% (0.3%) respectively. The annualized event rate for patients with a significant stenosis (≥50%) on MSCT was 6.3% (4.8%). When regarding plaque composition, the annualized event rate in patients with 2 or more segments with non-calcified plaque was 8.4% (6.7%) compared to 1.9% (1.2%) in patients with no or less than 2 segments with non-calcified plaque.

Combined use of MSCT and MPI resulted in significantly improved prediction of the composite hard endpoint of all cause mortality and non-fatal myocardial infarction (Log rank test p-value <0.005), as illustrated in the Kaplan-Meier survival curve in Figure 5. In patients with none or mild CAD (MSCT <50% stenosis) and a normal MPI (SSS <4) (n=256) the annualized event rate (annualized hard event rate in parenthesis) was 1.0% (0.6%). In patients with none or mild CAD (MSCT <50% stenosis) but an abnormal MPI (SSS ≥4)

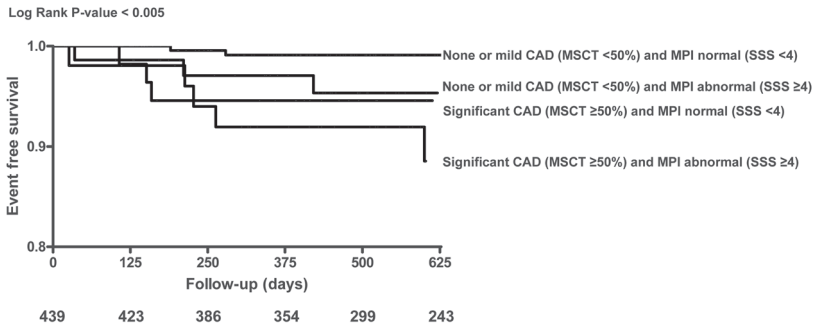


Figure 5. Kaplan-Meier curves for hard events (all cause mortality and non-fatal infarction) in patients with a normal MPI (SSS <4) and none or mild CAD (<50% stenosis) on MSCT, in patients with an abnormal MPI (SSS ≥ 4) and with none or mild CAD (<50% stenosis) on MSCT, in patients with a normal MPI (SSS <4) and significant CAD (MSCT ≥50% stenosis), and finally in patients with an abnormal MPI (SSS ≥ 4) and significant CAD (MSCT ≥50% stenosis).

(n=72), the annualized event rate increased to 3.7% (2.2%), whereas patients with significant CAD (MSCT ≥50% stenosis) and a normal MPI (SSS <4) (n=57) were associated with an annualized event rate of 3.8% (3.8%). Interestingly, the event rates between patients with none or mild CAD (<50%) stenosis and an abnormal MPI and patients with significant CAD (MSCT ≥50% stenosis) did not differ significantly. In patients with both significant CAD (MSCT ≥50% stenosis) and an abnormal MPI (SSS <4) (n=54), the annualized event rate was 9.0% (6.0%). In these patients the addition of plaque composition (presence of 2 or more segments with non-calcified plaque (n=20)) resulted in the highest event rate 10.8% (8.2%).

Discussion

The main finding of the current study is that when used in combination with MPI, MSCT not only provides complementary information about the presence, extent, and composition of atherosclerosis, but importantly, also results in improved risk stratification as compared to the use of MPI alone.

Risk stratification with MPI

A wealth of data have been published on the diagnostic accuracy and prognostic value of MPI.¹¹⁻¹⁶ In an extensive review of the available literature a low risk scan was associated with a low annualized hard event rate (cardiac death and non-fatal myocardial infarction) of 0.6% in a population of 69,655 patients.¹⁷ In a recent meta-analysis, Metz et al specifically focused on the prognostic value of a normal MPI.¹⁸ The pooled summary absolute event rate in their study was 1.21 (95%-CI: 0.98-1.48) for the occurrence of cardiac death and non-fatal myocardial infarction. The slightly higher absolute hard event rate in the current

study (2.2%) may have been caused by the inclusion of all cause mortality, and the fact that the majority of patients underwent pharmacological testing.^{17, 19} Importantly, event rates were significantly higher in patients with abnormal MPI ($SSS \geq 4$), in line with the previous literature.¹⁷

Risk stratification with MSCT

While MSCT coronary angiography is a relatively new technique, a considerable amount of evidence is available with calcium scoring.²⁰⁻²⁷ Moreover, in a systematic review of the available literature ($n=27,622$ patients) the presence of any coronary artery calcium was shown to confer a 4-fold increased risk of cardiac death or myocardial infarction ($p<0.0001$) as compared to the absence of coronary artery calcifications.²⁴ In contrast, an extremely low event rate of 0.4% was observed in patients without any coronary artery calcium.

Only limited data are available on the prognostic value of anatomic imaging with MSCT coronary angiography.²⁸⁻³⁰ In the present study, annual hard event rates of 0.3%, 2.0%, and 4.8% were observed in patients with respectively completely normal, non-significant and significant CAD on MSCT. Min et al evaluated 1,127 patients undergoing 16-slice MSCT with a mean follow-up of 15.3 ± 3.9 months. In line with our study, event rates for all cause mortality ranging between 0.3% for none or mild atherosclerosis (stenosis $<50\%$) to 15% for mild to moderate left main disease were observed in a period of 2 years.²⁹

Currently one previous study by Pundziute et al. has addressed the prognostic value of plaque components assessed by MSCT.³⁰ The number of mixed plaques was a significant predictor when corrected for baseline clinical variables. In the current study only non-calcified plaque remained an independent predictor of events. The discrepancy between the current results and the study by Pundziute et al. may be explained by differences in the studied patient populations as well as the use of optimized cutoffs and correction for MPI results in the current study.

Combination of MSCT and MPI

In previous studies, the prognostic value of anatomic imaging using calcium scoring in relation to MPI has been addressed.³¹⁻³⁴ Recently, Schenker et al showed that the risk of all cause mortality and myocardial infarction increased with increasing CS, both in patients with normal and in patients with abnormal perfusion on MPI.³⁴ The present study is the first to address the incremental prognostic value of MSCT when used in combination with MPI. Previous studies have shown that MPI provides incremental prognostic information over invasive coronary angiography.^{4, 5} Vice versa, the current study has revealed that the anatomic information on MSCT is not only an independent predictor of events but also provides incremental prognostic information over baseline clinical variables and MPI,

particularly in patients with a normal MPI. Although several MSCT variables were able to provide prognostic information, on a patient level the presence of significant CAD ($\geq 50\%$ stenosis) was identified as a robust independent predictor. This is an important finding as diagnostic MSCT examinations are often graded in this manner. In addition to stenosis severity, plaque composition was also identified to further enhance risk stratification. Indeed, the presence of non-calcified plaques provided incremental prognostic information over baseline clinical variables, MPI, and significant CAD on MSCT. This finding suggests that potentially assessment of plaque composition on MSCT may provide clinically relevant information in addition to stenosis severity.

Study limitations

Even though the diagnostic accuracy of MSCT is high, images are still uninterpretable in a small percentage of patients. It is however anticipated that the amount of uninterpretable studies will continue to decrease with newer generation scanners.^{35, 36} In contrast, none of the SPECT examinations were uninterpretable in this study. Another potential limitation is that the MSCT studies were evaluated visually; no validated accurate quantitative algorithms are currently available. In the current study a composite endpoint including all cause mortality was used, which is not a direct cardiac endpoint. An important advantage of all cause mortality however is the fact that it is not affected by verification bias.³⁷ Furthermore most deaths in adults are linked to cardiovascular disease. All cause mortality is therefore a commonly used endpoint allowing comparison of the current results to previous investigations.^{21, 26, 29, 34} Finally, the radiation burden associated with combined MSCT and MPI imaging is a limitation. However the radiation dose can decrease significantly when using dedicated dose reduction MSCT acquisition techniques that have recently become available.³⁸⁻⁴¹

Conclusion

MSCT is an independent predictor of events and provides incremental prognostic value to MPI. Furthermore, addition of plaque composition to stenosis severity was shown to provide incremental prognostic information. The results of this study suggest that combined anatomical and functional assessment may allow improved risk stratification.

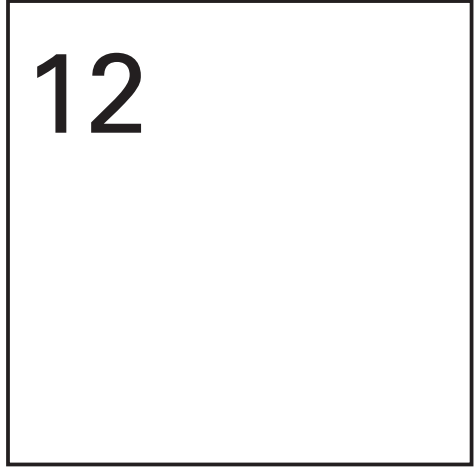
References

1. Gaemperli O, Schepis T, Koepfli P, et al. Accuracy of 64-slice CT angiography for the detection of functionally relevant coronary stenoses as assessed with myocardial perfusion SPECT. *Eur J Nucl Med Mol Imaging* 2007;34:1162-71.
2. Hacker M, Jakobs T, Hack N, et al. Sixty-four slice spiral CT angiography does not predict the functional relevance of coronary artery stenoses in patients with stable angina. *Eur J Nucl Med Mol Imaging* 2007;34:4-10.
3. Schuijff JD, Wijns W, Jukema JW, et al. Relationship between noninvasive coronary angiography with multi-slice computed tomography and myocardial perfusion imaging. *J Am Coll Cardiol* 2006;48:2508-14.
4. Iskandrian AS, Chae SC, Heo J, et al. Independent and incremental prognostic value of exercise single-photon emission computed tomographic (SPECT) thallium imaging in coronary artery disease. *J Am Coll Cardiol* 1993;22:665-70.
5. Pollock SG, Abbott RD, Boucher CA, et al. Independent and incremental prognostic value of tests performed in hierarchical order to evaluate patients with suspected coronary artery disease. Validation of models based on these tests. *Circulation* 1992;85:237-48.
6. Schroeder S, Kopp AF, Burgstahler C. Noninvasive plaque imaging using multislice detector spiral computed tomography. *Semin Thromb Hemost* 2007;33:203-9.
7. Diamond GA, Forrester JS. Analysis of probability as an aid in the clinical diagnosis of coronary-artery disease. *N Engl J Med* 1979;300:1350-8.
8. Germano G, Kavanagh PB, Waechter P, et al. A new algorithm for the quantitation of myocardial perfusion SPECT. I: technical principles and reproducibility. *J Nucl Med* 2000;41:712-9.
9. Leschka S, Husmann L, Desbiolles LM, et al. Optimal image reconstruction intervals for non-invasive coronary angiography with 64-slice CT. *Eur Radiol* 2006;16:1964-72.
10. Bassand JP, Hamm CW, Ardissino D, et al. Guidelines for the diagnosis and treatment of non-ST-segment elevation acute coronary syndromes. *Eur Heart J* 2007;28:1598-660.
11. Elhendy A, Schinkel A, Bax JJ, et al. Long-term prognosis after a normal exercise stress Tc-99m sestamibi SPECT study. *J Nucl Cardiol* 2003;10:261-6.
12. Elhendy A, Schinkel AFL, van Domburg RT, et al. Prognostic value of stress Tc-99m-tetrofosmin myocardial perfusion imaging in predicting all-cause mortality: a 6-year follow-up study. *European Journal of Nuclear Medicine and Molecular Imaging* 2006;33:1157-61.
13. Hachamovitch R, Berman DS, Kiat H, et al. Exercise myocardial perfusion SPECT in patients without known coronary artery disease: incremental prognostic value and use in risk stratification. *Circulation* 1996;93:905-14.
14. Stratmann HG, Williams GA, Wittry MD, et al. Exercise technetium-99m sestamibi tomography for cardiac risk stratification of patients with stable chest pain. *Circulation* 1994;89:615-22.
15. Thomas GS, Miyamoto MI, Morello AP, et al. Technetium 99m sestamibi myocardial perfusion imaging predicts clinical outcome in the community outpatient setting. The Nuclear Utility in the Community (NUC) Study. *J Am Coll Cardiol* 2004;43:213-23.
16. Underwood SR, Anagnostopoulos C, Cerqueira M, et al. Myocardial perfusion scintigraphy: the evidence - A consensus conference organised by the British Cardiac Society, the British Nuclear Cardiology Society and the British Nuclear Medicine Society, endorsed by the Royal College of Physicians of London and the Royal College of Radiologists. *European Journal of Nuclear Medicine and Molecular Imaging* 2004;31:261-91.
17. Shaw LJ, Iskandrian AE. Prognostic value of gated myocardial perfusion SPECT. *J Nucl Cardiol* 2004;11:171-85.
18. Metz LD, Beattie M, Hom R, et al. The prognostic value of normal exercise myocardial perfusion imaging and exercise echocardiography: a meta-analysis. *J Am Coll Cardiol* 2007;49:227-37.

19. Hachamovitch R, Hayes S, Friedman JD, et al. Determinants of risk and its temporal variation in patients with normal stress myocardial perfusion scans: what is the warranty period of a normal scan? *J Am Coll Cardiol* 2003;41:1329-40.
20. Arad Y, Spadaro LA, Goodman K, et al. Prediction of coronary events with electron beam computed tomography. *J Am Coll Cardiol* 2000;36:1253-60.
21. Budoff MJ, Shaw LJ, Liu ST, et al. Long-term prognosis associated with coronary calcification: observations from a registry of 25,253 patients. *J Am Coll Cardiol* 2007;49:1860-70.
22. Detrano R, Guerci AD, Carr JJ, et al. Coronary calcium as a predictor of coronary events in four racial or ethnic groups. *N Engl J Med* 2008;358:1336-45.
23. Greenland P, LaBree L, Azen SP, et al. Coronary artery calcium score combined with Framingham score for risk prediction in asymptomatic individuals. *JAMA* 2004;291:210-5.
24. Greenland P, Bonow RO, Brundage BH, et al. ACCF/AHA 2007 clinical expert consensus document on coronary artery calcium scoring by computed tomography in global cardiovascular risk assessment and in evaluation of patients with chest pain: a report of the American College of Cardiology Foundation Clinical Expert Consensus Task Force (ACCF/AHA Writing Committee to Update the 2000 Expert Consensus Document on Electron Beam Computed Tomography) developed in collaboration with the Society of Atherosclerosis Imaging and Prevention and the Society of Cardiovascular Computed Tomography. *J Am Coll Cardiol* 2007;49:378-402.
25. Kondos GT, Hoff JA, Sevrukov A, et al. Electron-beam tomography coronary artery calcium and cardiac events: a 37-month follow-up of 5635 initially asymptomatic low- to intermediate-risk adults. *Circulation* 2003;107:2571-6.
26. Shaw LJ, Raggi P, Schisterman E, et al. Prognostic value of cardiac risk factors and coronary artery calcium screening for all-cause mortality. *Radiology* 2003;228:826-33.
27. Taylor AJ, Bindeman J, Feuerstein I, et al. Coronary calcium independently predicts incident premature coronary heart disease over measured cardiovascular risk factors: mean three-year outcomes in the Prospective Army Coronary Calcium (PACC) project. *J Am Coll Cardiol* 2005;46:807-14.
28. Gilard M, Le Gal G, Cornily J, et al. Midterm Prognosis of Patients With Suspected Coronary Artery Disease and Normal Multislice Computed Tomographic Findings. *Arch Intern Med* 2007;165:1686-9.
29. Min JK, Shaw LJ, Devereux RB, et al. Prognostic value of multidetector coronary computed tomographic angiography for prediction of all-cause mortality. *J Am Coll Cardiol* 2007;50:1161-70.
30. Pundziute G, Schuijff JD, Jukema JW, et al. Prognostic value of multislice computed tomography coronary angiography in patients with known or suspected coronary artery disease. *J Am Coll Cardiol* 2007;49:62-70.
31. Anand DV, Lim E, Hopkins D, et al. Risk stratification in uncomplicated type 2 diabetes: prospective evaluation of the combined use of coronary artery calcium imaging and selective myocardial perfusion scintigraphy. *Eur Heart J* 2006;27:713-21.
32. Ramakrishna G, Miller TD, Breen JF, et al. Relationship and prognostic value of coronary artery calcification by electron beam computed tomography to stress-induced ischemia by single photon emission computed tomography. *Am Heart J* 2007;153:807-14.
33. Rozanski A, Gransar H, Wong ND, et al. Clinical outcomes after both coronary calcium scanning and exercise myocardial perfusion scintigraphy. *J Am Coll Cardiol* 2007;49:1352-61.
34. Schenker MP, Dorbala S, Hong EC, et al. Interrelation of coronary calcification, myocardial ischemia, and outcomes in patients with intermediate likelihood of coronary artery disease: a combined positron emission tomography/computed tomography study. *Circulation* 2008;117:1693-700.
35. Flohr TG, McCollough CH, Bruder H, et al. First performance evaluation of a dual-source CT (DSCT) system. *Eur Radiol* 2006;16:256-68.
36. Scheffel H, Alkhadi H, Plass A. Accuracy of dual-source CT coronary angiography: First experience in a high pre-test probability population without heart rate control. *Eur Radiol* 2006;16:2739-40.

37. Lauer MS, Blackstone EH, Young JB, et al. Cause of death in clinical research: time for a reassessment? *J Am Coll Cardiol* 1999;34:618-20.
38. Hausleiter J, Meyer T, Hadamitzky M, et al. Radiation dose estimates from cardiac multislice computed tomography in daily practice: impact of different scanning protocols on effective dose estimates. *Circulation* 2006;113:1305-10.
39. Hsieh J, Londt J, Vass M, et al. Step-and-shoot data acquisition and reconstruction for cardiac x-ray computed tomography. *Med Phys* 2006;33:4236-48.
40. Husmann L, Valenta I, Gaemperli O, et al. Feasibility of low-dose coronary CT angiography: first experience with prospective ECG-gating. *Eur Heart J* 2008;29:191-7.
41. Rybicki FJ, Otero HJ, Steigner ML, et al. Initial evaluation of coronary images from 320-detector row computed tomography. *Int J Cardiovasc Imaging* 2008;24:535-46.

Chapter 12



Incremental prognostic value of multi-slice
computed tomography coronary angiography
over coronary artery calcium scoring in patients
with suspected coronary artery disease

JM van Werkhoven, JD Schuijf, O Gaemperli, JW Jukema,
LJ Kroft, E Boersma, A Pazhenkottil, I Valenta, G Pundziute, A de Roos,
EE van der Wall, PA Kaufmann, JJ Bax

Abstract

The purpose of this study was to assess the relationship between calcium scoring (CS) and multi-slice computed tomography coronary angiography (MSCTA) and to determine if MSCTA has an incremental prognostic value to CS. In 432 patients (59% male, age 58 ± 11 years) referred for cardiac evaluation due to suspected coronary artery disease (CAD), CS and 64-slice MSCTA were performed. The following events were combined in a composite endpoint: all cause mortality, non-fatal infarction, and unstable angina requiring revascularization. CS was 0 in 147 (34%) patients, CS 1-99 was present in 122 (28%), CS 100-399 in 75 (17%), CS 400-999 in 56 (13%), and $CS \geq 1000$ in 32 (7%). MSCTA was normal in 133 (31%) patients, MSCTA 30-50% stenosis was observed in 190 (44%), and MSCTA $\geq 50\%$ stenosis in 109 (25%). During follow-up (median 670 days (25-75th percentile: 418-895), an event occurred in 21 patients (4.9%) patients. After multivariate correction for CS, MSCTA $\geq 50\%$ stenosis, the number of diseased segments, obstructive segments, and non-calcified plaques were independent predictors with an incremental prognostic value to CS. In conclusion, MSCTA provides additional information to CS regarding stenosis severity and plaque composition. This additional information was shown to translate into incremental prognostic value over CS.

Introduction

Non-invasive imaging plays an important role in the diagnosis and prognosis of coronary artery disease (CAD). The development of non-invasive anatomic imaging techniques such as coronary calcium scoring (CS) and multi-slice computed tomography coronary angiography (MSCTA) have resulted in substantially increased interest in non-invasive imaging of atherosclerosis.

Extensive data are available supporting the value of CS in risk stratification and patients with increased CS are generally considered to have a higher likelihood of future cardiac events. The majority of data however have been obtained in asymptomatic patients at low to intermediate risk although the technique may also be useful in symptomatic patients.¹⁻⁴

Direct non-invasive detection of luminal narrowing has become possible with the introduction of MSCTA. Preliminary studies addressing the prognostic value of MSCTA have demonstrated a low risk for events in case of a normal MSCTA study compared to a higher risk in the presence of significant CAD on MSCTA.⁵⁻⁸ Importantly, MSCTA is not restricted to luminography and the technique allows simultaneous visualization of the vessel wall. As a result, also non-stenotic lesions can be identified and even some information on plaque composition can be derived.⁹ This may be an important feature of the technique as several plaque characteristics observed on MSCTA have been linked to acute coronary syndromes in retrospective studies.^{10, 11} Nevertheless, only limited prospective data are currently available supporting this notion.

Accordingly, both CS and MSCTA may be useful for risk stratification in patients with suspected CAD, it is unclear however if the information regarding stenosis severity and plaque composition on MSCTA may provide additional prognostic information to CS. To answer this clinical question amongst others we have started a prospective registry that addresses the prognostic value of MSCTA in relation to baseline characteristics as well as other imaging techniques.¹² The purpose of the present study was to assess the relationship between observations on CS and MSCTA and to determine whether the information regarding stenosis severity and plaque composition on MSCTA translates into incremental prognostic value over CS alone.

Methods

Patient selection

The study population consisted of patients with suspected coronary artery disease (CAD) who were clinically referred for further cardiac assessment because of chest pain, a positive exercise ECG test, or a high risk profile for cardiovascular disease as part of an ongoing study protocol addressing the prognostic value of MSCTA in relation to other imaging techniques. From this prospective registry, results addressing the incremental prognostic value of MSCTA over myocardial perfusion imaging have been recently published.¹² Patients were enrolled at the University Hospital in Zurich, Switzerland, and at the Leiden University Medical Center, The Netherlands. The included patients prospectively underwent a CS scan followed by MSCTA. Exclusion criteria were: cardiac arrhythmias, renal insufficiency (defined as a glomerular filtration rate <30 ml/min), known hypersensitivity to iodine contrast media, and pregnancy. In addition, patients with an uninterpretable MSCTA examination were excluded. The pre-test likelihood of CAD was determined using the Diamond and Forrester method, with a risk threshold of <13.4% for low risk, >87.2% for high risk, and between 13.4 and 87.2% for intermediate risk, as previously described.¹³ The study was approved by the local ethics committee in both participating centers.

CS and MSCTA protocol

Patients were scanned using a 64-slice CT scanner (Aquillion64, Toshiba Medical Systems, Tokyo, Japan; or General Electrics LightSpeed VCT, Milwaukee, WI, US). Before CS and MSCTA examinations, the patient's heart rate and blood pressure were monitored. In the absence of contraindications, patients with a heart rate exceeding the threshold of 65 beats per minute were administered beta-blocking medication (50-100 mg metoprolol, oral or 5-10 mg metoprolol, intravenous). Before the helical scan, a non-enhanced low dose ECG-gated scan was performed to measure CS. The CS scan was prospectively triggered at 70% or 75% of the R-R interval and performed using the following scan parameters: 4x3.0 mm or 2.5 mm; gantry rotation time, 350-500 milliseconds; tube voltage, 120 kV; and tube current, 200-250 mA.

The CS scan was used to determine the start and end positions of the MSCTA examination. The helical scan was performed using a collimation of 64 x 0.5 mm or 64x0.625 mm. All scan parameters have been previously published.^{14, 15}

Datasets were reconstructed from the retrospectively gated raw data. Images were reconstructed with an effective slice thickness of 0.3 or 0.5. Coronary arteries were evaluated using the reconstruction dataset with the least motion artifacts, typically an end-diastolic phase.

The effective dose of the CS and MSCTA scans was estimated from the product of the dose-length product and an organ weighing factor [$k=0.014 \text{ mSv} \times (\text{mGy} \times \text{cm})^{-1}$] for the chest as the investigated anatomical region.¹⁶

Data Analysis

Post-processing of the CS and MSCTA examinations was performed on dedicated workstations (Vitrea2, Vital Images, USA and Advantage, GE healthcare, USA). The CS was calculated using the Agatston method.¹⁷ MSCTA angiograms were examined using the axial slices, curved multiplanar reconstructions (MPR), and maximum intensity projections (MIP). Coronary anatomy was assessed in a standardized manner by dividing the coronary artery tree into 17 segments according to the modified American Heart Association classification. First segments were classified based on the maximum luminal diameter stenosis. Normal MSCTA was defined as completely normal anatomy or minimal wall irregularities <30%, non-significant CAD was defined as the presence of luminal narrowing with a maximal luminal diameter stenosis <50%, and significant CAD was defined as the presence of an atherosclerotic lesion exceeding the threshold of 50% maximal luminal diameter stenosis. After assessment of stenosis severity, plaque composition was determined in all diseased segments (non-significant or significant CAD on MSCTA). Plaque composition was graded as non-calcified plaque (plaques having lower density compared with the contrast-enhanced lumen), calcified plaque (plaques with high density), and mixed plaque (containing elements of both non-calcified and calcified plaque).

Follow-up

Patient follow-up data were gathered using clinical visits or standardized telephone interviews. A composite endpoint was construed using the following events: all cause mortality, non-fatal myocardial infarction, and unstable angina requiring revascularization. Non-fatal infarction was defined based on criteria of typical chest pain, elevated cardiac enzyme levels, and typical changes on the ECG. Unstable angina was defined according to the European Society of Cardiology guidelines as acute chest pain with or without the presence of ECG abnormalities, and negative cardiac enzyme levels.¹⁸ Patients with stable complaints undergoing an early elective revascularization within 60 days after imaging with CS and MSCTA were excluded from the survival analysis.

Statistical analysis

Continuous variables were expressed as mean and standard deviation, and categorical baseline data were expressed in numbers and percentages. Cox regression analysis was used to determine the prognostic value of CS, and MSCTA variables. First univariate analysis of baseline CS and MSCTA variables was performed using the composite endpoint of all cause mortality, non-fatal infarction, and unstable angina requiring revascularization. For

each variable a hazard ratio with a 95%-confidence interval (95%-CI) was calculated. The predictive value of CS was assessed using binary cutoff values (CS >0, CS \geq 100, CS \geq 400, and CS \geq 1000). For the survival analysis of MSCTA, plaque burden (number of (non) significantly diseased segments) and plaque composition (number of segments with non-calcified, mixed or calcified plaque) were analyzed as continuous variables. Finally, multivariate models were created to assess the independent predictive value of MSCTA corrected for CS and baseline clinical variables. The incremental value of MSCTA over CS and baseline clinical variables was assessed by calculating the global chi-square. Statistical analyses were performed using SPSS software (version 12.0, SPSS Inc, Chicago, IL, USA). A p-value <0.05 was considered statistically significant.

Results

The current study population, derived from our prospective registry,¹² consisted of 533 patients presenting with suspected CAD at the University Hospital Zurich (n=270) and at the Leiden University Medical Center (n=263). The demographics in the two populations were similar. In 24 (4.5%) of these patients the MSCTA examination was uninterpretable due to the presence of motion artifacts, increased noise due to a high body mass index, and breathing. In addition, 35 patients (6.9%) were lost to follow-up, and an early revascularization occurred in 42 (8.3%) patients. After exclusion of these patients, a total of 432 remained for further analysis. The baseline characteristics of the patient population are presented in Table 1. In summary, the average age of the study cohort was 58 \pm 11 years and 58% of patients were men. A low or intermediate pre-test likelihood was observed in respectively 24% and 65% of patients. A high pre-test likelihood was observed in 11%.

Table 1. Patient characteristics

Gender (male)	59%
Age (yrs)	58 \pm 11
Risk Factors	
Diabetes	121 (28%)
Hypertension	244 (57%)
Hypercholesterolemia	170 (39%)
Family history CAD	157 (36%)
Current Smoking	119 (28%)
Obesity (BMI \geq 30)	92 (21%)
Pre-test likelihood of CAD	
Low	102 (24%)
Intermediate	281 (65%)
High	49 (11%)

CS and MSCTA results

The average CS of the cohort was 290 ± 730 . Calcium was absent in 117 (34%) patients, a CS of 1-99 was observed in 122 (28%), a CS between 100 and 399 in 75 (17%), a CS between 400 and 999 in 56 (13%), and a CS ≥ 1000 was present in 32 (7%) patients. MSCTA was normal in 133 (31%) patients, and atherosclerosis (non-significant or significant CAD) was present in the remaining 299 (69%) patients. Within the patients with atherosclerosis, non-significant CAD was observed in 190 (44%), and significant CAD was present in 109 (25%) patients. For the GE scanner the estimated average radiation dose for the MSCTA protocol was 18.3 ± 5.9 mSv, and the average radiation dose for the CS protocol was 1.2 ± 0.6 mSv. For the Toshiba scanner the estimated average radiation dose for the coronary angiography protocol was 17.6 ± 5.6 mSv and the estimated radiation dose for the CS protocol was 1.5 ± 0.7 mSv.

Relationship between CS and stenosis severity and plaque composition assessed on MSCTA

Stenosis severity

Figure 1 illustrates the MSCTA findings in patients with increasing CS values. In patients without any coronary calcium, MSCTA was normal in 80%. Non-calcified plaque was observed in the remaining 20% of patients (7% of the total study population). Importantly, significant CAD was observed in 4% of patients with a CS of 0. An example of a patient with a CS of 0 and a large non-calcified plaque on MSCTA, confirmed on conventional coronary

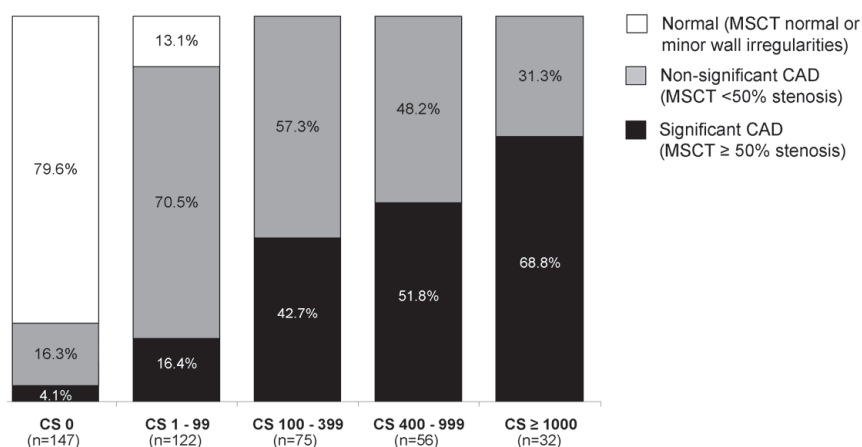


Figure 1. The relationship between increasingly higher CS categories and the prevalence of normal coronary anatomy (completely normal or minor wall irregularities), non-significant CAD (MSCTA < 50% stenosis) and significant CAD (MSCTA \geq 50% stenosis) on MSCTA.

angiography is shown in Figure 2. In patients with coronary calcifications non-significant and significant lesions were present in all but a few patients. However the relationship between CS and significant CAD on MSCTA was less evident. Particularly in patients with an intermediate CS between 100 and 1000, significant CAD was observed in approximately 50% of patients. In patients with a high CS ≥ 1000 , non-significant CAD was observed in 30% of patients.

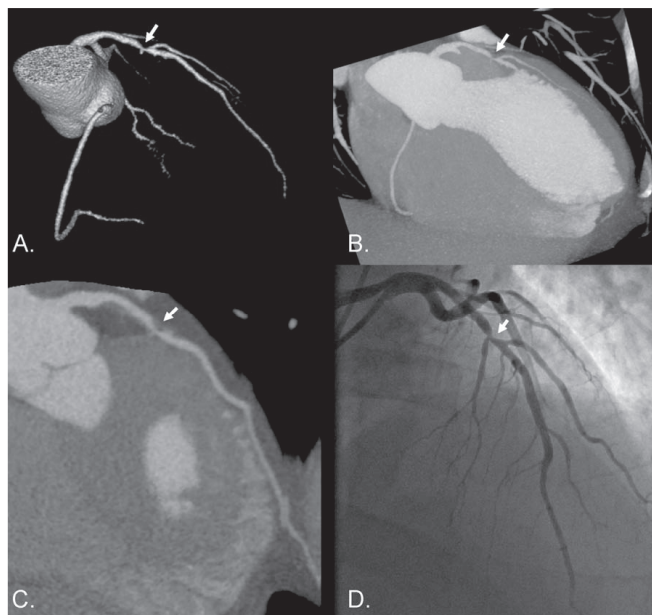


Figure 2. Case example of a 54-year old male patient presenting with atypical complaints. On CS no coronary calcifications were observed. However a large significant non-calcified plaque was detected in the left anterior descending artery on MSCTA (Panels A-C), which was confirmed on conventional coronary angiography (Panel D).

Plaque composition

MSCTA enables assessment of plaque composition in addition to stenosis severity. Figure 3 shows the distribution of segments with non-calcified plaque, mixed plaque and calcified plaque in each CS category as a percentage of the total diseased segments. In patients with CS of 0 all 76 diseased segments showed non-calcified plaque. With increasing CS categories the percentage of segments with calcified plaque contributing to the total of diseased segments increased. MSCTA was however able to identify a large proportion of diseased segments with elements of non-calcified plaque (either mixed plaque or non-calcified plaque) in each category.

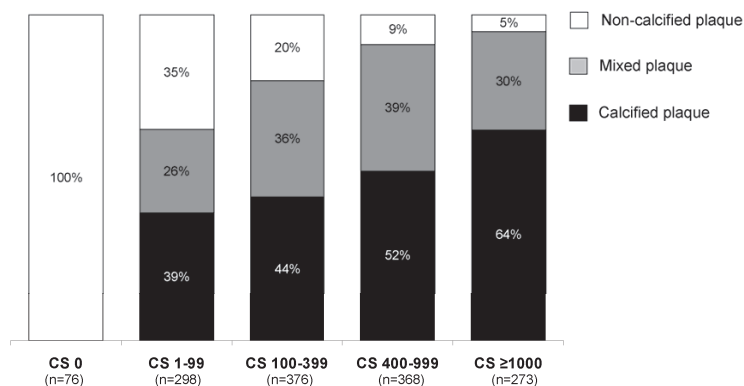


Figure 3. The distribution of segments with non-calcified plaque, mixed plaque and calcified plaque as a percentage of the total diseased segments on MSCTA per CS category. In patients with a CS 0, all 76 diseased segments showed non-calcified plaque. With increasing CS categories the percentage of diseased segments with calcified plaque increased. Nevertheless, non-calcified plaque and mixed plaque were still observed in a large proportion of diseased segments in each CS category.

Follow-up results

A median follow-up time of 670 days (25-75th percentile: 418-895) was obtained, during which the composite endpoint occurred in 21 patients (4.9%). All cause death was reported in 6 patients (1.4%), whereas non-fatal myocardial infarction occurred in 8 patients (1.8%) and 7 patients (1.6%) were revascularized due to unstable angina pectoris.

Survival analysis

Univariate analysis of CS and MSCTA categories is shown in Table 2. Within the CS cutoff categories CS ≥ 100 , CS ≥ 400 and CS ≥ 1000 were significant predictors of events. The

Table 2. Univariate CS and MSCTA predictors of coronary events

	HR (95%-CI)	p-value
CS		
Calcium score (per unit increase in CS score)	1.00 (1.00-1.01)	0.019
Any calcium	3.2 (0.9-10.9)	0.062
Calcium score ≥ 100	3.9 (1.5-10.2)	0.005
Calcium score ≥ 400	3.5 (1.5-8.3)	0.004
Calcium score ≥ 1000	4.1 (1.5-11.3)	0.006
MSCTA		
Atherosclerosis	4.3 (1.0-18.6)	0.048
Significant CAD	3.9 (1.7-9.3)	0.002
Nr. of Diseased segments	1.2 (1.08-1.3)	<0.001
Nr. Segments with significant CAD	1.4 (1.2-1.6)	<0.001
Nr. Segments with non-calcified plaque	1.2 (1.07-1.4)	0.003
Nr. Segments with mixed plaque	1.3 (1.07-1.5)	0.005
Nr. Segments with calcified plaque	1.09 (0.9-1.3)	0.254

highest hazard ratio was observed when using a cutoff of 1000. On MSCTA several variables reached statistical significance. The presence of any stenosis (non-significant (30-50% stenosis) or significant ($\geq 50\%$ stenosis) as well as the presence of significant CAD ($\geq 50\%$ stenosis) both were strong significant predictors. When regarding plaque burden, both the number of diseased segments as well as the number of segments with significant CAD were significant univariate predictors. When regarding plaque composition, the number of segments with non-calcified plaque and the number segments with mixed plaque were also significant predictors of events. The number of segments with calcified plaque was not a significant predictor of events.

Event rates

The annualized event rate in patients without any coronary calcium was 1.1%. Increasingly higher CS was associated with increasingly higher annualized event rates, the annualized event rate was 1.4% in patients with a CS 1-99, 3.7% in patients with a CS 100-399, and 4.8% in patients with a CS 400-999. The highest annualized event rate of 8.5% was observed in patients with a CS ≥ 1000 .

When regarding MSCTA, an event rate of 0.8% was observed in patients with a normal MSCTA (completely normal or minor wall irregularities); while in patients with atherosclerosis (non-significant and/or significant CAD) the annualized event rate was 3.5%. In patients with non-significant CAD the annualized event rate was 2.1%, versus 5.9% in patients with significant CAD.

Independent and incremental prognostic value of MSCTA over CS

To determine the independent prognostic value of MSCTA, multivariate models were created including all MSCTA variables corrected for age, gender and CS ≥ 1000 . Table 3 shows that the presence of significant CAD, the number of diseased segments, obstructive segments, segments with non-calcified plaque, and the number of segments with mixed plaque remained independent predictors. Furthermore plaque burden and plaque composition provided incremental prognostic value over clinical variables and MSCTA as shown in Figures 4 and 5. These results suggest that MSCTA may provide additional prognostic information. In particular, the number of segments with significant CAD and the number of segments with non-calcified plaque provided significant incremental prognostic value over CS. The number of mixed plaques provided borderline significant ($p=0.058$) incremental prognostic value to CS.

Table 3. Multivariate models for the prediction of coronary events

		HR (95%-CI)	p-value
Model 1	Atherosclerosis	4.5 (0.9-21.3)	0.056
	Calcium score ≥ 1000	4.0 (1.3-12.4)	0.016
Model 2	Significant CAD	3.6 (1.4-9.4)	0.009
	Calcium score ≥ 1000	2.9 (0.9-9.3)	0.064
Model 3	Nr. Diseased segments	1.2 (1.1-1.3)	0.006
	Calcium score ≥ 1000	2.0 (0.6-6.9)	0.268
Model 4	Nr. Segments with significant CAD	1.3 (1.1-1.5)	0.003
	Calcium score ≥ 1000	2.6 (0.7-9.3)	0.148
Model 5	Nr. Segments with non-calcified plaque	1.3 (1.1-1.4)	0.001
	Calcium score ≥ 1000	5.8 (1.9-18.2)	0.003
Model 6	Nr. Segments with mixed plaque	1.2 (1.0-1.4)	0.039
	Calcium score ≥ 1000	3.6 (1.1-11.6)	0.029

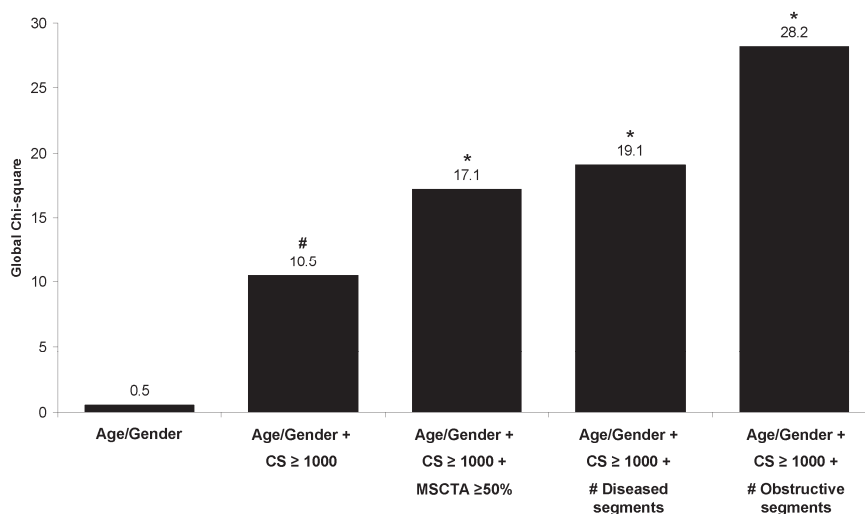


Figure 4. Bar graphs illustrating the incremental prognostic value (depicted by chi-square value on the y-axis) of significant CAD ($\geq 50\%$ stenosis) on MSCTA and plaque burden (defined as the number of diseased or segments with significant CAD on MSCTA) over age, gender and CS. CS has a significant incremental prognostic value over age and gender (#). A further incremental prognostic value over age, gender and CS was observed with the addition of MSCTA (*).

Discussion

The main finding of the current study was that MSCTA may provide additional anatomic information regarding stenosis severity and plaque composition compared to CS. Furthermore this information offers important prognostic information which is incremental to CS for risk stratification.

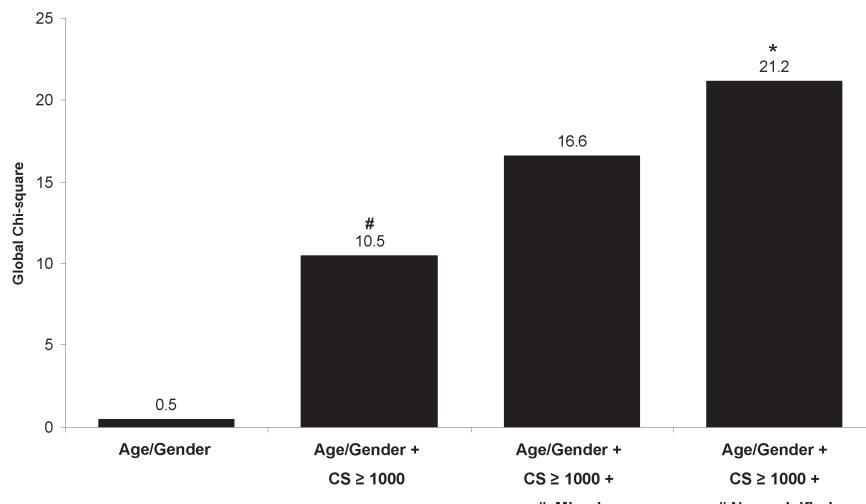


Figure 5. Bar graphs illustrating the incremental prognostic value (depicted by chi-square value on the y-axis) of MSCTA plaque composition variables over age, gender and CS. CS has a significant incremental prognostic value over age and gender (#). A further incremental prognostic value over age, gender and CS was observed with the addition of MSCTA (*).

CS and MSCTA for atherosclerosis detection

In asymptomatic patients, CS may be useful to identify the presence of atherosclerosis and thus identify patients that may be at higher risk than recognized based on traditional risk assessment.¹⁹ Vice versa, absence of calcium on the other hand in general implies a low likelihood of events.²⁰ However in a small proportion of patients with a negative CS, non-calcified plaque has been observed.^{21, 22} Indeed, in certain subpopulations, such as those at higher risk or in symptomatic patients the prevalence of non-calcified plaque may be higher.²³⁻²⁵ Akram et al. specifically studied the relationship between symptomatic status and the prevalence of non-significant and significant CAD in patients with a CS of 0 and observed 22% non-significant and significant CAD and 8% significant CAD in symptomatic patients.²³ In the current study non-significant or significant CAD was identified on MSCTA in 20% of patients with a CS of 0, whereas significant CAD was observed in 4%. Accordingly, particularly in symptomatic populations a small proportion of patients with atherosclerosis may not be recognized by CS.

Considering patients with evidence of coronary calcifications, a positive association has been observed between CS and the presence of significant CAD on MSCTA and conventional coronary angiography.^{26, 27} Indeed in the current study the prevalence of significant CAD paralleled increasing CS categories. Nevertheless, in a substantial proportion of patients with extensive calcifications, significant CAD was absent on MSCT, indicating somewhat lower specificity of CS to diagnose significant CAD in line with previous investigations.^{28, 29} Since

particularly in symptomatic patients identification of significant CAD is of importance for guiding clinical management (including decisions for potential revascularization), MSCTA may provide incremental diagnostic information to CS in this regard.

Prognostic value of CS and MSCTA

A considerable amount of evidence regarding risk stratification is available with CS in asymptomatic patients.^{19, 20, 30-33} Although less frequently studied, also in symptomatic patients CS has been shown to provide important prognostic information (¹⁻⁴ In the study by Detrano et al. a 6 times higher event rate was observed in patients with a CS above the median compared to those with a CS below the median.¹

The prognostic value of MSCTA has been studied less extensively.⁵⁻⁸ In the largest study thus far by Min et al, a cohort of 1,127 patients undergoing 16-slice MSCT was evaluated.⁶ The prognostic value of the Duke Prognostic Coronary Artery Disease Index was assessed and event rates for all cause mortality ranging between 0.3% for none or mild atherosclerosis (stenosis <50%) to 15% for mild to moderate left main disease were observed in a period of 2 years. Similar findings were reported in smaller studies by Gilard et al and Pundziute et al.^{5, 7} Furthermore, recently published results from our current prospective registry have demonstrated an incremental prognostic value of MSCTA over myocardial perfusion imaging using single photon emission computed tomography.¹²

To our knowledge the current study is the first study assessing the incremental prognostic value of both stenosis severity and plaque composition on MSCTA over CS. In a previous study however, the incremental value of plaque burden, derived by non-invasive coronary angiography with electron beam computed tomography, over CS was assessed by Ostrom and colleagues.³⁴ The authors showed that plaque burden, defined as the number of non-significantly or significantly diseased vessels, had independent and incremental value in predicting all-cause mortality independent of age, gender, conventional risk factors, and CS. Similar findings were recently reported by Rubinshtein et al.⁸ Accordingly, in combination with our own observations, it appears that non-invasive measures of the extent and severity of stenosis provide incremental prognostic information over CS.

Importantly, assessment of plaque composition may further enhance risk stratification. However, only limited prospective data are available addressing the potential relationship between plaque composition on MSCTA and outcome. When exploring plaque composition in the current study, the number of segments with non-calcified plaque as well as the number of segments with mixed plaque was shown to be independently associated with increased risk for events. Interestingly, no such relation was observed for the number of segments with calcified plaque. An explanation may be that CS is more accurate at quantifying

calcium burden. Furthermore when regarding only the number of calcified plaques on MSCT the calcium in mixed plaques is disregarded. Secondly, another explanation may be that non-calcified plaque is more important from a prognostic standpoint. Currently two previous studies have addressed the prognostic value of plaque composition assessed by MSCTA.^{7, 12} Pundziute et al observed that the number of mixed plaques was a significant predictor when corrected for baseline clinical variables.⁷ In addition, we recently showed that plaque composition on MSCTA provides incremental prognostic value over myocardial perfusion imaging.¹²

Limitations

Even though the diagnostic accuracy of MSCTA is high, uninterpretable images are still encountered in a small percentage of patients due to motion because of high or irregular heart rates or breathing during the examination. It is however anticipated that the number of uninterpretable studies will continue to decrease with newer generation scanners. Another potential limitation of MSCTA is the use of iodinated contrast media. As a result MSCTA is contraindicated in patients with renal insufficiency or known hypersensitivity to iodine contrast media. Currently 64-slice MSCTA is still associated with a significantly higher radiation exposure than CS, although the radiation dose of MSCTA will decrease with the use of dedicated dose reduction techniques that have recently become available.³⁵⁻³⁸

Conclusion

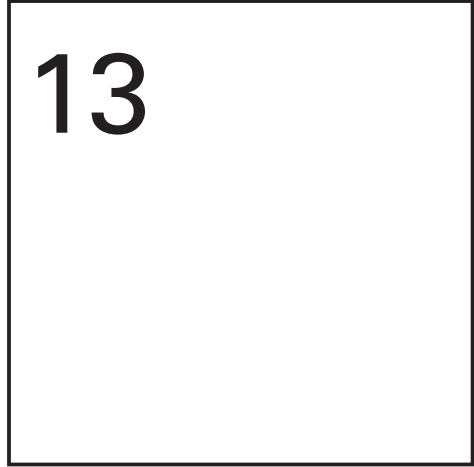
Non-invasive anatomic imaging using CS and MSCTA is useful for the detection of atherosclerosis; MSCTA however provides additional information to CS regarding stenosis severity and plaque composition. This additional information was shown to translate into incremental value for risk stratification.

References

1. Detrano R, Hsiai T, Wang S, et al. Prognostic value of coronary calcification and angiographic stenoses in patients undergoing coronary angiography. *J Am Coll Cardiol* 1996;27:285-90.
2. Georgiou D, Budoff MJ, Kaufer E, et al. Screening patients with chest pain in the emergency department using electron beam tomography: a follow-up study. *J Am Coll Cardiol* 2001;38:105-10.
3. Schenker MP, Dorbala S, Hong EC, et al. Interrelation of coronary calcification, myocardial ischemia, and outcomes in patients with intermediate likelihood of coronary artery disease: a combined positron emission tomography/computed tomography study. *Circulation* 2008;117:1693-700.
4. Keelan PC, Bielak LF, Ashai K, et al. Long-term prognostic value of coronary calcification detected by electron-beam computed tomography in patients undergoing coronary angiography. *Circulation* 2001;104:412-7.
5. Gilard M, Le Gal G, Cornily J, et al. Midterm Prognosis of Patients With Suspected Coronary Artery Disease and Normal Multislice Computed Tomographic Findings. *Arch Intern Med* 2007;165:1686-9.
6. Min JK, Shaw LJ, Devereux RB, et al. Prognostic value of multidetector coronary computed tomographic angiography for prediction of all-cause mortality. *J Am Coll Cardiol* 2007;50:1161-70.
7. Pundziute G, Schuijff JD, Jukema JW, et al. Prognostic value of multislice computed tomography coronary angiography in patients with known or suspected coronary artery disease. *J Am Coll Cardiol* 2007;49:62-70.
8. Rubinshtein R, Halon DA, Gaspar T, et al. Cardiac computed tomographic angiography for risk stratification and prediction of late cardiovascular outcome events in patients with a chest pain syndrome. *Int J Cardiol* 2008;137:108-15.
9. Schroeder S, Kopp AF, Baumbach A, et al. Noninvasive detection and evaluation of atherosclerotic coronary plaques with multislice computed tomography. *J Am Coll Cardiol* 2001;37:1430-5.
10. Hoffmann U, Moselewski F, Nieman K, et al. Noninvasive assessment of plaque morphology and composition in culprit and stable lesions in acute coronary syndrome and stable lesions in stable angina by multidetector computed tomography. *J Am Coll Cardiol* 2006;47:1655-62.
11. Schuijff JD, Beck T, Burgstahler C, et al. Differences in plaque composition and distribution in stable coronary artery disease versus acute coronary syndromes; non-invasive evaluation with multi-slice computed tomography. *Acute Card Care* 2007;9:48-53.
12. van Werkhoven JM, Schuijff JD, Gaemperli O, et al. Prognostic value of multislice computed tomography and gated single-photon emission computed tomography in patients with suspected coronary artery disease. *J Am Coll Cardiol* 2009;53:623-32.
13. Diamond GA, Forrester JS. Analysis of probability as an aid in the clinical diagnosis of coronary-artery disease. *N Engl J Med* 1979;300:1350-8.
14. Schuijff JD, Wijns W, Jukema JW, et al. The relationship between non-invasive coronary angiography with multi-slice computed tomography and myocardial perfusion imaging. *J Am Coll Cardiol* 2006;48:2508-14.
15. Gaemperli O, Schepis T, Kalff V, et al. Validation of a new cardiac image fusion software for three-dimensional integration of myocardial perfusion SPECT and stand-alone 64-slice CT angiography. *Eur J Nucl Med Mol Imaging* 2007;34:1097-106.
16. Hausleiter J, Meyer T, Hermann F, et al. Estimated radiation dose associated with cardiac CT angiography. *JAMA* 2009;301:500-7.
17. Agatston AS, Janowitz WR, Hildner FJ, et al. Quantification of coronary artery calcium using ultrafast computed tomography. *J Am Coll Cardiol* 1990;15:827-32.
18. Bassand JP, Hamm CW, Ardissino D, et al. Guidelines for the diagnosis and treatment of non-ST-segment elevation acute coronary syndromes. *Eur Heart J* 2007;28:1598-660.
19. Taylor AJ, Bindeman J, Feuerstein I, et al. Coronary calcium independently predicts incident premature coronary heart disease over measured cardiovascular risk factors: mean three-year outcomes in the Prospective Army Coronary Calcium (PACC) project. *J Am Coll Cardiol* 2005;46:807-14.

20. Budoff MJ, Shaw LJ, Liu ST, et al. Long-term prognosis associated with coronary calcification: observations from a registry of 25,253 patients. *J Am Coll Cardiol* 2007;49:1860-70.
21. Cheng VY, Lepor NE, Madyoon H, et al. Presence and severity of noncalcified coronary plaque on 64-slice computed tomographic coronary angiography in patients with zero and low coronary artery calcium. *Am J Cardiol* 2007;99:1183-6.
22. Rubinshtein R, Gaspar T, Halon DA, et al. Prevalence and extent of obstructive coronary artery disease in patients with zero or low calcium score undergoing 64-slice cardiac multidetector computed tomography for evaluation of a chest pain syndrome. *Am J Cardiol* 2007;99:472-5.
23. Akram K, O'Donnell RE, King S, et al. Influence of symptomatic status on the prevalence of obstructive coronary artery disease in patients with zero calcium score. *Atherosclerosis* 2008;203:533-7.
24. Ramakrishna G, Miller TD, Breen JF, et al. Relationship and prognostic value of coronary artery calcification by electron beam computed tomography to stress-induced ischemia by single photon emission computed tomography. *Am Heart J* 2007;153:807-14.
25. Shemesh J, Apter S, Itzchak Y, et al. Coronary calcification compared in patients with acute versus in those with chronic coronary events by using dual-sector spiral CT. *Radiology* 2003;226:483-8.
26. Kennedy J, Shavelle R, Wang S, et al. Coronary calcium and standard risk factors in symptomatic patients referred for coronary angiography. *Am Heart J* 1998;135:696-702.
27. Ho JS, FitzGerald SJ, Stolfus LL, et al. Relation of a coronary artery calcium score higher than 400 to coronary stenoses detected using multidetector computed tomography and to traditional cardiovascular risk factors. *Am J Cardiol* 2008;101:1444-7.
28. Knez A, Becker A, Leber A, et al. Relation of coronary calcium scores by electron beam tomography to obstructive disease in 2,115 symptomatic patients. *Am J Cardiol* 2004;93:1150-2.
29. Budoff MJ, Georgiou D, Brody A, et al. Ultrafast computed tomography as a diagnostic modality in the detection of coronary artery disease: a multicenter study. *Circulation* 1996;93:898-904.
30. Detrano R, Guerci AD, Carr JJ, et al. Coronary calcium as a predictor of coronary events in four racial or ethnic groups. *N Engl J Med* 2008;358:1336-45.
31. Greenland P, LaBree L, Azen SP, et al. Coronary artery calcium score combined with Framingham score for risk prediction in asymptomatic individuals. *JAMA* 2004;291:210-5.
32. Greenland P, Bonow RO, Brundage BH, et al. ACCF/AHA 2007 clinical expert consensus document on coronary artery calcium scoring by computed tomography in global cardiovascular risk assessment and in evaluation of patients with chest pain: a report of the American College of Cardiology Foundation Clinical Expert Consensus Task Force (ACCF/AHA Writing Committee to Update the 2000 Expert Consensus Document on Electron Beam Computed Tomography) developed in collaboration with the Society of Atherosclerosis Imaging and Prevention and the Society of Cardiovascular Computed Tomography. *J Am Coll Cardiol* 2007;49:378-402.
33. Shaw LJ, Raggi P, Schisterman E, et al. Prognostic value of cardiac risk factors and coronary artery calcium screening for all-cause mortality. *Radiology* 2003;228:826-33.
34. Ostrom MP, Gopal A, Ahmadi N, et al. Mortality incidence and the severity of coronary atherosclerosis assessed by computed tomography angiography. *J Am Coll Cardiol* 2008;52:1335-43.
35. Hausleiter J, Meyer T, Hadamitzky M, et al. Radiation dose estimates from cardiac multislice computed tomography in daily practice: impact of different scanning protocols on effective dose estimates. *Circulation* 2006;113:1305-10.
36. Hsieh J, Londt J, Vass M, et al. Step-and-shoot data acquisition and reconstruction for cardiac x-ray computed tomography. *Med Phys* 2006;33:4236-48.
37. Husmann L, Valenta I, Gaemperli O, et al. Feasibility of low-dose coronary CT angiography: first experience with prospective ECG-gating. *Eur Heart J* 2008;29:191-7.
38. Rybicki FJ, Otero HJ, Steigner ML, et al. Initial evaluation of coronary images from 320-detector row computed tomography. *Int J Cardiovasc Imaging* 2008;24:535-46.

Chapter 13



Incremental prognostic value of left ventricular function analysis over non-invasive coronary angiography with multi-detector computed tomography

FR de Graaf, JM van Werkhoven, JE van Velzen, ML Antoni,
MJ Boogers, LJ Kroft, A de Roos, MJ Schaliij, JW Jukema,
EE van der Wall, JD Schuijf, JJ. Bax

Abstract

The purpose of this study was to determine the prognostic value of CTA derived left ventricular (LV) function analysis and to assess its incremental prognostic value over the detection of significant stenosis using CTA. In 728 patients (400 males, mean age 55 ± 12 years) with known or suspected CAD the presence of significant stenosis ($\geq 50\%$ stenosis) and LV function were assessed using CTA. LV end-systolic volume (LVESV), LV end-diastolic volume (LVEDV) and LV ejection fraction (LVEF) were calculated. LV function was assessed as a continuous variable and using cutoff values (LVEDV > 215 ml, LVESV > 90 ml, LVEF $< 49\%$). The following events were combined in a composite end-point: all-cause mortality, non-fatal myocardial infarction, and unstable angina pectoris requiring hospitalization. On CTA, a significant stenosis was observed in 221 patients (30%). During follow-up [median 765 days, 25th–75th percentile: 493–978] an event occurred in 45 patients (6.2%). After multivariate correction for clinical risk factors and CTA, LVEF $< 49\%$ and LVESV > 90 ml were independent predictors of events with an incremental prognostic value over clinical risk factors and CTA. In conclusion, the present results suggest that LV function analysis provides independent and incremental prognostic information beyond anatomic assessment of CAD using CTA.

Introduction

Multidetector computed tomography coronary angiography (CTA) has emerged as an important non-invasive imaging modality by providing direct anatomic assessment of coronary artery disease (CAD).¹⁻³ Recently, several studies have shown that, in addition to its value for the diagnosis of CAD, stenosis detection with CTA may also be useful for risk stratification.⁴⁻⁷ Furthermore, besides the assessment of coronary anatomy, left ventricular (LV) function may be evaluated using information derived from the same CTA data set.⁸⁻¹⁰ LV function is an established prognostic marker, as has been demonstrated using several imaging modalities including left ventriculography, echocardiography, magnetic resonance imaging (MRI) and single photon emission computed tomography (SPECT).¹¹⁻¹⁴ However, no data are currently available concerning the prognostic significance of CTA derived LV function assessment. The purpose of the present study was therefore to determine the prognostic value of CTA derived LV function analysis and to assess its incremental prognostic value over the detection of significant coronary artery stenosis using CTA.

Methods

The study group consisted of consecutive patients with suspected or known CAD who were clinically referred for CTA because of chest pain, a positive or inconclusive exercise electrocardiogram (ECG) test, or an elevated risk profile for cardiovascular disease. The study population is part of a large ongoing registry exploring the prognostic value of CTA.¹⁵ For the current analysis, only patients with a CTA examination of diagnostic image quality and with additional LV function data were included. Exclusion criteria for CTA examination were: 1) (supra)ventricular arrhythmias, 2) renal failure (glomerular filtration rate < 30 ml/min), 3) known allergy to iodine contrast material, 4) severe claustrophobia or 5) pregnancy.

CTA Data Acquisition

CTA studies were performed using a 64-row (n=647) or 320-row (n=81) multidetector scanner (Aquilion 64, and Aquilion ONE, respectively, Toshiba Medical Systems, Otawara, Japan). One hour prior to the examination, a single dose of oral beta-blocker medication was administered to patients with a heart rate \geq 65 bpm, unless contraindicated. Based on a pre-defined beta-blocking medication administration protocol, patients with a heart rate between 65 and 75 bpm received 50 mg metoprolol while patients with a heart rate \geq 75 bpm received 100 mg metoprolol. The total amount of non-ionic contrast media (Iomeron 400; Bracco, Milan, Italy) injected into the antecubital vein was 60-100 ml (depending on body weight and scanner type) at a flow rate of 5.0 ml/s or 6.0 ml/s, followed by a saline flush of 25-50 ml. In order to synchronize the arrival of the contrast media, bolus arrival was

detected using a real-time bolus tracking technique.¹⁶ All images were acquired during a single inspiratory breath-hold of maximally 12 seconds. For 64-row CTA, a helical-scanning technique was used as previously described.^{17, 18} In brief, during the scan, the ECG was registered simultaneously for retrospective gating of the data. A collimation of 64 x 0.5 mm was used. Additional scan parameters were: 400 ms or 500 ms gantry rotation time depending on cardiac frequency, 120 kV tube voltage and 300-350 mA (depending on body-mass index (BMI) and thoracic geometry). During 320-row CTA, the ECG was registered simultaneously for prospective triggering of the data. In order to perform LV function analysis, ECG-triggered tube modulation was used, as previously described.¹⁹

The entire heart was imaged in a single heart beat, attaining maximal tube current during 75% of R-R interval (in patients with stable heart rate < 60 beats per minute (bpm)), during 65-85% of R-R interval (in patients with a heart rate 60-65 bpm) or during 30-80% of R-R interval (in patients with a heart rate >65 bpm). Outside the pre-defined interval, tube current was 25% of the maximal tube current. In patients with a heart rate > 65 bpm images were acquired during multiple heart beats (typically two). A collimation of 320 x 0.5 mm was used. Additional scan parameters were: 350 ms gantry rotation time, 120-135 kV tube voltage and 400-580 mA (depending on BMI and thoracic geometry). For the 64-row CTA scanner, the estimated average radiation dose for CTA was 17.6 ± 5.6 mSv. For the 320-row CTA scanner, the estimated average radiation dose for single heart beat CTA's using ECG-triggered tube modulation was 10.7 ± 3.6 mSv. In patients in whom CTA image acquisition was performed during multiple heart beats average estimated radiation dose was 16.7 ± 6.3 mSv.

Coronary arteries were evaluated using the reconstruction dataset with the least motion artifacts, typically acquired during an end-diastolic phase. To assess LV function and LV volumes, 10 series of 2.0-mm slices were reconstructed from the same dataset at every 10% throughout the cardiac cycle, starting at early systole (0% of cardiac cycle) to end-diastole (90% of cardiac cycle).

Data Analysis

CTA and LV function reconstructions were transferred to a remote workstation with dedicated analysis software (for 64-row CTA reconstructions: Vitrea 2, Vital Images, Minnetonka, MN, USA; for 320-row CTA reconstructions: Vitrea FX 1.0, Vital Images, Minnetonka, MN, USA). The presence of coronary stenosis was assessed by scrolling through axial images, combined with visual assessment of curved multiplanar reconstructions in ≥ 2 orthogonal planes. CTA examinations were evaluated on a patient basis for the presence of a significant stenosis ($\geq 50\%$ luminal narrowing) by two experienced observers. Discrepancies in interpretation were resolved by consensus.

For the purpose of LV function analysis, appropriate phases for LV end-systolic volume (LVESV) and LV end-diastolic volume (LVEDV) were acquired, by selecting the smallest and largest cross-sectional LV cavity areas respectively. Upper limit of the LV was determined at the basal level of the mitral valve and the start of the LV outflow tract, as previously described.²⁰ Endocardial borders were outlined using a semi-automated method from the base to the apex on the short-axis cine images by an independent observer. Papillary muscles were excluded from the ventricular cavity. The LVEDV and LVESV volumes were calculated and the LVEF was derived by subtracting the LVESV from the LVEDV and dividing the result by the LVEDV.⁹ Observers for LV function analysis were blinded to CTA data.

End-points

Patient follow-up data were gathered by a single observer, blinded to the baseline CTA results, using clinical visits and/or standardized telephone interviews. A composite end-point was constructed using the following events: all-cause mortality, non-fatal myocardial infarction, and unstable angina pectoris requiring hospitalization. Non-fatal infarction was defined based on criteria of typical chest pain, elevated cardiac enzyme levels, and typical changes on the ECG.²¹ Unstable angina was defined according to the European Society of Cardiology guidelines as acute chest pain with or without the presence of ECG abnormalities, and negative cardiac enzyme levels.²²

Statistical Analysis

Statistical analysis was performed using SPSS software (version 16.0, SPSS Inc., Chicago, Illinois). Quantitative data were expressed as mean \pm standard deviation (SD). Categorical variables were described as numbers and percentages. Cox regression analysis was used to determine the prognostic value of the presence of significant stenosis and LV function parameters on CTA. First, univariate analysis of baseline characteristics, the presence of significant stenosis and LV function parameters was performed using a composite end-point of all-cause mortality, non-fatal infarction, and unstable angina. For each variable, a hazard ratio (HR) with a 95%-confidence interval (CI) was calculated. Increased LVEDV and LVESV were defined as LVEDV $>$ 215 ml, LVESV $>$ 90 ml and reduced LVEF was defined as LVEF $<$ 49%, as described previously.²³ These values were determined using the 95% confidence interval boundaries for 3-dimensional LV dimensions and function as determined by CTA.²³ After univariate analysis, several multivariate models were created to correct LV function parameters for clinical risk factors and the presence of significant stenosis on CTA. In case variables showed strong interrelation (Pearson's correlation coefficient $>$ 0.8), variables were excluded from the same multivariate model. Finally, the incremental value of LV function variables over clinical risk factors (age, gender, smoking and known CAD) and the presence of significant stenosis on CTA was assessed by calculating the global chi-square values. A p-value $<$ 0.05 was considered statistically significant.

Results

From the registry, additional LV function measurements (derived from CTA) were available in 813 patients. In 29 patients (3.6%) the CTA examination was of non-diagnostic image quality and these patients were excluded from the study. Furthermore, a total of 56 patients (6.9%) were lost to follow up. As a result, the patient group consisted of 728 individuals. The main clinical characteristics of the population are listed in Table 1. In summary, 55% was male and the mean age was 55 ± 12 years.

Table 1. Patient characteristics

Gender (male / female)	328 / 400
Age (years)	55 ± 12
Reason for Referral	
Typical chest pain	83 (12%)
Atypical chest pain	189 (26%)
Non-anginal chest pain	132 (18%)
Elevated risk profile	213 (29%)
Positive or inconclusive exercise ECG	111 (15%)
Clinical Risk Factors	
Diabetes	222 (31%)
Hypercholesterolemia	261 (36%)
Hypertension	317 (44%)
Family history of coronary artery disease	309 (42%)
Smoking	137 (19%)
Obesity (BMI ≥ 30 kg/m ²)	143 (20%)
Known CAD	96 (13%)

Baseline CTA and LV function

In the study population of 728 patients, a significant stenosis (luminal narrowing $\geq 50\%$) was identified on CTA in 221 patients (30%). When evaluating LV volumes, an average LVEDV of 138 ± 38 ml was observed. For LVESV an average value of 52 ± 29 ml was observed. As a result, average LVEF was $64 \pm 10\%$. Increased LVEDV (> 215 ml) and LVESV (> 90 ml) were present in 31 patients (4.3%) and 50 patients (6.9%), respectively. A reduced LVEF ($< 49\%$) was present in 43 patients (7.3%).

Follow-up

The median follow-up period was 765 days (25th–75th percentile: 493–978); an event occurred in 45 patients (6.2%). All-cause death was reported in 23 patients (3.2%), non-fatal myocardial infarction occurred in 7 patients (1.0%), and 15 patients (2.0%) were admitted to the hospital due to unstable angina.

Survival Analysis

Univariate analysis of clinical risk factors, significant stenosis on CTA and LV function analysis parameters is depicted in Table 2. Of the clinical risk factors, age, smoking and known CAD were significant predictors of events. Also, the presence of a significant stenosis on CTA was identified as a significant predictor of events. Regarding LV function, all three parameters (LVEDV, LVESV and LVEF) were significant univariate predictors when assessed as continuous variables and categorical variables, using predefined cutoff values.

Table 2. Univariate predictors of events

	HR (95%-CI)	p-value
Baseline clinical Characteristic		
Age	1.04 (1.01-1.07)	0.005
Male gender	1.36 (0.75-2.49)	0.315
Diabetes	1.03 (0.55-1.93)	0.939
Hypercholesterolemia*	0.73 (0.38-1.39)	0.333
Hypertension [†]	0.89 (0.53-1.73)	0.958
Family history of coronary artery disease [‡]	0.61 (0.32-1.15)	0.125
Smoking	2.31 (1.25-4.25)	0.007
Obesity (BMI \geq 30 kg/m ²)	0.55 (0.22-1.39)	0.205
Known CAD	2.74 (1.46-5.13)	0.002
CTA		
Significant stenosis	3.52 (1.59-7.83)	0.002
LV function (continuous)		
LVEDV (per 10 ml increase)	1.07 (1.00-1.14)	0.048
LVESV (per 10 ml increase)	1.10 (1.03-1.18)	0.006
LVEF (per % increase)	0.97 (0.94-0.99)	0.006
LV function (categorical)		
LVEDV > 215 ml	2.89 (1.22-6.86)	0.016
LVESV > 90 ml	3.95 (1.99-7.84)	<0.001
LVEF < 49%	3.82 (1.93-7.57)	<0.001

Multivariate models were created correcting for clinical risk factors (age, gender, smoking and known CAD) and significant stenosis on CTA. The prognostic value of LV volumes and LVEF are shown in Table 3. A total of six models were created. In the first three models LVEDV, LVESV and LVEF were assessed as continuous variables. In the last three models the predictive value of LV function was determined using the pre-defined cutoff values to indicate reduced LV function. Although none of the continuous LV function variables remained independent predictors of events, using the pre-defined cutoff values as markers for reduced LV function, increased LVESV and reduced LVEF provided additional prognostic information over clinical risk factors (age, gender, smoking, known CAD) and significant stenosis on CTA. Figure 1 illustrates the incremental prognostic value, depicted by chi-square value, of LVESV > 90 ml over age, gender, smoking, known CAD and significant stenosis on CTA ($p <$

0.05). Similarly, Figure 2 shows that LVEF < 49% has incremental value ($p < 0.05$), and thus enhanced risk stratification beyond the detection of significant stenosis using CTA.

Table 3. Multivariate models for the prediction of events

	HR (95%-CI)	p-value
LV function (continuous)		
LVEDV (per 10 ml increase)	1.05 (0.99-1.13)	0.123
LVESV (per 10 ml increase)	1.06 (0.98-1.15)	0.119
LVEF (per % increase)	0.98 (0.96-1.01)	0.177
LV function (categorical)		
LVEDV > 215 ml	1.98 (0.79-4.95)	0.143
LVESV > 90 ml	3.11 (1.45-6.67)	0.004
LVEF < 49%	2.61 (1.22-5.60)	0.014

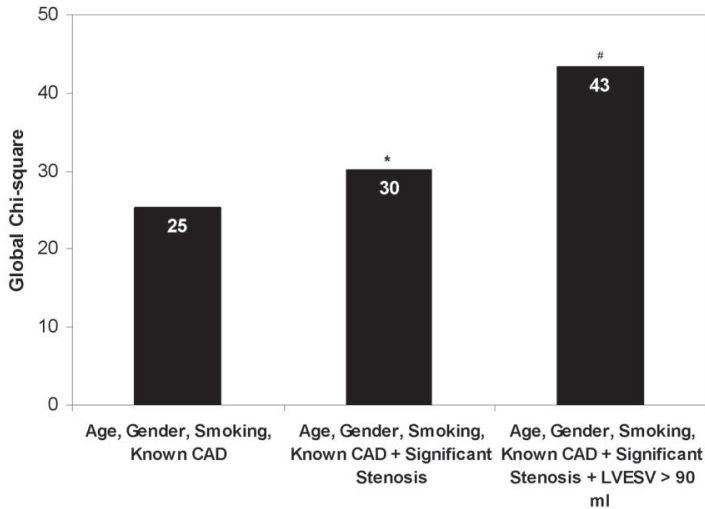


Figure 1. Bar graph illustrating the incremental prognostic value (depicted by chi-square values on the y-axis) of LVESV > 90 ml over age, gender, smoking, known CAD and significant stenosis. The presence of significant stenosis on CTA has a significant incremental prognostic value over age, gender, smoking and known CAD (*). A further incremental prognostic value over clinical risk factors and significant stenosis on CTA is observed with the addition of LVESV > 90 ml (#).

Discussion

The main finding of the current study is that CTA derived LV function may provide important prognostic information beyond the detection of significant stenosis on CTA.

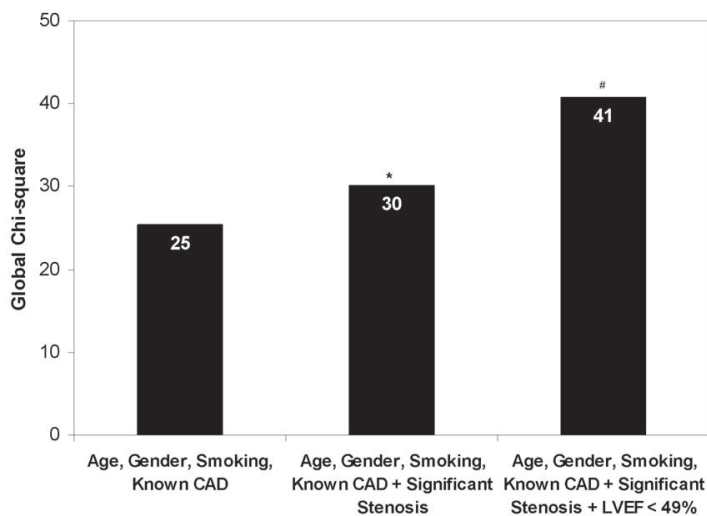


Figure 2. Bar graph illustrating the incremental prognostic value (depicted by chi-square values on the y-axis) of LVEF < 49% over age, gender, smoking, known CAD and significant stenosis on CTA. The presence of significant stenosis on CTA has a significant incremental prognostic value over age, gender, smoking and known CAD (*). A further incremental prognostic value over clinical risk factors and significant stenosis on CTA is observed with the addition of LVEF < 49% (#).

LV volumes and LVEF are used extensively as clinical markers of cardiac function. In patients with known CAD, LV function analysis provides important information for risk assessment and further management.^{11, 24} Post myocardial infarction patients with a normal LVEF have a relatively good prognosis, whereas the risk of future events has been shown to increase with deteriorating LVEF.²⁵ LV function analysis may also be useful in patients with suspected CAD. Using 2-dimensional echocardiography in 2,948 patients without prevalent CAD, Devereux and colleagues showed that LVEF < 40% was a strong predictor of cardiovascular death (RR 6.9, CI 3.0-15.9, $p < 0.001$) and all-cause mortality (RR 4.8, CI 2.8-8.1, $p < 0.001$), independent of clinical risk factors.¹² In a study by Sharir and colleagues, evaluating 1680 patients referred for gated SPECT, LVEF < 45% and ESV > 70 ml were identified as optimal thresholds to accurately stratify patients into high risk and low risk groups.¹⁴ Importantly, patients with a normal LVEF or LVESV had a substantially lower annual mortality rate (regardless of the degree of perfusion abnormalities on SPECT) than patients with reduced LVEF or increased LVESV. In the current study, the prognostic value of LV function measurements on CTA was evaluated. LV volumes and LVEF provided prognostic information independent of baseline clinical variables. These findings illustrate that measurements of LV function (and volumes) from CTA acquisitions can be beneficial in defining patient risk and if available, should be incorporated into the clinical report.

Importantly, patients undergoing CTA are primarily referred for assessment of CAD. As this anatomic information has been established to provide prognostic information, ⁽⁴⁻⁶⁾ an important objective of the current study was to determine the additional value of LV function analysis beyond the detection of significant CAD. Limited information is available regarding the additional prognostic value of LV function over the non-invasive angiographic assessment of CAD using CTA. In a recent study by Min and colleagues, evaluating 5330 consecutive patients without known CAD with a mean follow up of 2.3 ± 0.6 years, the addition of LV function measured by CTA significantly increased risk correlation for death. Annualized mortality rates in patients with significant CAD and LVEF $\leq 50\%$ was significantly higher (3.79%) than in patients with significant CAD and LVEF $> 50\%$ (1.76%).²⁶ Furthermore, Chow and co-workers recently determined the incremental prognostic value of LV function measured with CTA in 2,076 consecutive patients with a mean follow up of 16 ± 8 months. It was shown that LVEF had incremental prognostic value over CAD severity (HR 1.47, 95% CI 1.17-1.86).²⁷ These data indicate that LV function is an important predictor of survival with incremental value to CTA. In line with these results, the present study suggests that, although the assessment of significant CAD on CTA is a powerful predictor, LV function parameters provide independent incremental value in predicting adverse events. Thus, the addition of LV function analysis to CTA may further improve risk stratification of patients with known or suspected CAD referred for stenosis detection.

Limitations

Several limitations of the present study merit consideration. First, 6.9% of patients were lost to follow-up. Second, regional wall motion abnormalities were not assessed in the present study. Third, the present study is limited by a relatively small patient number. Fourth, CTA is inherently associated with radiation exposure.²⁸ As a result, prospective ECG triggering was recently introduced for the purpose of radiation reduction.^{29, 30} This technique allows image acquisition during a small portion of the cardiac cycle which significantly reduces the radiation exposure. However, as a result data are no longer acquired throughout the entire cardiac cycle, thereby eliminating the possibility of simultaneous LV function analysis from the same dataset. Although LV function may still be assessed, it has become at the expense of increased radiation exposure, also when using ECG-triggered tube current modulation. Therefore, the necessity of LV function analysis using CTA should be carefully weighed against the increase in radiation burden. Importantly, LV function analysis may also be performed using radiation free modalities, such as echocardiography or magnetic resonance imaging. Accordingly, although in the present study LV function was derived from CTA, LV function analysis may enhance risk stratification beyond the presence of significant stenosis on CTA regardless of the modality used to derive this information. Additional studies are warranted to gain better understanding of the integration of angiographic and LV function data to refine risk stratification.

Conclusion

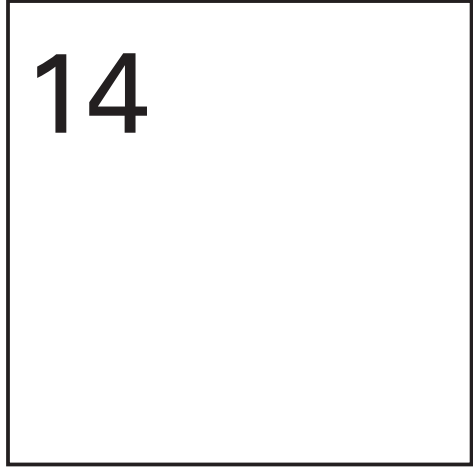
The present results suggest that LV function analysis provides independent and incremental prognostic information beyond anatomic assessment of CAD using CTA.

References

1. Budoff MJ, Dowe D, Jollis JG, et al. Diagnostic performance of 64-multidetector row coronary computed tomographic angiography for evaluation of coronary artery stenosis in individuals without known coronary artery disease: results from the prospective multicenter ACCURACY (Assessment by Coronary Computed Tomographic Angiography of Individuals Undergoing Invasive Coronary Angiography) trial. *J Am Coll Cardiol* 2008;52:1724-32.
2. Meijboom WB, Meijs MF, Schuijf JD, et al. Diagnostic accuracy of 64-slice computed tomography coronary angiography: a prospective, multicenter, multivendor study. *J Am Coll Cardiol* 2008;52:2135-44.
3. Miller JM, Rochitte CE, Dewey M, et al. Diagnostic performance of coronary angiography by 64-row CT. *N Engl J Med* 2008;359:2324-36.
4. Ostrom MP, Gopal A, Ahmadi N, et al. Mortality incidence and the severity of coronary atherosclerosis assessed by computed tomography angiography. *J Am Coll Cardiol* 2008;52:1335-43.
5. van Werkhoven JM, Schuijf JD, Gaemperli O, et al. Incremental prognostic value of multi-slice computed tomography coronary angiography over coronary artery calcium scoring in patients with suspected coronary artery disease. *Eur Heart J* 2009;30:2622-9.
6. Min JK, Shaw LJ, Devereux RB, et al. Prognostic value of multidetector coronary computed tomographic angiography for prediction of all-cause mortality. *J Am Coll Cardiol* 2007;50:1161-70.
7. Carrigan TP, Nair D, Schoenhagen P, et al. Prognostic utility of 64-slice computed tomography in patients with suspected but no documented coronary artery disease. *Eur Heart J* 2009;30:362-71.
8. Kim TH, Hur J, Kim SJ, et al. Two-phase reconstruction for the assessment of left ventricular volume and function using retrospective ECG-gated MDCT: comparison with echocardiography. *AJR Am J Roentgenol* 2005;185:319-25.
9. Henneman MM, Schuijf JD, Jukema JW, et al. Assessment of global and regional left ventricular function and volumes with 64-slice MSCT: a comparison with 2D echocardiography. *J Nucl Cardiol* 2006;13:480-7.
10. Yamamuro M, Tadamura E, Kubo S, et al. Cardiac functional analysis with multi-detector row CT and segmental reconstruction algorithm: comparison with echocardiography, SPECT, and MR imaging. *Radiology* 2005;234:381-90.
11. de Feyter PJ, van Eenige MJ, Dighton DH, et al. Prognostic value of exercise testing, coronary angiography and left ventriculography 6-8 weeks after myocardial infarction. *Circulation* 1982;66:527-36.
12. Devereux RB, Roman MJ, Palmieri V, et al. Prognostic implications of ejection fraction from linear echocardiographic dimensions: the Strong Heart Study. *Am Heart J* 2003;146:527-34.
13. Hundley WG, Morgan TM, Neagle CM, et al. Magnetic resonance imaging determination of cardiac prognosis. *Circulation* 2002;106:2328-33.
14. Sharir T, Germano G, Kavanagh PB, et al. Incremental prognostic value of post-stress left ventricular ejection fraction and volume by gated myocardial perfusion single photon emission computed tomography. *Circulation* 1999;100:1035-42.
15. van Werkhoven JM, Schuijf JD, Gaemperli O, et al. Prognostic value of multislice computed tomography and gated single-photon emission computed tomography in patients with suspected coronary artery disease. *J Am Coll Cardiol* 2009;53:623-32.
16. Cademartiri F, Nieman K, van der Lugt A, et al. Intravenous contrast material administration at 16-detector row helical CT coronary angiography: test bolus versus bolus-tracking technique. *Radiology* 2004;233:817-23.
17. Schuijf JD, Wijns W, Jukema JW, et al. Relationship between noninvasive coronary angiography with multi-slice computed tomography and myocardial perfusion imaging. *J Am Coll Cardiol* 2006;48:2508-14.

18. Leschka S, Husmann L, Desbiolles LM, et al. Optimal image reconstruction intervals for non-invasive coronary angiography with 64-slice CT. *Eur Radiol* 2006;16:1964-72.
19. de Graaf FR, Schuijf JD, van Velzen JE, et al. Diagnostic Accuracy of 320-Row Multidetector Computed Tomography Coronary Angiography in the Non-Invasive Evaluation of Significant Coronary Artery Disease. *Eur Heart J* 2009;In Press.
20. de Graaf FR, Schuijf JD, van Velzen JE, et al. Assessment of global left ventricular function and volumes with 320-row multidetector computed tomography: A comparison with 2D-echocardiography. *J Nucl Cardiol* 2010;17:225-31.
21. Thygesen K, Alpert JS, White HD. Universal definition of myocardial infarction. *Eur Heart J* 2007;28:2525-38.
22. Bassand JP, Hamm CW, Ardissino D, et al. Guidelines for the diagnosis and treatment of non-ST-segment elevation acute coronary syndromes. *Eur Heart J* 2007;28:1598-660.
23. Lin FY, Devereux RB, Roman MJ, et al. Cardiac chamber volumes, function, and mass as determined by 64-multidetector row computed tomography: mean values among healthy adults free of hypertension and obesity. *JACC Cardiovasc Imaging* 2008;1:782-6.
24. Hachamovitch R, Rozanski A, Hayes SW, et al. Predicting therapeutic benefit from myocardial revascularization procedures: are measurements of both resting left ventricular ejection fraction and stress-induced myocardial ischemia necessary? *J Nucl Cardiol* 2006;13:768-78.
25. Schulman SP, Achuff SC, Griffith LS, et al. Prognostic cardiac catheterization variables in survivors of acute myocardial infarction: a five year prospective study. *J Am Coll Cardiol* 1988;11:1164-72.
26. Min JK, Lin FY, Dunning AM, et al. Incremental prognostic significance of left ventricular dysfunction to coronary artery disease detection by 64-detector row coronary computed tomographic angiography for the prediction of all-cause mortality: results from a two-centre study of 5330 patients. *Eur Heart J* 2010.
27. Chow BJ, Wells GA, Chen L, et al. Prognostic value of 64-slice cardiac computed tomography severity of coronary artery disease, coronary atherosclerosis, and left ventricular ejection fraction. *J Am Coll Cardiol* 2010;55:1017-28.
28. Einstein AJ, Henzlova MJ, Rajagopalan S. Estimating risk of cancer associated with radiation exposure from 64-slice computed tomography coronary angiography. *JAMA* 2007;298:317-23.
29. Husmann L, Valenta I, Gaemperli O, et al. Feasibility of low-dose coronary CT angiography: first experience with prospective ECG-gating. *Eur Heart J* 2008;29:191-7.
30. Shuman WP, Branch KR, May JM, et al. Prospective versus retrospective ECG gating for 64-detector CT of the coronary arteries: comparison of image quality and patient radiation dose. *Radiology* 2008;248:431-7.

Chapter 14



Multi-slice computed tomography coronary angiography for risk stratification in patients with an intermediate pre-test likelihood

JM van Werkhoven, O Gaemperli, JD Schuijf, JW Jukema, LJ Kroft,
S Leschka, H Alkadhi, I Valenta, G Pundziute, A de Roos,
EE van der Wall, PA Kaufmann, JJ Bax

Abstract

The purpose of this study was to assess whether MSCTA may be useful for risk stratification of patients with suspected CAD at intermediate pre-test likelihood according to Diamond and Forrester. MSCTA images were evaluated for the presence of significant CAD in 316 included patients (60% male, average age 57 ± 11 years) with suspected CAD and an intermediate pre-test likelihood according to Diamond and Forrester. Patients were followed in time for the occurrence of an event. A combined endpoint of all cause mortality, non-fatal infarction, and unstable angina requiring revascularization. Significant CAD was observed in 89 patients (28%), whereas normal MSCTA or non-significant CAD was observed in the remaining 227 (72%) patients. During follow-up (median 621 days (95%-confidence interval: 408-835) an event occurred in 13 patients (4.8%). The annualized event rate was 0.8% in patients with normal MSCT, 2.2% in patients with non-significant CAD and 6.5% in patients with significant CAD. Moreover, MSCTA remained a significant predictor ($p < 0.05$) of events after multivariate correction. In conclusion, our results suggest that in an intermediate pre-test likelihood population, MSCTA is highly effective in re-stratifying patients into either a low or high post-test risk group. These results further emphasize the usefulness of non-invasive imaging with MSCTA in this patient population.

Introduction

Coronary artery disease (CAD) is a leading cause of mortality and morbidity worldwide. The diagnosis and management of this disease is increasingly dependent on non-invasive imaging strategies. With the introduction of multi-slice computed tomography coronary angiography (MSCTA) non-invasive assessment of coronary anatomy has become possible, allowing early identification of atherosclerosis. MSCTA has a high diagnostic accuracy for the detection of significant CAD ($\geq 50\%$ luminal narrowing) on conventional coronary angiography,¹⁻⁷ and may be particularly useful for diagnosis in patients with an intermediate pre-test likelihood for significant CAD.⁸ Although the prognostic value of MSCTA has been evaluated in previous studies^(7, 9-16), no studies have specifically addressed the target population for MSCTA. The purpose of this study therefore was to assess if MSCTA may be useful for risk stratification in patients with suspected CAD and an intermediate pre-test likelihood.

Methods

The study population consisted of 331 patients with suspected CAD and an intermediate pre-test likelihood. Patients were clinically referred for further cardiac assessment as part of an ongoing study protocol addressing the prognostic value of MSCTA. From this prospective registry, results addressing the incremental prognostic value of MSCTA over myocardial perfusion imaging have been recently published.¹³

Baseline clinical demographic values were recorded from the electronic patient file based on physician documented history. Symptoms were classified as typical angina, atypical angina, non-anginal chest pain and asymptomatic. Typical anginal chest pain was defined as combination of: 1) discomfort in the anterior chest, neck, shoulders, jaw, or arms; 2) precipitated by physical exertion or psychic stress; and 3) relieved by rest or nitroglycerin within minutes. Atypical chest pain was defined as chest pain with two of these 3 factors and non-anginal chest pain was defined as chest pain with less than 2 of these 3 factors.¹⁷ Pre-test likelihood was defined according to Diamond and Forrester criteria which are based on age, gender and symptomatic status.¹⁸ Intermediate likelihood was defined as a pre-test likelihood between 13.4 and 87.2%. In addition, asymptomatic diabetic patients were also classified as having an intermediate pre-test likelihood according to the increased prevalence of CAD and increased risk of events in this population.¹⁹⁻²¹ Exclusion criteria were: cardiac arrhythmias, renal insufficiency (defined as a glomerular filtration rate < 30 ml/min), known hypersensitivity to iodine contrast media, and pregnancy. In addition, patients with an uninterpretable MSCTA examination were excluded from further analysis. The study was approved by the local ethics committee in both participating centers.

Patients were scanned using a 64-slice CT scanner (Aquilion64, Toshiba Medical Systems, Tokyo, Japan; General Electrics LightSpeed VCT, Milwaukee, WI, US; or Sensation64, Siemens, Forchheim, Germany). For each patient, the heart rate and blood pressure were monitored before the scan. In the absence of contraindications, patients with a heart rate exceeding the threshold of 65 beats per minute were administered beta-blocking medication (50-100 mg metoprolol, oral or 5-10 mg metoprolol, intravenous). The contrast enhanced helical scan was performed using 80-140 ml of non-ionic contrast agent (Xenetix 300; Iomeron 400; or Iodixanol 370) administered at a flow rate of 3.5-5 ml/s followed by a bolus of saline flush (30-50 ml at 3.5-5 ml/s). All scan parameters have been previously published.²²⁻²⁴

Datasets were reconstructed from the retrospectively gated raw data. Images were reconstructed with an effective slice thickness of 0.3, 0.5 or 0.625 mm with the Toshiba, Siemens, and GE systems respectively. Coronary arteries were evaluated using the reconstruction dataset with the least motion artifacts, typically an end-diastolic phase. Post-processing was performed on dedicated workstations (Vitrea2, Vital Images, USA, Advantage, GE healthcare, USA, Leonardo, Siemens, Germany). The interpretation of MSCTA angiograms was performed in a standardized manner using the axial slices, curved multiplanar reconstructions (MPR), and maximum intensity projections (MIP). MSCTA examinations were scored on a patient basis by two experienced observers in each center, based on the maximum luminal diameter stenosis. Discrepancies in interpretation were resolved by consensus. Normal MSCTA was defined as completely normal anatomy, non-significant stenosis was defined as the presence of luminal narrowing with a maximal luminal diameter stenosis <50%, and significant stenosis was defined as the presence of an atherosclerotic lesion exceeding the threshold of $\geq 50\%$ luminal narrowing. The effective dose of the CS and MSCTA scans was estimated from the product of the dose-length product and an organ weighing factor [$k=0.014 \text{ mSv} \times (\text{mGy} \times \text{cm})^{-1}$] for the chest as the investigated anatomical region.²⁵

Patient follow-up data were gathered using clinical visits or standardized telephone interviews. The following events were regarded as clinical endpoints: all cause mortality, non-fatal myocardial infarction, and unstable angina requiring revascularization. Two combined endpoints were used: a combined endpoint of all events; and a combined hard endpoint including only all cause mortality and non-fatal myocardial infarction. Non-fatal infarction was defined based on criteria of typical chest pain, elevated cardiac enzyme levels, and typical changes on the ECG. Unstable angina was defined according to the European Society of Cardiology guidelines as acute chest pain with or without the presence of ECG abnormalities, and negative cardiac enzyme levels.²⁶ Patients with stable complaints undergoing an early elective revascularization within 60 days after MSCTA were excluded from the survival analysis.

Continuous variables were expressed as mean and standard deviation, and categorical baseline data were expressed in numbers and percentages. Cox regression analysis was used to determine the prognostic value of MSCTA. First univariate analysis of baseline clinical variables and MSCTA variables was performed using a composite endpoint of all cause mortality, non-fatal infarction, and unstable angina requiring revascularization. For each variable a hazard ratio with a 95%-confidence interval (95%-CI) was calculated. Finally a multivariate model was created using backward stepwise selection to assess the independent predictive value of MSCTA corrected for baseline clinical variables. At each step, the least significant variable was discarded from the model, until all variables in the model reached a p-value <0.25.

Cumulative event rates for MSCTA were obtained by the Kaplan-Meier method, and the survival curves were compared using the log-rank test. Statistical analyses were performed using SPSS software (version 12.0, SPSS Inc, Chicago, IL, USA). A p-value <0.05 was considered statistically significant.

Results

Patient characteristics

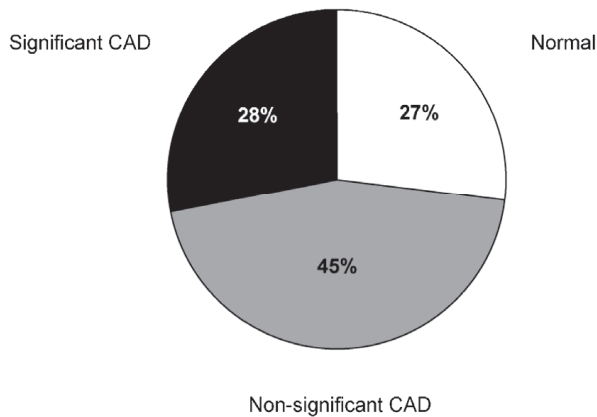
The study population, derived from our prospective registry,²⁷ consisted of 331 patients with suspected CAD and an intermediate pre-test likelihood. The MSCTA examination was uninterpretable in 15 patients (4.5%). Reasons for uninterpretability were the presence of motion artifacts, increased noise due to high body mass index, and breathing. After exclusion of these patients, a total of 316 patients remained for analysis. The average age of the study cohort was 57±11 years and 60% of patients were men. Patients presented with asymptomatic diabetes (25%) non-anginal chest pain (22%), atypical chest pain (48%), and typical chest pain (5%). A complete overview of the baseline characteristics of the study population is presented in Table 1.

MSCT results

During MSCTA image acquisition, an average heart rate of 63±10 beats per minute was recorded. MSCTA was classified as normal in 85 (27%) of patients. Atherosclerosis was detected in the remaining 231 (73%) patients, classified as non-significant CAD (<50% luminal narrowing) in 142 (45%) and significant CAD (≥50% luminal narrowing) in 89 (28%) patients.(Figure 1) The estimated average radiation dose for the coronary angiography protocol was 18.1±5.9 mSv and the estimated radiation dose for the CS protocol was 1.4±0.6 mSv.

Table 1. Patient characteristics.

Gender (male)	190 (60.1%)
Age (yrs)	57±11
Risk Factors	
Diabetes	127 (40.2%)
Hypertension	174 (55.1%)
Hypercholesterolemia	125 (39.6%)
Family history CAD	123 (38.9%)
Current Smoking	102 (32.3%)
Obesity (BMI ≥ 30)	71 (22.5%)
Symptoms	
Asymptomatic	78 (24.7%)
Dyspnoea	34 (10.8%)
Non-anginal chest pain	36 (11.4%)
Atypical chest pain	151 (47.8%)
Typical chest pain	17 (5.4%)

**Figure 1.** Pie chart illustrating the distribution of MSCTA findings.

Follow-up results

In total, 26 (8%) patients were lost to follow-up and 21 (7%) patients underwent early revascularization. In the remaining 269 patients the median follow-up time achieved was 621 days (25-75th percentile: 408-835). During the follow-up period an event occurred in 13 patients (5%). All cause mortality was reported in 5 patients (2%), whereas non-fatal myocardial infarction occurred in 3 patients (1%) and 5 patients (2%) were revascularized due to unstable angina pectoris. In the excluded patients with an early revascularization myocardial infarction occurred in 1 of 21 patients.

Event rates

In patients with a normal MSCTA an annualized event rate (annualized event rate for hard events between parentheses) of 0.8% (0%) was observed, while in patients with atherosclerosis (non-significant and/or significant CAD) the annualized event rate was 3.5% (2.6%). Significant CAD ($\geq 50\%$ luminal narrowing) on MSCTA resulted in an event rate of 6.5% (4.6%). The total event rates (all cause mortality, non-fatal myocardial infarction and unstable angina requiring revascularization) and the hard event rates (all cause mortality and non-fatal myocardial infarction) in all patients and stratified according to MSCTA are shown in Figure 2.

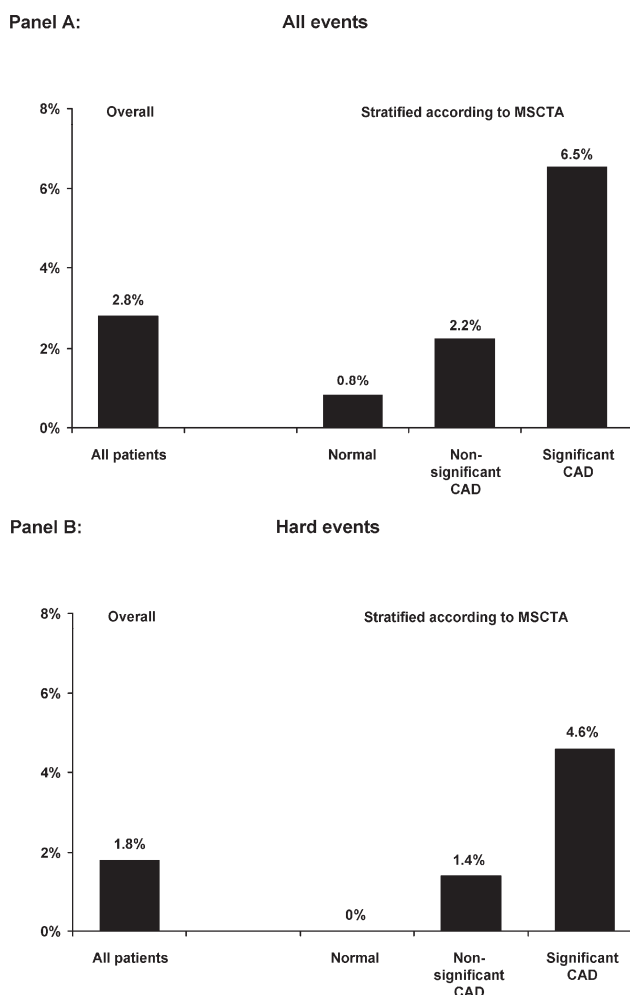


Figure 2. The annualized event rate in all patients and stratified according to MSCTA results. Panel A: Bar graph for all events (all cause mortality, non-fatal myocardial infarction, and unstable angina requiring revascularization); Panel B: Bar graph for hard events (all cause mortality, and non-fatal myocardial infarction).

Survival analysis

Baseline univariate predictors of events are listed in Table 2. Significant CAD ($\geq 50\%$ luminal narrowing) was the best univariate predictor of events with a hazard ratio of 3.9 (95%-confidence interval: 1.3-11.7). After correcting for smoking in a multivariate model this variable remained an independent predictor of events. Table 2) The Kaplan-Meier survival analysis in Figure 3 further illustrates the usefulness of $\geq 50\%$ luminal narrowing on MSCTA as a cutoff for risk stratification. A significant difference (Logrank P-value 0.008) in survival was observed between patients with normal or non-significant CAD and patients with significant CAD ($\geq 50\%$ luminal narrowing) on MSCTA. Similar results were obtained when using a combined hard endpoint of all cause mortality and non-fatal myocardial infarction (Logrank P-value 0.0077). (Figure 3)

Table 2. Univariate and Multivariate predictors of events.

	Univariate analysis		Multivariate analysis	
	HR (95%-CI)	p-value	HR (95%-CI)	p-value
Risk factors				
Gender (male)	0.84 (0.28-2.50)	0.754		
Age (yrs)	1.00 (0.95-1.05)	0.814		
Diabetes	0.98 (0.32-3.01)	0.981		
Hypertension	0.85 (0.28-2.55)	0.781		
Hypercholesterolemia	1.25 (0.42-3.72)	0.685		
Family history CAD	0.96 (0.31-2.95)	0.951		
Current Smoking	2.54 (0.85-7.57)	0.093		
Obesity (BMI ≥ 30)	1.27 (0.34-4.65)	0.714		
MSCTA				
Atherosclerosis	4.71 (0.61-36.30)	0.136		
Significant CAD	3.92 (1.31-11.68)	0.014	3.46 (1.14-10.48)	0.028

Discussion

The main finding of the current study is that in an intermediate pre-test likelihood population, MSCTA has a good prognostic value and may effectively identify patients at higher or lower risk for coronary events. These results further emphasize the usefulness of non-invasive imaging with MSCTA in this patient population.

MSCTA is increasingly used in the diagnosis of CAD, and may be specifically useful for the rule out of CAD. The diagnostic accuracy of MSCTA has been studied extensively, and in early single center studies an average weighted sensitivity of 97.5 (95%-confidence interval 96-99) and specificity of 91 (95%-confidence interval 87.5-95) has been observed.⁵ More recently several prospective multi-center studies have been published showing similar

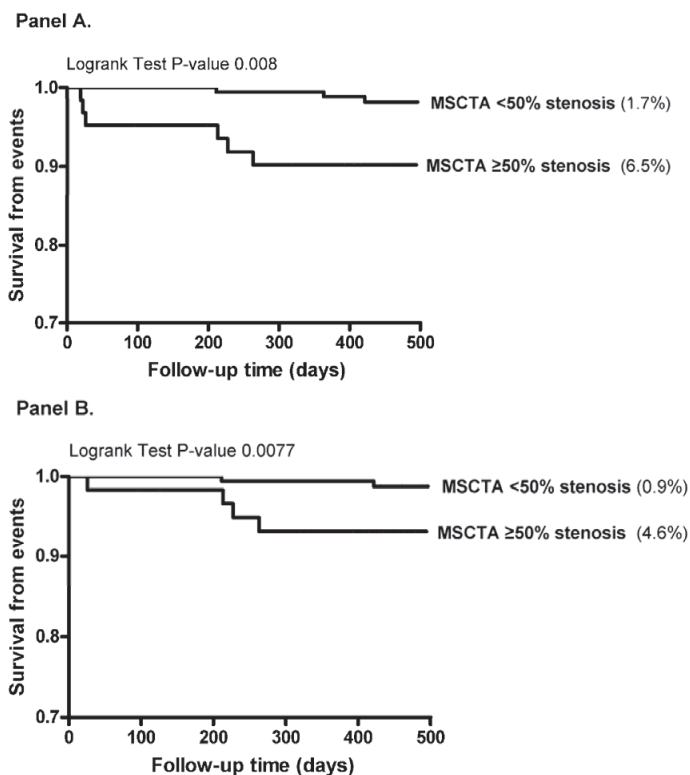


Figure 3. Kaplan-Meier survival curves in patients with normal or non-significant CAD (<50% luminal narrowing) compared to patients with significant CAD (≥50% luminal narrowing). Panel A: Kaplan-Meier curves for all events (all cause mortality, non-fatal myocardial infarction, and unstable angina requiring revascularization); Panel B: Kaplan-Meier curves for hard events (all cause mortality, and non-fatal myocardial infarction).

sensitivities and specificities.^{1, 3, 4} Importantly however, in the majority of these diagnostic accuracy studies patients were included who were referred for conventional diagnostic coronary angiography and thus with high pre-test probability. Accordingly, when interpreting these observations, it is important to take into account the pre-test probability, as according to Bayes theorem, pre-test probability may have a major influence on the positive and negative predictive value. With increasingly higher pre-test probability, the prevalence of disease is higher and as a consequence the positive predictive value will increase, with a subsequent decrease in negative predictive value. Conversely, in lower pre-test probability populations, with lower disease prevalence, positive predictive value will decrease, but negative predictive value will improve.

The relationship between pre-test probability and the diagnostic accuracy of MSCTA was recently studied by Meijboom et al. among patients with a high, intermediate, or low pre-test likelihood. In patients with a high pre-test likelihood for CAD, the post-test probability

for significant CAD after MSCT was not substantially different from the pre-test probability. As a result, a normal examination did not result in sufficient reduction of post-test probability to reliably rule out the presence of significant CAD. These observations indicate that the clinical value of MSCTA is limited in this patient group. In contrast, in patients with a low and intermediate pre-test likelihood, a negative MSCTA scan was able to reduce the post test probability of CAD to 0%.²⁸ The effectiveness of MSCTA in patients with an intermediate pre-test likelihood was also confirmed by Henneman et al.²⁹ The authors assessed the prevalence of completely normal MSCTA, and thus the efficacy to rule out CAD, in patients with suspected CAD and related these observations to the pre-test likelihood of CAD. The authors showed that normal MSCTA was observed in only 17% of patients with a high pre-test likelihood further underlining the limited clinical value in those patients. Conversely, MSCTA was able to rule out the presence of atherosclerosis in 33% of patients with an intermediate pre-test likelihood.

However, in addition to diagnosis, prognostication is an important component of imaging tests and determines subsequent management. Thus far, several prognostic studies have addressed the potential prognostic value of MSCTA. (7, 9-11, 13) However, most of these observations have been derived from heterogeneous patient populations including patients with known CAD. In several more recent publications the prognostic value of MSCT has been determined specifically in patients with suspected CAD.¹⁴⁻¹⁶ In the study by Carrigan et al. 227 patients without documented CAD were included.¹⁶ The absence of obstructive CAD was associated with a 99% freedom from cardiac death, myocardial infarction and revascularization during an average of 2.3 years of follow-up. In patients with one or more vessels with obstructive CAD a significantly increased event rate was observed (Log rank p-value 0.01). Similar findings were recently reported by Hadamitzky et al.¹⁴

Although these observations underline the usefulness of MSCT for prognosis in patients with suspected CAD, dedicated data in the target population for MSCT, patients with an intermediate pre-test likelihood, are lacking. Importantly, the results of the current study confirm the prognostic value of MSCT in this particular patient population as MSCTA was shown to be highly effective for risk stratification. Indeed, hard event rates were <1% for patients without significant stenosis on MSCTA, indicating that these patients may be safely reassured. In contrast, the presence of a significant stenosis implied a substantially increased risk approaching 5% of coronary events.

Limitations

Several limitations need to be acknowledged. Even though the diagnostic accuracy of MSCTA is high, uninterpretable images are still being encountered in a small percentage of patients due to motion because of high or irregular heart rates or breathing during the examination. It

is however anticipated that the number of uninterpretable studies will continue to decrease with newer generation scanners. Currently 64-slice MSCTA is still associated with a high radiation exposure, although the radiation dose of MSCTA will decrease with the use of dedicated dose reduction techniques that have recently become available.³⁰⁻³³ Importantly, low-dose computed tomography with prospective ECG-triggering has recently been shown to reduce radiation burden while maintaining diagnostic image quality and a high diagnostic accuracy.^{34, 35}

Conclusion

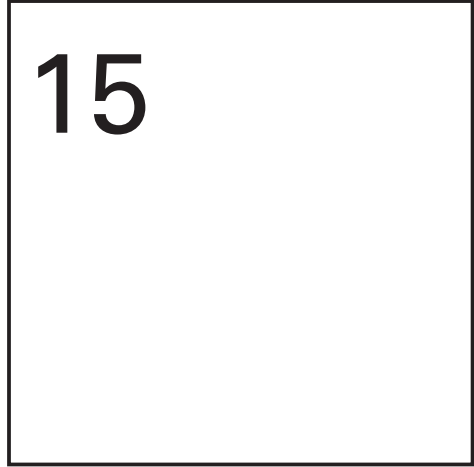
These results suggest that in an intermediate pre-test likelihood population, MSCTA is highly effective in re-stratifying patients into either a low or high post-test risk group. These results further emphasize the usefulness of non-invasive imaging with MSCTA in this patient population.

References

1. Miller JM, Rochitte CE, Dewey M, et al. Diagnostic Performance of Coronary Angiography by 64-Row CT. *N Engl J Med* 2008;359:2324-36.
2. Schuijf JD, Pundziute G, Jukema JW, et al. Diagnostic accuracy of 64-slice multislice computed tomography in the noninvasive evaluation of significant coronary artery disease. *Am J Cardiol* 2006;98:145-8.
3. Budoff MJ, Dowe D, Jollis JG, et al. Diagnostic performance of 64-multidetector row coronary computed tomographic angiography for evaluation of coronary artery stenosis in individuals without known coronary artery disease: results from the prospective multicenter ACCURACY (Assessment by Coronary Computed Tomographic Angiography of Individuals Undergoing Invasive Coronary Angiography) trial. *J Am Coll Cardiol* 2008;52:1724-32.
4. Meijboom WB, Meijs MFL, Schuijf JD, et al. Diagnostic Accuracy of 64-slice Computed Tomography Coronary Angiography: A Prospective Multicenter, Multivendor Study. *J Am Coll Cardiol* 2008;52:2135-44.
5. Abdulla J, Abildstrom SZ, Gotzsche O, et al. 64-multislice detector computed tomography coronary angiography as potential alternative to conventional coronary angiography: a systematic review and meta-analysis. *Eur Heart J* 2007;28:3042-50.
6. Mowatt G, Cook JA, Hillis GS, et al. 64-Slice computed tomography angiography in the diagnosis and assessment of coronary artery disease: systematic review and meta-analysis. *Heart* 2008;94:1386-93.
7. Pundziute G, Schuijf JD, Jukema JW, et al. Prognostic value of multislice computed tomography coronary angiography in patients with known or suspected coronary artery disease. *J Am Coll Cardiol* 2007;49:62-70.
8. Meijboom WB, Van Mieghem CA, Mollet NR, et al. 64-slice computed tomography coronary angiography in patients with high, intermediate, or low pretest probability of significant coronary artery disease. *J Am Coll Cardiol* 2007;50:1469-75.
9. Gilard M, Le Gal G, Cornily J, et al. Midterm Prognosis of Patients With Suspected Coronary Artery Disease and Normal Multislice Computed Tomographic Findings. *Arch Intern Med* 2007;165:1686-9.
10. Min JK, Shaw LJ, Devereux RB, et al. Prognostic value of multidetector coronary computed tomographic angiography for prediction of all-cause mortality. *J Am Coll Cardiol* 2007;50:1161-70.
11. Rubinshtein R, Halon DA, Gaspar T, et al. Cardiac computed tomographic angiography for risk stratification and prediction of late cardiovascular outcome events in patients with a chest pain syndrome. *Int J Cardiol* 2008;137:108-15.
12. Gaemperli O, Valenta I, Schepis T, et al. Coronary 64-slice CT angiography predicts outcome in patients with known or suspected coronary artery disease. *Eur Radiol* 2008;18:1162-73.
13. van Werkhoven JM, Schuijf JD, Gaemperli O, et al. Prognostic value of multislice computed tomography and gated single-photon emission computed tomography in patients with suspected coronary artery disease. *J Am Coll Cardiol* 2009;53:623-32.
14. Hadamitzky M, Freissmuth B, Meyer T, et al. Prognostic Value of Coronary Computed Tomographic Angiography for Prediction of Cardiac Events in Patients With Suspected Coronary Artery Disease. *J Am Coll Cardiol Img* 2009;2:524-6.
15. Aldrovandi A, Maffei E, Palumbo A, et al. Prognostic value of computed tomography coronary angiography in patients with suspected coronary artery disease: a 24-month follow-up study. *Eur Radiol* 2009;19:1653-60.
16. Carrigan TP, Nair D, Schoenhagen P, et al. Prognostic utility of 64-slice computed tomography in patients with suspected but no documented coronary artery disease. *Eur Heart J* 2009;30:362-71.
17. Diamond GA. A clinically relevant classification of chest discomfort. *J Am Coll Cardiol* 1983;1:574-5.

18. Diamond GA, Forrester JS. Analysis of probability as an aid in the clinical diagnosis of coronary-artery disease. *N Engl J Med* 1979;300:1350-8.
19. Haffner SM, Lehto S, Ronnemaa T, et al. Mortality from coronary heart disease in subjects with type 2 diabetes and in nondiabetic subjects with and without prior myocardial infarction. *N Engl J Med* 1998;339:229-34.
20. Scholte AJ, Schuijf JD, Kharagjitsingh AV, et al. Prevalence of coronary artery disease and plaque morphology assessed by multi-slice computed tomography coronary angiography and calcium scoring in asymptomatic patients with type 2 diabetes. *Heart* 2008;94:290-5.
21. Wackers FJ, Young LH, Inzucchi SE, et al. Detection of silent myocardial ischemia in asymptomatic diabetic subjects: the DIAD study. *Diabetes Care* 2004;27:1954-61.
22. Leschka S, Husmann L, Desbiolles LM, et al. Optimal image reconstruction intervals for non-invasive coronary angiography with 64-slice CT. *Eur Radiol* 2006;16:1964-72.
23. Schuijf JD, Wijns W, Jukema JW, et al. The relationship between non-invasive coronary angiography with multi-slice computed tomography and myocardial perfusion imaging. *J Am Coll Cardiol* 2006;48:2508-14.
24. Leschka S, Alkadhi H, Plass A, et al. Accuracy of MSCT coronary angiography with 64-slice technology: first experience. *Eur Heart J* 2005;26:1482-7.
25. Hausleiter J, Meyer T, Hermann F, et al. Estimated radiation dose associated with cardiac CT angiography. *JAMA* 2009;301:500-7.
26. Bassand JP, Hamm CW, Ardissino D, et al. Guidelines for the diagnosis and treatment of non-ST-segment elevation acute coronary syndromes. *Eur Heart J* 2007;28:1598-660.
27. van Werkhoven JM, Schuijf JD, Gaemperli O, et al. Prognostic Value of Multi-slice Computed Tomography and Gated Single Photon Emission Computed Tomography in Patients with Suspected Coronary Artery Disease. *J Am Coll Cardiol* 2009;53:623-32.
28. Meijboom WB, Van Mieghem CA, Mollet NR, et al. 64-slice computed tomography coronary angiography in patients with high, intermediate, or low pretest probability of significant coronary artery disease. *J Am Coll Cardiol* 2007;50:1469-75.
29. Henneman MM, Schuijf JD, van Werkhoven JM, et al. Multi-slice computed tomography coronary angiography for ruling out suspected coronary artery disease: what is the prevalence of a normal study in a general clinical population? *Eur Heart J* 2008;29:2006-13.
30. Hausleiter J, Meyer T, Hadamitzky M, et al. Radiation dose estimates from cardiac multislice computed tomography in daily practice: impact of different scanning protocols on effective dose estimates. *Circulation* 2006;113:1305-10.
31. Hsieh J, Londt J, Vass M, et al. Step-and-shoot data acquisition and reconstruction for cardiac x-ray computed tomography. *Med Phys* 2006;33:4236-48.
32. Husmann L, Valenta I, Gaemperli O, et al. Feasibility of low-dose coronary CT angiography: first experience with prospective ECG-gating. *Eur Heart J* 2008;29:191-7.
33. Rybicki FJ, Otero HJ, Steigner ML, et al. Initial evaluation of coronary images from 320-detector row computed tomography. *Int J Cardiovasc Imaging* 2008;24:535-46.
34. Herzog BA, Husmann L, Burkhard N, et al. Accuracy of low-dose computed tomography coronary angiography using prospective electrocardiogram-triggering: first clinical experience. *Eur Heart J* 2008;29:3037-42.
35. Scheffel H, Alkadhi H, Leschka S, et al. Low-dose CT coronary angiography in the step-and-shoot mode: diagnostic performance. *Heart* 2008;94:1132-7.

Chapter 15



Diabetes: prognostic value of computed tomography coronary angiography--comparison with a nondiabetic population

JM Van Werkhoven, F Cademartiri, S Seitun, E Maffei, A Palumbo, C Martini, G Tarantini, LJ Kroft, A de Roos, AC Weustink, J W Jukema, D Ardissino, NR Mollet, JD Schuijf, JJ Bax

Abstract

The purpose of this study was to evaluate the prognostic value of multi-detector computed tomography coronary angiography (MDCT-CA) in a diabetic population with known or suspected coronary artery disease (CAD) compared with non-diabetic individuals. 313 type-2 Diabetes Mellitus (DM) patients, group I (males 213; age 62 ± 11 years), and 303 non DM patients, group II (males 203; age 63 ± 11 years), underwent 64-row MDCT with a non-contrast enhanced calcium score followed by CT angiography. MDCT-CA were retrospectively classified as normal, non-obstructive CAD ($\leq 50\%$ luminal narrowing, and obstructive CAD ($>50\%$ luminal narrowing). During follow-up after CTA, major events (cardiac death, nonfatal myocardial infarction, and unstable angina requiring hospitalization) and total events (major events plus coronary revascularizations) were recorded in each patient. Cox proportional hazards analysis and Kaplan-Meier analysis were used to compare survival. The number of diseased segments (mean, 5.6 vs. 4.4, $p=0.001$) and the rate of obstructive CAD ($>50\%$ luminal narrowing (51% vs. 37%, $p<0.001$)) were higher in DM patients. Patients were followed for a mean of 20 ± 5 (range 6-44) months. At multivariate analysis DM ($p<0.001$) and evidence of obstructive CAD ($p<0.001$) were independent predictors of outcome. Obstructive CAD remained a significant multivariate predictor both in DM and in non DM patients. Both in DM and non DM patients with absence of disease the event rate was 0%. The event rate increased to 36% in non-DM patients with obstructive CAD and was highest (47%) in DM patients with obstructive CAD. In conclusion, both in DM and non DM patients, MDCT-CA provides incremental prognostic information over baseline clinical variables, and the absence of atherosclerosis on MDCT-CA is associated with an excellent prognosis. MDCT-CA might be a clinically useful tool to improve risk stratification in both DM and non DM patients.

Introduction

Type-2 Diabetes Mellitus (DM) is a major public health concern. At present, 200 million people worldwide have DM and its prevalence is expected to continue increasing exponentially.¹ It is well established that DM is associated with coronary artery disease (CAD), cardiovascular disease and total mortality that is two-to-four times higher than that occurring in non-diabetic patients.² Previous studies have shown that patients with DM but no history of CAD have a similar risk of cardiovascular death as non-diabetic patients who have a history of myocardial infarction (MI).³ In order to select appropriate management strategies, risk stratification is therefore essential in this population.

Due to the high prevalence of CAD, the role of coronary imaging in diabetic patients may not be to document the presence of coronary atherosclerosis but rather to identify those patients with more extensive disease versus those without any atherosclerosis. In patients with extensive CAD, further testing may be warranted to identify those with significant inducible myocardial ischemia who may be candidates for coronary angiography and subsequent revascularization.^{4, 5} The prognostic utility of stress imaging studies, including myocardial perfusion scintigraphy and dobutamine stress echocardiography, have been validated in numerous studies and, in general, patients with a normal imaging study have an annual cardiac ischemic event rate of <1%. However this risk is increased more than two-fold in diabetic patients.⁶ Therefore, assessing prognosis in patients with DM remains challenging and further refinement of risk stratification is necessary in this high-risk population

Recently, multi-detector computed tomography coronary angiography (MDCT-CA) has emerged as a non-invasive tool for the diagnosis of CAD, which enables assessment of the vascular lumen together with the arterial wall. As a result, the technique allows accurate assessment of the presence or absence of CAD with sensitivity and negative predictive value near to 100%.⁷⁻¹¹ Therefore the purpose of our study was to evaluate the prognostic value of MDCT-CA in a diabetic population with known or suspected CAD compared with non-diabetic individuals that underwent MDCT-CA with the aim of excluding CAD.

Methods

Study Group

The study group consisted of 646 eligible patients: 328 consecutive diabetic patients and 318 consecutive non-diabetic patients. All patients were imaged between January 2005 and June 2006, and were referred for further evaluation of suspected CAD on the basis of symptoms, elevated risk profile or abnormal diagnostic test results at the Azienda Ospedaliero-Universitaria di Parma, Italy, and at the Leiden University Medical Center, the

Netherlands. The study was a double-center prospective observational study as a part of a larger on-going registry. In all patients MDCT-CA was performed as part of the standard clinical diagnostic work up involving exercise electrocardiogram, myocardial scintigraphy, and/or echocardiography. The study was approved by the institutional review boards of both participating centers, and patients gave informed consent.

From the 646 patients who had an MDCT-CA scan, 30 (5%) were lost to follow-up resulting in a final study cohort of 616 individuals. Of these 616 patients, 313 had DM while 303 were without DM. At the baseline examination, demographic information, CAD risk factors, and clinical signs were collected by F.C., E.M., A.P., and J.D.S.

History of CAD was defined as history of myocardial infarction or coronary revascularization and/or presence of at least one angiographically documented coronary stenosis of >50% lumen narrowing. DM was defined as a fasting plasma glucose level of ≥ 126 mg/dL treated currently with either diet intervention, oral glucose-lowering agents or insulin.¹² Information as to the following risk factors were acquired: systemic hypertension (blood pressure of $\geq 140/90$ mmHg or the use of antihypertensive medication),¹³ hypercholesterolemia (total cholesterol level of ≥ 200 mg/dL or treatment with lipid-lowering drugs);¹⁴ obesity (body mass index of ≥ 30 kg/m²);¹⁵ positive family history of CAD (presence of CAD in a first-degree female [< 65 years] or male [< 55 years] relative);¹⁶ and smoking (previous or current smoking). We classified typical and atypical chest pain according to the criteria of Diamond.¹⁷ In the category “other symptoms” we included patients with dyspnea.

Exclusion criteria for the scan were previous allergic reaction to iodine contrast medium, renal insufficiency (creatinine clearance < 60 mL/min), pregnancy, respiratory impairment and unstable clinical status.

MDCT-CA scan protocol

All examinations were performed with a 64-detector row CT scanner (Sensation 64, Siemens, Forchheim, Germany or Aquilion 64, Toshiba Medical Systems, Tokyo, Japan). If the heart rate was > 65 bpm, oral or intravenous beta-blockers were provided when tolerated. In 511 patients (83%) sublingual nitroglycerin (0.3 mg) was also administered immediately prior to the exam to optimize visualization of small coronary vessels.

Examinations were performed as follows. First, a prospectively ECG triggered coronary calcium CT data set was obtained using standardized 20×1.2 mm collimation for the Siemens scanner and 4×3.0 mm collimation for the Toshiba scanner. Then, MDCT-CA was performed after administration of 100 ml of non ionic contrast material (Iomeprol 400 mg/ml, Iomeron 400®, Bracco, Milan, Italy) at a flow rate of 4-6 ml/s depending on patient

status. All injections were performed by dual head power injector (Stellant®, MedRad, USA) via an antecubital vein and were followed by 50 ml of saline bolus chaser at the same flow rate. A bolus tracking technique was used to determine the initiation of CT data acquisition. Using the Siemens scanner MDCT-CA was performed with: collimation (32x2)×0.6mm, gantry rotation time 330ms, tube voltage 120kV, tube current 700-900mAs, pitch 0.24, and Field-of-view 140-160mm. The Toshiba protocol consisted of: 64 × 0.5-mm collimation, gantry rotation time 400ms, tube voltage 120 or 135 kV, tube current 300 mA (range 250 to 400), and pitch 0.2 to 0.3. Datasets were reconstructed at least at two points of the cardiac cycle using a retrospective ECG gating algorithm (one diastolic cardiac phase usually at -350 msec from the R waves and one end-systolic phase at +275 msec). In the presence of motion artifacts, as in the case of cardiac arrhythmias, additional reconstructions were made at different time points of the R-R interval (steps of ±50ms). At the time of the study, tube current modulation was not used in both centers. The radiation dose estimated was 15-21mSv. Axial data sets were transferred to a remote workstation for post-processing and subsequent evaluation.

MDCT-CA data analysis

An overall Agatston score was recorded for each patient. All MDCT-CA angiograms were evaluated by two experienced observers in each center (F.C. Radiologist with 9 years of experience in cardiac CT/coronary CTA interpretation, E.M. Radiologist with 4 years of experience in cardiac CT/coronary CTA interpretation, J.D.S. cardiovascular researcher with 7 years of experience in cardiac CT/coronary CTA interpretation, and J.W.J. Interventional Cardiologist with 8 years of experience in cardiac CT/coronary CTA interpretation) unaware of the clinical history of the patients. Images were assessed on a dedicated workstation (MMWS®, Siemens Medical Solutions, Forchheim, Germany; Vitrea 2; Vital Images, Minnetonka, Minnesota) using different software tools. Axial images, multiplanar reformats, coronary cross-section views, curved multiplanar reconstructions, maximum intensity projections and volume rendering of the coronary arterial circulation were used for the assessment. The individual readings were performed retrospectively in approximately 20 sessions of 30 patients each. In case of disagreement, a joint reading was performed and a consensus decision was reached. All 16 coronary segments as established in the American Heart Association classification⁽¹⁸⁾ were considered in the analysis. All interpretable segments were evaluated for the presence of any atherosclerotic plaque.¹⁹ Atherosclerotic lesions were classified visually as obstructive (>50% luminal narrowing) or non-obstructive (≤50% luminal narrowing).

Follow-up

All patients were followed up for a minimum of 6 months after the MDCT-CA examination. Telephone interviews were performed with each patient, with his or her direct relative or

with the referring physician to discuss symptoms, the occurrence of new events or coronary revascularization procedures, any change in clinical status, and hospital admission (E.M., S.S., J.D.S., J.M.vW.). Hospital records of all patients were carefully screened to confirm the information obtained (E.M., S.S., J.D.S., J.M.vW.). The principal study end-point was a composite endpoint of cardiac death, non fatal MI, unstable angina and the need for elective revascularization. Major cardiac events included cardiac death, non fatal MI, and unstable angina requiring hospitalization. MI was defined based on criteria of typical chest pain, elevated cardiac enzyme levels, and typical changes on the electrocardiogram.²⁰

Statistical analysis

Continuous variables are expressed as mean values (\pm SD). Differences between groups were compared using the Student t and chi-square tests. Cumulative event rates of the composite end-point and major cardiac events were estimated using the Kaplan-Meier method and compared using the log-rank test. A parallel survival model was constructed in which total cardiac events included cardiac death, nonfatal MI, unstable angina and late coronary revascularization (>60 days from the MDCT-CA examination). Patients undergoing coronary revascularization were censored at the time of the procedure. Only the first event was taken into account.

The association of selected variables with outcome was assessed using Cox's proportional hazards survival model involving univariate and stepwise multivariate procedures. A composite end-point of cardiac revascularization, cardiac death, nonfatal MI and unstable angina was used. A significance level of 0.05 was required for a MDCT-CA variable to be included in the multivariate model, whereas a level of 0.1 was the cut-off value for exclusion. Multivariate analysis was corrected for all baseline clinical patient characteristics. Hazard ratios with the corresponding 95% confidence intervals were estimated. Statistical analysis were performed with SPSS software (version 16.0, SPSS Inc., Chicago, Illinois) and significance was set at $p < 0.05$.

Results

All 616 patients included in the study underwent MDCT-CA without complications. The clinical and demographic characteristics of the patients are given in Table 1. The diabetic group consisted of 213 male patients and the average age was 62 ± 11 years. The non-diabetic group consisted of 203 male patients and the average age was 63 ± 11 years. Overall, 210 (67%) diabetic patients and 203 (67%) non-diabetic patients had no history of CAD at the time of the MDCT-CA examination.

Table 1. Baseline Characteristics of Diabetics Compared with Non-diabetics

	Diabetics (n = 313)	Non-diabetics (n = 303)	p Value
Clinical characteristics			
Age (years; mean [SD])	62 (11)	63 (11)	0.25
Age male	62 (11)	62 (11)	0.91
Age female	63 (11)	66 (10)	0.03
Male gender (%)	213 (68)	203 (67)	0.85
BMI (kg/m ² ; mean [SD])	28 (4)	26 (3)	< 0.001
Mean heart rate (bpm; mean [SD])	61 (10)	62 (10)	0.28
Follow-up (months; mean [SD])	20 (7)	20 (3)	0.96
History of CAD			
Absent (%)	210 (67)	203 (67)	0.95
Present (%)	103 (33)	100 (33)	0.95
Previous MI (%)	19 (6)	22 (7)	0.66
Previous revascularization (%)	28 (9)	31 (10)	0.68
Previous MI + revascularization (%)	56 (18)	47 (15)	0.49
Risk factors			
N. of risk factors (mean [SD])	2.3 (1.2)	2.4 (1.1)	0.46
Hypertension	214 (68)	196 (65)	0.38
Hypercholesterolemia (%)	169 (54)	180 (59)	0.20
Obesity (BMI ≥ 30 kg/m ²) (%)	100 (32)	54 (18)	< 0.001
Current smoking (%)	91 (29)	136 (45)	< 0.001
Family history of CAD (%)	142 (45)	150 (49)	0.34
Symptoms			
Asymptomatic (%)	103 (33)	96 (32)	0.81
Typical angina pectoris (%)	61 (19)	42 (14)	0.08
Atypical angina pectoris (%)	92 (29)	101 (33)	0.33
Other symptoms (%)	57 (18)	64 (21)	0.42

MDCT-CA findings

A total of 189 (2%) coronary segments were considered to be of non-diagnostic quality (n=158 with motion artifacts due to elevated heart rate, n=31 with extensive calcification) and were excluded from evaluation. Plaque burden was therefore evaluated in 9297 segments. As shown in Table 2, significant differences were observed between diabetic and non-diabetic patients concerning the prevalence of normal coronary arteries (19% vs. 26%, respectively, p=0.04) and the prevalence of obstructive disease (51% vs. 37%, respectively, p<0.001). Furthermore, diabetic patients showed a higher average number of diseased coronary segments (5.6 vs. 4.4, respectively, p=0.001), with either obstructive (1.7 vs. 1.2, respectively, p=0.01) or non-obstructive (3.9 vs. 3.1, respectively, p=0.005) CAD. The total Agatston calcium score, which reflects plaque burden, was higher in diabetic patients than non-diabetic patients (440 vs. 195, respectively, p<0.001).

Table 2. MDCT-CA Characteristics of Diabetics compared with Non-diabetics

	Diabetics (n=313)	Non-diabetics (n=303)	p Value
Patients			
Absence of CAD (%)	59 (19)	79 (26)	0.04
Non-obstructive CAD (%)	94 (30)	112 (37)	0.08
Obstructive CAD (%)	160 (51)	112 (37)	< 0.001
Total Agaston CS (mean [SD])	440 (786)	195 (404)	< 0.001
Segments			
No. of diseased segments (mean [SD])	5.6 (4.8)	4.4 (4.5)	0.001
No. of segments (mean [SD]) with obstructive plaques	1.7 (2.8)	1.2 (2.4)	0.01
non-obstructive plaques	3.9 (3.9)	3.1 (3.3)	0.005

Follow-up results

During a mean follow-up period of 20 ± 5.4 months (range: 6-44 months), 88 cardiac events occurred in diabetic patients compared with 45 in non-diabetic patients (28% vs. 15%, $p < 0.001$). A total of 27 major cardiac events were observed, 22 among DM patients (fatal acute MI, $n=7$ [2%], non-fatal acute MI, $n=8$ [3%], unstable angina requiring hospitalization $n=7$ [2%]) and 5 among non DM patients (non-fatal acute MI, $n=4$ [1%], unstable angina requiring hospitalization $n=1$ [0.3%]). The overall difference in incidence was significant (7% vs. 2%, $p=0.002$).

As shown in Table 3, patients with cardiac events ($n=133$) had a greater baseline risk factor profile than patients without cardiac events ($n=483$). The principal risk factors among patients with events were a more advanced age and prevalence of male gender (101 [76%] subjects), the presence of known CAD (76 [57%] subjects) or DM (88 [66%] subjects), a higher number of risk factors (mean, 3.3 vs. 2.7, respectively, $p < 0.001$) and a higher prevalence of symptoms, with typical pain the more frequent (58 [44%] subjects). Furthermore, patients with cardiac events had a larger plaque burden as CAD tended to be more severe and extensive (Table 4).

Of the 88 diabetic patients who had cardiac events, 74 (46%) had obstructive disease while 14 (15%) had non-obstructive disease ($p < 0.001$). Conversely, the 45 non-diabetic patients to suffer cardiac events comprised 40 (36%) with obstructive disease, and 5 (4%) with non-obstructive disease ($p < 0.001$).

A total of 78 (25%) diabetic and 42 (14%) non-diabetic patients ($p < 0.001$) underwent coronary revascularization (16 surgical and 114 percutaneous coronary interventions). Fourteen revascularizations were performed after the occurrence of a major cardiac event in 12 DM

Table 3. Baseline Characteristics of Patients with Events compared with Patients without Events

	Patients With Events (n = 133)	Patients Without Events (n = 483)	p Value
Clinical characteristics			
Age (years; mean [SD])	66 (10)	62 (11)	< 0.001
Male gender (%)	101 (76)	318 (66)	0.03
BMI (kg/m ² ; mean [SD])	27 (4)	27 (4)	0.81
Mean heart rate (bpm; mean [SD])	60 (9)	61 (11)	0.21
Follow-up (months; mean [SD])	20 (4)	20 (3)	0.76
History of CAD			
Absent (%)	57 (43)	356 (74)	< 0.001
Present (%)	76 (57)	127 (26)	< 0.001
Previous MI (%)	18 (13)	23 (5)	< 0.001
Previous revascularization (%)	18 (13)	41 (8)	0.11
Previous MI + revascularization (%)	40 (30)	63 (13)	< 0.001
Risk factors			
N. of risk factors (mean [SD])	3.3 (1.1)	2.7 (1.3)	<0.001
Diabetes Mellitus	88 (66)	225 (47)	< 0.001
Hypertension	97 (73)	313 (65)	0.09
Hypercholesterolemia (%)	99 (74)	250 (52)	< 0.001
Obesity (BMI ≥ 30 kg/m ²) (%)	27 (20)	127 (26)	0.19
Current smoking (%)	60 (45)	167 (35)	0.03
Family history of CAD (%)	67 (50)	225 (47)	0.49
Symptoms			
Asymptomatic (%)	16 (12)	183 (38)	< 0.001
Typical angina pectoris (%)	58 (44)	45 (9)	< 0.001
Atypical angina pectoris (%)	26 (19)	167 (35)	0.001
Other symptoms (%)	33 (25)	88 (18)	0.12

Table 4. MDCT-CA Characteristics of Patients with Events compared with Patients without Events

	Patients with events (n=133)	Patients without events (n=483)	p Value
Patients			
Absence of CAD (%)	0 (0)	138 (28)	< 0.001
Non-obstructive CAD (%)	19 (14)	187 (39)	< 0.001
Obstructive CAD (%)	114 (86)	158 (33)	< 0.001
Total Agatston CS (mean [SD])	657.4 (883)	226.8 (517)	< 0.001

patients and in 2 non DM patients. Sixty-four (53%) patients underwent revascularization because of single vessel disease. Fifty-nine (49%) patients underwent early revascularization (<60 days from the MDCT-CA examination).

Outcome prediction

Univariate and multivariate predictors of total events in all patients and for DM and non DM patients are reported in Tables 5 and 6. Both diabetes, and obstructive CAD were independently associated with cardiac events in all patients (n=616). When assessing the predictive value of MDCT-CA in DM patients and in non DM patients, obstructive CAD was a strong predictor of events ($p<0.0001$) corrected for baseline clinical variables.

Table 5. Univariate and Multivariate Predictors of Total Cardiac Events in All Patients

Clinical Characteristics	All Patients (n=616)			
	Univariate Analysis		Multivariate Analysis	
	HR (95% CI)	p Value	HR (95% CI)	p Value
Age (>65 yrs)	1.81 (1.29-2.55)	<0.001		
Male gender	1.53 (1.03-2.28)	0.03		
Diabetes Mellitus	2.06 (1.44-2.96)	<0.001	1.94 (1.33-2.84)	0.001
Hypertension	1.41 (0.96-2.06)	0.08		
Family history	1.13 (0.81-1.59)	0.46		
Smoking	1.45 (1.03-2.04)	0.03		
Hypercholesterolemia	2.46 (1.67-3.62)	<0.001	1.63 (1.08-2.46)	0.02
Obesity	0.73 (0.48-1.11)	0.14		
Previous infarction	2.83 (2.01-3.98)	<0.001		
Previous revascularization	2.35 (1.67-3.31)	<0.001		
MDCT-CA Characteristics				
Obstructive CAD	9.59 (5.91-15.6)	<0.001	7.66 (4.34-13.43)	<0.001

Survival analysis

In both DM and non DM patients a higher total event rate occurred in patients with obstructive CAD (51.1% in DM patients vs. 35.7% in non DM patients) compared with patients with non-obstructive CAD (14.8% in DM patients vs. 4.5% in non-DM patients) or normal coronary arteries (0% vs. 0% in both DM and non DM patients)(p value <0.001)(Fig 1).

Excluding the overall revascularizations, major cardiac event rates of 18.5% and 3.6% were observed in DM and non DM patients with obstructive disease, respectively, which was higher than the corresponding rates observed in patients with non-obstructive disease (1.2% vs. 0.9%) and normal coronary arteries (0% vs. 0%), respectively (Fig 1). This difference in survival according to stenosis severity was significant in DM patients ($p<0.001$) but did not reach statistical significance in non DM patients ($p=0.1$).

As shown in Fig 2 Panel A, the total event rate was significantly higher ($p<0.05$) in DM patients with presence of atherosclerosis (non-obstructive or obstructive disease) compared to non DM patients with presence of atherosclerosis (35% vs. 21%) ($p<0.001$). Notably, the cardiac event rate among patients with absence of disease was 0% both in DM and non DM

Table 6. Univariate and Multivariate Predictors of Total Cardiac Events in Diabetics and Non-diabetics

Clinical Characteristics	Diabetics (n=313)			Non-diabetics (n=303)		
	Univariate Analysis HR (95% CI)	p Value	Multivariate Analysis HR (95% CI)	Univariate Analysis HR (95% CI)	p Value	Multivariate Analysis HR (95% CI)
Age (>65 yrs)	2.57 (1.65-3.99)	<0.001		1.05 (0.59-1.86)	0.86	
Male gender	1.29 (0.8-2.07)	0.29		2.05 (0.99-4.24)	0.05	
Hypertension	1.47 (0.91-2.38)	0.12		1.22 (0.65-2.29)	0.52	
Family history	0.94 (0.62-1.43)	0.78		1.74 (0.95-3.17)	0.07	
Smoking	1.45 (0.94-2.24)	0.09		2.13 (1.17-3.88)	0.01	
Hypercholesterolemia	2.18 (1.39-3.42)	<0.001		4.03 (1.80-8.98)	<0.001	0.40 (0.29-1.92)
Obesity	0.65 (0.40-1.06)	0.09		0.56 (0.22-1.40)	0.22	
Previous infarction	3.16 (2.08-4.80)	<0.001		2.35 (1.29-4.25)	0.005	
Previous revascularization	2.47 (1.63-3.76)	<0.001		2.16 (1.20-3.89)	0.01	0.48 (0.25-0.95)
MDCT-CA Characteristics						
Obstructive CAD	6.57 (3.72-11.6)	<0.001	5.04 (2.59-9.82)	16.29 (6.45-41.11)	<0.001	21.64 (7.60-61.57)
						<0.001

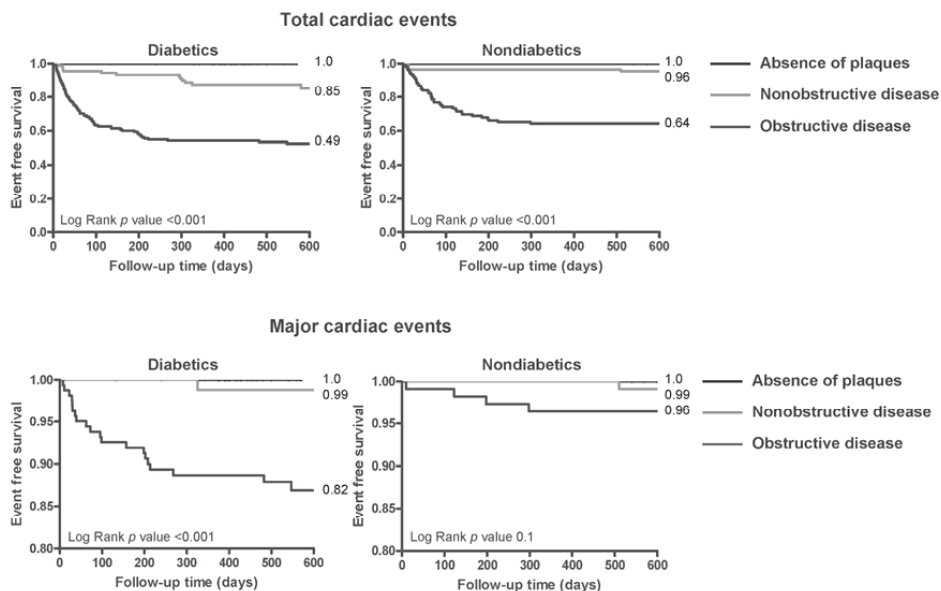


Figure 1. Kaplan-Meier Survival Curves for Total and Major Events According to the Severity of CAD on MDCT-CA in Diabetics and Non-diabetics. Statistically significant differences in survival according to the severity of CAD on MDCT-CA were observed in diabetics and non-diabetics when assessing total event free survival (Log Rank p -value <0.001). When assessing major event free survival the difference in survival according to severity of CAD on MDCT-CA was statistically significant in diabetics (Log Rank p value <0.001), but did not reach a statistically significant difference in non-diabetics (Log Rank p value 0.1).

Major cardiac events indicate cardiac death, nonfatal infarction, and unstable angina requiring hospitalization. Total cardiac events indicate major events and cardiac revascularizations.

patients. Similar findings were observed when assessing the predictive value of MDCT-CA for major cardiac events both in DM and non DM patients. When assessing the predictive value of obstructive disease, as shown in Fig 2 Panel B, an increased event rate of 47% was observed in DM patients with obstructive CAD compared to 36% in non DM patients with obstructive CAD which reached borderline statistical significance ($p=0.052$). When assessing the predictive value of obstructive disease on MDCT-CA for major cardiac events this difference was statistically significant ($p<0.05$) with a major event rate of 13% in DM patients with obstructive CAD compared to 4% in non DM patients with obstructive CAD.

Discussion

DM is associated with a substantially elevated risk of cardiovascular morbidity and mortality. However identifying CAD at an early stage in diabetic patients is challenging.⁶ Small-vessel and diffuse disease may not be detected easily by myocardial perfusion scintigraphy and dobutamine stress echocardiography. Furthermore, potential confounders are a high

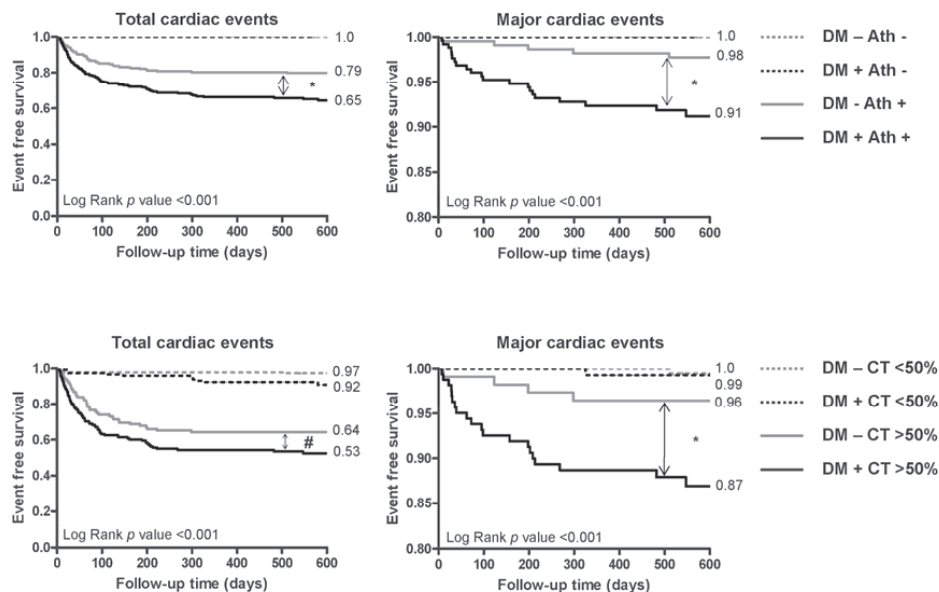


Figure 2. Kaplan-Meier Survival Curves for Total and Major Events in Diabetics and Non-diabetics Stratified for the Presence of Atherosclerosis on MDCT-CA (non-obstructive or obstructive disease) in Panel A, and Stratified for the presence of Obstructive disease on MDCT-CA in Panel B. A statistically higher event rate was observed in diabetics compared to non-diabetics in the presence of atherosclerosis on MDCT-CA (Log Rank p value <0.05), both when assessing total and major event free survival. When assessing total event free survival in diabetics with obstructive disease a borderline significantly higher event rate was observed compared to non-diabetic patients with obstructive disease (Log Rank p value 0.052). The higher event rate observed in diabetic patients with obstructive disease was however significantly higher when assessing major event free survival (Log Rank p value <0.05)

Major cardiac events indicate cardiac death, nonfatal infarction, and unstable angina requiring hospitalization. Total cardiac events indicate major events and cardiac revascularizations. Statistical comparisons between curves are indicated by arrows. An asterisk indicates statistical significance (p value <0.05). A borderline statistical significance ($p=0.052$) was observed between the DM - CT $>50\%$ and DM + CT $>50\%$ groups, as indicated by #.

threshold for pain owing to autonomic dysfunction, the often multivessel nature of CAD, baseline electrocardiographic abnormalities, the frequently poor exercise performance of diabetic patients, the coexistence of peripheral artery disease, and the use of multiple medications.²¹ Numerous previous studies have confirmed that diabetics with normal stress imaging results have an annual cardiac event rate (myocardial infarction or cardiac death) of 3–6%, which is more than twice that of non-diabetic patients with normal stress imaging findings.^{22–24}

To our knowledge this is the first study to address the prognostic value of MDCT-CA in diabetic patients. In our study a normal MDCT-CA examination was associated with a 100% event-free survival in both diabetic and non-diabetic patients. MDCT-CA allows for assessment of coronary atherosclerosis at an earlier stage compared to imaging techniques that assess myocardial perfusion. As a result MDCT-CA has a high negative predictive value for

the rule out of CAD both in non-diabetic as well as in diabetic patients.^{25, 26} As is shown in our study this high negative predictive value for CAD translates into an excellent negative predictive value for future events. Previous studies in general populations referred for MDCT-CA have also demonstrated very low event rates in patients with normal MDCT-CA examinations with annualized event rates of <0.7%.²⁷⁻³⁵ The excellent outcome in diabetic patients with completely absent CAD is of clinical relevance, because it suggests that MDCT-CA can identify truly low risk patients in contrast to other modalities. These findings are similar to those observed in a study addressing the prognostic value of coronary calcium score testing, patients suffering from diabetes with no coronary artery calcium demonstrated a survival similar to that of non-diabetics and no detectable calcium (98.8% and 99.4%, respectively, $p = 0.5$).³⁶ Survival analysis showed that both diabetic and non-diabetic patients with non-obstructive CAD had a higher risk as compared with patients without CAD. Indeed, it is known that acute coronary syndromes are frequently attributable to non-obstructive lesions (<50%) owing to plaque disruption with superimposed thrombosis.³⁷ Nonetheless, severe lesions have the highest progression compared with non-obstructive lesions. Serial angiographic studies have indicated that the more obstructive a plaque is, the more frequently it progresses to coronary occlusion (³⁸ and/or gives rise to myocardial infarction.³⁹ In agreement, our analysis revealed that a higher event rate occurred among patients with obstructive CAD. Recently, several studies have reported on the prognostic value of obstructive CAD on MDCT-CA in general populations.^{31, 33, 34, 40} In our study assessing the prognostic value in diabetic and non-diabetic patients, multivariate analysis demonstrated that evidence of obstructive disease on MDCT-CA remained a strong independent predictor of events in both groups ($p < 0.0001$)

When comparing the predictive value of atherosclerosis and obstructive CAD in DM and non DM, significantly increased event rates were observed in DM patients. These findings are in agreement with those made in previous larger multicenter studies. For any degree of perfusion abnormality, diabetics had a much greater risk of cardiac events and death compared to non-diabetics for any degree of demonstrable perfusion abnormality.^{41, 42} Similar findings have been reported for stress echocardiographic techniques (⁴³ and electron-beam computed tomography studies. In the study by Raggi et al. similar findings to our study were observed when assessing the prognostic value of coronary calcium score in diabetics and non-diabetics.³⁶ In their study the average coronary calcium score for subjects with and for those without diabetes was 281 ± 567 and 119 ± 341 , respectively ($p < 0.0001$). The observed death rate in diabetics was higher for every increase in calcium score compared to non-diabetics ($p < 0.0001$). Taken together, these findings suggest that for any extent of plaque burden cardiovascular risk is higher in diabetic patients than in non-diabetic individuals. Thus, MDCT-CA may be a useful tool to risk-stratify diabetic and non-diabetic subjects with the objective being to better define appropriate individual management.

Limitations

There are some limitations of our study. Complete information concerning the degree of metabolic control of DM, the status of secondary organ involvement, and of autonomic dysfunction, were not obtained. This limitation was mainly due to the exploratory nature of the study, which was aimed at investigating the prognostic role of MDCT-CA on outcome in “real world” DM patients with or without CAD rather than on the degree of diabetes control. Furthermore, a more detailed analysis of the group of patients without known CAD may have been interesting. However, due to the relatively low number of events this analysis was not possible. Another potential limitation of our study was that we included in the multivariate model patients who underwent early revascularization procedures (<60 days after the exam) that generally are performed as a direct consequence of the MDCT-CA imaging findings. Conversely, decisions to perform late revascularization procedures (≥ 60 days after MDCT-CA exam) usually are not significantly influenced by the results of the exam. Late revascularization are the result of worsening clinical status, such that late revascularizations represent a surrogate for disease progression. This issue has been recently addressed by another study in which the prognostic ability of MDCT-CA was assessed including patients who underwent early revascularization procedures.²⁸

However, it is worthwhile noting that all decisions regarding revascularization were based on symptoms and/or the presence of concomitant ischemia on non-invasive testing, rather than the arbitrary evidence of obstructive CAD on MDCT-CA. In our study, however, a parallel survival model for total cardiac events excluding early revascularizations demonstrated that DM patients remained associated with worse outcome; furthermore, the presence of obstructive CAD on MDCT-CA remained associated with outcome in both DM and non DM patients. Therefore, our results do not appear to be affected by treatment bias.

Conclusion

This is the first study to our knowledge to assess the prognostic value of MDCT-CA in diabetic patients with known or suspected CAD compared with non-diabetic individuals. MDCT-CA provides incremental prognostic information over baseline clinical variables in both groups of patients when obstructive CAD is present. The absence of atherosclerosis on MDCT-CA is associated with an excellent prognosis in both groups of patients. MDCT-CA might therefore be a clinically useful tool to improve risk stratification in DM patients.

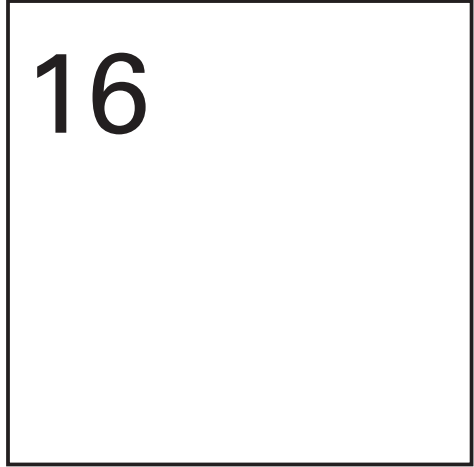
References

1. King H, Aubert RE, Herman WH. Global burden of diabetes, 1995-2025: prevalence, numerical estimates, and projections. *Diabetes Care* 1998;21:1414-31.
2. Nathan DM, Meigs J, Singer DE. The epidemiology of cardiovascular disease in type 2 diabetes mellitus: how sweet it is ... or is it? *Lancet* 1997;350:SI4-SI9.
3. Haffner SM, Lehto S, Ronnema T, et al. Mortality from coronary heart disease in subjects with type 2 diabetes and in nondiabetic subjects with and without prior myocardial infarction. *N Engl J Med* 1998;339:229-34.
4. Hachamovitch R, Hayes SW, Friedman JD, et al. Comparison of the short-term survival benefit associated with revascularization compared with medical therapy in patients with no prior coronary artery disease undergoing stress myocardial perfusion single photon emission computed tomography. *Circulation* 2003;107:2900-7.
5. Sorajja P, Chareonthaitawee P, Rajagopalan N, et al. Improved survival in asymptomatic diabetic patients with high-risk SPECT imaging treated with coronary artery bypass grafting. *Circulation* 2005;112:I311-I6.
6. Kamalesh M, Feigenbaum H, Sawada S. Assessing prognosis in patients with diabetes mellitus--the Achilles' heel of cardiac stress imaging tests? *Am J Cardiol* 2007;99:1016-9.
7. Leschka S, Alkadhi H, Plass A, et al. Accuracy of MSCT coronary angiography with 64-slice technology: first experience. *Eur Heart J* 2005;26:1482-7.
8. Mollet NR, Cademartiri F, Van Mieghem CAG, et al. High-resolution spiral computed tomography coronary angiography in patients referred for diagnostic conventional coronary angiography. *Circulation* 2005;112:2318-23.
9. Nikolaou K, Knez A, Rist C, et al. Accuracy of 64-MDCT in the diagnosis of ischemic heart disease. *AJR* 2006;187:111-7.
10. Pugliese F, Mollet NR, Runza G, et al. Diagnostic accuracy of non-invasive 64-slice CT coronary angiography in patients with stable angina pectoris. *Eur Radiol* 2006;16:575-82.
11. Raff GL, Gallagher MJ, O'Neill WW, et al. Diagnostic accuracy of noninvasive coronary angiography using 64-slice spiral computed tomography. *J Am Coll Cardiol* 2005;46:552-7.
12. Report of the expert committee on the diagnosis and classification of diabetes mellitus. *Diabetes Care* 2003;26:S5-20.
13. 2003 European Society of Hypertension-European Society of Cardiology guidelines for the management of arterial hypertension. *J Hypertens* 2003;21:1011-53.
14. Executive Summary of The Third Report of The National Cholesterol Education Program (NCEP) Expert Panel on Detection, Evaluation, and Treatment of High Blood Cholesterol In Adults (Adult Treatment Panel III). *JAMA* 2001;285:2486-97.
15. Clinical Guidelines on the Identification, Evaluation, and Treatment of Overweight and Obesity in Adults--The Evidence Report. National Institutes of Health. *Obes Res* 1998;6 Suppl 2:S1S-209S.
16. Taylor AJ, Bindeman J, Feuerstein I, et al. Coronary calcium independently predicts incident premature coronary heart disease over measured cardiovascular risk factors: mean three-year outcomes in the Prospective Army Coronary Calcium (PACC) project. *J Am Coll Cardiol* 2005;46:807-14.
17. Diamond GA. A clinically relevant classification of chest discomfort. *J Am Coll Cardiol* 1983;1:574-5.
18. Austen WG, Edwards JE, Frye RL, et al. A reporting system on patients evaluated for coronary artery disease. Report of the Ad Hoc Committee for Grading of Coronary Artery Disease, Council on Cardiovascular Surgery, American Heart Association. *Circulation* 1975;51:5-40.
19. Achenbach S, Moselewski F, Ropers D, et al. Detection of calcified and noncalcified coronary atherosclerotic plaque by contrast-enhanced, submillimeter multidetector spiral computed tomography: a segment-based comparison with intravascular ultrasound. *Circulation* 2004;109:14-7.

20. Alpert JS, Thygesen K, Antman E, et al. Myocardial infarction redefined--a consensus document of The Joint European Society of Cardiology/American College of Cardiology Committee for the redefinition of myocardial infarction. *J Am Coll Cardiol* 2000;36:959-69.
21. Ryden L, Standl E, Bartnik M, et al. Guidelines on diabetes, pre-diabetes, and cardiovascular diseases: executive summary. The Task Force on Diabetes and Cardiovascular Diseases of the European Society of Cardiology (ESC) and of the European Association for the Study of Diabetes (EASD). *Eur Heart J* 2007;28:88-136.
22. Chaowalit N, Arruda AL, McCully RB, et al. Dobutamine stress echocardiography in patients with diabetes mellitus: enhanced prognostic prediction using a simple risk score. *J Am Coll Cardiol* 2006;47:1029-36.
23. Marwick TH, Case C, Sawada S, et al. Use of stress echocardiography to predict mortality in patients with diabetes and known or suspected coronary artery disease. *Diabetes Care* 2002;25:1042-8.
24. Sozzi FB, Elhendy A, Roelandt JR, et al. Prognostic value of dobutamine stress echocardiography in patients with diabetes. *Diabetes Care* 2003;26:1074-8.
25. Schuijf JD, Bax JJ, Jukema JW, et al. Noninvasive angiography and assessment of left ventricular function using multislice computed tomography in patients with type 2 diabetes. *Diabetes Care* 2004;27:2905-10.
26. Meijboom WB, Meijs MFL, Schuijf JD, et al. Diagnostic accuracy of 64-slice computed tomography coronary angiography: a prospective multicenter, multivendor study. *J Am Coll Cardiol* 2008;52:2135-44.
27. Aldrovandi A, Maffei E, Palumbo A, et al. Prognostic value of computed tomography coronary angiography in patients with suspected coronary artery disease: a 24-month follow-up study. *Eur Radiol* 2009;19:1653-60.
28. Carrigan TP, Nair D, Schoenhagen P, et al. Prognostic utility of 64-slice computed tomography in patients with suspected but no documented coronary artery disease. *Eur Heart J* 2009;30:362-71.
29. Gaemperli O, Valenta I, Schepis T, et al. Coronary 64-slice CT angiography predicts outcome in patients with known or suspected coronary artery disease. *Eur Radiol* 2008;18:1162-73.
30. Gilard M, Le Gal G, Cornily J, et al. Midterm prognosis of patients with suspected coronary artery disease and normal multislice computed tomographic findings. *Arch Intern Med* 2007;165:1686-9.
31. Ostrom MP, Gopal A, Ahmadi N, et al. Mortality incidence and the severity of coronary atherosclerosis assessed by computed tomography angiography. *J Am Coll Cardiol* 2008;52:1335-43.
32. Pundziute G, Schuijf JD, Jukema JW, et al. Prognostic value of multislice computed tomography coronary angiography in patients with known or suspected coronary artery disease. *J Am Coll Cardiol* 2007;49:62-70.
33. van Werkhoven JM, Schuijf JD, Gaemperli O, et al. Prognostic value of multislice computed tomography and gated single-photon emission computed tomography in patients with suspected coronary artery disease. *J Am Coll Cardiol* 2009;53:623-32.
34. Gopal A, Nasir K, Ahmadi N, et al. Cardiac computed tomographic angiography in an outpatient setting: an analysis of clinical outcomes over a 40-month period. *J Cardiovasc Comput Tomogr* 2009;3:90-5.
35. Van Lingen R, Kakani N, Veitch A, et al. Prognostic and accuracy data of multidetector CT coronary angiography in an established clinical service. *Clin Radiol* 2009;64:601-7.
36. Raggi P, Shaw LJ, Berman DS, et al. Prognostic value of coronary artery calcium screening in subjects with and without diabetes. *J Am Coll Cardiol* 2004;43:1663-9.
37. Falk E, Shah PK, Fuster V. Coronary plaque disruption. *Circulation* 1995;92:657-71.
38. Alderman EL, Corley SD, Fisher LD, et al. Five-year angiographic follow-up of factors associated with progression of coronary artery disease in the Coronary Artery Surgery Study (CASS). CASS Participating Investigators and Staff. *J Am Coll Cardiol* 1993;22:1141-54.

39. Giroud D, Li JM, Urban P, et al. Relation of the site of acute myocardial infarction to the most severe coronary arterial stenosis at prior angiography. *Am J Cardiol* 1992;69:729-32.
40. Hadamitzky M, Freissmuth B, Meyer T, et al. Prognostic value of coronary computed tomographic angiography for prediction of cardiac events in patients with suspected coronary artery disease. *J Am Coll Cardiol Img* 2009;2:404-11.
41. Giri S, Shaw LJ, Murthy DR, et al. Impact of diabetes on the risk stratification using stress single-photon emission computed tomography myocardial perfusion imaging in patients with symptoms suggestive of coronary artery disease. *Circulation* 2002;105:32-40.
42. Kang X, Berman DS, Lewin HC, et al. Incremental prognostic value of myocardial perfusion single photon emission computed tomography in patients with diabetes mellitus. *Am Heart J* 1999;138:1025-32.
43. Cortigiani L, Bigi R, Sicari R, et al. Prognostic value of pharmacological stress echocardiography in diabetic and nondiabetic patients with known or suspected coronary artery disease. *J Am Coll Cardiol* 2006;47:605-10.

Chapter 16



Influence of smoking on the prognostic value of cardiovascular computed tomography coronary angiography

JM van Werkhoven, JD Schuijf, A Pazhenkottil, BA Herzog, JR Ghadri,
JW Jukema, E Boersma, LJ Kroft, A de Roos, PA Kaufmann, JJ Bax

Abstract

Computed tomography coronary angiography (CTA) is an important non-invasive imaging modality increasingly used for the diagnosis and prognosis of coronary artery disease (CAD). The purpose of the current study was to determine the influence of smoking status on the prognostic value of CTA in patients with suspected or known CAD. In 1207 patients (57% male, age 57 ± 12 years) referred for CTA, the presence of significant CAD ($\geq 50\%$ stenosis) was determined. During follow-up the following events were recorded: all cause mortality, and non-fatal infarction. The prognostic value of CTA in smokers and non-smokers was compared using an interaction term in the Cox proportional hazard regression analysis. Significant CAD was observed in 327 patients (27%), and 273 patients (23%) were smokers. During a median follow-up time of 2.2 years, an event occurred in 50 patients. After correction for baseline characteristics including smoking in a multivariate model, significant CAD remained an independent predictor of events. Furthermore, a significant interaction ($p < 0.05$) was observed between significant CAD and smoking. The annualized event rate in smokers with significant CAD was 8.78% compared to 0.99% in smokers without significant CAD ($p < 0.001$). In non-smokers with significant CAD the annualized event rate was 2.07% compared to 1.01% in non-smokers without significant CAD ($p = 0.058$). In conclusion, the prognostic value of CTA was significantly influenced by smoking status. The event rates in patients with significant CAD were approximately 4-fold higher in smokers compared to non-smokers. These findings suggest that smoking cessation needs to be aggressively pursued, especially in smokers with significant CAD.

Introduction

The introduction of multi-slice computed tomography coronary angiography (CTA) has changed the field of non-invasive imaging. In contrast to functional imaging techniques assessing myocardial perfusion and wall motion, CTA can provide direct non-invasive anatomic assessment of the coronary arteries. Because of the high negative predictive value for detection of significant CAD (defined as $\geq 50\%$ stenosis),¹ the technique is increasingly used as a gatekeeper for further diagnostic testing. In the last 3-4 years, several single and multi-center studies have suggested that CTA may also provide important prognostic information. These studies have shown that patients with significant CAD detected on CTA are associated with worse outcome compared to patients without significant CAD.²⁻⁷

Although the prognostic value of CTA and its incremental value over baseline clinical variables have thus been previously described, no reports have specifically focused on the prognostic value of CTA in smokers. This may be of interest, as smoking is an important but also modifiable risk factor resulting in an approximately 2 to 4 times increased risk of coronary heart disease compared to non-smokers.^{8, 9} Furthermore, smoking has recently been shown to significantly increase the risk of events in asymptomatic individuals with evidence of atherosclerosis according to the coronary calcium score (CS), when compared to non-smokers with a similar calcium burden.¹⁰ It is conceivable that smoking has a similar effect on risk stratification with CTA. The purpose of the current study was therefore to determine the influence of smoking status on the prognostic value of CTA in patients with suspected or known CAD.

Methods

The study population consisted of patients who were clinically referred for CTA because of chest pain symptoms or a high risk profile for cardiovascular disease. Patients were enrolled at the University Hospital in Zurich, Switzerland, and at the Leiden University Medical Center, The Netherlands. Results from this prospective registry have been previously published.⁵ Exclusion criteria were: cardiac arrhythmias, renal insufficiency (defined as a glomerular filtration rate < 30 ml/min), known hypersensitivity to iodine contrast media, and pregnancy. In addition, patients with an uninterpretable CTA examination or coronary artery bypass grafts were excluded. Clinical patient characteristics were collected by the referring physician. Patients provided informed consent and the study was approved by the local ethics committees in both participating centers.

CTA acquisition and data analysis

Patients were scanned using a 64-row CT scanner (Aquilion64, Toshiba Medical Systems, Otawara, Japan; and General Electrics LightSpeed VCT, Milwaukee, WI, US) or with a 320-row CT scanner (Toshiba Multi-slice Aquilion ONE system, Toshiba Medical Systems, Otawara, Japan). Before the examination, the patient's heart rate and blood pressure were monitored. In the absence of contraindications, patients with a heart rate exceeding 65 beats per minute were administered beta-blocking medication (50-100 mg metoprolol, oral or 5-10 mg metoprolol, intravenous). All scan parameters have been previously published.¹¹⁻¹³

Post-processing of the CTA examinations was performed on dedicated workstations (Vitrea2 and VitreaFx, Vital Images, USA; and Advantage GE Healthcare, USA). CTA examinations were read by two experienced readers at both participating centers, blinded to follow-up results. Coronary anatomy was assessed using a 17 segment model according to a modified American Heart Association classification.¹⁴ Normal CTA was defined as completely normal anatomy or minimal wall irregularities <30%, non-significant CAD was defined as the presence of luminal narrowing with a maximal luminal diameter stenosis <50%, and significant CAD was defined as the presence of a lesion exceeding ≥50% maximal luminal diameter stenosis.

Follow-up results

Patient follow-up data were gathered using clinical visits or standardized telephone interviews. A composite endpoint was constructed using all cause mortality, and non-fatal myocardial infarction. Non-fatal infarction was defined based on criteria of typical chest pain, elevated cardiac enzyme levels, and typical changes on the ECG.¹⁵ Patients with stable complaints undergoing an early elective revascularization within 60 days after CTA were excluded from the survival analysis.

Statistical analysis

Normally distributed continuous variables were expressed as mean values (\pm standard deviation). Non-normally distributed continuous variables were expressed as median values with a 25th-75th percentile. Categorical baseline data were expressed in numbers and percentages. Differences between smokers and non-smokers were compared using the Student t and chi-square tests. Cox regression analysis was used to determine the prognostic value of significant (\geq 50% luminal narrowing) CAD on CTA. First univariate analysis of baseline clinical variables, and CTA was performed using a composite endpoint of all cause mortality, and non-fatal infarction. For each variable a hazard ratio with a 95%-confidence interval (95%-CI) was calculated. A multivariate model was created to assess the independent prognostic value of CTA. To compare the prognostic value of CTA in smokers and non-smokers a final multivariate model was constructed to test for interaction between smoking

and CTA. Multivariate models were created using stepwise backward elimination; first all baseline clinical variables were included in the model, subsequently the least significant variable was excluded one at a time until all variables in the model reached a p-value <0.5. Annualized event rates were calculated based on the number of events per 100 patient years follow-up (FU). Survival curves were estimated with the Kaplan-Meier method, and curves were compared using the log-rank test. Statistical analyses were performed using SPSS software (version 16.0, SPSS Inc, Chicago, IL, USA). A p-value <0.05 was considered statistically significant.

Results

The study population consisted of 1467 patients presenting at the University Hospital Zurich (n=468), and at the Leiden University Medical Center (n=999). In 44 (3%) patients the CTA examination was uninterpretable due to the presence of motion artifacts, increased noise due to a high body mass index, and breathing. In addition, 117 patients (8%) were lost to follow-up. Finally 99 patients (7%) were excluded due to early revascularization. After exclusion, a total of 1207 remained for analysis. The majority of patients were symptomatic (67%), the remaining 33% of patients were referred because of a high risk profile with or without an abnormal exercise ECG. An overview of the baseline characteristics of the study population is presented in Table 1.

Table 1. Patient characteristics

	Total (n = 1207)	Non-smokers (n=934)	Smokers (n=273)	P-value
Age (years)	56.8±11.9	57.4±12.2	54.8±10.9	0.002
Gender (male)	690 (57%)	514 (55%)	176 (64%)	0.006
Risk Factors				
Diabetes	299 (25%)	226 (24%)	73 (27%)	0.39
Hypertension	587 (49%)	455 (49%)	132 (49%)	0.92
Hypercholesterolemia	461 (38%)	341 (37%)	120 (44%)	0.03
Family history of CAD	475 (39%)	342 (37%)	133 (49%)	<0.001
Obesity (BMI ≥ 30 kg/m ²)	220 (18%)	176 (19%)	44 (16%)	0.26
History				
Previous MI	96 (8%)	68 (7%)	28 (10%)	0.11
Previous PCI	116 (10%)	82 (9%)	34 (13%)	0.07
Known CAD	135 (11%)	96 (10%)	39 (14%)	0.07

CTA results

Significant CAD was observed on CTA in 327 patients (27%). In the remaining 880 patients (73%) non-significant CAD was observed in 425 patients (35%) and 455 patients (38%) were

classified as normal. Figure 1 illustrates the prevalence of significant CAD on CTA according to smoking status. In non-smokers (n=934), significant stenosis was observed on CTA in 229 patients (25%), compared to 98 (36%) of the 273 patients who smoked ($p<0.001$).

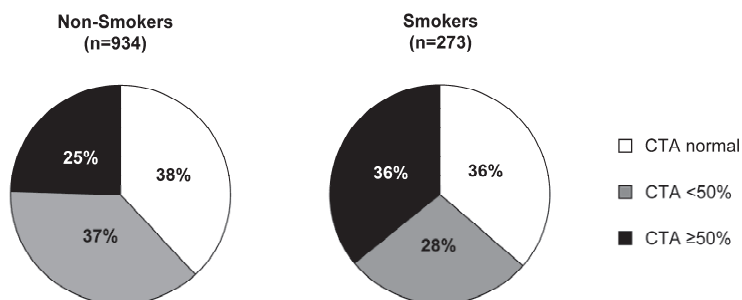


Figure 1. Relationship between CTA findings and Smoking.

Follow-up results

The median FU time was 2.2 years (25-75th percentile: 1.3-3.2 years). During the FU period a myocardial infarction occurred in 12 patients and all cause mortality was registered in 40 patients. The composite endpoint of all cause mortality and myocardial infarction occurred in 50 patients. This resulted in an event rate of 1.8 per 100 patient years FU.

Survival analysis

The presence of significant CAD on CTA was a significant univariate predictor of events (Table 2). After correction for baseline clinical variables including smoking status, significant CAD remained an independent predictor of events (Table 2). An event rate of 4.01 events per 100 patient years FU was observed in patients with significant CAD compared to 1.0 event per 100 patient years FU in patients without significant CAD.

To assess the prognostic value of significant CAD on CTA in smokers and non-smokers, a second multivariate model was constructed to test for interaction (Table 3). The prognostic value of CTA was significantly higher in smokers compared to the prognostic value of CTA in non-smokers (interaction $p = 0.031$, and $p = 0.045$ adjusted for age, diabetes, hypercholesterolemia, obesity, and known CAD). The event rate in smokers with significant CAD was 8.78 events per 100 patient years FU compared to 0.99 events per 100 patient years FU in smokers without significant CAD ($p<0.001$). In non-smokers with significant CAD the event rate was 2.07 events per 100 patient years FU compared to 1.01 events per 100 patient years FU in non-smokers without significant CAD ($p=0.058$). The survival rate following CTA according to smoking status is illustrated in Figure 2.

Table 2. Univariate and Multivariate predictors of events

	Univariate		Multivariate	
	HR (95%-CI)	p-value	HR (95%-CI)	p-value
Age (years)	1.1 (1.0-1.1)	<0.001	1.1 (1.0-1.1)	<0.001
Gender (male)	1.1 (0.6-1.9)	0.68		
Diabetes	1.6 (0.9-2.9)	0.11	1.8 (1.0-3.5)	0.07
Hypertension	1.2 (0.7-2.2)	0.46		
Hypercholesterolemia	1.1 (0.6-1.9)	0.67		
Family history CAD	0.9 (0.5-1.6)	0.68		
Obesity (BMI \geq 30 kg/m ²)	0.49 (0.2-1.2)	0.13	0.5 (0.2-1.3)	0.2
Known CAD	2.3 (1.2-4.3)	0.01	1.8 (0.9-3.5)	0.1
Current Smoking	2.9 (1.6-4.9)	<0.001	2.6 (1.4-4.7)	<0.05
Significant CAD	4.1 (2.3-7.2)	<0.001	2.4 (1.3-4.4)	<0.05

Table 3. Interaction between Smoking and significant CAD on CTA

Exposure	Patients	Event	HR (95%-CI)	p-value
No Smoking				
CTA <50%	705	16	1.0 (reference)	
CTA \geq 50%	229	11	2.1 (0.9-4.5)	0.06
Smoking				
CTA <50%	175	4	1.0 (reference)	
CTA \geq 50%	98	19	8.9 (3.0-26.5)	<0.001

Discussion

The main finding of the current study comparing the prognostic value of CTA in smokers and non-smokers is that the prognostic value of significant CAD on CTA was significantly influenced by smoking status. The event rate in patients with significant CAD was approximately 4-fold higher in smokers compared to non-smokers. On the other hand, in patients without significant CAD, the event rate was similar in smokers and non-smokers.

Although several studies have been published on the prognostic value of CTA, to our knowledge this is the first report to describe the effect of smoking on risk stratification with CTA. The effect of smoking on the prognostic value of atherosclerosis as detected by CS has been studied.¹⁰ CS is generally used in asymptomatic cohorts as a measure of atherosclerotic plaque burden, and elevated CS are associated with an increased risk of events. In the study by Shaw et al. in a large cohort of 10,377 asymptomatic individuals, the value of CS for risk stratification has been compared between smokers and non-smokers. The authors observed a significant interaction between smoking and CS for the prediction of all cause mortality. In each CS category the event rates in smokers were higher than observed in non-smokers. In addition to this imaging study in asymptomatic individuals, elevated event rates in

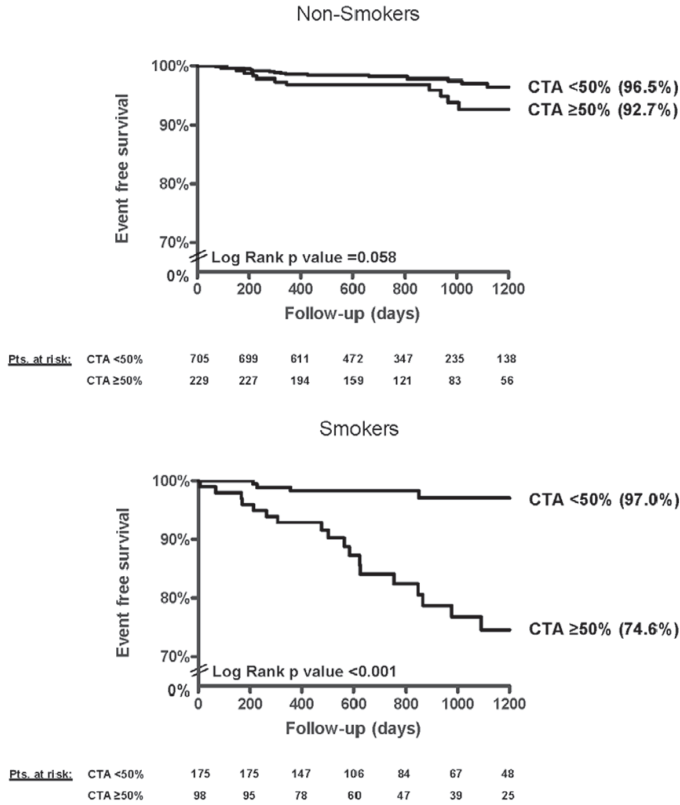


Figure 2. Survival according to CTA in non-smokers (panel a) and smokers (panel b).

smokers as compared to non-smokers have also been reported in symptomatic patients with established CAD. For instance, several studies have shown that following revascularization, smokers have a higher event rate than non-smokers.¹⁶⁻¹⁸ The results of the current study are in line with these findings and further strengthen the evidence that smokers with CAD have a higher risk of events than non-smokers with similar levels of CAD.

The observations in the current study may be explained in part by the influence of smoking on the formation and progression of atherosclerosis through its negative effects on vasomotor dysfunction, inflammation and lipid modification.¹⁹ Indeed multiple reports have described the effects of smoking on the formation of atherosclerosis both at autopsy,²⁰ as well as in clinical studies using coronary angiography,^{21, 22} CS²³⁻²⁵ and intima media thickness (IMT) measurements.^{26, 27} Coronary angiography studies have described that smoking is an important and independent predictor of CAD, which is in line with the increased prevalence of significant CAD observed in the current study.^{21, 22} Of interest, the atherosclerotic process seems to occur earlier in life in smokers.^{25, 28} Earlier formation of CAD explains the

increased levels of CAD observed in smokers; however this may also be linked to increased progression of CAD. Smoking has been associated with CAD progression both on coronary angiography, IMT, and CTA. In a sub study of the CCAIT trial, Waters et al. observed that smoking resulted in both plaque progression and new plaque formation on serial quantitative coronary angiography.²⁹

The rapid decrease in the risk of myocardial infarction observed after smoking cessation suggests that in addition to the effects of smoking on CAD formation and progression, smoking may also be seen as a trigger for myocardial infarction.³⁰ Smoking may affect all three major factors defining high risk patients that are vulnerable to myocardial infarction or sudden cardiac death: vulnerable plaque, vulnerable blood, and vulnerable myocardium.³¹ Smoking has been associated with inflammatory processes, and endothelial dysfunction which may increase plaque vulnerability resulting in a higher risk of intracoronary thrombus formation. In addition platelet function, antithrombotic/prothrombotic and fibrinolytic factors may be altered by smoking resulting in an increased thrombotic tendency which in turn may cause more frequent and severe thrombus formation in response to plaque rupture.³²⁻³⁵ Finally, smoking results in activation of the sympathetic nervous system thereby increasing heart rate and myocardial contractility resulting in increased oxygen demand, while at the same time decreasing myocardial oxygen supply due to vasoconstriction of the coronary arteries.³⁶ This mismatch in oxygen demand/supply may increase the myocardial vulnerability to ischemia thereby unfavorably altering myocardial response to thrombotic occlusions.

Clinical implications

Further studies are needed to confirm our finding that the relative risk of events associated with significant CAD on CTA is significantly higher in smokers compared to non-smokers. Nevertheless, our results do suggest that strategies aimed at preventing future cardiovascular events should be intensified in patients with significant CAD who smoke. This is further strengthened by the fact that smoking is a modifiable risk factor, and that smoking cessation has been shown to improve survival.^{37, 38}

Interestingly, when regarding patients without significant CAD, the risk of events in smokers without significant CAD was similar to the risk observed in their non-smoking counterparts. Based on previous studies assessing effect of smoking on CAD, it is expected that new formation and progression of (non-significant) CAD should also be increased in patients without significant CAD who smoke. The similar event rates observed in the current study suggest that this effect may be more gradual. Longer follow-up studies are necessary to determine the influence of smoking status in patients without significant CAD.

Limitations

A limitation of the current study is that no exact data regarding quantification of smoking were available. This would have been of interest as several studies have suggested a dose response relationship between smoking and the severity of CAD. In addition, the occurrence of passive smoking in the non-smoking sub group was not systematically recorded. Because passive smoking has also been associated with an increased risk of events,³⁹⁻⁴² a similar interaction as observed between significant CAD and active smoking may exist in passive smokers. Future studies are necessary to further study these concepts.

A general limitation of CTA imaging is the high radiation dose associated with traditional 64-slice CTA protocols, although the radiation dose of CTA has decreased substantially with the implementation of dose saving algorithms and novel acquisition techniques.⁴³⁻⁴⁶ Importantly, low-dose CTA with prospective ECG-triggering has recently been shown to reduce radiation burden while maintaining image quality and a high diagnostic accuracy.⁴⁷ Currently, the radiation burden with these novel acquisition techniques is approaching ≤ 2 mSv.⁴⁸

Conclusion

The prognostic value of CTA was significantly influenced by smoking status. The event rates in patients with significant CAD were approximately 4-fold higher in smokers compared to non-smokers. These results need to be confirmed in larger follow-up studies, but suggest that smoking cessation needs to be aggressively pursued, especially in smokers with significant CAD.

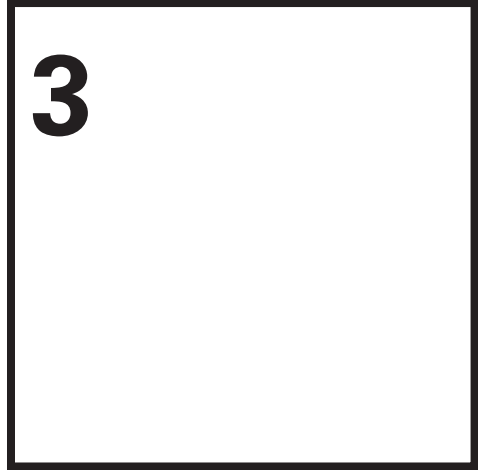
References

1. Meijboom WB, Meijjs MFL, Schuijf JD, et al. Diagnostic accuracy of 64-slice computed tomography coronary angiography: a prospective multicenter, multivendor study. *J Am Coll Cardiol* 2008;52:2135-44.
2. Gopal A, Nasir K, Ahmadi N, et al. Cardiac computed tomographic angiography in an outpatient setting: an analysis of clinical outcomes over a 40-month period. *J Cardiovasc Comput Tomogr* 2009;3:90-5.
3. Hadamitzky M, Freissmuth B, Meyer T, et al. Prognostic Value of Coronary Computed Tomographic Angiography for Prediction of Cardiac Events in Patients With Suspected Coronary Artery Disease. *J Am Coll Cardiol Img* 2009;2:404-11.
4. Ostrom MP, Gopal A, Ahmadi N, et al. Mortality incidence and the severity of coronary atherosclerosis assessed by computed tomography angiography. *J Am Coll Cardiol* 2008;52:1335-43.
5. van Werkhoven JM, Schuijf JD, Gaemperli O, et al. Prognostic value of multislice computed tomography and gated single-photon emission computed tomography in patients with suspected coronary artery disease. *J Am Coll Cardiol* 2009;53:623-32.
6. Chow BJ, Wells GA, Chen L, et al. Prognostic value of 64-slice cardiac computed tomography severity of coronary artery disease, coronary atherosclerosis, and left ventricular ejection fraction. *J Am Coll Cardiol* 2010;55:1017-28.
7. Min JK, Lin FY, Dunning AM, et al. Incremental prognostic significance of left ventricular dysfunction to coronary artery disease detection by 64-detector row coronary computed tomographic angiography for the prediction of all-cause mortality: results from a two-centre study of 5330 patients. *European Heart Journal* 2010;31:1212-9.
8. http://www.cdc.gov/tobacco/data_statistics/sgr/2004/index.htm (5 May 2009)
9. http://profiles.nlm.nih.gov/NN/B/B/X/S/_/nnbbxs.pdf (5 May 2009)
10. Shaw LJ, Raggi P, Callister TQ, et al. Prognostic value of coronary artery calcium screening in asymptomatic smokers and non-smokers. *Eur Heart J* 2006;27:968-75.
11. Schuijf JD, Wijns W, Jukema JW, et al. The relationship between non-invasive coronary angiography with multi-slice computed tomography and myocardial perfusion imaging. *J Am Coll Cardiol* 2006;48:2508-14.
12. Gaemperli O, Schepis T, Kalff V, et al. Validation of a new cardiac image fusion software for three-dimensional integration of myocardial perfusion SPECT and stand-alone 64-slice CT angiography. *Eur J Nucl Med Mol Imaging* 2007;34:1097-106.
13. de Graaf FR, Schuijf JD, van Velzen JE, et al. Diagnostic accuracy of 320-row multidetector computed tomography coronary angiography in the non-invasive evaluation of significant coronary artery disease. *Eur Heart J* 2010;31:1908-15.
14. Austen WG, Edwards JE, Frye RL, et al. A reporting system on patients evaluated for coronary artery disease. Report of the Ad Hoc Committee for Grading of Coronary Artery Disease, Council on Cardiovascular Surgery, American Heart Association. *Circulation* 1975;51:5-40.
15. Thygesen K, Alpert JS, White HD. Universal definition of myocardial infarction. *Eur Heart J* 2007;28:2525-38.
16. Goldenberg I, Jonas M, Tenenbaum A, et al. Current smoking, smoking cessation, and the risk of sudden cardiac death in patients with coronary artery disease. *Arch Intern Med* 2003;163:2301-5.
17. van Domburg RT, Meeter K, van Berkel DF, et al. Smoking cessation reduces mortality after coronary artery bypass surgery: a 20-year follow-up study. *J Am Coll Cardiol* 2000;36:878-83.
18. Hasdai D, Garratt KN, Grill DE, et al. Effect of smoking status on the long-term outcome after successful percutaneous coronary revascularization. *N Engl J Med* 1997;336:755-61.
19. Ambrose JA, Barua RS. The pathophysiology of cigarette smoking and cardiovascular disease: an update. *J Am Coll Cardiol* 2004;43:1731-7.

20. Strong JP, Richards ML. Cigarette smoking and atherosclerosis in autopsied men. *Atherosclerosis* 1976;23:451-76.
21. Wang XL, Tam C, McCredie RM, et al. Determinants of severity of coronary artery disease in Australian men and women. *Circulation* 1994;89:1974-81.
22. Weintraub WS, Klein LW, Seelaus PA, et al. Importance of total life consumption of cigarettes as a risk factor for coronary artery disease. *Am J Cardiol* 1985;55:669-72.
23. Goel M, Wong ND, Eisenberg H, et al. Risk factor correlates of coronary calcium as evaluated by ultrafast computed tomography. *Am J Cardiol* 1992;70:977-80.
24. Loria CM, Liu K, Lewis CE, et al. Early adult risk factor levels and subsequent coronary artery calcification: the CARDIA Study. *J Am Coll Cardiol* 2007;49:2013-20.
25. Jockel KH, Lehmann N, Jaeger BR, et al. Smoking cessation and subclinical atherosclerosis--results from the Heinz Nixdorf Recall Study. *Atherosclerosis* 2009;203:221-7.
26. Howard G, Burke GL, Szklo M, et al. Active and passive smoking are associated with increased carotid wall thickness. The Atherosclerosis Risk in Communities Study. *Arch Intern Med* 1994;154:1277-82.
27. Howard G, Wagenknecht LE, Burke GL, et al. Cigarette smoking and progression of atherosclerosis: The Atherosclerosis Risk in Communities (ARIC) Study. *JAMA* 1998;279:119-24.
28. Herbert WH. Cigarette smoking and arteriographically demonstrable coronary artery disease. *Chest* 1975;67:49-52.
29. Waters D, Lesperance J, Gladstone P, et al. Effects of cigarette smoking on the angiographic evolution of coronary atherosclerosis. A Canadian Coronary Atherosclerosis Intervention Trial (CCAIT) Substudy. CCAIT Study Group. *Circulation* 1996;94:614-21.
30. Rosenberg L, Kaufman DW, Helmrich SP, et al. The risk of myocardial infarction after quitting smoking in men under 55 years of age. *N Engl J Med* 1985;313:1511-4.
31. Naghavi M, Libby P, Falk E, et al. From vulnerable plaque to vulnerable patient: a call for new definitions and risk assessment strategies: Part I. *Circulation* 2003;108:1664-72.
32. Hioki H, Aoki N, Kawano K, et al. Acute effects of cigarette smoking on platelet-dependent thrombin generation. *Eur Heart J* 2001;22:56-61.
33. Sambola A, Osende J, Hathcock J, et al. Role of risk factors in the modulation of tissue factor activity and blood thrombogenicity. *Circulation* 2003;107:973-7.
34. Burke AP, Farb A, Malcom GT, et al. Coronary risk factors and plaque morphology in men with coronary disease who died suddenly. *N Engl J Med* 1997;336:1276-82.
35. Hung J, Lam JY, Lacoste L, et al. Cigarette smoking acutely increases platelet thrombus formation in patients with coronary artery disease taking aspirin. *Circulation* 1995;92:2432-6.
36. Quillen JE, Rossen JD, Oskarsson HJ, et al. Acute effect of cigarette smoking on the coronary circulation: constriction of epicardial and resistance vessels. *J Am Coll Cardiol* 1993;22:642-7.
37. van Berkel TF, Boersma H, Roos-Hesselink JW, et al. Impact of smoking cessation and smoking interventions in patients with coronary heart disease. *Eur Heart J* 1999;20:1773-82.
38. Gordon T, Kannel WB, McGee D, et al. Death and coronary attacks in men after giving up cigarette smoking. A report from the Framingham study. *Lancet* 1974;2:1345-8.
39. Glantz SA, Parmley WW. Passive smoking and heart disease. Mechanisms and risk. *JAMA* 1995;273:1047-53.
40. Wells AJ. Passive smoking as a cause of heart disease. *J Am Coll Cardiol* 1994;24:546-54.
41. Wells AJ. Heart disease from passive smoking in the workplace. *J Am Coll Cardiol* 1998;31:1-9.
42. Steenland K, Thun M, Lally C, et al. Environmental tobacco smoke and coronary heart disease in the American Cancer Society CPS-II cohort. *Circulation* 1996;94:622-8.
43. Hausleiter J, Meyer T, Hadamitzky M, et al. Radiation dose estimates from cardiac multislice computed tomography in daily practice: impact of different scanning protocols on effective dose estimates. *Circulation* 2006;113:1305-10.

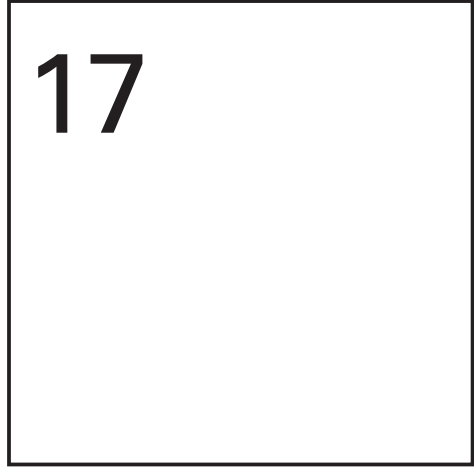
44. Hsieh J, Londt J, Vass M, et al. Step-and-shoot data acquisition and reconstruction for cardiac x-ray computed tomography. *Med Phys* 2006;33:4236-48.
45. Husmann L, Valenta I, Gaemperli O, et al. Feasibility of low-dose coronary CT angiography: first experience with prospective ECG-gating. *Eur Heart J* 2008;29:191-7.
46. Rybicki FJ, Otero HJ, Steigner ML, et al. Initial evaluation of coronary images from 320-detector row computed tomography. *Int J Cardiovasc Imaging* 2008;24:535-46.
47. Herzog BA, Husmann L, Burkhard N, et al. Accuracy of low-dose computed tomography coronary angiography using prospective electrocardiogram-triggering: first clinical experience. *Eur Heart J* 2008;29:3037-42.
48. Herzog BA, Wyss CA, Husmann L, et al. First Head-to-Head Comparison of Effective Radiation Dose from Low-Dose CT with Prospective ECG-Triggering versus Invasive Coronary Angiography. *Heart* 2009;95:1656-61.

Part 3



Future perspectives

Chapter 17



Myocardial perfusion imaging to assess ischemia using multislice computed tomography

Abstract

Multi-slice computed tomography (MSCT) coronary angiography is an accurate non-invasive imaging technique, but cannot determine the functional relevance of the lesions it detects. However, MSCT perfusion imaging can detect the presence of myocardial infarction during rest and can assess viability using delayed enhancement. With recent developments in MSCT scanner technology it has become possible to image myocardial perfusion and the capability of MSCT to determine the presence of ischemia through perfusion imaging during stress is currently investigated. Although only limited data are available, non-invasive imaging with MSCT has the potential to assess both coronary anatomy and myocardial perfusion in one procedure. This review describes the feasibility of myocardial perfusion imaging using MSCT and its potential use in clinical practice.

Introduction

Imaging plays an important role in the diagnosis of coronary artery disease (CAD). In the last decades several non-invasive techniques such as single photon emission computed tomography (SPECT), MRI and contrast echocardiography have become readily available to assess myocardial perfusion in order to demonstrate the presence of ischemia. In recent years, non-invasive assessment of cardiac anatomy has also become possible with the introduction of multi-slice computed tomography (MSCT). MSCT coronary angiography (MSCTA) has emerged as an accurate and robust imaging technique,¹⁻⁴ which is able to detect the presence of atherosclerosis at an early stage and can accurately rule out the presence of significant CAD.⁵ However, when significant CAD is detected, MSCTA is unable to assess the hemodynamic consequences, i.e. the effect on myocardial perfusion.⁶⁻⁹ Accordingly, treatment decisions remain uncertain in case of a positive MSCTA as information on the presence of ischemia is needed.

The combination of this important limitation and recent progress in scan technology has renewed interest in the innovation of MSCT perfusion imaging. This review describes the feasibility and technical aspects of myocardial perfusion imaging using state of the art MSCT. In addition, the currently available evidence and its potential use in clinical practice will be discussed.

Feasibility of myocardial perfusion imaging using MSCT

CT perfusion imaging is based on myocardial tissue attenuation changes during the infusion of contrast medium. The ability to assess myocardial perfusion using CT technology was first studied around 1980.^{10, 11} Following this breakthrough, others have studied CT perfusion imaging using electron beam computed tomography (EBCT) scanners first in animal models,¹²⁻¹⁴ and later in humans.^{15,16} The introduction of MSCT scanning technology resulted in a higher spatial resolution and enabled increasingly larger volume coverage in shortened acquisition times. With each new generation MSCT scanner the number of detectors increased, from 4 to 16 to 64, and up to 320 with the current state of the art systems. These advancements have enabled fast acquisition of coronary anatomy, and may also allow reliable visualization of myocardial perfusion. Moreover, because of its high spatial resolution MSCT perfusion imaging may even allow assessment of transmural perfusion.

MSCT acquisition techniques for perfusion imaging

Depending on the scanner system, different protocols can be applied to assess myocardial perfusion. Early studies have used a dynamic imaging protocol for absolute quantification of myocardial perfusion. With dynamic imaging the table is fixed and image data are acquired during the entire infusion of contrast. By measuring the changes in tissue attenuation over time, attenuation curves of the myocardium can be calculated. (Figure 1, panel A) In a recent study by George et al. myocardial perfusion was quantified in 6 mongrel dogs using dynamic 64-slice MSCT.¹⁷ The authors employed two methods to quantify myocardial perfusion. The first approach was a semi-quantitative method based on the upslope of the time attenuation

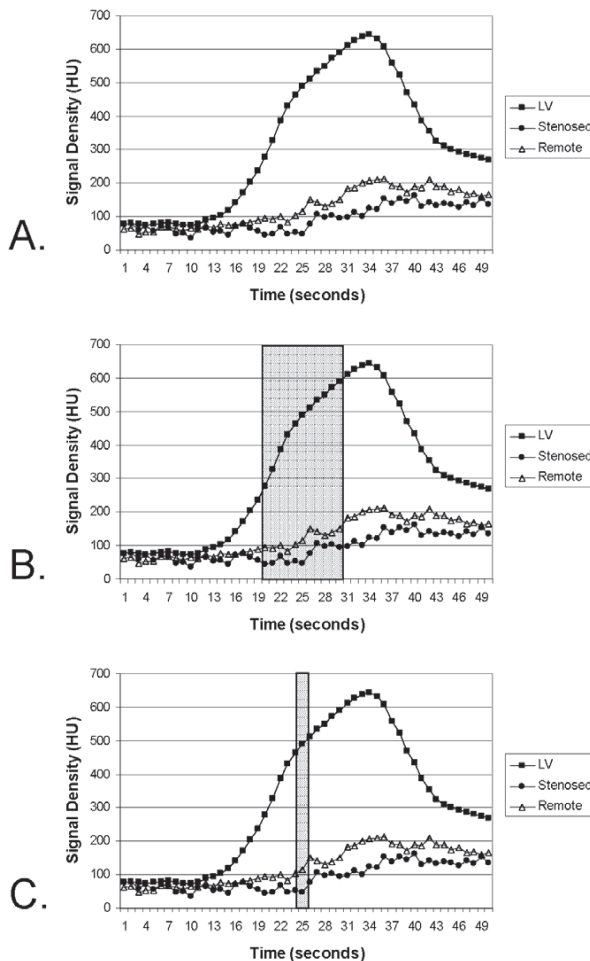


Figure 1. MSCT signal density time curves during infusion of adenosine and iodinated contrast agent using a dynamic imaging approach (panel A). The highlighted regions in panels A and B illustrate the acquisition window of retrospective ECG gated 64-slice helical scanning mode (panel B) and the acquisition window for prospective ECG gated 320-slice volumetric scanning mode (panel C). Adapted and reprinted with permission from reference 17.

curves of ischemic myocardium, normalized for the arterial/input function by dividing myocardial upslope by the left ventricular blood flow upslope or the upslope in a remote myocardial region. With the second approach the authors aimed to perform absolute quantification of myocardial blood flow by combining the time attenuation curves in a model representing the blood tissue exchange in the myocardium. Both methods resulted in an excellent correlation with microsphere derived myocardial blood flow. Although dynamic MSCT allows quantification of myocardial blood flow it is dependant on a prolonged acquisition time which is associated with a high radiation dose. Furthermore dynamic imaging with the current industry standard 64-slice MSCT only provides limited coverage; selected slices are acquired rather than the entire heart which limits its clinical utility.

A second approach to myocardial perfusion imaging with MSCT is ECG gated helical scanning or spiral imaging. This approach is currently used in 64-slice MSCTA protocols and can be used to cover a large area by moving the table slowly through the MSCT tube during acquisition of several heart beats. By gating the images to the ECG, it is possible to create reconstructions of the entire heart during different phases of the R-R interval. By selecting a phase with the least motion the heart can essentially be 'frozen' allowing motion free assessment of the coronary arteries but also of myocardial perfusion. With helical scanning data acquisition is started when a sufficiently high concentration of contrast agent has reached the coronary arteries. As a result, myocardial perfusion can be assessed with this approach only during the upslope of the contrast infusion and at the peak of contrast enhancement. (Figure 1, panel B) The cardiac reconstructions that are derived in this manner combine the information obtained from different heart beats, therefore absolute quantification is not possible. However myocardial perfusion may be assessed semi-quantitatively by measuring myocardial signal density in hypoenhanced regions of the myocardium and normalizing it to the signal density in remote myocardial segments or the left ventricular cavity.¹⁸ This approach results in a signal density ratio which has been shown to correlate very well with microsphere derived blood flow measurements in animal models. Helical scanning enables larger coverage and reduces the scan time and therefore the radiation dose as compared to dynamic imaging. Nevertheless, imaging is still performed during several heart beats resulting in attenuation variations between base and apex. Furthermore helical scanning employs a considerable overlap; accordingly, radiation exposure remains substantial with this technique.

With the introduction of the novel 256- and 320-slice MSCT scanners, allowing true volumetric imaging, the difficulties associated with dynamic and helical scanning using current 64-slice scanners may be eliminated.¹⁹⁻²² These state-of-the-art scanners have sufficient coverage to scan the entire heart within a single rotation. Through scanning in a dynamic mode, myocardial perfusion of the entire ventricle can be quantified. Furthermore, a full volume scan of the heart can be performed within a single heart beat, thereby reducing scan

time and radiation dose compared to helical scanning. The implementation of prospective ECG-triggering allows further reduction in radiation dose by scanning only during a small part of the R-R interval. The short scan time also results in more homogenous attenuation of the myocardium. With this new technique myocardial perfusion can be assessed during the upslope of contrast infusion by comparing uptake in stenosed and remote regions either visually, or semi-quantitatively using signal density ratios (Figure 1, panel C).^{23, 24}

Rest and stress imaging

Assessment of myocardial perfusion at rest has been performed in animals and humans in several studies using first pass perfusion to determine the presence of resting perfusion defects indicating myocardial infarction.²⁵⁻³⁰ Hypodense areas during arterial phase CT imaging may represent viable as well as necrotic myocardium. A distinction between viable and necrotic myocardium may however be made using delayed enhancement imaging.³¹⁻³⁴ In a study by Henneman et al. MSCT perfusion imaging was compared to SPECT imaging in 69 patients with previous infarction, of which 62 (90%) displayed a perfusion defect on SPECT.²⁵ The presence of hypoenhanced regions was identified on MSCT in all 62 patients. Nieman et al. showed that MSCT can also accurately detect late enhanced regions in a comparative study with MRI.³⁴

Only few studies have evaluated stress imaging protocols for detection of inducible perfusion defects. In the previously mentioned studies by George et al. in dogs,^{17,18} MSCT was able to assess ischemia during hyperemia in comparison to microsphere derived myocardial blood flow both quantitatively in dynamic mode as well as semi-quantitatively in helical scan mode. When using the semi-quantitative approach, mean myocardial signal density was significantly lower in stenosed (92.3 ± 39.5 HU) versus remote myocardium (180.04 ± 41.9), and a significant linear relationship was observed between the signal density ratio on MSCT and microsphere derived myocardial blood flow in both stenosed and remote territories within the clinically important range of flows (<8 ml/g/min). Importantly, further research is needed to assess the accuracy of flow measurements also at lower ranges. An example of a myocardial perfusion abnormality observed on MSCT is shown in Figure 2. Recently, reports have been published on the feasibility of stress/rest myocardial perfusion imaging with MSCT in humans.^{23, 35, 36} Kurata et al. performed a study in 12 patients undergoing both stress and rest perfusion imaging using 16-slice MSCT.³⁶ Myocardial perfusion was visually assessed and compared to SPECT. The authors observed an agreement of 83% between the MSCT and SPECT perfusion scans. In preliminary work by George et al. myocardial perfusion was assessed during rest and stress using a prototype 256-slice MSCT scanner.²⁴ Myocardial perfusion was quantified by comparing the attenuation values between sub-endocardial and subepicardial regions. This resulted in a transmural perfusion ratio which accurately detected the presence of significant CAD as compared to SPECT.

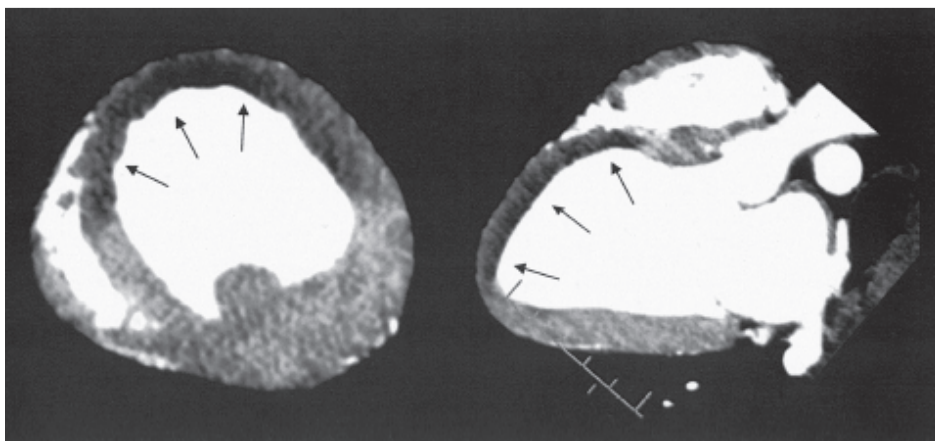


Figure 2. An example of a perfusion defect observed on MSCT using a helical acquisition mode. The stenosis in the left anterior descending coronary artery results in a perfusion defect of the anteroseptal, anterior, and anterolateral wall of the myocardium (arrows) as observed in the axial slice in panel A. In the long axis multi-planar reconstruction in panel B, the perfusion defect extends from the anteroseptal wall to the apex. Reprinted with permission from reference 17.

Alternative approaches

In preliminary studies with dual source CT myocardial tissue iodine content could be evaluated by using two detectors with different X ray spectra. Ruzsics et al showed in 35 patients with suspected or known CAD a good correlation between observations on MSCT and SPECT data.³⁷ A limitation of dual source CT technology however is the lack of cardiac coverage which may result in longer scan time with increased risk of contrast variations from base to apex. Another approach to perfusion imaging is the use of perfusion weighted color maps. Although they do not represent true perfusion imaging, they provide a surrogate of perfusion and enhance the ability to detect perfusion deficits.³⁸ Future research is however needed to further develop these techniques and establish their feasibility in clinical practice.

Potential clinical implications

Although only limited data are available, the studies that have been performed illustrate the potential of MSCT perfusion imaging. Because of its high spatial resolution and fast acquisition time MSCT may potentially have an advantage over conventional perfusion imaging using SPECT. Furthermore the ability to investigate patients with metal implants provides an advantage over MR perfusion imaging. Potentially, MSCT may serve as an alternative myocardial perfusion imaging technique in patients with contraindications to MRI. However, the major advantage of MSCT perfusion imaging may be the ability to combine perfusion with anatomy. This could allow comprehensive assessment of coronary anatomy and perfusion

during a single imaging procedure. With the use of new generation wide coverage scanners and prospectively triggered scan protocols, myocardial perfusion can potentially be assessed semi-quantitatively in combination with MSCTA with an acceptable radiation dose.³⁹ Such an integrated imaging approach has several advantages for the diagnosis and potentially the prognosis of CAD.

Complementary value for diagnosis of CAD

Anatomic and functional imaging modalities provide complementary information as has been demonstrated by previous studies comparing MSCTA to conventional perfusion imaging using SPECT.⁶⁻⁹ In the study by Schuijff et al., only 50% of patients with a significant (>50%) lesion on MSCTA had an abnormal perfusion on SPECT.⁹ Conversely, normal perfusion on SPECT was unable to rule out the presence of significant CAD or atherosclerosis in general. (Figure 3) The combination of anatomic and functional imaging in a single procedure may facilitate patient management. Patients with normal coronary anatomy without perfusion abnormalities can be discharged, while patients with significant CAD and abnormal perfusion may be directly referred for conventional coronary angiography followed by revascularization. Finally, those with (significant) atherosclerosis but without evidence of perfusion abnormalities will most likely benefit from risk factor modification and strict control at the

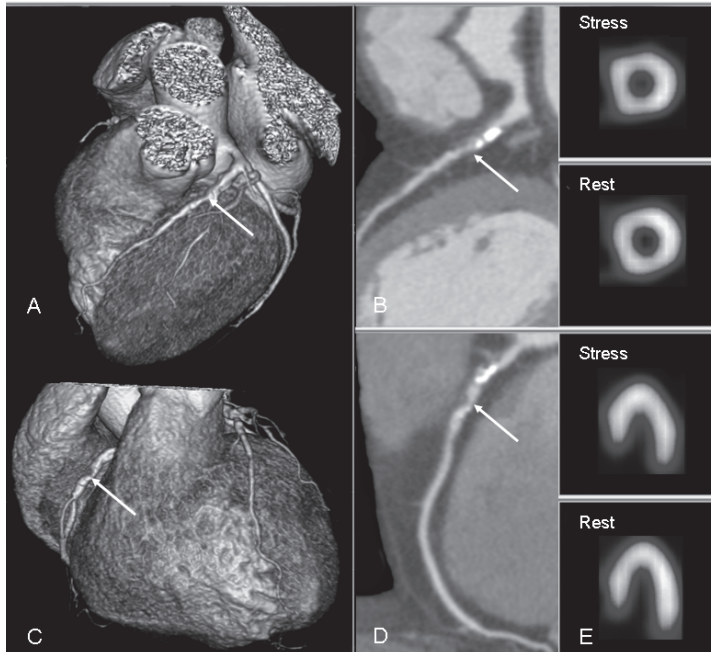


Figure 3. Case example of a patient with significant atherosclerotic lesions in both the left anterior descending coronary artery (arrows panels A, and B) as well as in the right coronary artery (arrows panels C, and D), while normal myocardial perfusion was observed (panel E).

outpatient clinic. Although improved management has not yet been proven, initial data support the notion that combined assessment of anatomy and perfusion may result in a higher diagnostic accuracy for the detection of hemodynamically significant coronary artery lesions.⁴⁰ By fusing both anatomic and perfusion datasets into a single, three-dimensional anatomic representation of the heart with overlying coronary anatomy, diagnostic accuracy may also improve on a vessel basis. This approach may enable accurate allocation of perfusion defects to the corresponding arteries. Gaemperli et al. assessed the accuracy of cardiac image fusion by combining MSCTA and SPECT.⁴¹ The authors concluded that in almost one third of patients, fusion of MSCTA and SPECT provided additional diagnostic information, especially in functionally relevant lesions in distal segments and diagonal branches and in vessels with extensive disease or calcifications. Fusion of MSCTA and MSCT perfusion datasets may provide similar information with higher accuracy as misalignment between datasets will occur less frequently.

Complementary value for prognosis

MSCT is a relatively new imaging technique. So far only limited studies are available assessing the prognostic value of MSCTA. Preliminary work by Pundziute et al. and by Min et al. has shown promising results.^{42, 43} The presence of significant CAD is associated with an increased risk for cardiac events, while a completely normal MSCTA confers a very low risk. Conversely, perfusion imaging using SPECT has been well validated for risk stratification, and can accurately distinguish between patients at low and high risk for future cardiac events.⁴⁴⁻⁴⁶ As MSCT and SPECT provide complementary information about the presence and extent of CAD, it is intuitively expected that their combined use may further improve risk stratification.⁴⁷ Although no prognostic data are available, combined assessment of myocardial perfusion imaging and coronary anatomy with MSCT may also provide increased risk stratification compared to the use of MSCTA or MSCT perfusion imaging alone.

Limitations

Several issues need to be resolved before MSCT perfusion imaging can be added to MSCTA in clinical practice. An important issue is radiation dose. Dynamic mode scanning is attractive since it allows quantification of myocardial blood flow, but is associated with a high radiation dose. Therefore imaging during first pass infusion of contrast using a semi-quantitative approach will probably be more feasible as exposure time and resulting radiation dose is less. Further developments in wide coverage scanners and prospective ECG-triggering, can potentially reduce the radiation dose to 7-11 mSv for combined perfusion and coronary angiography imaging.³⁹

Secondly, when combining MSCTA with perfusion imaging, the combination of beta blockade - which is frequently required for MSCTA - and pharmacological stress needed for stress imaging may pose a problem. The use of beta blockers may alter the resting and hyperemic myocardial blood flow resulting in increased myocardial flow reserve, which may decrease the sensitivity for the detection of myocardial ischemia.^{48, 49} Furthermore MSCTA will be less reliable during stress imaging as image quality decreases with increasing heart rates.

Finally a general limitation of MSCT is its limited temporal resolution, which can result in motion artefacts in the myocardium that can be mistaken for perfusion deficits. Other artefacts that may be observed are those caused by beam hardening. To circumvent this problem, extensive effort is currently invested to develop and validate beam hardening correction algorithms.⁵⁰ Furthermore temporal resolution has increased with dual source CT technology.^{51, 52}

Conclusion

With the introduction of wide volume scanners enabling prospective ECG-triggering, MSCT perfusion imaging has become increasingly feasible. MSCT has the potential to visualize myocardial perfusion during rest and stress in combination with anatomic assessment of the coronary arteries. This may enable use of MSCT as a “one stop shop” for the diagnosis and potentially the prognosis of CAD. However, before MSCT perfusion imaging can be implemented in clinical practice, more clinical data are needed.

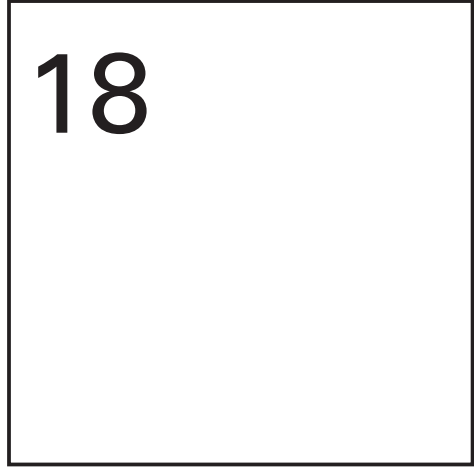
References

1. Leschka S, Alkadhi H, Plass A et al. Accuracy of MSCT coronary angiography with 64-slice technology: first experience. *Eur Heart J* 2005;26:1482-7.
2. Mollet NR, Cademartiri F, Van Mieghem CA et al. High-resolution spiral computed tomography coronary angiography in patients referred for diagnostic conventional coronary angiography. *Circulation* 2005;112:2318-23.
3. Raff GL, Gallagher MJ, O'Neill WW, et al. Diagnostic accuracy of noninvasive coronary angiography using 64-slice spiral computed tomography. *J Am Coll Cardiol* 2005;46:552-7.
4. Schuijf JD, Pundziute G, Jukema JW et al. Diagnostic accuracy of 64-slice multislice computed tomography in the noninvasive evaluation of significant coronary artery disease. *Am J Cardiol* 2006;98:145-8.
5. Henneman MM, Schuijf JD, van Werkhoven JM et al. Multi-slice computed tomography coronary angiography for ruling out suspected coronary artery disease: what is the prevalence of a normal study in a general clinical population? *Eur Heart J* 2008;29:2006-13.
6. Gaemperli O, Schepis T, Koepfli P et al. Accuracy of 64-slice CT angiography for the detection of functionally relevant coronary stenoses as assessed with myocardial perfusion SPECT. *Eur J Nucl Med Mol Imaging* 2007;34:1162-71.
7. Gaemperli O, Schepis T, Valenta I et al. Functionally Relevant Coronary Artery Disease: Comparison of 64-Section CT Angiography with Myocardial Perfusion SPECT. *Radiology* 2008;248:414-23.
8. Hacker M, Jakobs T, Hack N et al. Sixty-four slice spiral CT angiography does not predict the functional relevance of coronary artery stenoses in patients with stable angina. *Eur J Nucl Med Mol Imaging* 2007;34:4-10.
9. Schuijf JD, Wijns W, Jukema JW et al. Relationship between noninvasive coronary angiography with multi-slice computed tomography and myocardial perfusion imaging. *J Am Coll Cardiol* 2006;48:2508-14.
10. Scanlan JG, Gustafson DE, Chevalier PA, et al. Evaluation of ischemic heart disease with a prototype volume imaging computed tomographic (CT) scanner: preliminary experiments. *Am J Cardiol* 1980;46:1263-8.
11. Adams DF, Hessel SJ, Judy PF, et al. Differing attenuation coefficients of normal and infarcted myocardium. *Science* 1976;192:467-9.
12. Gould RG, Lipton MJ, McNamara MT, et al. Measurement of regional myocardial blood flow in dogs by ultrafast CT. *Invest Radiol* 1988;23:348-53.
13. Rumberger JA, Feiring AJ, Lipton MJ, et al. Use of ultrafast computed tomography to quantitate regional myocardial perfusion: a preliminary report. *J Am Coll Cardiol* 1987;9:59-69.
14. Wolfkiel CJ, Ferguson JL, Chomka EV et al. Measurement of myocardial blood flow by ultrafast computed tomography. *Circulation* 1987;76:1262-73.
15. Bell MR, Lerman LO, Rumberger JA. Validation of minimally invasive measurement of myocardial perfusion using electron beam computed tomography and application in human volunteers. *Heart* 1999;81:628-35.
16. Ludman PF, Coats AJ, Burger P et al. Validation of measurement of regional myocardial perfusion in humans by ultrafast x-ray computed tomography. *Am J Card Imaging* 1993;7:267-79.
17. George RT, Jerosch-Herold M, Silva C et al. Quantification of myocardial perfusion using dynamic 64-detector computed tomography. *Invest Radiol* 2007;42:815-22.
18. George RT, Silva C, Cordeiro MA et al. Multidetector computed tomography myocardial perfusion imaging during adenosine stress. *J Am Coll Cardiol* 2006;48:153-60.
19. Kido T, Kurata A, Higashino H et al. Cardiac imaging using 256-detector row four-dimensional CT: preliminary clinical report. *Radiat Med* 2007;25:38-44.

20. Kondo C, Mori S, Endo M et al. Real-time volumetric imaging of human heart without electrocardiographic gating by 256-detector row computed tomography: initial experience. *J Comput Assist Tomogr* 2005;29:694-8.
21. Mori S, Kondo C, Suzuki N et al. Volumetric cine imaging for cardiovascular circulation using prototype 256-detector row computed tomography scanner (4-dimensional computed tomography): a preliminary study with a porcine model. *J Comput Assist Tomogr* 2005;29:26-30.
22. Rybicki FJ, Otero HJ, Steigner ML et al. Initial evaluation of coronary images from 320-detector row computed tomography. *Int J Cardiovasc Imaging* 2008;24:535-46.
23. George RT, Lardo AC, Kitagawa K et al. Combined Perfusion and Non-Invasive Coronary Angiography in Patients with Suspected Coronary Disease using 256 Row, 0.5 mm Slice Thickness Non-Helical Multi-Detector Computed Tomography. Presented at: American Heart Association Scientific Sessions. Orlando, FL, USA, 4-7 November 2007.
24. George RT, Yousuf O, Kitagawa K et al. Quantification of Myocardial Perfusion in Patients Using 256-Row Multidetector Computed Tomography: Evaluation of Endocardial vs. Epicardial Blood Flow. Presented at: American Heart Association Scientific Sessions. Orlando, FL, USA, 4-7 November 2007.
25. Henneman MM, Schuijf JD, Dibbets-Schneider P et al. Comparison of multislice computed tomography to gated single-photon emission computed tomography for imaging of healed myocardial infarcts. *Am J Cardiol* 2008;101:144-8.
26. Hoffmann U, Millea R, Enzweiler C et al. Acute myocardial infarction: contrast-enhanced multi-detector row CT in a porcine model. *Radiology* 2005;231:697-701.
27. Mahnken AH, Bruners P, Katoh M, et al. Dynamic multi-section CT imaging in acute myocardial infarction: preliminary animal experience. *Eur Radiol* 2006;16:746-52.
28. Nieman K, Cury RC, Ferencik M et al. Differentiation of recent and chronic myocardial infarction by cardiac computed tomography. *Am J Cardiol* 2006;98:303-8.
29. Nikolaou K, Sanz J, Poon M et al. Assessment of myocardial perfusion and viability from routine contrast-enhanced 16-detector-row computed tomography of the heart: preliminary results. *Eur Radiol* 2005;15:864-71.
30. Sanz J, Weeks D, Nikolaou K et al. Detection of healed myocardial infarction with multidetector-row computed tomography and comparison with cardiac magnetic resonance delayed hyperenhancement. *Am J Cardiol* 2006;98:149-55.
31. Habis M, Capderou A, Ghostine S et al. Acute myocardial infarction early viability assessment by 64-slice computed tomography immediately after coronary angiography: comparison with low-dose dobutamine echocardiography. *J Am Coll Cardiol* 2007;49:1178-85.
32. Lardo AC, Cordeiro MA, Silva C et al. Contrast-enhanced multidetector computed tomography viability imaging after myocardial infarction: characterization of myocyte death, microvascular obstruction, and chronic scar. *Circulation* 2006;113:394-404.
33. Mahnken AH, Koos R, Katoh M et al. Assessment of myocardial viability in reperfused acute myocardial infarction using 16-slice computed tomography in comparison to magnetic resonance imaging. *J Am Coll Cardiol* 2005;45:2042-7.
34. Nieman K, Shapiro MD, Ferencik M et al. Reperfused myocardial infarction: contrast-enhanced 64-Section CT in comparison to MR imaging. *Radiology* 2008;247:49-56.
35. Kido T, Kurata A, Higashino H et al. Quantification of regional myocardial blood flow using first-pass multidetector-row computed tomography and adenosine triphosphate in coronary artery disease. *Circ J* 2008;72:1086-91.
36. Kurata A, Mochizuki T, Koyama Y et al. Myocardial perfusion imaging using adenosine triphosphate stress multi-slice spiral computed tomography: alternative to stress myocardial perfusion scintigraphy. *Circ J* 2005;69:550-7.
37. Ruzsics B, Lee H, Zwerner PL, et al. Dual-energy CT of the heart for diagnosing coronary artery stenosis and myocardial ischemia-initial experience. *Eur Radiol* 2008;18:2414-24.

38. Mahnken AH, Lautenschlager S, Fritz D, et al. Perfusion weighted color maps for enhanced visualization of myocardial infarction by MSCT: preliminary experience. In *J Cardiovasc Imaging* 2008;24:883-90.
39. George RT, Lima JA. Radiation Dose Measurements on Subjects Undergoing Combined CT Perfusion and CT Angiography Imaging with a Prototype 256-row MDCT Scanner Presented at: American Heart Association Scientific Sessions. Orlando, FL, USA, 4-7 November 2007.
40. Rispler S, Keidar Z, Ghersin E et al. Integrated single-photon emission computed tomography and computed tomography coronary angiography for the assessment of hemodynamically significant coronary artery lesions. *J Am Coll Cardiol* 2007;49:1059-67.
41. Gaemperli O, Schepis T, Valenta I et al. Cardiac image fusion from stand-alone SPECT and CT: clinical experience. *J Nucl Med* 2007;48:696-703.
42. Min JK, Shaw LJ, Devereux RB et al. Prognostic value of multidetector coronary computed tomographic angiography for prediction of all-cause mortality. *J Am Coll Cardiol* 2007;50:1161-70.
43. Pundziute G, Schuijff JD, Jukema JW et al. Prognostic value of multislice computed tomography coronary angiography in patients with known or suspected coronary artery disease. *J Am Coll Cardiol* 2007;49:62-70.
44. Elhendy A, Schinkel A, Bax JJ, et al. Long-term prognosis after a normal exercise stress Tc-99m sestamibi SPECT study. *J Nucl Cardiol* 2003;10:261-6.
45. Hachamovitch R, Berman DS, Kiat H et al. Exercise myocardial perfusion SPECT in patients without known coronary artery disease: incremental prognostic value and use in risk stratification. *Circulation* 1996;93:905-14.
46. Shaw LJ, Iskandrian AE. Prognostic value of gated myocardial perfusion SPECT. *J Nucl Cardiol* 2004;11:171-85.
47. van Werkhoven JM, Schuijff JD, Gaemperli O et al. Prognostic Value of Multi-Slice Computed Tomography and Gated Single Photon Emission Computed Tomography in a Cohort of 426 Patients with Known or Suspected Coronary Artery Disease. Presented at: American Heart Association Scientific Sessions. Orlando, FL, USA, 4-7 November 2007.
48. Bottcher M, Czernin J, Sun K, et al. Effect of beta 1 adrenergic receptor blockade on myocardial blood flow and vasodilatory capacity. *J Nucl Med* 1997;38:442-6.
49. Koepfli P, Wyss CA, Namdar M et al. Beta-adrenergic blockade and myocardial perfusion in coronary artery disease: differential effects in stenotic versus remote myocardial segments. *J Nucl Med* 2004;45:1626-31.
50. Kitagawa K, George RT et al. Myocardial Perfusion Assessment Using Dynamic-mode 256-Row Multidetector Computed Tomography: Influence of Beam Hardening Correction. Presented at: The annual meeting of the Society of Cardiovascular Computed Tomography. Orlando, FL, USA, 17-20 July 2008.
51. Ropers U, Ropers D, Pflederer T et al. Influence of heart rate on the diagnostic accuracy of dual-source computed tomography coronary angiography. *J Am Coll Cardiol* 2007;50:2393-8.
52. Weustink AC, Meijboom WB, Mollet NR et al. Reliable high-speed coronary computed tomography in symptomatic patients. *J Am Coll Cardiol* 2007;50:786-94.

Chapter 18



Diastolic heart function assessed with MDCT:
feasibility study in comparison with tissue
doppler

MJ Boogers, JM van Werkhoven, JD Schuijf, V Delgado, G Nucifora,
RJ van der Geest, LJ Kroft, JHC Reiber, A de Roos, JJ Bax, HJ Lamb

Abstract

Diastolic left ventricular (LV) function plays an important role in patients with cardiovascular disease. Currently, 2D echocardiography using TDI has been used most commonly to evaluate diastolic LV function. Although the role of MDCT imaging for evaluation of coronary atherosclerosis has been explored extensively, its feasibility to evaluate diastolic function has not been studied. The purpose of this study was to demonstrate the feasibility of multidetector row computed tomography (MDCT) for assessment of diastolic function in comparison with 2-dimensional (2D) echocardiography using tissue Doppler imaging (TDI). Seventy patients who had undergone 64-MDCT and 2D echocardiography with TDI were enrolled. Diastolic function was evaluated using early (E) and late (A) transmitral peak velocity (cm/s) and peak mitral septal tissue velocity (Ea) (cm/s). Peak transmitral velocity (cm/s) was calculated by dividing peak diastolic transmitral flow (mL/s) by the corresponding mitral valve area (cm²). Mitral septal tissue velocity was calculated from changes in LV length per cardiac phase. Subsequently, the estimation of LV filling pressures (E/Ea) was determined. Good correlations were observed between MDCT and 2D echocardiography for assessment of E ($r=0.73$, $p<0.01$), E/A ($r=0.87$, $p<0.01$), Ea ($r=0.82$, $p<0.01$) and E/Ea ($r=0.88$, $p<0.01$). Moreover, a good diagnostic accuracy was found for detection of diastolic dysfunction using MDCT (79%). In conclusion, MDCT imaging is a feasible technique to evaluate diastolic LV function. MDCT imaging showed good correlation for the estimation of LV filling pressures when compared to 2D echocardiography. Additionally, a good agreement was found for detection of diastolic dysfunction using MDCT.

Introduction

Diastolic left ventricular (LV) function plays an important role in the evaluation of clinical symptoms, therapeutic options and prognosis in patients with cardiovascular disease.¹⁻⁴ More specifically, it has been shown that diastolic dysfunction represents an important pathological condition in patients with coronary artery disease (CAD).^{5, 6}

Currently, the concept of diastology has been explored with different imaging techniques, wherein Doppler echocardiography represents the most commonly used approach for evaluation of diastolic function.⁷⁻¹² For the evaluation of diastolic function, transmitral velocity has been used frequently as a non-invasive alternative to directly measured LV filling pressures.^{7, 9} However, it is important to note that several confounding factors may influence transmitral velocity and consequently transmitral velocity alone may not be the best marker for diastolic LV dysfunction.^{8, 9, 13} Combined assessment of early peak transmitral velocity and early peak mitral septal tissue velocity may be more accurate for the evaluation of diastolic LV function, predominantly in patients with depressed or increased LV filling pressures.^{8, 12, 13} Multidetector row computed tomography (MDCT) has emerged as a potent non-invasive imaging modality for evaluation of coronary atherosclerosis.^{14, 15} Despite the introduction of prospective triggering techniques to lower the radiation dose, retrospective electrocardiographic gating remains at present the most frequently applied approach to perform cardiac MDCT in clinical practice.¹⁶ Furthermore, it is important to note that prospective triggering can only be performed in selected patients with stable and low heart rates. Accordingly, in a large number of patients MDCT images may still be acquired using retrospective ECG gating to ensure diagnostic image quality of the coronary arteries. Importantly, in these patients, functional analysis can be performed retrospectively without additional image acquisitions.

Thus far, studies have been restricted to LV systolic function analysis,¹⁷ and no information is available on the feasibility of MDCT imaging to assess diastolic LV function. Accordingly, the present study aimed to evaluate the feasibility of MDCT for assessment of diastolic function in a direct comparison with 2D echocardiography using TDI.

Methods

Patient population, study design

Seventy consecutive patients who had been referred for 64-MDCT imaging were retrospectively selected from our clinical registry. MDCT imaging was performed to evaluate known or established CAD, and 2D echocardiography with TDI was performed to evaluate therapeutic options. Both examinations had been performed sequentially, in random order. Known CAD

was defined as previous myocardial infarction, revascularization or evidence of CAD on previous diagnostic tests. Patients without evidence of CAD on previous diagnostic tests were suspected to have CAD (and therefore referred for CT angiography). Study exclusion was based on: (1) poor MDCT image quality (2) absence of Doppler echocardiography examination within 3 months (3) valvulopathy (mitral or aortic valve dysfunction), and (4) (supra) ventricular arrhythmias. Additionally, patients with unstable angina pectoris or acute coronary syndrome were excluded from further analysis. Our Institutional Review Board does not require its approval for retrospective technical analysis of clinically obtained data, as was the case in this study.

MDCT - Data Acquisition and Analysis

MDCT imaging was performed with a 64-slice MDCT scanner (Aquilion 64, Toshiba Medical Systems, Otawara, Japan). Prior to MDCT imaging, patients were monitored for blood pressure and heart rate. Patients with a heart rate ≥ 65 beats/min were given metoprolol 50 or 100 mg orally, unless contra-indicated.

For the contrast-enhanced helical scan, collimation was 64×0.5 mm with a rotation time of 400 ms. Tube current and voltage were 350 mA and 120 kV. At an injection rate of 5 mL/min, 95 to 130 mL of nonionic contrast medium (Iomeron 400; Bracco, Milan, Italy) was infused in the antecubital vein. After start of contrast infusion, recurrent low-dose examinations were performed to monitor contrast arrival within the region of interest, placed in the descending aorta. The electrocardiogram (ECG) gated helical scan was automatically triggered once the predetermined threshold level of baseline +100 Hounsfield units was reached. After a preset delay of 2 seconds, scanning was performed during an inspiratory breath hold of 8 to 12 seconds.

Data were reconstructed with a slice thickness of 1 mm and a reconstruction interval of 1 mm. With the use of half reconstruction algorithms, the actual temporal resolution was 200 milliseconds. Segmented reconstruction algorithms yielded a temporal resolution of up to 50 milliseconds, depending on the actual imaging acquisition conditions (pitch, rotation time and heart rate). ECG-gated post processing software was used for to reconstruct data in short-axis orientation. Images were reconstructed at 20 intervals (0% to 95% of the R-R interval) and transferred to a separate workstation with dedicated cardiac function analysis software (Mass V2008-EXP, LKEB, Leiden, The Netherlands).¹⁸ Contrast-enhanced scans were analyzed by an independent observer who was blinded to all other data. Significant coronary artery stenosis was defined as $\geq 50\%$ luminal narrowing, whereas non-significant stenosis was defined as $< 50\%$ luminal narrowing.

MDCT - Transmitral velocity

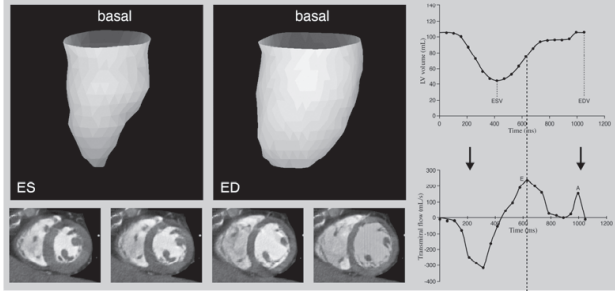
Peak transmitral velocity (cm/s) was measured in early (E) and late (A) diastole. The peak value represents the highest mean value of the measurements obtained during early and late diastole. Late peak transmitral velocity (cm/s) was measured at atrial contraction. Transmitral velocity (cm/s) measurements were based on several processing steps (Figure 1). At first, LV volumes were calculated for 20 cardiac phases (each phase represented 5% of the cardiac cycle). For each phase, automatic contour detection was performed on 1 mm sliced reconstructed short-axis images ranging from mitral valve annulus to the cardiac apex (Figure 1A, left panel). Manual corrections could be made to improve contour detection. Papillary muscles were regarded as part of the LV cavity and were included in the LV volume analyses.¹⁹ Automatic contour detection was performed using dedicated in-house developed MASS research software package (Mass V2008-EXP, LKEB, Leiden, The Netherlands).¹⁸ Next, LV volumes were plotted in a volume versus time curve (Figure 1A, right upper curve). In addition, changes in LV volumes between two consecutive phases (first derivative) were derived and used to calculate the transmitral flow (mL/s) per phase (Figure 1A, right lower curve). Subsequently, the maximal transmitral flow (mL/s) in early and late diastole was derived using the transmitral flow versus time curve. To allow direct comparison with 2D echocardiography, the maximal transmitral flow (mL/s) in early and late diastole was divided by their corresponding mitral valve area (cm²) (which was measured during early and late diastole, as described below), yielding an early and late peak transmitral velocity (cm/s) and the E/A.

MDCT - Mitral septal tissue velocity

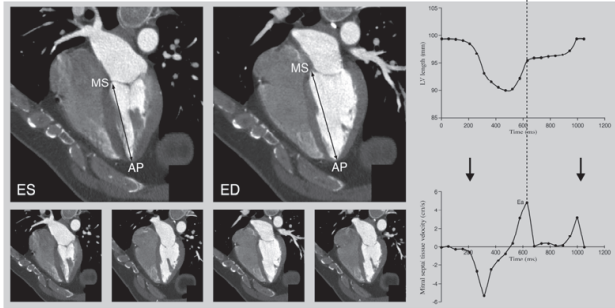
Myocardial tissue velocity (cm/s) was measured at the septal level of the mitral valve annulus attachment. Measurements of peak mitral septal tissue velocity (cm/s) during early diastole (Ea) are illustrated (Figure 1B). For 20 phases, LV length (mm) was calculated as the distance between two anatomical markers, positioned at the mitral septal annulus (MA) and cardiac apex (AP) (Figure 1B, left panel). Anatomical markers were positioned at reconstructed 4-chamber views. Reconstruction of a 4-chamber view was based on several reconstruction steps. At first, a 2-chamber view was reconstructed from axial slices, directing the image slice (cardiac axis) through the cardiac apex. Consecutively, a 4-chamber view was reconstructed by positioning the image slice at two-third of the mitral valve annulus (perpendicular to the interventricular septum) using the 2-chamber view.

The LV length (mm) per phase was plotted in a LV length versus time curve (Figure 1B, right upper panel). Changes in LV length between two consecutive phases were calculated and used to generate a velocity versus time curve (Figure 1B, right lower panel). In this curve, mitral septal tissue velocities were plotted against time. For each phase, mitral septal tissue velocity (cm/s) was computed using changes in LV length and heart rate. The maximal tis-

A. Transmitral Flow



B. Mitral Septal Tissue Velocity



C. Mitral Valve Area

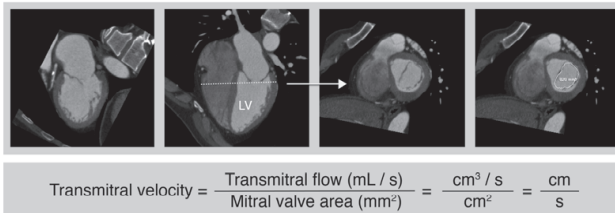


Figure 1. Diastolic left ventricular (LV) function assessed with multidetector row computed tomography (MDCT).

A Transmitral flow. LV volumes (mL) were measured for 20 phases per cardiac cycle. LV volumes (mL) were measured using short-axis images by outlining endocardial contours in each phase. LV volumes (mL) were plotted in a volume versus time curve (right upper panel). These curves were used to define the diastole, ranging from end-systolic (ES) to end-diastolic (ED) phase. Consecutively, changes in LV volumes between two consecutive phases were plotted against time (transmitral flow versus time curve) (right lower curve). Subsequently, early and late peak transmitral flow (mL/s) were derived.

B Mitral septal tissue velocity. Anatomical markers were positioned at the mitral septal annulus (MA) and the cardiac apex (AP). LV length (mm) (the distance between anatomical markers) was calculated for each phase (left panel). The LV length (mm) was plotted in a LV length versus time curve (right upper curve). Next, changes in LV length between two consecutive phases were calculated. Based on these numbers, mitral septal tissue velocities (cm/s) were calculated for each phase (velocity versus time curve, right lower panel). The early peak mitral septal tissue velocity (cm/s) (Ea) represented the maximal tissue velocity during early diastole.

C Mitral valve area. Measurements were performed at the most distal level of the mitral valve leaflets (smallest mitral valve area) using reconstructed images at peak early and late transmitral velocity. LV axis was positioned perpendicular to mid-mitral valve annulus on sagittal and coronal views (left panel), yielding a 2-chamber view (panel 1). Consecutively, the 4-chamber view was reconstructed (panel 2) and mitral valve area was measured at the tip of the leaflets (panels 3 and 4) on short-axis views. To allow direct comparison, transmitral velocity (cm/s) was calculated using the following formula: peak diastolic transmitral flow (mL/s) divided by the corresponding mitral valve area (cm²).

sue velocity (cm/s) during early diastole represented early peak mitral septal tissue velocity (cm/s) (Ea). Measurements were performed using the MASS research software package.¹⁸

Finally, the estimation of LV filling pressures (E/Ea) was calculated by dividing early transmitral velocity (E) (cm/s) by the mitral septal tissue velocity (Ea) (cm/s).

Reproducibility of the mitral septal tissue velocity measurements was evaluated in a subset of 15 patients who were randomly selected from the patient population. Mitral septal tissue velocity was measured twice in the subset of 15 patients according to the standardized protocol, as described above.

MDCT - Mitral valve area

Mitral valve area (cm²) was measured to enable direct comparison of volumetric indices derived from MDCT with velocity-based parameters as assessed with 2D echocardiography. In Figure 1C, the processing steps involved in mitral valve area (cm²) measurements are illustrated. Images were reconstructed with a slice thickness of 0.5 mm and a reconstruction interval of 0.3 mm.

Mitral valve area (cm²) measurements were based on different steps: the LV axis was positioned perpendicular to mid-mitral valve annulus on sagittal and coronal views, yielding a 2-chamber view (panel 1). Subsequently, a 4-chamber view (panel 2) was reconstructed and manual contour detection was performed at the most distal level of the mitral valve leaflets in short-axis views (panel 3 and 4). Measurements were performed during early and late peak transmitral flow (mL/s) using a dedicated workstation (Vitrea 2; Vital Images, Minnetonka, Minnesota, USA).

The mitral valve area (cm²) was calculated to enable direct comparison with 2D echocardiography. Transmitral velocity (cm/s) was calculated by the following formula: transmitral velocity = transmitral flow (mL/s) / corresponding mitral valve area (cm²) (Figure 1). Reproducibility of the mitral valve area measurements was evaluated in a subset of 20 patients who were randomly selected from the patient population. In these patients, the mitral valve area was measured twice using the same processing steps, as described above.

Transthoracic 2D echocardiography using tissue Doppler imaging

Acquisition

Transthoracic 2D echocardiography was performed in left lateral decubitus position using a commercially available system (Vingmed Vivid-7, General Electric, Horten, Norway). Standard parasternal (long- and short-axis) and apical views (2- and 4-chamber) were obtained. In addition, continuous-wave and pulsed-wave Doppler examinations were performed. From the

4-chamber view, TDI was obtained with color Doppler frame rates exceeding 115 frames/second, depending on the sector width of the range of interest. Aliasing velocities varied between 16 and 32 cm/s and resulted from pulse repetition frequencies ranging from 500 Hz and 1 kHz. Echocardiographic analyses were performed by an independent and blinded observer.

2D echocardiography - Transmitral velocity

Transmitral velocity (cm/s) was recorded at the end of respiratory expiration (Figure 2, upper panel). Transmitral velocity (cm/s) measurements were performed using dedicated offline software (EchoPAC 7.0.0.; General Electric, Horten, Norway. Standard pulsed-wave Doppler imaging was performed to assess early (E) and late (A) peak transmitral peak velocity (cm/s). Early and late peak transmitral velocity (cm/s) were used to calculate the E/A. Doppler sample volume was placed at the tip of the mitral valve leaflets, on a 4-chamber view (20). Subsequently, early and late peak transmitral velocities (cm/s) were obtained in diastole.

2D echocardiography - Mitral septal tissue velocity

Early peak mitral septal tissue velocity (cm/s) (Ea) was assessed using color-coded TDI on a 4-chamber view. Images were obtained in end-expiration in a patient in left lateral decubitus position. Doppler velocities (cm/s) were measured from the apical 4-chamber view using a 6x6 mm sample volume positioned at the basal septal mitral valve annulus, as illustrated in Figure 2 (lower panel) (20). Color-coded images from three consecutive heartbeats were analyzed using dedicated offline software (EchoPAC 7.0.0.; General Electric, Horten, Norway). Reliable tissue Doppler curves were obtained in 67 patients.

Detection of diastolic dysfunction

To evaluate the accuracy of MDCT to detect diastolic dysfunction, diastolic function was graded in four categories using the following criteria; normal diastolic function (≥ 1 E/A < 2 and E/Ea ≤ 8), impaired relaxation pattern (diastolic dysfunction grade I) (E/A < 1 and E/Ea ≤ 8), pseudonormal pattern (diastolic dysfunction grade II) (≥ 1 E/A < 2 and ≥ 9 E/Ea ≤ 12) and restrictive filling pattern (diastolic dysfunction grade III) (E/A ≥ 2 and E/Ea ≥ 13).²¹ Based on these criteria, the patient population was divided into two groups; patients with normal diastolic function and patients with diastolic dysfunction (including impaired LV relaxation, pseudonormal and restrictive LV filling pattern).

Statistical analysis

Continuous data are presented as mean \pm standard deviation, and categorical data are presented as absolute numbers or percentages. Comparison of MDCT and 2D echocardiography with TDI was performed using Pearson's linear regression analysis. The 95% limits of agreement were calculated using Bland-Altman analysis that plotted the mean value of differences of each pair against the average value of similar pair of data. MDCT was subtracted from 2D echocardiography

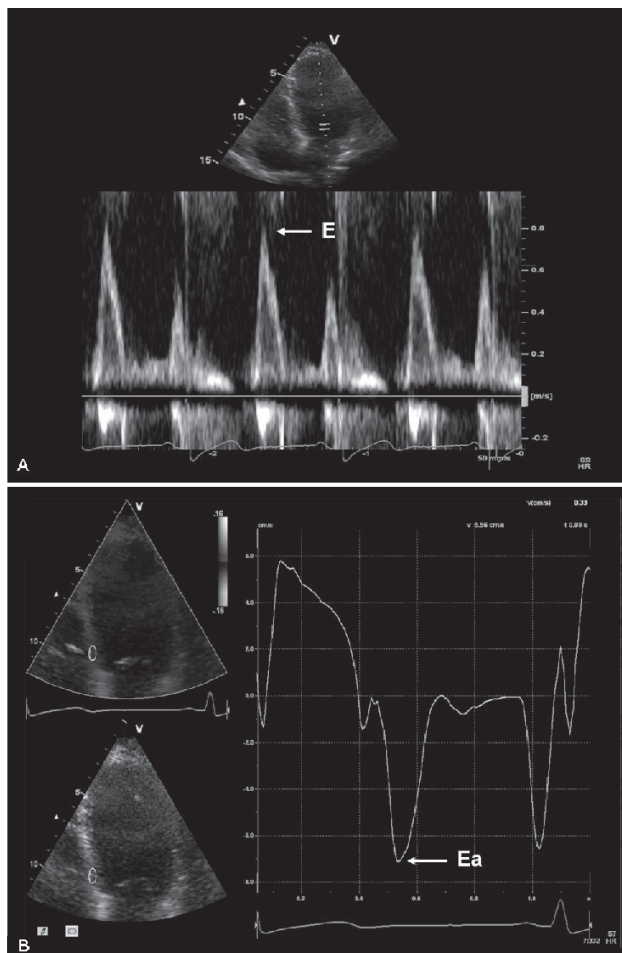


Figure 2. Evaluation of diastolic function with 2-dimensional (2D) echocardiography using tissue Doppler imaging (TDI). 2D echocardiographic assessment of pulsed-wave Doppler of early (E) transmital velocity (cm/s) (panel A) and early diastolic peak mitral septal tissue velocity (cm/s) (Ea) at basal septal segment by TDI (panel B). The E (white arrow, panel A) and Ea (white arrow, panel B) were 0.80 m/s and -7.1 cm/s. Accordingly, the E/Ea was 11.27.

with TDI as the latter was considered the clinical standard. Reproducibility was evaluated by calculating the intraclass correlation coefficients (ICC) and an excellent agreement was defined as an ICC >0.8. Diagnostic accuracy of MDCT for detection of diastolic dysfunction was assessed using a binary approach; normal diastolic function and diastolic dysfunction (including impaired LV relaxation, pseudonormal and restrictive LV filling pattern). Corresponding sensitivity and specificity values were calculated. For these values, the 95% confidence intervals (CI) were calculated using the following formula: $p \pm 1.96 \times \text{standard error (SE)}$ and the SE was estimated by $\sqrt{[p(1-p)/n]}$. Statistical analyses were performed with SPSS release 16.0 (SPSS Inc, Chicago, Illinois, USA). All tests $p < 0.05$ were considered statistically significant.

Results

Patient population

A total of 70 patients (46 (66%) men, mean age 55 ± 11 years) were included. Baseline characteristics of the patient population are listed in Table 1. MDCT and 2D echocardiography were performed within 3 months and no acute coronary events or worsening of angina occurred between the examinations. No changes in the use of medication occurred between both examinations. Clinical referral for MDCT was based on suspected CAD in 58 patients and known CAD in 12 patients. Patients with known CAD included patients with previous myocardial infarction ($n=10$), percutaneous coronary intervention ($n=7$) and patients with indications of CAD on earlier diagnostic tests ($n=3$). Significant coronary artery stenosis ($\geq 50\%$ luminal narrowing) was reported in 21 (30%) patients. In total, 31 (44%) patients received beta-blocking therapy prior to MDCT imaging.

Transmitral velocity

Transmitral flow versus time curves were obtained in all patients. Mean LV end-systolic and LV end-diastolic volumes were 70 ± 50 mL and 149 ± 52 mL on MDCT. Accordingly, the mean LV ejection fraction was $56 \pm 13\%$ (Table 1). Mean values for transmitral velocity are shown in Table 2. Pearson's correlation showed a good correlation for E ($r=0.73$, $p<0.01$) and E/A ($r=0.87$, $p<0.01$) (Figures 3A and 4A). Bland-Altman analysis for E showed a mean difference of 2.4 ± 12.0 cm/s, with 95% limits of agreement ranging from -21.2 to 26.0 cm/s, whereas for E/A the mean value of difference was -0.1 ± 0.2 with 95% limits of agreement ranging from -0.5 to 0.4 (Figures 3B and 4B). An excellent reproducibility was observed for assessment of mitral valve area (ICC 0.85, 95% CI 0.67 - 0.94).

Mitral septal tissue velocity

Velocity versus time curves were obtained for all patients. Mean values for E_a and E/E_a are shown in Table 2. A good correlation ($r=0.82$, $p<0.01$) (Figure 5A) for E_a was found. Bland-Altman analysis showed a mean value of difference of -0.5 ± 1.6 cm/s with 95% limits of agreement ranging from -3.6 to 2.5 cm/s (Figure 5B). In addition, good correlation ($r=0.88$, $p<0.01$, Figure 6A) was reported for E/E_a with a mean value of difference of 1.0 ± 2.9 and 95% limits of agreement ranging from -4.6 to 6.7 (Figure 6B).

An excellent reproducibility was observed for assessment of mitral septal tissue velocity (ICC 0.94, 95% CI 0.80 - 0.99).

Detection of diastolic dysfunction

Finally, diagnostic accuracy of MDCT to detect diastolic dysfunction in comparison to Doppler echocardiography was calculated (21). In total, 19 (27%) patients showed normal diastolic function, whereas 51 (73%) patients showed diastolic dysfunction using Doppler

Table 1. Baseline characteristics of study population

Men	46 (66)
Age (yrs)	55 ± 11
Suspected CAD	58 (83)
Known CAD	12 (17)
Significant coronary stenosis	21 (30)
Cardiovascular risk factors	
Diabetes mellitus	35 (50)
Systemic hypertension	43 (61)
Hypercholesterolemia	40 (57)
Current smoking	11 (16)
Positive family history	27 (39)
Medication use	
β-blockers	24 (34)
ACE-I / AT II antagonists	35 (50)
Statins	29 (41)
Diuretics	15 (21)
Anticoagulants	30 (43)
MDCT	
Heart rate (bpm)	58 ± 10
LV end-systolic volume (mL)	70 ± 50
LV end-diastolic volume (mL)	149 ± 52
LV ejection fraction (%)	56 ± 13

Table 2. Diastolic function parameters for MDCT and 2D echocardiography

	MDCT	2D echocardiography	P-value
Transmitral velocity			
E (cm/s)	59.0 ± 16.6	61.8 ± 14.5	<0.05
A (cm/s)	56.2 ± 17.4	64.8 ± 18.2	<0.05
E/A	1.1 ± 0.4	1.1 ± 0.5	<0.05
Mitral septal tissue velocity			
Ea (cm/s)	6.6 ± 2.7	6.2 ± 2.3	<0.05
E/Ea	10.5 ± 5.5	11.6 ± 6.0	<0.05

echocardiography. Of the patients with diastolic dysfunction on Doppler echocardiography, 40 patients were scored similarly using MDCT, yielding a sensitivity of 78% (95% CI 67-89%). Normal diastolic function was found in 15 of the 19 patients using MDCT, yielding a specificity of 79% (95% CI 61-97%). Overall, diagnostic accuracy for assessment of diastolic dysfunction was 79% (95% CI 69-89%).

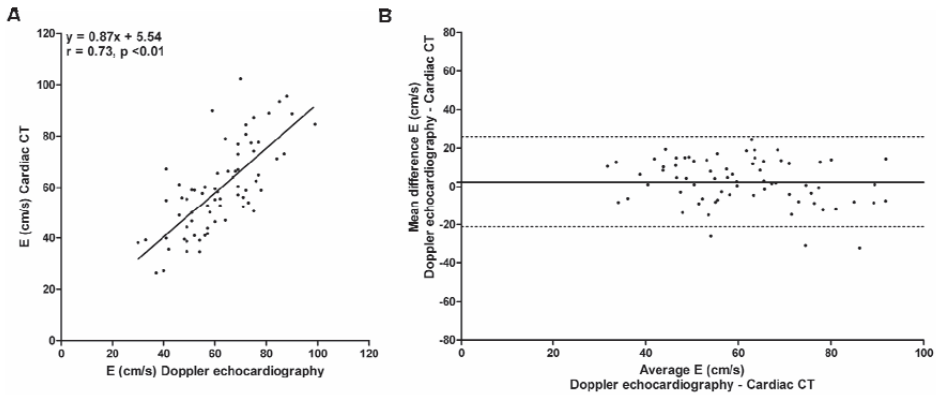


Figure 3. Comparison between 2-dimensional (2D) echocardiography and multidetector row computed tomography (MDCT) for assessment of early maximal diastolic transmitral velocity (E). A. Good correlation was observed between both techniques. B. Bland-Altman analysis showing the difference of each pair plotted against the average value of same pair of values.

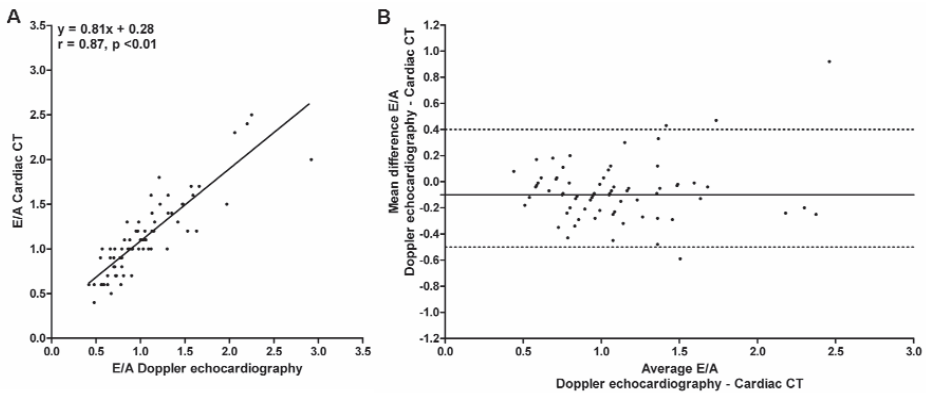


Figure 4. Comparison between 2-dimensional (2D) echocardiography and multidetector row computed tomography (MDCT) for E/A. A. Good correlation was observed between both techniques. B. Bland-Altman analysis showing the difference of each pair plotted against the average value of same pair of values.

Discussion

This study demonstrated good correlations for transmitral velocity (E and E/A) and mitral septal tissue velocity (Ea). Additionally, combined assessment of transmitral and mitral septal tissue velocity (E/Ea) representing an estimation of LV filling pressures showed good correlation between MDCT and 2D echocardiography with TDI. Finally, a good agreement was found for the detection of diastolic dysfunction using MDCT. Accordingly, the current study showed that MDCT is a feasible method for assessment of diastolic function.

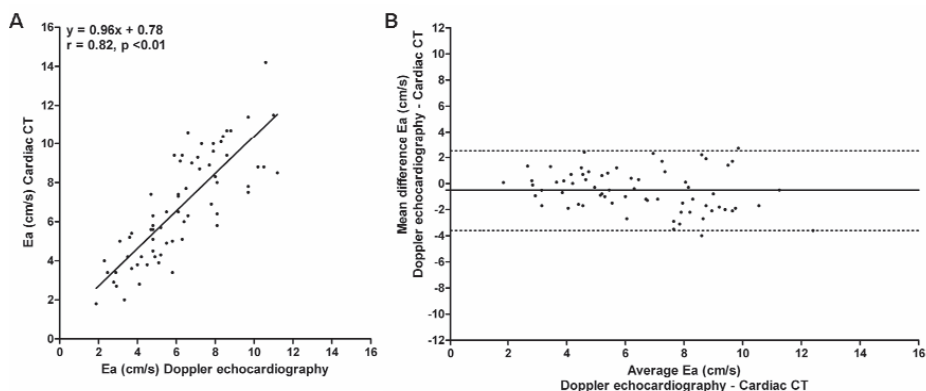


Figure 5. Comparison between 2-dimensional (2D) echocardiography and multidetector row computed tomography (MDCT) for assessment of early peak mitral septal tissue velocity (Ea). A. Good correlation was observed between both imaging techniques. B. Bland-Altman analysis showing the difference of each pair plotted against the average value of same pair of values.

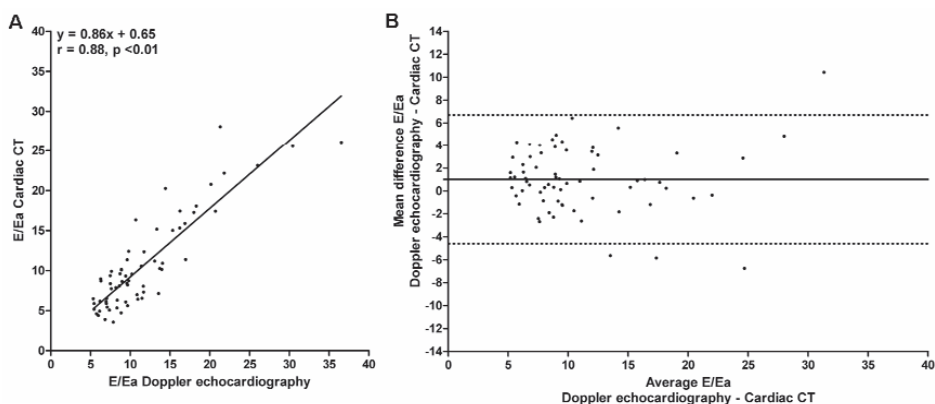


Figure 6. Comparison between 2-dimensional (2D) echocardiography and multidetector row computed tomography (MDCT) for E/Ea. A. Good correlation for E/Ea was observed between both techniques. B. Bland-Altman analysis showing the difference of each pair plotted against the average value of same pair of values.

The importance of diastolic function in patients with coronary atherosclerosis has been demonstrated in several studies.^{5, 6} A recent meta-analysis pooled 3396 patients with documented myocardial infarction from 12 prospective studies and demonstrated that patients with a restrictive LV filling pattern had a significantly higher mortality rate than patients with a non-restrictive LV filling pattern (11.3 % vs. 28.7%, $p < 0.01$).^{5, 6}

Although invasive measurements of LV filling pressure are considered the most accurate approach for evaluation of diastolic LV function, they are not ideal for widespread application and follow-up examinations. Consequently, several cardiac imaging techniques (particularly Doppler echocardiography) have been used to assess transmitral velocity as a

noninvasive alternative.^{7,9} Even though complex interacting pathophysiologic mechanisms may underlie diastolic dysfunction, evaluation of diastolic LV function is most frequently based on transmitral velocity measurements alone.^{7,9,13}

Transmitral velocity

Doppler echocardiography has been validated for the assessment of transmitral velocity as a noninvasive alternative of direct LV filling pressures.⁷ Additionally, Doppler echocardiography has been compared to magnetic resonance imaging (MRI) for assessment of transmitral velocity.^{11,12} Hartiala and colleagues evaluated whether velocity-encoded cine MRI was feasible for evaluation of transmitral velocity in 10 normal volunteers.¹¹ Good correlations were found between Doppler echocardiography and MRI for early and late transmitral velocity and E/A ratio. In the present study, the feasibility of MDCT was demonstrated indicating good correlations between MDCT and Doppler echocardiography for early transmitral velocity ($r=0.73$, $p<0.01$) and E/A ratio ($r=0.87$, $p<0.01$). In line with the study by Hartiala et al.,¹¹ a systematic underestimation of transmitral velocity was observed when compared to Doppler echocardiography (Table 2). These findings may be related to technical differences between MDCT and Doppler echocardiography; in particular differences in temporal resolution may play a role in the systematic underestimation of transmitral velocity with MDCT. In both studies, correlations were not excellent for transmitral velocity and this may be related to other parameters that could influence transmitral velocity measurements, including filling pressures, degree of LV relaxation, myocardial elastic recoil and stiffness.^{9,10} To overcome these limitations, additional measurements have been proposed, including the evaluation of pulmonary venous velocity, M-mode echocardiography flow velocity curves, and altering pre- and afterload conditions (Valsalva maneuver or nitroglycerin administration).^{22,23} In the current study however, these measurements were not performed as this study was only performed to evaluate the feasibility of MDCT.

Additionally, it has been suggested to combine transmitral velocity and mitral septal tissue velocity measurements when evaluating diastolic heart function. Importantly, the combined assessment of transmitral velocity and mitral septal tissue velocity represents a better estimate of LV filling pressures as it is a normalization of LV filling gradient for filling LV volume.^{8,12,13}

Mitral septal tissue velocity

Ommen and colleagues⁸ studied the clinical use of TDI for evaluation of diastolic LV function in 100 patients. Comparison between invasive LV filling pressures and combined assessment of early transmitral velocity and mitral septal tissue velocity showed improved correlation ($r=0.64$) as compared to transmitral velocity ($r=0.59$) or mitral septal tissue velocity ($r=0.36$) alone.⁸ In addition, MRI has been compared to TDI for assessment of

tissue velocities.¹² Paelinck et al.¹² used phase-contrast MRI and Doppler echocardiography to measure transmitral and mitral septal tissue velocities in 18 patients with hypertrophic cardiomyopathy. Importantly, combined assessment of early transmitral velocity and mitral septal tissue velocity (E/Ea) showed a good correlation between Doppler echocardiography and MRI ($r=0.89$, $p<0.01$). Moreover, invasive measurements were well correlated to E/Ea derived from Doppler echocardiography ($r=0.85$, $p<0.01$) and MRI ($r=0.80$, $p<0.01$). Likewise, the current study reported good correlations for transmitral velocity (E/A, $r=0.87$, $p<0.01$) and E/Ea ($r=0.88$, $p<0.01$). Furthermore, both studies showed that mitral septal tissue velocity was slightly overestimated when compared to Doppler echocardiography. With Doppler echocardiography, tissue velocities are quantified using changes in Doppler signal over time. Doppler patterns are only displayed for the region of interest (sample volume), located at the basal septal mitral valve annulus. With MDCT however, tissue velocities are measured using a different region of interest; ranging from the basal septal mitral valve annulus to the apex. The different regions of interest may have caused a slight overestimation of tissue velocity using MDCT.

Diastolic left ventricular function

Good agreement for detection of diastolic dysfunction was found when compared to Doppler echocardiography. This represents an important finding as the assessment of diastolic dysfunction provides important diagnostic, therapeutic and prognostic information in patients with cardiovascular disease, and more specifically, in patients with coronary atherosclerosis.¹⁻⁶ Additionally, it has been shown that patients with coronary atherosclerosis and normal LV systolic function may already exhibit diastolic dysfunction.²⁴ Accordingly, additional post-processing for diastolic dysfunction may have the potential to enhance the clinical evaluation derived from cardiac CT, particularly in patients with evidence of coronary atherosclerosis but normal LV systolic function. Moreover, the feasibility of MDCT for assessment of diastolic function is of particular interest as the number of patients referred for noninvasive evaluation of known or suspected coronary atherosclerosis with MDCT imaging has increased substantially over the recent years. In these patients, retrospective gating represents the most commonly used approach for cardiac CT.¹⁶ In a large multicenter observational study, including 21 university hospitals and 29 community hospitals, Hausleiter et al.¹⁶ recently showed that retrospective electrocardiographic gating was still applied in 94% of the 1965 enrolled patients. Importantly, in patients imaged with retrospective gating evaluation of diastolic LV function provides important additional information without additional radiation exposure.

Limitations

Some limitations need to be considered. At first, transmitral velocity parameters were assessed with Doppler echocardiography and MDCT as a noninvasive alternative to directly

measured LV filling pressures. Although direct measurements of LV filling pressures would have been preferred, they are not ideal for routine clinical examination. In addition, the assessment of LV filling pressures was performed by measuring early diastolic mitral septal tissue velocity with color-coded TDI. This technology provides lower values of tissue velocities as compared to pulsed-wave TDI.²⁵ Second, patients with valvular regurgitation were excluded. Severe valvular regurgitation may disturb accurate velocity measurements, leading to an inaccurate diastolic LV function analysis. Additional studies are needed to evaluate this potential confounding effect. Finally, one has to take into consideration that the effect of intravenous infusion of contrast media for cardiac CT angiography imaging on diastolic function indices is currently unknown.

Conclusions

Good correlations were observed for transmitral velocity, mitral septal tissue velocity and estimation of LV filling pressures when compared to 2D echocardiography using TDI. Moreover, a good agreement was found for detection of diastolic dysfunction using MDCT. Accordingly, MDCT is a feasible technique for assessment of diastolic function.

References

1. Zile MR, Brutsaert DL. New concepts in diastolic dysfunction and diastolic heart failure: Part I: diagnosis, prognosis, and measurements of diastolic function. *Circulation* 2002;105:1387-93.
2. Zile MR, Brutsaert DL. New concepts in diastolic dysfunction and diastolic heart failure: Part II: causal mechanisms and treatment. *Circulation* 2002;105:1503-8.
3. Bursi F, Weston SA, Redfield MM, et al. Systolic and diastolic heart failure in the community. *JAMA* 2006;296:2209-16.
4. Bhatia RS, Tu JV, Lee DS, et al. Outcome of heart failure with preserved ejection fraction in a population-based study. *N Engl J Med* 2006;355:260-9.
5. Perrone-Filardi P, Bacharach SL, Dilsizian V, et al. Impaired left ventricular filling and regional diastolic asynchrony at rest in coronary artery disease and relation to exercise-induced myocardial ischemia. *Am J Cardiol* 1991;67:356-60.
6. Moller JE, Whalley GA, Dini FL, et al. Independent prognostic importance of a restrictive left ventricular filling pattern after myocardial infarction: an individual patient meta-analysis: Meta-Analysis Research Group in Echocardiography acute myocardial infarction. *Circulation* 2008;117:2591-8.
7. Nishimura RA, Appleton CP, Redfield MM, et al. Noninvasive doppler echocardiographic evaluation of left ventricular filling pressures in patients with cardiomyopathies: a simultaneous Doppler echocardiographic and cardiac catheterization study. *J Am Coll Cardiol* 1996;28:1226-33.
8. Ommen SR, Nishimura RA, Appleton CP, et al. Clinical utility of Doppler echocardiography and tissue Doppler imaging in the estimation of left ventricular filling pressures: A comparative simultaneous Doppler-catheterization study. *Circulation* 2000;102:1788-94.
9. Nishimura RA, Tajik AJ. Evaluation of diastolic filling of left ventricle in health and disease: Doppler echocardiography is the clinician's Rosetta Stone. *J Am Coll Cardiol* 1997;30:8-18.
10. Oh JK, Appleton CP, Hatle LK, et al. The noninvasive assessment of left ventricular diastolic function with two-dimensional and Doppler echocardiography. *J Am Soc Echocardiogr* 1997;10:246-70.
11. Hartiala JJ, Mostbeck GH, Foster E, et al. Velocity-encoded cine MRI in the evaluation of left ventricular diastolic function: measurement of mitral valve and pulmonary vein flow velocities and flow volume across the mitral valve. *Am Heart J* 1993;125:1054-66.
12. Paelinck BP, de Roos A, Bax JJ, et al. Feasibility of tissue magnetic resonance imaging: a pilot study in comparison with tissue Doppler imaging and invasive measurement. *J Am Coll Cardiol* 2005;45:1109-16.
13. Nagueh SF, Middleton KJ, Kopelen HA, et al. Doppler tissue imaging: a noninvasive technique for evaluation of left ventricular relaxation and estimation of filling pressures. *J Am Coll Cardiol* 1997;30:1527-33.
14. Raff GL, Gallagher MJ, O'Neill WW, et al. Diagnostic accuracy of noninvasive coronary angiography using 64-slice spiral computed tomography. *J Am Coll Cardiol* 2005;46:552-7.
15. Mollet NR, Cademartiri F, van Mieghem CA, et al. High-resolution spiral computed tomography coronary angiography in patients referred for diagnostic conventional coronary angiography. *Circulation* 2005;112:2318-23.
16. Hausleiter J, Meyer T, Hermann F, et al. Estimated radiation dose associated with cardiac CT angiography. *JAMA* 2009;301:500-7.
17. Henneman MM, Bax JJ, Schuijf JD, et al. Global and regional left ventricular function: a comparison between gated SPECT, 2D echocardiography and multi-slice computed tomography. *Eur J Nucl Med Mol Imaging* 2006;33:1452-60.
18. van der Geest RJ, Reiber JH. Quantification in cardiac MRI. *J Magn Reson Imaging* 1999;10:602-8.

19. Pattynama PM, Lamb HJ, van der Velde EA, et al. Left ventricular measurements with cine and spin-echo MR imaging: a study of reproducibility with variance component analysis. *Radiology* 1993;187:261-8.
20. Lester SJ, Tajik AJ, Nishimura RA, et al. Unlocking the mysteries of diastolic function: deciphering the Rosetta Stone 10 years later. *J Am Coll Cardiol* 2008;51:679-89.
21. Nagueh SF, Appleton CP, Gillebert TC, et al. Recommendations for the evaluation of left ventricular diastolic function by echocardiography. *J Am Soc Echocardiogr* 2009;22:107-33.
22. Nishimura RA, Abel MD, Hatle LK, et al. Relation of pulmonary vein to mitral flow velocities by transesophageal Doppler echocardiography. Effect of different loading conditions. *Circulation* 1990;81:1488-97.
23. Takatsuji H, Mikami T, Urasawa K, et al. A new approach for evaluation of left ventricular diastolic function: spatial and temporal analysis of left ventricular filling flow propagation by color M-mode Doppler echocardiography. *J Am Coll Cardiol* 1996;27:365-71.
24. Garcia-Fernandez MA, Azevedo J, Moreno M, et al. Regional diastolic function in ischaemic heart disease using pulsed wave Doppler tissue imaging. *Eur Heart J* 1999;20:496-505.
25. Yu CM, Sanderson JE, Marwick TH, et al. Tissue Doppler imaging a new prognosticator for cardiovascular diseases. *J Am Coll Cardiol* 2007;49:1903-14.

Summary and Conclusions

Summary and Conclusions

The general introduction of the thesis (Chapter 1) describes the epidemiology of CAD worldwide, and specifically in the Netherlands. The concepts underlying atherosclerosis formation and progression are briefly discussed followed by an overview of different invasive and non-invasive imaging techniques available to identify CAD, including novel anatomic imaging using CTA. This introduction of the different imaging techniques is followed by the objective and outline of the thesis.

Part 1

In Part 1 of the thesis the value of CTA for diagnosis of CAD, and its relationship to existing diagnostic imaging modalities is described. Chapter 2 provides an overview of the advances in CTA technique, and describes the potential value of CTA in clinical practice compared to existing non-invasive imaging techniques. Based on this review, it was concluded that the combined use of these techniques may enhance the assessment of the presence and extent of coronary artery disease. The diagnostic accuracy of CTA for detection of significant CAD on invasive coronary angiography, in patients with an intermediate pre-test likelihood is evaluated in Chapter 3. On a segmental level, sensitivity, specificity, positive predictive value and negative predictive value were 79%, 98%, 61%, and 99% respectively. On a patient level, sensitivity, specificity, positive predictive value, and negative predictive value were respectively 100%, 89%, 76%, and 100%. CTA therefore has an excellent diagnostic accuracy in the target population of patients with an intermediate pre-test likelihood. Importantly, CTA allowed accurate rule out of significant CAD in 66% of the total population. In Chapters 4-7, the anatomic data obtained on CTA is compared to functional imaging techniques (SPECT, FFR, and MRI). In Chapter 4 the diagnostic information obtained from CTA is compared to SPECT. These findings are further correlated to invasive coronary angiography and IVUS. Of 26 patients with an abnormal MPI study, 23 (88%) showed significant stenosis on CTA. As compared with QCA, CTA showed a sensitivity of 96% and specificity of 67% for the detection of stenoses $\geq 50\%$ diameter narrowing in these patients. On the other hand, 27 (84%) of 44 patients with normal MPI had evidence of coronary atherosclerosis on CTA (luminal stenosis $\geq 50\%$: $n = 15$, luminal stenosis $< 50\%$: $n = 12$, sensitivity of 100% and specificity of 83% as compared with QCA). Using IVUS, we found substantial plaque burden (mean 58.9 \pm 18.1% of cross-sectional area). It was concluded that a considerable plaque burden can be observed with CTA even in the absence of myocardial perfusion abnormalities. This finding reflects the fact that CTA can detect atherosclerotic lesions that are not flow-limiting. In Chapter 5 the presence of atherosclerosis on CTA in patients with a normal MPI is further explored. In 97 patients with a normal MPI, a total of 38 patients

(39%) showed normal coronary anatomy, whereas non-significant and significant CAD was observed in respectively 37 (38%), and 18 (19%) patients. Importantly, only 4 (4%) patients presented with high risk CAD (2 with left main and 2 with 3-vessel disease). These results suggest that a normal MPI can be associated with a wide range of anatomical observations and cannot exclude the presence of both non-obstructive and obstructive CAD. In Chapter 6 CTA is compared to invasive functional imaging using FFR in 36 vessels of men with known CAD. An abnormal FFR was observed in only 58% of vessels with lesions >50% on CTA. Nevertheless, the agreement between normal CTA and FFR was excellent; FFR was normal in all 11 vessels with normal CTA. It was concluded that significant stenoses on CTA frequently do not result in reduced FFR. A normal CTA study however can accurately rule out the presence of hemodynamically significant lesions in men with known CAD. In Chapter 7 the anatomic findings observed on CTA are compared to MRI perfusion imaging and conventional coronary angiography. In the 38 patients without significant stenosis on CTA, normal perfusion was observed in 29 (76%). In patients with a significant stenosis on CTA, ischemia was observed in 10 (67%). In all patients without significant stenosis on CTA and normal perfusion on MRI (n=29), significant stenosis was absent on conventional coronary angiography. All patients with both CTA and MRI abnormal (n=10) had significant stenoses on conventional coronary angiography. As a result the anatomic and functional data obtained with CTA and MRI is complementary for the assessment of CAD and these findings support the sequential or combined assessment of anatomy and function.

Several studies have correlated the presence of significant CAD on CTA to the presence of myocardial perfusion defects on SPECT. In Chapter 8 multiple CTA variables of atherosclerosis are compared to SPECT imaging in order to determine the different predictors of ischemia. On a patient basis, multivariate analysis showed that the degree of stenosis (presence of $\geq 70\%$ stenosis, OR 3.5), plaque extent and composition (mixed plaques ≥ 3 , OR 1.7 and calcified plaques ≥ 3 , OR 2.0) and location (atherosclerotic disease in left main coronary artery and/or proximal left anterior descending coronary artery, OR 1.6) were independent predictors for ischemia on MPI. Therefore, in addition to the degree of stenosis, CTA variables of atherosclerosis describing plaque extent, composition and location are predictive of the presence of ischemia on MPI. In Chapter 9 the impact of clinical presentation and pre-test likelihood on the relationship between CS and CTA was determined in order to determine the role of CS as a gatekeeper to CTA. In patients with CS 0, the prevalence of significant CAD increased from 3.9% to 4.1% and 14.3% in respectively non-anginal, atypical and typical chest pain, and from 3.4% to 3.9% and 27.3% with respectively a low, intermediate and high pre-test likelihood. In patients with CS 1-400, the prevalence of significant CAD increased from 27.4% to 34.7% and 51.7% in respectively non-anginal, atypical and typical chest pain, and from 15.4% to 35.6% and 50% in respectively low, intermediate and high pre-test likelihood. In patients with CS >400, the prevalence of significant CAD on CTA

remained high (>72%) regardless of clinical presentation and pre-test likelihood. It was concluded that the relation between CCS and CTA is influenced by clinical presentation and pre-test likelihood, and these factors should be taken into account when using CS as a gatekeeper for CTA.

Part 2

In Part 2 of the thesis the value of CTA for risk stratification is evaluated; in addition, the prognostic value of CTA is compared to other non-invasive imaging techniques used for risk stratification. Chapter 10 reviews published data on the prognostic value of CTA. Based on this literature overview it was concluded that characterization of atherosclerosis non-invasively has the potential to provide important prognostic information enabling a more patient tailored approach to disease management. Chapters 11-13 describe the incremental prognostic value of CTA over SPECT perfusion imaging, coronary CS, and CT derived LV volumes and LV function respectively. In Chapter 11, CTA emerged as an independent predictor of events with an incremental prognostic value to SPECT. CTA and MPI were synergistic and combined use resulted in significantly improved prediction (Log-rank test p -value<0.005). It was therefore concluded that combined anatomical and functional assessment may allow improved risk stratification. In Chapter 12, after multivariate correction for CS, CTA $\geq 50\%$ stenosis, the number of diseased segments, obstructive segments, and non-calcified plaques were independent predictors with an incremental prognostic value to CS. The additional information on stenosis severity and plaque composition obtained using CTA was shown to translate into incremental prognostic value over CS. When assessing the incremental prognostic value of CTA over CT derived LV volumes and LV function in Chapter 13, LVEF < 49% and LVESV > 90 mL were independent predictors of events with an incremental prognostic value over clinical risk factors and CTA. These results suggest that LV function analysis provides incremental prognostic information beyond anatomic assessment of CAD using CTA. Chapters 14-16 discuss the prognostic value of CTA in patients with an intermediate pre-test likelihood, patients with diabetes mellitus (DM) and in smokers. In patients with an intermediate pre-test likelihood for CAD the annualized event rate was 0.8% in patients with normal CTA, 2.2% in patients with non-significant CAD and 6.5% in patients with significant CAD (Chapter 14). Moreover, CTA remained a significant predictor (p <0.05) of events after multivariate correction. These results suggest that CTA is highly effective in re-stratifying patients into either a low or high post-test risk group. These results further emphasize the usefulness of non-invasive imaging with CTA in this patient population. In Chapter 15 the prognostic value of CTA was compared between DM and non-DM patients. Obstructive CAD was a significant multivariate predictor both in DM and in non DM patients. Both in DM and non DM patients with absence of disease the event rate was 0%. The event rate

increased to 36% in non-DM patients with obstructive CAD and was highest (47%) in DM patients with obstructive CAD. CTA might therefore be a clinically useful tool to improve risk stratification in both DM and non DM patients. The influence of smoking on the prognostic value of CTA was assessed in Chapter 16. A significant interaction ($p < 0.05$) was observed between significant CAD and smoking for the prediction of events. The annualized event rate in smokers with significant CAD was 8.78% compared to 0.99% in smokers without significant CAD ($p < 0.001$). In non-smokers with significant CAD the annualized event rate was 2.07% compared to 1.01% in non-smokers without significant CAD ($p = 0.058$). The prognostic value of CTA was significantly influenced by smoking status. These findings suggest that smoking cessation needs to be aggressively pursued, especially in smokers with significant CAD.

Part 3

In Part 3 of the thesis potential future perspectives of CTA imaging are discussed. In addition to non-invasive coronary angiography and LV volume and function assessment, CTA also has the potential to assess myocardial perfusion imaging. Chapter 17 reviews the limited data available regarding the feasibility of CTA perfusion imaging and discusses its potential clinical value. The evaluation of both coronary anatomy and myocardial perfusion using a single imaging modality has the potential to allow for accurate and quick assessment of the presence of coronary artery stenosis and its effects on myocardial hemodynamics. In Chapter 18 assessment of diastolic function on CTA is compared with 2-dimensional (2D) echocardiography using tissue Doppler imaging (TDI). Good correlations were observed between CTA and 2D echocardiography for assessment of E ($r = 0.73$, $p < 0.01$), E/A ($r = 0.86$, $p < 0.01$), Ea ($r = 0.82$, $p < 0.01$) and E/Ea ($r = 0.88$, $p < 0.01$). It was therefore concluded that CTA imaging is a feasible technique to evaluate diastolic LV function.

Conclusions

The objective of the thesis was to explore the value of CTA for diagnosis and risk stratification of CAD in patients presenting with suspected and known CAD, in order to further define the role of non-invasive anatomic imaging in clinical practice. CTA has a good diagnostic accuracy for the detection of significant CAD on conventional coronary angiography, and an especially high negative predictive value in patients with an intermediate pre-test likelihood for CAD, the target population for non-invasive imaging. As a result it may be used as an effective gatekeeper to invasive coronary angiography.

In order to define the role of CTA relative to other non-invasive imaging techniques used for this purpose, several comparative studies were performed. These studies have demonstrated that CTA is capable of identifying atherosclerosis at an early stage, and can distinguish between atherosclerosis and completely normal coronary anatomy. Completely normal coronary anatomy is associated with normal coronary blood flow on FFR and with an excellent prognosis. In patients with atherosclerosis, CTA is able to define the extent, severity, location and composition of atherosclerotic lesions throughout the coronary artery tree and can identify atherosclerosis even in a large proportion of patients with normal perfusion on SPECT or MRI. The detailed assessment of atherosclerosis provides important prognostic information incremental to perfusion imaging, and can be used to guide medical treatment decision making. However, decision making regarding referral to revascularization procedures cannot be made solely on the basis of anatomical information. Although significant CAD on CTA is associated with abnormal blood flow, approximately half of patients with significant CAD do not show any perfusion defects. Functional imaging therefore remains mandatory in order to determine which patients will benefit from revascularization.

CTA supplies complementary information to existing non-invasive imaging techniques, and has the potential to provide a more patient tailored approach to patient management. What remains to be determined is how CTA and non-invasive functional imaging should be integrated into clinical practice. The concept of combined imaging in all patients referred for non-invasive imaging has led to the introduction of hybrid SPECT/CTA or PET/CTA scanners and to the further development of perfusion imaging with CTA in order to obtain anatomical and functional imaging from a single procedure. Dual testing however may be redundant in some patients and may increase the cost of diagnostic testing. Sequential imaging approaches have therefore been proposed in which the decision to undergo further testing is based on preceding test results. Prospective follow-up studies assessing both the efficacy and more importantly cost-effectiveness of such algorithms are highly anticipated and necessary to further define the role of non-invasive anatomic imaging in clinical practice.

Samenvattingen en Conclusies

Samenvattingen en Conclusies

De algemene inleiding van het proefschrift (Hoofdstuk 1) beschrijft de epidemiologie van CAD wereldwijd, en specifiek in Nederland. De onderliggend principes van atherosclerose vorming en progressie worden kort besproken, gevolgd door een overzicht van de verschillende invasieve en niet-invasieve beeldvormingstechnieken die beschikbaar zijn om CAD te identificeren, inclusief de anatomische beeldvorming met behulp van CTA. Dit overzicht van de verschillende beeldvormende technieken wordt gevolgd door de doelstelling en de opzet van het proefschrift.

Deel 1

In Deel 1 van het proefschrift wordt de waarde van CTA voor diagnose van CAD, en de relatie tot bestaande diagnostische beeldvormende technieken beschreven. Hoofdstuk 2 geeft een overzicht van de ontwikkelingen op het gebied van CTA techniek en beschrijft de potentiële klinische waarde van CTA ten opzicht van bestaande niet-invasieve functionele beeldvormende technieken. Op basis van deze review, werd geconcludeerd dat de combinatie van deze technieken de beoordeling van de aanwezigheid en de omvang van coronaire hartziekten vergroten. De diagnostische waarde van CTA voor de beoordeling van significant coronairlijden op invasieve coronair angiografie, bij patiënten met een intermediaire “pre-test likelihood” wordt geëvalueerd in Hoofdstuk 3. Op een segmentaal niveau, waren sensitiviteit, specificiteit, positief voorspellende waarde en negatief voorspellende waarde respectievelijk 79%, 98%, 61% en 99%. Op patiënt niveau, waren de sensitiviteit, specificiteit, positief voorspellende waarde en negatief voorspellende respectievelijk 100%, 89%, 76% en 100%. CTA heeft dus een uitstekende diagnostische nauwkeurigheid in de doelgroep van patiënten met een intermediaire “pre-test likelihood”. CTA kon de aanwezigheid van significant coronairlijden nauwkeurig uitsluiten in 66% van de onderzoekspopulatie. In de Hoofdstukken 4-7, wordt de anatomische informatie verkregen met CTA vergeleken met functionele beeldvormingstechnieken (SPECT, FFR, en MRI). In Hoofdstuk 4 wordt de diagnostische informatie verkregen uit CTA vergeleken met SPECT. Deze bevindingen zijn verder gerelateerd aan invasieve coronair angiografie en IVUS. Van 26 patiënten met een abnormaal MPI onderzoek, hadden 23 (88%) een aanzienlijke vernauwing op CTA. Bij de vergelijking met invasieve coronair angiografie had CTA een sensitiviteit van 96% en een specificiteit van 67% voor de beoordeling van significant stenosen ($\geq 50\%$ vernauwing van het lumen). In 27 (84%) van 44 patiënten met een normale MPI werd atherosclerose op de CTA gevonden (stenose $\geq 50\%$: $n = 15$, stenose $< 50\%$: $n = 12$, met een sensitiviteit van 100% en specificiteit van 83% ten opzichte van QCA). Met behulp van IVUS, werd een aanzienlijke “plaque burden” gevonden (gemiddeld $58,9 \pm 18,1\%$ van het dwarsdoorsnede oppervlakte).

Er werd geconcludeerd dat een aanzienlijke “plaque burden” kan worden waargenomen met CTA, zelfs bij het ontbreken van perfusie afwijkingen. Deze bevinding weerspiegelt de mogelijkheid van CTA om atherosclerose op te sporen die nog geen beperking oplevert voor de myocard perfusie. In Hoofdstuk 5 wordt de aanwezigheid van atherosclerose op CTA bij patiënten met een normale MPI verder onderzocht. In 97 patiënten met een normale MPI, hadden in totaal 38 patiënten (39%) een normale coronaire anatomie, terwijl niet-significante en significante CAD werd waargenomen bij respectievelijk 37 (38%) en 18 (19%) patiënten. Een belangrijke bevinding was dat slechts 4 (4%) patiënten presenteerden met hoog risico CAD (2 met een hoofdstam stenose en 2 met 3-vats lijden). Deze resultaten suggereren dat een normale MPI is geassocieerd met een breed scala aan anatomische afwijkingen op CTA en daarmee de aanwezigheid van zowel niet-obstructieve als obstructieve CAD niet kan uitsluiten. In Hoofdstuk 6 wordt CTA vergeleken met invasieve functionele beeldvorming met FFR in 36 vaten mannen met bekend coronairlijden. Een abnormale FFR werd waargenomen in slechts 58% van de vaten met $\geq 50\%$ stenose op CTA. Echter, de overeenkomst tussen normale CTA en FFR was uitstekend; FFR was normaal bij alle 11 vaten met een normale CTA. Geconcludeerd werd dat een significante stenose op CTA vaak niet resulteert in een verminderde FFR. Een normale CTA onderzoek kan echter nauwkeurig de aanwezigheid van hemodynamisch significante laesies uitsluiten bij mannen met bekend coronairlijden. In Hoofdstuk 7 werden de anatomische bevindingen waargenomen op CTA vergeleken met MRI perfusie beeldvorming en conventionele coronaire angiografie. In de 38 patiënten zonder significante stenose op de CTA, werd normale perfusie waargenomen in 29 (76%) patiënten. Bij patiënten met een significante stenose op CTA werd ischemie waargenomen in 10 (67%) patiënten. Bij alle patiënten zonder significante stenose op de CTA en normale perfusie op de MRI ($n = 29$), was significante stenose afwezig op conventionele coronair angiografie. Alle patiënten met zowel een abnormale CTA en abnormale MRI ($n = 10$) hadden een significante stenose op conventionele coronaire angiografie. De anatomische en functionele gegevens, verkregen met CTA en MRI geven complementaire informatie bij de beoordeling van CAD. Deze bevindingen ondersteunen sequentiële of gecombineerde beeldvorming strategieën waarbij zowel anatomische als functionele informatie wordt verkregen.

Verschillende onderzoeken hebben atherosclerose gedetecteerd met CTA gecorreleerd aan de aanwezigheid van myocard perfusie defecten op SPECT. In Hoofdstuk 8 werden meerdere CTA variabelen voor atherosclerose vergeleken met SPECT-beeldvorming om verschillende voorspellers van ischemie te bepalen. Op patient niveau bleek uit de multivariate analyse dat de mate van stenose (aanwezigheid van, een $\geq 70\%$ stenose, OR 3.5), de uitgebreidheid en de samenstelling van plaque (mixed plaque, ≥ 3 OR 1,7 en verkalkte plaques, ≥ 3 , OR 2.0) en de locatie (atherosclerose in de hoofdstam en / of proximale ramus descendens anterior, OR 1,6) onafhankelijke voorspellers waren voor ischemie op MPI. Naast de mate

van stenose, zijn de uitgebreidheid en samenstelling van plaque en de locatie belangrijke voorspellers voor de aanwezigheid van ischemie op MPI. In Hoofdstuk 9 wordt het effect van klinische presentatie en “pre-test likelihood” op de relatie tussen CS en CTA beoordeeld, om de rol van CS als poortwachter voor CTA te bepalen. Bij patiënten met CS 0, steeg de prevalentie van significant coronairlijden van 3,9% tot 4,1% en 14,3% in respectievelijk niet-angineuze, atypische en typische pijn op de borst, en van 3,4% tot 3,9% en 27,3% in respectievelijk een lage, middelhoge en hoge “pre-test likelihood”. Bij patiënten met CS 100-400, steeg de prevalentie van significant coronairlijden van 27,4% tot 34,7% en 51,7% in respectievelijk niet-angineuze, atypische en typische pijn op de borst, en van 15,4% tot 35,6% en 50% in respectievelijk lage, middelhoge en een hoge “pre-test likelihood”. Bij patiënten met CS > 400, bleef prevalentie van significant coronairlijden op CTA hoog (> 72%), ongeacht de klinische presentatie en “pre-test likelihood”. Geconcludeerd werd dat de relatie tussen CS en CTA wordt beïnvloed door de klinische presentatie en “pre-test likelihood”. Deze factoren moeten daarom in acht worden genomen bij het gebruik van CS als poortwachter voor CTA.

Deel 2

In Deel 2 van het proefschrift wordt de waarde van CTA voor risicostratificatie geëvalueerd; daarnaast wordt de prognostische waarde van CTA vergeleken met de prognostische waarde van andere niet-invasieve beeldvormende technieken. Hoofdstuk 10 geeft een overzicht van de artikelen die zijn gepubliceerd over de prognostische waarde van CTA. Op basis van dit literatuuronderzoek werd geconcludeerd dat de non-invasieve karakterisering van atherosclerose belangrijke prognostische informatie geeft die potentieel gebruikt kan worden om een meer patiëntgerichte aanpak voor ziekte management mogelijk te maken. Hoofdstukken 11-13 beschrijven de incrementele prognostische waarde van CTA bovenop SPECT perfusie beeldvorming, coronaire CS, en CT-afgeleide LV volumina en LV functie bepaling. In Hoofdstuk 11, bleek CTA een onafhankelijke voorspeller van cardiovasculaire eindpunten te zijn met een incrementele prognostische waarde bovenop SPECT. CTA en MPI waren synergetische en het gecombineerde gebruik van de twee resulteerde in een significant betere voorspelling van de prognose (log-rank test p-waarde <0,005). Derhalve werd geconcludeerd dat de gecombineerde anatomische en functionele evaluatie mogelijk de risicostratificatie van mensen verwezen voor niet-invasieve beeldvorming verbeterd. In Hoofdstuk 12, bleken na multivariate correctie voor CS, zowel CTA $\geq 50\%$ stenose, het aantal aangetaste segmenten, het aantal significant aangetaste segmenten, en het aantal segmenten met niet-verkalkte plaques onafhankelijke voorspellers, met een incrementele prognostische waarde bovenop CS. De incrementele prognostische waarde van CTA bovenop LV functie bepalingen van LV volume en LV functie wordt besproken in Hoofdstuk 13. LVEF <49% en

LVESV > 90 ml waren onafhankelijke voorspellers van eindpunten met een incrementele prognostische waarde bovenop klinische risicofactoren en CTA. Deze resultaten suggereren dat LV functie analyse incrementele prognostische informatie bovenop anatomische beoordeling van CAD met behulp van CTA biedt. Hoofdstukken 14-16 bespreken de prognostische waarde van CTA bij patiënten met een intermediaire “pre-test likelihood”, patiënten met diabetes mellitus (DM) en bij rokers. Bij patiënten met een intermediaire “pre-test likelihood” was bedroeg de incidentie van eindpunten 0,8% per jaar bij patiënten met een normale CTA, 2,2% bij patiënten niet-significante CAD en 6,5% bij patiënten met significant coronairlijden (Hoofdstuk 14). Bovendien, CTA bleef een significante voorspeller ($p < 0,05$) na multivariate correctie. Deze resultaten suggereren dat CTA zeer effectief is in de re-stratificatie van patiënten in ofwel een laag danwel een hoog risico. Deze resultaten onderstrepen het nut van niet-invasieve beeldvorming met CTA bij deze patiëntenpopulatie. In Hoofdstuk 15 wordt de prognostische waarde van CTA vergeleken tussen de DM en niet-DM patiënten. Obstructieve CAD was een belangrijke multivariate voorspeller zowel in DM als in niet DM patiënten. Zowel in DM en niet DM patiënten zonder atherosclerose, was de incidentie van eindpunten 0% per jaar. De incidentie 36% in niet-DM patiënten met obstructieve CAD en was het hoogst (47%) in DM patiënten met obstructieve CAD. Dit onderzoek toont aan dat CTA van nut kan zijn bij risicostratificatie zowel in DM als in niet-DM patiënten. De invloed van roken op de prognostische waarde van CTA, werd onderzocht in Hoofdstuk 16. Een significante interactie ($p < 0,05$) voor het voorspellen van het eindpunt werd waargenomen tussen significante CAD en roken. Op jaarbasis bedroeg de incidentie bij rokers met significant CAD 8,78% in vergelijking met 0,99% bij rokers zonder significant CAD ($p < 0,001$). Bij niet-rokers met significant CAD was de incidentie op jaarbasis 2,07% in vergelijking tot 1,01% bij niet-rokers zonder significant CAD ($p = 0,058$). De prognostische waarde van CTA werd significant beïnvloed door rookgedrag. Deze bevindingen suggereren dat stoppen met roken agressief moet worden nagestreefd, met name bij rokers met significant CAD.

Deel 3

In Deel 3 van het proefschrift worden potentiële toekomstige mogelijkheden van CTA beeldvorming besproken. In aanvulling op niet-invasieve coronaire angiografie en LV functie bepaling, heeft CTA ook het potentieel om myocardperfusie te beoordelen. Hoofdstuk 17 beschrijft het beperkt aantal onderzoeken die zijn gepubliceerd over de mogelijkheid van CTA perfusie beeldvorming en bespreekt de potentiële klinische waarde hiervan. De evaluatie van zowel coronair anatomie en myocard perfusie met behulp van één beeldvormende modaliteit heeft het potentieel om nauwkeurig en snel zowel de aanwezigheid van een stenose alsmede het effect van deze stenose op myocard hemodynamiek te bepalen.

In Hoofdstuk 18 wordt de beoordeling van diastolische functie op CTA vergeleken met 2-dimensionale (2D) echocardiografie met tissue Doppler imaging (TDI). Goede correlaties werden waargenomen tussen CTA en 2D-echocardiografie voor de beoordeling van E ($r = 0,73$, $p < 0,01$), E / A ($r = 0,86$, $p < 0,01$), EA ($r = 0,82$, $p < 0,01$) en de E / EA ($r = 0,88$, $p < 0,01$). Daarom werd geconcludeerd dat het mogelijk is om met CTA de diastolische LV functie te evalueren.

Conclusies

Het doel van dit proefschrift was om de waarde van CTA voor de diagnose en risicostratificatie van CAD te evalueren bij patiënten met verdenking op coronairlijden en met bekend coronairlijden, om de rol van niet-invasieve anatomische beeldvorming te begrijpen in de kliniek. CTA heeft een goede diagnostische waarde voor de detectie van significant coronairlijden op conventionele coronaire angiografie, en een bijzonder hoge negatief voorspellende waarde bij patiënten met een intermediaire “pre-test likelihood” voor CAD, de doelgroep van niet-invasieve beeldvorming. Daardoor kan CTA worden gebruikt als een effectieve poortwachter voor invasieve coronairangiografie.

Om de rol van CTA te bepalen ten opzichte van andere niet-invasieve beeldvormingstechnieken die worden gebruikt als poortwachter voor invasieve coronaire angiografie zijn verschillende vergelijkende onderzoeken uitgevoerd. Deze onderzoeken hebben aangetoond dat CTA in staat is om atherosclerose te detecteren in een vroeg stadium, en onderscheid kan maken tussen atherosclerose en normale coronair anatomie. Normale coronair anatomie is geassocieerd met een normale coronaire bloedstroom op de FFR en met een uitstekende prognose. Bij patiënten met atherosclerose is CTA in staat om de uitgebreidheid, de ernst, de locatie en samenstelling van atherosclerotische laesies te definiëren, ook in een groot deel van de patiënten met een normale perfusie op SPECT of MRI. De gedetailleerde beoordeling van atherosclerose levert belangrijke incrementele prognostische informatie bovenop perfusie beeldvorming, en kan worden gebruikt als handleiding voor farmacologische therapie. Echter, de keuze om patiënten te verwijzen voor een revascularisatieprocedure kan niet alleen worden gemaakt op basis van de anatomische informatie. Hoewel significant CAD op de CTA is geassocieerd met abnormale perfusie, vertonen maar ongeveer de helft van de patiënten met significant coronairlijden een perfusie defect. Functionele beeldvorming blijft dus nodig om te kunnen bepalen welke patiënten zullen profiteren van revascularisatie.

CTA levert aanvullende informatie ten opzichte van bestaande niet-invasieve beeldvormende technieken, en heeft het potentieel om een meer patiëntgerichte ziekte management mogelijk te maken. Wat echter nog moet worden bepaald, is hoe CTA en niet-invasieve

functionele beeldvormingstechnieken moeten worden geïntegreerd in de kliniek. Het concept van de gecombineerde beeldvorming bij alle patiënten die worden verwezen voor niet-invasieve beeldvorming heeft geleid tot de introductie van hybride SPECT / CTA en PET / CTA scanners en tot de verdere ontwikkeling van de perfusie beeldvorming met CTA om anatomische en functionele beeldvorming te verkrijgen uit een enkele procedure. Dubbele testen kunnen echter overbodig zijn in sommige patiënten en kunnen de kosten van diagnostiek onnodig verhogen. Sequentiële beeldvorming benaderingen zijn daarom voorgesteld waarin het besluit tot verwijzing voor verdere diagnostiek, is gebaseerd op de voorgaande onderzoeksresultaten. Prospectieve follow-up onderzoeken zijn nodig om te kijken welk aanpak het beste en meest kosten-effectief is. Dergelijke algoritmen zijn hoogst nodig om de klinische rol van niet-invasieve anatomische beeldvorming beter te definiëren.

List of Publications

List of Publications

van Werkhoven JM, Schuijf JD, Jukema JW, van der Wall EE, Bax JJ. Multi-slice computed tomography coronary angiography: anatomic vs functional assessment in clinical practice. *Minerva Cardioangiol* 2008;56:215-26.

van Werkhoven JM, Schuijf JD, Jukema JW, Kroft LJ, Stokkel MP, Dibbets-Schneider P, Pundziute G, Scholte AJ, van der Wall EE, Bax JJ. Anatomic correlates of a normal perfusion scan using 64-slice computed tomographic coronary angiography. *Am J Cardiol* 2008;101:40-5.

van Werkhoven JM, Bax JJ, Nucifora G, Jukema JW, Kroft LJ, de Roos A, Schuijf JD. The value of multi-slice-computed tomography coronary angiography for risk stratification. *J Nucl Cardiol* 2009;16:970-80.

van Werkhoven JM, Schuijf JD, Jukema JW, Pundziute G, de Roos A, Schalijs MJ, van der Wall EE, Bax JJ. Comparison of non-invasive multi-slice computed tomography coronary angiography versus invasive coronary angiography and fractional flow reserve for the evaluation of men with known coronary artery disease. *Am J Cardiol* 2009;104:653-6.

van Werkhoven JM, Gaemperli O, Schuijf JD, Jukema JW, Kroft LJ, Leschka S, Alkadhi H, Valenta I, Pundziute G, de Roos A, van der Wall EE, Kaufmann PA, Bax JJ. Multislice computed tomography coronary angiography for risk stratification in patients with an intermediate pretest likelihood. *Heart* 2009;95:1607-11.

van Werkhoven JM, Schuijf JD, Gaemperli O, Jukema JW, Kroft LJ, Boersma E, Pazhenkottil A, Valenta I, Pundziute G, de Roos A, van der Wall EE, Kaufmann PA, Bax JJ. Incremental prognostic value of multi-slice computed tomography coronary angiography over coronary artery calcium scoring in patients with suspected coronary artery disease. *Eur Heart J* 2009;30:2622-9.

van Werkhoven JM, Schuijf JD, Gaemperli O, Jukema JW, Boersma E, Wijns W, Stolzmann P, Alkadhi H, Valenta I, Stokkel MP, Kroft LJ, de Roos A, Pundziute G, Scholte A, van der Wall EE, Kaufmann PA, Bax JJ. Prognostic value of multislice computed tomography and gated single-photon emission computed tomography in patients with suspected coronary artery disease. *J Am Coll Cardiol* 2009;53:623-32.

van Werkhoven JM, Schuijf JD, Bax JJ. Myocardial perfusion imaging to assess ischemia using multislice computed tomography.

Expert Rev Cardiovasc Ther 2009;7:49-56.

van Werkhoven JM, de Boer SM, Schuijf JD, Cademartiri F, Maffei E, Jukema JW, Boogers MJ, Kroft LJ, de Roos A, Bax JJ. Impact of clinical presentation and pretest likelihood on the relation between calcium score and computed tomographic coronary angiography.

Am J Cardiol 2010;106:1675-9.

van Werkhoven JM, Cademartiri F, Seitun S, Maffei E, Palumbo A, Martini C, Tarantini G, Kroft LJ, de Roos A, Weustink AC, Jukema JW, Ardissino D, Mollet NR, Schuijf JD, Bax JJ. Diabetes: prognostic value of CT coronary angiography--comparison with a nondiabetic population.

Radiology 2010;256:83-92.

van Werkhoven JM, Heijnenbrok MW, Schuijf JD, Jukema JW, Boogers MM, van der Wall EE, Schreur JH, Bax JJ. Diagnostic accuracy of 64-slice multislice computed tomographic coronary angiography in patients with an intermediate pretest likelihood for coronary artery disease.

Am J Cardiol 2010;105:302-5.

van Werkhoven JM, Heijnenbrok MW, Schuijf JD, Jukema JW, van der Wall EE, Schreur JH, Bax JJ. Combined non-invasive anatomical and functional assessment with MSCT and MRI for the detection of significant coronary artery disease in patients with an intermediate pretest likelihood.

Heart 2010;96:425-31.

van Werkhoven JM, Schuijf JD, Pazhenkottil AP, Herzog BA, Ghadri JR, Jukema JW, Boersma E, Kroft LJ, de Roos A, Kaufmann PA, Bax JJ. Influence of smoking on the prognostic value of cardiovascular computed tomography coronary angiography.

Eur Heart J 2011;32:365-70.

Boogers MJ, Schuijf JD, Kitslaar PH, van Werkhoven JM, de Graaf FR, Boersma E, van Velzen JE, Dijkstra J, Adame IM, Kroft LJ, de Roos A, Schreur JH, Heijnenbrok MW, Jukema JW, Reiber JH, Bax JJ. Automated quantification of stenosis severity on 64-slice CT: a comparison with quantitative coronary angiography.

JACC Cardiovasc Imaging 2010;3:699-709.

de Graaf FR, van Werkhoven JM, van Velzen JE, Antoni ML, Boogers MJ, Kroft LJ, de Roos A, Schalijs MJ, Jukema JW, van der Wall EE, Schuijff JD, Bax JJ. Incremental prognostic value of left ventricular function analysis over non-invasive coronary angiography with multidetector computed tomography.

J Nucl Cardiol 2010;17:1034-40.

Djaberi R, Schuijff JD, van Werkhoven JM, Nucifora G, Jukema JW, Bax JJ. Relation of epicardial adipose tissue to coronary atherosclerosis.

Am J Cardiol 2008;102:1602-7.

Henneman MM, Schuijff JD, Pundziute G, van Werkhoven JM, van der Wall EE, Jukema JW, Bax JJ. Noninvasive evaluation with multislice computed tomography in suspected acute coronary syndrome: plaque morphology on multislice computed tomography versus coronary calcium score.

J Am Coll Cardiol 2008;52:216-22.

Henneman MM, Schuijff JD, van Werkhoven JM, Pundziute G, van der Wall EE, Jukema JW, Bax JJ. Multi-slice computed tomography coronary angiography for ruling out suspected coronary artery disease: what is the prevalence of a normal study in a general clinical population?

Eur Heart J 2008;29:2006-13.

Meijboom WB, Meijs MF, Schuijff JD, Cramer MJ, Mollet NR, van Mieghem CA, Nieman K, van Werkhoven JM, Pundziute G, Weustink AC, de Vos AM, Pugliese F, Rensing B, Jukema JW, Bax JJ, Prokop M, Doevendans PA, Hunink MG, Krestin GP, de Feyter PJ. Diagnostic accuracy of 64-slice computed tomography coronary angiography: a prospective, multi-center, multivendor study.

J Am Coll Cardiol 2008;52:2135-44.

Nucifora G, Marsan NA, Siebelink HM, van Werkhoven JM, Schuijff JD, Schalijs MJ, Poldermans D, Holman ER, Bax JJ. Safety of contrast-enhanced echocardiography within 24 h after acute myocardial infarction.

Eur J Echocardiogr 2008;9:816-8.

Nucifora G, Schuijff JD, Tops LF, van Werkhoven JM, Kajander S, Jukema JW, Schreur JH, Heijenbrok MW, Trines SA, Gaemperli O, Turta O, Kaufmann PA, Knuuti J, Schalijs MJ, Bax JJ. Prevalence of coronary artery disease assessed by multislice computed tomography coronary angiography in patients with paroxysmal or persistent atrial fibrillation.

Circ Cardiovasc Imaging 2009;2:100-6.

Nucifora G, Schuijf JD, van Werkhoven JM, Djaberi R, van der Wall EE, de Roos A, Scholte AJ, Schalij MJ, Jukema JW, Bax JJ. Relation between Framingham risk categories and the presence of functionally relevant coronary lesions as determined on multislice computed tomography and stress testing.

Am J Cardiol 2009;104:758-63.

Nucifora G, Marsan NA, Holman ER, Siebelink HM, van Werkhoven JM, Scholte AJ, van der Wall EE, Schalij MJ, Bax JJ. Real-time 3-dimensional echocardiography early after acute myocardial infarction: incremental value of echo-contrast for assessment of left ventricular function.

Am Heart J 2009;157:882-8.

Nucifora G, Schuijf JD, van Werkhoven JM, Jukema JW, Marsan NA, Holman ER, van der Wall EE, Bax JJ. Usefulness of echocardiographic assessment of cardiac and ascending aorta calcific deposits to predict coronary artery calcium and presence and severity of obstructive coronary artery disease.

Am J Cardiol 2009;103:1045-50.

Nucifora G, Schuijf JD, van Werkhoven JM, Jukema JW, Djaberi R, Scholte AJ, de Roos A, Schalij MJ, van der Wall EE, Bax JJ. Prevalence of coronary artery disease across the Framingham risk categories: coronary artery calcium scoring and MSCT coronary angiography.

J Nucl Cardiol 2009;16:368-75.

Nucifora G, Schuijf JD, van Werkhoven JM, Trines SA, Kajander S, Tops LF, Turta O, Jukema JW, Schreur JH, Heijenbrok MW, Gaemperli O, Kaufmann PA, Knuuti J, van der Wall EE, Schalij MJ, Bax JJ. Relationship between obstructive coronary artery disease and abnormal stress testing in patients with paroxysmal or persistent atrial fibrillation.

Int J Cardiovasc Imaging 2010.

Nucifora G, Bax JJ, van Werkhoven JM, Boogers MJ, Schuijf JD. Coronary Artery Calcium Scoring in Cardiovascular Risk Assessment.

Cardiovasc Ther 2010.

Nucifora G, Marsan NA, Bertini M, Delgado V, Siebelink HM, van Werkhoven JM, Scholte AJ, Schalij MJ, van der Wall EE, Holman ER, Bax JJ. Reduced left ventricular torsion early after myocardial infarction is related to left ventricular remodeling.

Circ Cardiovasc Imaging 2010;3:433-42.

Nucifora G, Bertini M, Marsan NA, Delgado V, Scholte AJ, Ng AC, van Werkhoven JM, Siebelink HM, Holman ER, Schalij MJ, van der Wall EE, Bax JJ. Impact of left ventricular dyssynchrony early on left ventricular function after first acute myocardial infarction. *Am J Cardiol* 2010;105:306-11.

Nucifora G, Schuijff JD, Delgado V, Bertini M, Scholte AJ, Ng AC, van Werkhoven JM, Jukema JW, Holman ER, van der Wall EE, Bax JJ. Incremental value of subclinical left ventricular systolic dysfunction for the identification of patients with obstructive coronary artery disease. *Am Heart J* 2010;159:148-57.

Pundziute G, Schuijff JD, Jukema JW, van Werkhoven JM, Boersma E, de Roos A, van der Wall EE, Bax JJ. Gender influence on the diagnostic accuracy of 64-slice multislice computed tomography coronary angiography for detection of obstructive coronary artery disease. *Heart* 2008;94:48-52.

Pundziute G, Schuijff JD, Jukema JW, van Werkhoven JM, Nucifora G, Decramer I, Sarno G, Vanhoenacker PK, Reiber JH, Wijns W, Bax JJ. Type 2 diabetes is associated with more advanced coronary atherosclerosis on multislice computed tomography and virtual histology intravascular ultrasound. *J Nucl Cardiol* 2009;16:376-83.

Pundziute G, Schuijff JD, van Werkhoven JM, Nucifora G, van der Wall EE, Wouter JJ, Bax JJ. Head-to-head comparison between bicycle exercise testing and coronary calcium score and coronary stenoses on multislice computed tomography. *Coron Artery Dis* 2009;20:281-7.

Pundziute G, Schuijff JD, van Velzen JE, Jukema JW, van Werkhoven JM, Nucifora G, van der Kley F, Kroft LJ, de Roos A, Boersma E, Reiber JH, Schalij MJ, van der Wall EE, Bax JJ. Assessment with multi-slice computed tomography and gray-scale and virtual histology intravascular ultrasound of gender-specific differences in extent and composition of coronary atherosclerotic plaques in relation to age. *Am J Cardiol* 2010;105:480-6.

Scholte AJ, Roos CJ, van Werkhoven JM. Function and anatomy: SPECT-MPI and MSCT coronary angiography. *EuroIntervention* 2010;6 Suppl G:G94-G100.

Schuijff JD, van Werkhoven JM, Woo A, Rakowski H. Imaging highlights from the 2008 Scientific Session of the American College of Cardiology.

JACC Cardiovasc Imaging 2008;1:525-35.

Schuijf JD, van Werkhoven JM, Pundziute G, Jukema JW, Decramer I, Stokkel MP, Dibbets-Schneider P, Schalij MJ, Reiber JH, van der Wall EE, Wijns W, Bax JJ. Invasive versus noninvasive evaluation of coronary artery disease.

JACC Cardiovasc Imaging 2008;1:190-9.

van Velzen JE, Schuijf JD, van Werkhoven JM, Herzog BA, Pazhenkottil AP, Boersma E, de Graaf FR, Scholte AJ, Kroft LJ, de Roos A, Stokkel MP, Jukema JW, Kaufmann PA, van der Wall EE, Bax JJ. Predictive value of multislice computed tomography variables of atherosclerosis for ischemia on stress-rest single-photon emission computed tomography.

Circ Cardiovasc Imaging 2010;3:718-26.

Dankwoord

Dankwoord

De afgelopen jaren heb ik met veel plezier onderzoek gedaan. Dit is mede te danken aan de vele mensen die mij daarbij direct en indirect hebben geholpen en gesteund.

Als eerste wil ik jou bedanken Joanne. Ik heb onze samenwerking altijd enorm kunnen waarderen. Daarnaast, wil ik natuurlijk het CT team met daarin Gabija en later ook Mark, Joella, Fleur, Gaetano, Kees, Noor en Caroline bedanken voor al die jaren fijne samenwerking met de acquisitie, het uitwerken en het wegstijven van de scans en natuurlijk voor al het plezier tijdens het werk, op congres en daarbuiten. Eric, ik wil jou erg bedanken voor al het statistisch onderwijs dat ik door de jaren heen van je heb mogen ontvangen. Talitha, Cora, Marina en Monique, bedankt voor al jullie administratieve hulp tijdens mijn promotie.

In zeer grote mate is mijn tijd als promovendus in het LUMC onvergetelijk geworden door alle collega's en vrienden in de tuin. Naast de ongelooflijke hoeveelheid lol die we hebben gemaakt in de tuin, op congres en in de kroeg stond er ook altijd wel iemand klaar met advies op elk gebied. Toen ik aankwam als student werd ik gelijk opgenomen door de voor mij "oude" tuin met Tops, Mollema, Graus, Ivo, Maureen, Claudia, Saskia, en natuurlijk Pijnappels. Na mijn wetenschapsstage, toen ik als promovendus kwam werken, gingen de meeste van de "oude" tuin weg en kwam de "nieuwe" tuin met in het bijzonder Jan, Jan Willem, Roderick en Rutger aan en later ook Louisa, Mihaly, Hans, Joep en Carine erbij in de tuin. Ik wil jullie allemaal bedanken voor een geweldige tijd! Rutger, ik wil je ook speciaal bedanken voor al je hulp als paranmf.

Naast alle collega's in het LUMC zijn er nog vele andere mensen in mijn leven erg belangrijk geweest bij de totstandkoming van dit proefschrift. Pap, Mam, Jan en Judith, jullie hebben mij altijd gesteund en geadviseerd in alles wat ik deed en mij gestimuleerd om succesvol maar vooral gelukkig te zijn. Judith ik wil jou ook speciaal heel erg bedanken voor al je werk met de vormgeving van mijn proefschrift en het werk als paranmf. Ook de rest van mijn familie wil ik bedanken en dan in het bijzonder opa en oma Van Werkhoven voor jullie altijd aanwezige warmte en interesse en natuurlijk ook oma Romeijn, aan jou heb ik dit promotieonderzoek uiteindelijk te danken! Nelly, Lex en Cindy ik wil ook jullie bedanken voor al jullie steun. Op de middelbare school heb ik samen met Wim Jaap de eerste stappen in de richting gezet van de wetenschap, Wim Jaap ik ben je dankbaar voor je vriendschap en advies door de jaren heen. Laten we dat nog heel lang zo houden. Natuurlijk wil ik ook mijn club bedanken, tijdens mijn onderzoek was het erg fijn om naast onze goede vriendschap een wijdere blik in het leven buiten het ziekenhuis te blijven behouden.

Lieve Marielle jij hebt mijn onderzoek van heel dichtbij meegemaakt en je hebt mij altijd met je liefde, advies en relativerend vermogen gesteund zowel in de leuke tijden maar ook in de soms minder leuke tijden, dit is erg belangrijk voor mij geweest en ik ben je daar ontzettend dankbaar voor.

Curriculum Vitae

Curriculum Vitae

De auteur van dit proefschrift is geboren op 25 oktober 1983 te 's Gravenhage. In 2002 deed hij het eindexamen VWO aan het Eerste Christelijke Lyceum te Haarlem. In hetzelfde jaar startte hij met de studie Geneeskunde aan de Universiteit van Leiden. Tijdens zijn studie was hij werkzaam als redacteur bij de studenteneditie van het Nederlands Tijdschrift voor Geneeskunde en was hij betrokken bij wetenschappelijk onderzoek op de afdeling Cardiologie van het Leids Universitair Medisch Centrum. In januari 2007 behaalde hij het doctoraalexamen Geneeskunde en startte hij met onderzoek op het gebied van niet-invasieve beeldvorming bij de afdeling Cardiologie en Radiologie van het Leids Universitair Medisch Centrum onder begeleiding van Prof. Dr. Bax, Prof. Dr. Jukema en Prof. Dr. De Roos. Dit project, ondersteund door de Nederlandse Vereniging voor Cardiologie en het Interuniversitair Cardiologisch Instituut van Nederland, heeft geleid tot dit proefschrift.

In juni 2010 is hij gestart met de klinische fase van de opleiding Geneeskunde aan de Universiteit van Leiden.

